Oxidative Coupling Reactions and Organic Electrochemical Cells based on Electron Transfer Reactions

A Thesis

Submitted for the Degree of

DOCTOR OF PHILOSOPHY

By

M RAMUSAGAR



SCHOOL OF CHEMISTRY
UNIVERSITY OF HYDERABAD
HYDERABAD-500 046
INDIA

November-2018

Contents

Abbr	eviations	i
Abstr	ract	iii
Chap	ter 1	
Synth	netic Methods based on Electron Transfer Reactions	-naphthol 1 2 4 7 8 11 2-naphthol 11 opy 17 mines 19 23 23 33 33 36 36 36 37
Section	on 1: Reaction of Oxygen Adsorbed Carbon Materials with 2-napht	hol
1.1.1	Introduction	1
1.1.2.	Oxidative coupling of 2-naphthol	2
1.1.3	Previous reports on 1,1'-bi-2-naphthol from this laboratory	4
1.1.4	Carbon materials	7
1.1.4.	1 Surface characterization and properties of activated carbon	8
1.1.5	Results and Discussion	11
1.1.5.	1 Reactions of molecular oxygen adsorbed carbon materials with 2-napl	hthol 11
1.1.5.	2Evidence for paramagnetic species through EPR spectroscopy	17
Section	on 2: Oxidative Coupling of 2-naphthol and 1-naphthylamines	
with	I ₂ /O ₂ Reagent System	
1.2.1	Introduction	19
1.2.2	Results and Discussion	23
1.2.2.	1 Reactions of I ₂ with 2-naphthol	23
Section	on 3: Reaction of p-Doped N-Methylpolypyrrole with	
Sodiu	ım borohydride	
1.3.1	Introduction	31
1.3.2	Results and Discussion	33
1.3.2.	1 Synthesis of <i>p</i> -doped N-methylpolypyrrole (NMPPY)	33
1.3.2.	2 Preparation of Lewis base borane complexes using the	
	NMPPY/NaBH ₄ reagent system.	33
1.3.2.	3 Estimation of radical cation sites present in N-methylpolypyrrole	35
1.4	Conclusions	43

1.5	Experimental Section	45
1.6	References	57
Chapt	er 2	
Electr	on Transfer Reaction of Amine Donors with Quinone Acceptors	
2.1	Introduction	67
2.1.1	Electron transfer (ET) reactions in organic donor and acceptor system	67
2.1.2	ET and Polar processes in quinone chemistry	69
2.1.3	Addition and substitution reaction of quinones with amines	70
2.1.4	Charge transfer and electron transfer reactions of quinones	71
2.2	Results and Discussion	75
2.2.1	Reaction of secondary amines with quinone acceptors	76
2.2.2	EPR studies of aminoquinone in solid state	82
2.2.3	Reaction of tertiary amines with quinone acceptors	84
2.2.4	EPR studies of isopropyl amine and diisopropylamine with p-chloranil	92
2.2.5	Preparation of amide derivatives	95
2.2.6	EPR studies of amides with <i>p</i> -chloranil	97
2.2.7	Effect of TiO ₂ in EPR studies of amides with <i>p</i> -chloranil	106
2.2.7.5	UV-Visible spectral studies of amides with <i>p</i> -chloranil	116
2.2.8	Reaction of 2-naphthol and bi-2-naphthol with <i>p</i> -chloranil	121
2.2.9	Reaction of N-methylpyrrolidone (NMP) with p-chloranil	123
2.3	Conclusions	127
2.4	Experimental Section	129
2.5	References	145
Chapt	er 3	
Electr	icity Harvesting Organic Electrochemical Cell	
Exploi	iting Reversible Electron Transfer Reaction between	
Tertia	ry Amine Donors and Quinone Acceptors	
3.1	Introduction	151
3.1.1	Electron transfer (ET) mechanism for Birch reduction	151
3.1.2	ET mechanism in acyloin condensation	152

3.1.3	ET mechanism in Grignard reaction	153
3.1.4	ET mechanism in Aldol condensation	154
3.1.5	ET mechanism in Cannizarro reaction	154
3.1.6	ET mechanism in Meerwein-Pondorf-Verley (MPV) reduction	155
3.1.7	ET mechanism for nucleophilic substitution reactions	156
3.1.8	Electron transfer (ET) reactions in electrochemical process	157
3.2	Electron transfer in photochemical reactions	161
3.3	Organic solar cells	163
3.3.1	Single layer organic cells	164
3.3.2	Bilayer donor-acceptor solar cells	165
3.4	Results and Discussion	169
3.4.1	Construction of energy harvesting electro chemical cell	169
3.4.1.1	Two layer cell configuration	169
3.4.1.2	Multi layer cell configuration	171
3.5	Conclusions	189
3.6	Experimental Section	191
3.7	References	209
Apper	ndix I (Representative spectra)	215
Apper	ndix II (X-ray Crystallographic Data)	251
List of	publications	253

Abbreviations

Ac acetyl

AC activated carbon

Al aluminium anhyd. anhydrous aq. aqueous

Ar aryl

Bn benzyl

BINOL 1,4-benzoquinone 2,2' bi-2-naphthol

br broad (in spectroscopy)

Bu butyl

CB carbon black
CT charge transfer

DABCO 1,4-diazabicyclo[2.2.2]octane

DDQ 2,3-dichloro-5,6-dicyano-p-benzoquinone

DiPrBA *N,N*-diisopropylbenzamide

DIPEA N, N-diisopropylethylamine

d doublet (in spectroscopy)

DMF *N,N*-dimethylformamide

DMSO dimethyl sulfoxide

ee enantiomeric excess

EC ethylene carbonate

EPR electron paramagnetic resonance

ET electron transfer

equiv equivalent

Et ethyl

FF fill factor
h hour(s)
IR infrared

J coupling constant (in NMR spectroscopy)

m multiplet (in spectroscopy)

Me methyl

min minute(s)

mp melting point

NMP N-methyl-2-pyrrolidone

NMR nuclear magnetic resonance

NQ 1,4-naphthaquinone
PC propylene carbonate

PEO polyethylene oxide

PMMA poly(methyl methacrylate)

Nu nucleophile

Ph phenyl

PhNEt₂ *N,N*-diethylaniline

PNMA poly(*N*-methylaniline)

ppm parts per million

Pr propyl

q quartet (in spectroscopy)

ref reference number

rt room temperature

s singlet (in spectroscopy)

sat. saturated sec secondary

SET single electron transfer

soln solution

SS stainless steel
T temperature

TEMPO (2,2,6,6-tetrmethylpiperidin-1-yl)oxyl

t tertiary

t triplet (in spectroscopy)

THF tetrahydrofuran

TMPDA N, N, N', N'-tetramethylethylenediamine

TPA triphenylamine
TMS trimethylsilyl

UV ultraviolet

Abstract

This thesis entitled "Oxidative Coupling Reactions and Organic Electrochemical Cells based on Electron Transfer reactions" comprises of three chapters. The three chapters are subdivided into four sections namely Introduction, Results and Discussion, Conclusions and Experimental Section along with References. The work described in this thesis is exploratory in nature.

In chapter 1, we have described the development of new synthetic methods using oxygen doped carbon materials. We have carried out the reaction of 2-naphthol 1 with the oxygen doped carbon materials in presence of *t*-BuOK as base in THF. The resulting coupled product bi-2-naphthol 2 was obtained up to 95% yield in the case of oxygen adsorbed activated carbon (AC) and in 70% yield using oxygen adsorbed carbon black (CB). In the case of graphite which undergoes only physisorption with O₂, no bi-2-naphthol product was isolated (Scheme 1).

Scheme 1

We have also developed a method for the synthesis of racemic bi-2-naphthol **2**, by the coupling of 2-naphthol **1** in the presence of I₂/O₂ reagent in DCM solvent through electron transfer mechanism (Scheme 2).

Scheme 2

We have also prepared naphthidines 4 by using I_2/O_2 reagent system (Scheme 3).

Scheme 3

$$R^{1}_{N}, R^{2}$$

$$I_{2}/O_{2}$$

$$DCM, 25 °C$$

$$12 h$$

$$R^{1}_{N}, R^{2}$$

$$R^{1}_{N} = 12 \text{ A}$$

$$R^{1}_{N} = 12 \text{ A}$$

$$R^{2}_{N} = 12 \text{$$

A simple method was developed for estimating the doping levels in N-methylpolypyrrole salt **6** by using NaBH₄. The polymer has been readily prepared through polymerization of N-methylpyrrole **5** by FeCl₃ catalysed oxidation.

The reaction of N-methylpolypyrrole salt **6** with NaBH₄ and PPh₃ in the presence of THF solvent to gave Ph₃P:BH₃ **8** up to 1.35 mmol (20-55% yield) (Scheme 4). When the reaction was carried out in presence of pyridine **7** pyridine:BH₃ complex **8** was formed in 39-74% yield (Scheme 4).

Similarly, we have observed that the reaction of N-methylpolypyrrole salt **6** with NaBH₄ in the presence of amines in THF gave the amine:BH₃ complexes **10** in 40-60% yield (Scheme 5).

Scheme 5

In chapter2, we have described studies on the electron transfer reaction of quinone acceptors with donors like amines, amides and 2-naphthol derivatives. We have prepared a series of aminoquinone derivatives by the reaction of amines like N-substituted piperazine 11 reacts with quinones 12 and 13 in DCM solvent to obtain paramagnetic species. The reaction goes through electron transfer pathway and paramagnetic species with subsequent formation of aminoquinone as products (Scheme 6).

The reaction secondary amines like piperazines **11** with quinones **12** and **13** gave the corresponding diamagnetic aminoquinone product **14** and **15** *via* electron transfer reactions and charge transfer complexes (Scheme 7). Formation of radical ion intermediates were confirmed by epr spectral analysis.

Scheme 7

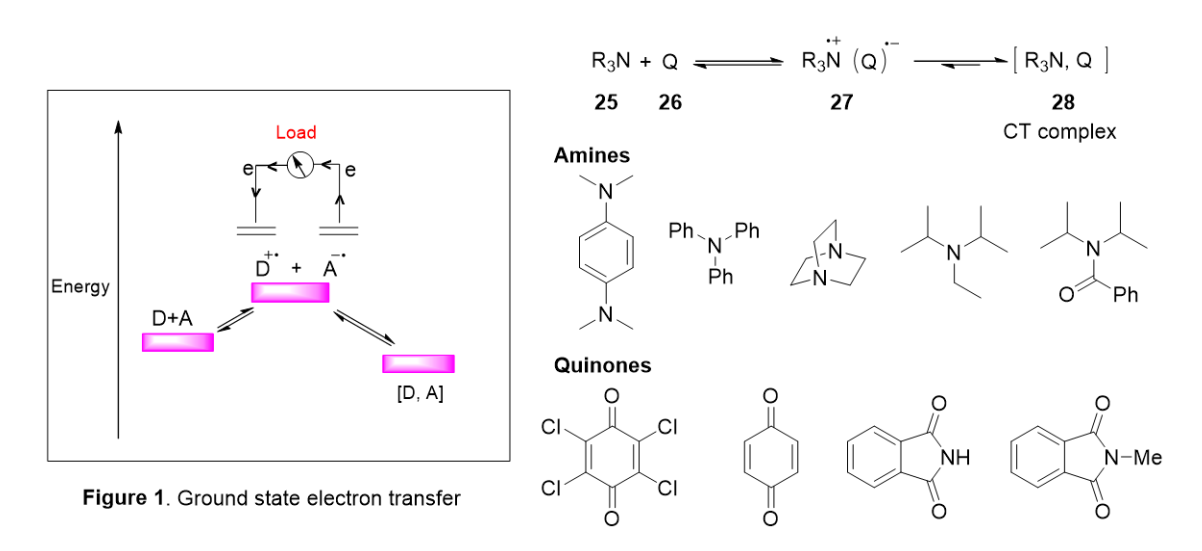
Similarly, the reaction of tertiary amines like piperazine **18** and quinones **12** gave the charge transfer complexes *via* the initially formed radical cation-anion pair as revealed by epr spectral analysis (Scheme 8).

The electron transfer complex and charge transfer complexes of amide derivatives **22** with *p*-chloranil **12b** were also studied through EPR and UV-Visible studies (Scheme 9).

Scheme 9

In the third chapter, we have developed an electrochemical cell based on the reversible electron transfer reactions using tertiary amine (R_3N) as electron donor and p-chloranil (Q) as an electron acceptor (Scheme 10). The electrochemical cell was constructed by making pastes of tertiary amines and p-chloranil pastes with propylene carbonate PC, titanium dioxide TiO₂ and poly(ethylene oxide) PEO.

Scheme 10



We have examined the performance of these electrochemical cells at the temperatures $28\,^{\circ}\text{C}$ to $40\,^{\circ}\text{C}$ by measuring current (I) and voltage (V) characteristics.

The results presented in this thesis are discussed considering mechanisms involved in these transformations and comparison with literature reports.

Note: Scheme numbers and compound numbers given in this abstract are different from those given in the chapters.

Chapter 1

Synthetic Methods based on Electron Transfer Reactions

Section 1: Reaction of Oxygen Adsorbed Carbon Materials with 2-naphthol Derivatives.

Section 2: Oxidative Coupling of 2-naphthol and 1-naphthylamines using I_2/O_2 Reagent System.

Section 3: Reaction of *p*-Doped N-Methylpolypyrrole with Sodium borohydride.

1.1 Reaction of Oxygen Adsorbed Carbon Materials with 2-Naphthol Derivatives

1.1.1 Introduction

Chiral bi-2-naphthyl derivatives have been used widely in asymmetric organic synthesis. Bi-2-naphthol (BINOL) is one of the most important compounds, as it exists in chiral atropisomers (R)-(+)-1a and (S)-(-)-1a. It is thermally stable and hence useful in numerous asymmetric transformations under various experimental conditions.

Figure. 1

The bi-2-naphthol **1a** derivatives generated immense interest because of their versatile backbone can be modified, thereby affecting the reaction environment.^{3,4} Optically active bi-2-napthol derivatives **1** have been widely used in both catalytic and stoichiometric transformations (Chart 1).^{5,6}

Chart 1

1.1.2 Oxidative coupling of 2-naphthol

Ding *et al.* reported⁷ oxidative coupling of 2-naphthol **17a** in aqueous medium at 50 °C using FeCl₃ (Scheme 1).

Brusse *et al.* reported⁸ the oxidative dimerization of 2-naphthol **17a** in the presence of copper(II)amine complexes. The optically active bi-2-naphthol **1a** compound was obtained by using (+) amphetamine as complexing amine which lead to selective precipitation of the copper(II)-(+)amphetamine-(-)binaphthol complex (Scheme 2).

Scheme 2

Doussot *et al.* reported⁹ oxidative coupling of electron rich naphthalene derivatives **17** using TiCl₄ in nitromethane solvent (Scheme 3).

Scheme 3

Wang *et al.* reported¹⁰ biaryl coupling of 2-naphthol derivatives **17** by using FeCl₃ catalyst in the presence of m-CPBA in DCM solvent (Scheme 4).

Morioku *et al.* prepared bi-2-naphthol **1a** from 2-naphthol **17a** using graphene oxide in the presence of BF₃.OEt₂ in DCE solvent at reflux conditions (Scheme 5).¹¹

Scheme 5

Grant-Overton and co-workers¹² reported the synthesis of bi-2-naphthol derivatives **1** under microwave conditions, using ${}^{t}Bu_{2}O_{2}$ in chlorobenzene solvent at 200 ${}^{o}C$ (Scheme 6).

Scheme 6

1.1.3 Previous reports on 1,1'-bi-2-naphthol from this laboratory

Methods have been developed in this laboratory to readily access chiral bi-2-naphthol **1a** in optically pure form. For example, the racemic bi-2-naphthol **1a** was resolved using (*S*)-proline^{13a-c} **18** as well as boric acid and chiral α -methylbenzylamine^{13d} **19**. The racemic BINOL was also resolved using (*S*)-amino naphthol **20** and boric acid in acetonitrile solvent (Scheme 7).^{13e}

Scheme 7

Diastereomeric mixture of amino alcohol **21**, compound **22** and the aminonaphthol derivatives **23** could be readily resolved using the chiral bi-2-napthol and boric acid (Scheme 8).¹⁴

Enantiomerically pure 2,3-diphenyl-1,4-butanediol **26** was prepared in good yields through intramolecular oxidative coupling of the titanium enolates of phenylacetic acid esters containing chiral 1,1'-bi-2-naphthol moiety followed by reduction using the $NaBH_4/I_2$ reagent system (Scheme 9).¹⁵

Scheme 9

Convenient methods were also developed for the preparation of chiral 1,1'-bi-2-naphthol derived amino ether derivatives **29**, **30** and **31** through opening of aziridinium ion intermediate, prepared from trans-(±)-2-(1-pyrrolidinyl)cyclohexanol **27** (Scheme 10).¹⁶

We have investigated the synthesis of bi-2-naphthol derivatives by electron transfer reactions using oxygen adsorbed carbon materials as described. A brief review of reports on the oxygen adsorbed carbon materials would facilitate the discussion.

1.1.4 Carbon materials

Carbon materials are useful in producing, transmitting and storing energy. ^{17a} The carbon materials are help in developing cheaper, cleaner and more energy-efficient technologies. ¹⁷ Based on its structural characteristics, carbon materials are useful in aerospace structures, aircraft brakes, concrete structures and lubrication. ¹⁸ Carbon materials are advantageous in practical applications like heat conduction and thermal insulation, environmental applications and in biomedical applications. ¹⁹ These materials may be collectively called as a family of carbon obtained from carbonization of organic raw materials. Generally, carbon materials are subjected to heat treatment at inert atmosphere to increase carbon content and to decrease the heteroatom content. ^{20,21} Carbonization is the process of heating, carbon materials such as coal, wood, nutshell etc. In this process of heating there is elimination of small molecules, such as water, methanol, carbon dioxide and carbon monoxide. ²² The resultant movement of atoms over short atomic distances creates a space network of porosity.

Recently, investigations were carried out on in this laboratory on the production of pyrolysis gas from woody biomass for use in electricity generation. In this carbonization process the commercially important charcoal is a byproduct. In continuation of these studies we became interested in developing organic reactions using readily accessible activated charcoal and related materials. Accordingly, a brief review on the nature and properties of activated charcoal and other readily accessible carbon materials like carbon

black and graphite for applications in organic transformations would facilitate the discussion.

Activated charcoal has potential for use in storage of electricity in electrochemical double layer capacitors (supercapacitors). It has also potential for harvesting the "IR" (heat) portion of the solar spectrum as it is a semiconductor with a narrow band gap of 34 meV.

1.1.4.1 Surface characterization and properties of activated carbon

The surface characteristics of carbon materials and the chemistry of the carbon materials are depending on the heteroatoms present in the carbon matrix. The heteroatom like molecular oxygen is responsible for the presence of different acidic functional groups such as carboxyl, carbonyl, phenol, quinone and lactones. In carbon materials, unsaturated sites are also present in the matrix.²⁴

Figure 2. Surface groups present in the carbon material. It indicates the presence of σ (*) and π (•) electrons at the zigzag sites and the presence of triple bonds at the armchair sites.

Carbon materials containing bulk atoms are neutral but the surface sites could adsorb molecules. These sites are very reactive and react even with metals. It is well known that chemical treatment of carbon materials increases the concentration of surface oxygen functional groups. Earlier, it was reported²⁵ that upon chemisorptions, the oxygen acquires a partial negative charge. It was also reported²⁶ that the carbon materials have a

free-flowing sp^{2- π} -electrons, which are useful in electron transfer reactions. The oxygen reduction reaction (ORR) of oxygen generates superoxide radical bound to carbon material and it acts as oxidatising agent in electron transfer reactions (Scheme 11).²⁷

Scheme 11

The characteristics of carbon materials and chemistry of their surface depends on the heteroatom presence which is in turn dependent on the nature of the materials and methods used for their preparation.²⁸ Further, it was suggested that the heteroatom like oxygen free graphene edge sites in carbon materials are neither H terminated nor free radicals. Instead, the edge sites are carbene-like zigzag sites with triplet ground state **36** or aryne-like (arm chair) sites with singlet ground state **35** (Figure 3).²⁹

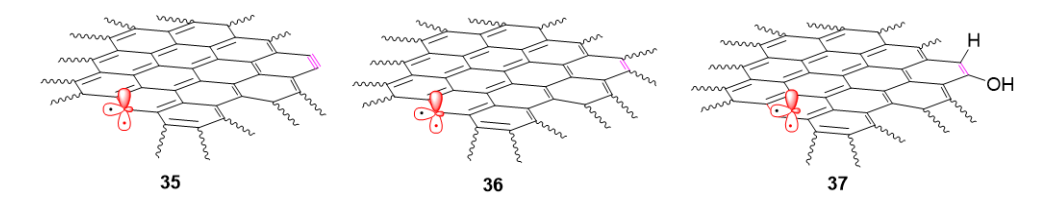
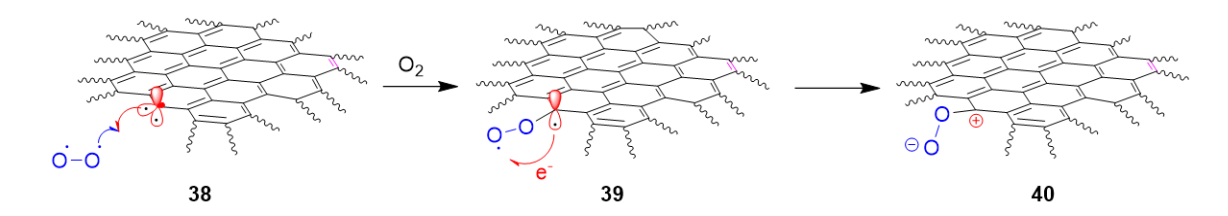


Figure 3. Reactive sites present in the carbon materials.

The aryne-like sites in **35** are expected to undergo trimerization to give benzenoid aggregates under ambient atmospheric condition. It is also expected to give phenolic groups upon reaction with moisture resulting in phenolic structure as in **37**. However, the magnetic properties and chemisorptions with molecular oxygen reported for the carbon materials are in accordance with the proposal that the graphene edge sites are carbene-like with triplet ground state. ²⁹

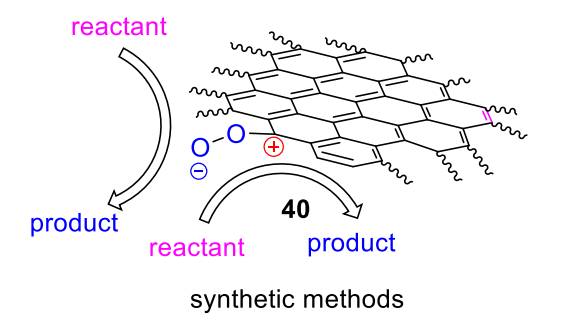
Previously, it was reported that chemisorption of molecular oxygen by activated carbon materials leads to formation of negatively charged oxygen (C-O-O $^{\delta}$ -) species. 30,31 Accordingly, we envisaged the formation of such species **40** through electron transfer from the carbon radical site in **39** formed by reaction with molecular oxygen with activated carbon **38** (Scheme 12).

Scheme 12



It is of our interest to develop reactions for practical use of the reactive intermediate **40** in the oxygen doped activated charcoal in synthetic transformations (Scheme 13).

Scheme 13

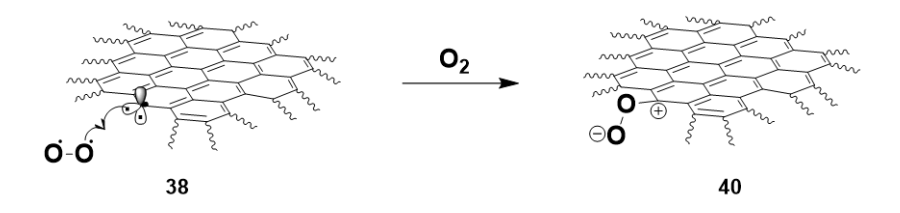


Therefore, we have investigated the molecular oxygen adsorbed carbon materials for the development of new synthetic methods based on reaction with electron rich compounds and reducing agents. The results are presented in the next section.

1.1.5.1 Reactions of molecular oxygen adsorbed carbon materials with 2-Naphthol

As outlined in the introduction section, activated carbon and carbon black react with molecular oxygen to give the intermediate species **40**. It was observed that very little oxygen gets adsorbed in the case of graphite (Table 1).

Table 1. Adsorption of molecular oxygen on carbon materials^a



Entry	CM 38 (g)	M/O ₂ (g)	O ₂ , (mmol)
1	AC (1) CB (1) Gr (1)	1.034 1.053 1.000	1.06 1.65
2	AC (2)	2.071	2.22
	CB (2)	2.078	2.43
3	AC (3)	3.092	2.88
	CB (3)	3.119	3.72
4	AC (4)	4.120	3.75
	CB (4)	4.152	4.75
5	AC (5)	5.175	5.46
	CB (5)	5.190	5.93
	Gr(5)	5.006	0.19
6	AC (10)	10.203	6.34
	CB (10)	10.236	7.37
	Gr(10)	10.013	0.41
7	AC (15)	15.312	9.75

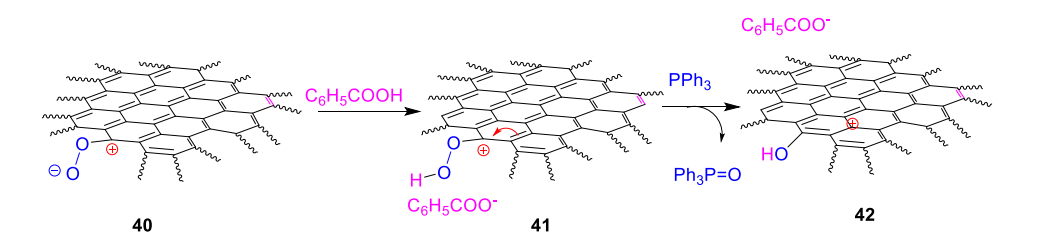
^aCarbon materials were heated at 200 °C under high vacuum for 2 h and brought to rt under N_2 . Then dry oxygen was passed to CM for 1 h.

12 Results and Discussion

The carbon material was preheated to 200 °C under high vacuum and brought to room temperature under N₂ atmosphere. Then the resulting carbon material was exposed to dry oxygen. The difference in the weight of carbon material before and after oxygen adsorption indicates the amount of oxygen molecule adsorbed (Table 1).

The carbon skeleton of the oxygen adsorbed intermediate 40 is expected to behave like electron acceptor and the negatively charged oxygen end is expected to undergo reaction with proton donors. Previously, it was observed from this laboratory that triphenylphosphine oxide (Ph₃P=O) was obtained in the reaction of benzoic acid with oxygen adsorbed intermediate 42 (Scheme 14).

Scheme 14



We became interested in using the oxygen adsorbed AC in oxidative coupling reactions. We have carried out the reaction of 2-naphthol **17a** using one gram of oxygen adsorbed AC in solvents like THF, methanol and toluene but only in toluene the bi-2-naphthol **1a** was obtained in 25% yield (Table 3). When the reaction was carried out in the presence of *t*-BuOK, the yield increased to 48%. The yield further improved to 67% when the reaction with *t*-BuOK was carried out in THF, presumably due to greater solubility of *t*-BuOK in THF solvent. When 2 g of activated carbon was used, the bi-2-naphthol **1a** product was obtained in 95% yield (Table 2).

Table 2. Reaction of Molecular Oxygen Adsorbed Carbon Materials with 2-naphthol **17a.**^a

Entry	CM (g)	t-BuOK (mmol)	Solvent (mL)	1a (%) ^b
1	AC (1)	-	Toluene (15)	25
2	AC (1)	2	Toluene (15)	48
3	AC (1)	2	THF (15)	67
4	AC (2)	2	THF (30)	95
5°	AC (2)	2	THF (30)	76
6	CB (2)	2	THF (45)	70
7^{d}	AC (2)	2	THF (30)	93

^aThe reactions were carried out with 2 mmol of 2-naphthol **17a** at 25 °C for 48 h. ^byield.

We have also observed that the 2-naphthol **17a** undergoes oxidative coupling reaction in the presence of carbon black (2 g) to give bi-2-naphthol **1a** in 70% yield under the same conditions. Whereas, the bi-2-naphthol **1a** product was not formed when the reaction was carried out using graphite (2 g), again indicating that molecular oxygen is mainly physisorbed in the case of graphite. In the absence of carbon additives, there was no formation of the bi-2-naphthol product **1a**.

The substituted 2-naphthol derivatives **17b** and **17c**, gave the corresponding bi-2-naphthol derivatives **1b** and **1c** in 83% and 68% yields, respectively (Scheme 15).

^cThe reaction was carried out for 24 h. ^dThe reaction was carried out with reoxidised activated carbon material.

14 Results and Discussion

Scheme 15

We have also observed that the bi-2-naphthol **1a** product was obtained in 93% yield when the recovered and re-oxidized activated carbon³³ was reused in this transformation (Table 2, entry 7).

The oxidative coupling reactions of 2-naphthol 17a using molecular oxygen adsorbed carbon materials can be rationalized by considering the mechanism outlined in Scheme 16. Initial deprotonation of the 2-naphthol 17a by *t*-BuOK base would give the 2-naphtholate 43a which could transfer one electron to the positively charged superoxide radical bound carbon material 40 to give the naphtholate radical 45. Dimerization of this naphtholate radical 45 followed by aromatization would give the bi-2-naphthol product 1a (Scheme 16).

1.1.5.2Evidence for presence of paramagnetic species through EPR spectral analysis

EPR spectra were recorded for the activated carbon samples at various stages and the spectra are presented below.

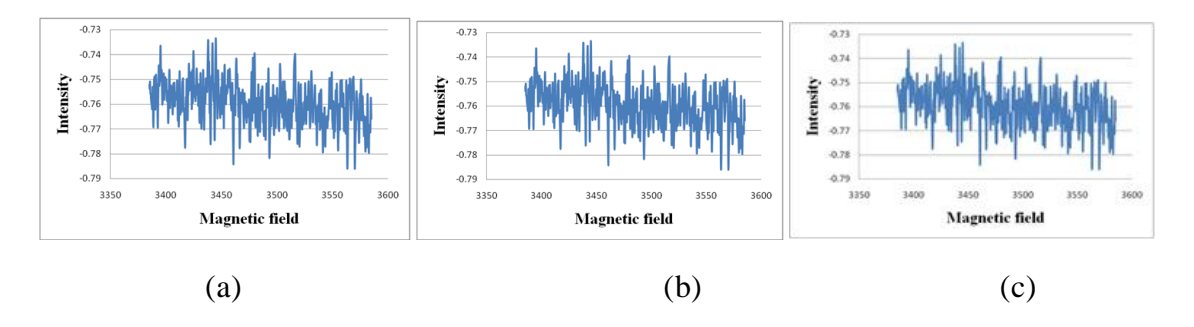
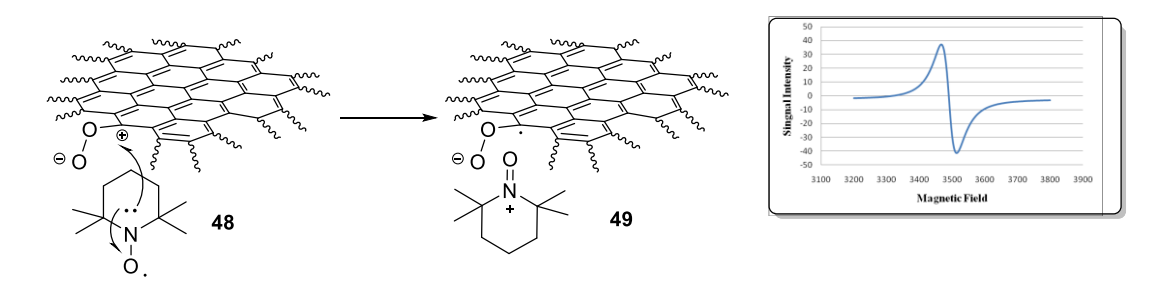


Figure 4. a) EPR spectrum of commercial carbon material. b) EPR spectrum of vacuum dried carbon material. c) EPR spectrum of oxygen doped carbon material.

The coupled product **1a** was not formed when the reaction was carried out in the presence of TEMPO, indicating that the expected TEMPO⁺ oxonium ion intermediate formed in the reaction of TEMPO with oxygen doped activated carbon may not oxidize 2-naphtholate **43a.** EPR Spectrum of paramagnetic species formed upon reaction of oxygen adsorbed activated carbon with TEMPO exhibits a broad singlet epr signal which corresponds to the species **49** (Scheme 17).

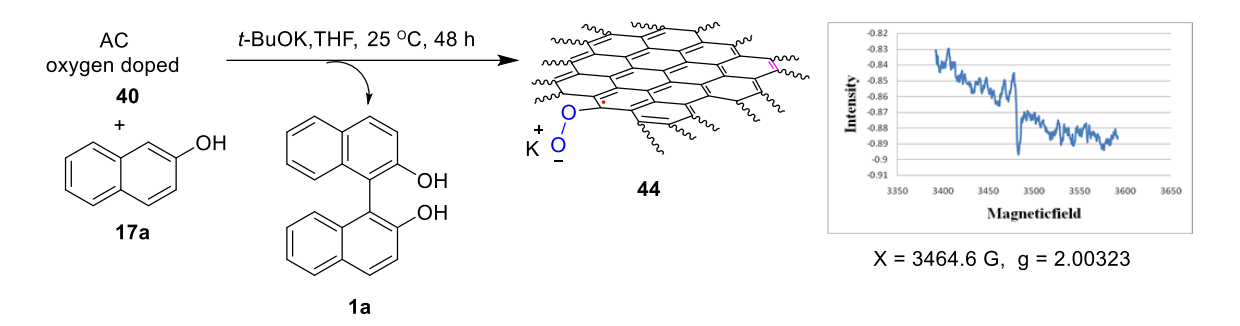
Scheme 17



The formation of paramagnetic species **44** upon addition of 2-naphthol/KO^tBu was also confirmed by EPR spectroscopy

16 Results and Discussion

Scheme 18



The EPR signals observed are in accordance with that expected for the paramagnetic species present in residual activated carbon samples.

It was observed in this laboratory that alcohols 56 are obtained in the reaction of organoboranes 53 with activated carbon 40 in the presence of aq. NaOH (Scheme 19).

Scheme 19

Also, it was found in this laboratory that when the oxygen adsorbed activated carbon **40** reacts with NaBH₄/PPh₃ in THF H₃B:PPh₃ **59** was obtained in 21-77% yield. When the reaction was carried out in presence of pyridine, the corresponding borane **62** complex was formed in 42-52% yield (Scheme 20).³⁴

Scheme 20

Dehydrogenative cross coupling reactions were also developed in this laboratory by carrying out the reaction of tetrahydroisoquinoline **63** with activated carbon in the presence of nucleophiles. The corresponding products were formed in good yields (Scheme 21).³⁵

Scheme 21

We have also observed that aromatic coupling reactions using 2-naphthol and 1-naphthylamines can be readily carried out using I_2 . The results are presented in the next section.

1.2 Oxidative coupling of 2-naphthol and 1-naphthylamines using I_2/O_2 Reagent System

1.2.1 Introduction

The charge transfer complexes formed by the reaction of electron donors and acceptors have been widely studied over the years. Such complexes were initially reported by Benesi and Hildebrand in 1949³⁶ and later characterized by R. S. Mulliken.³⁷ The electron donor and acceptor complexes of halogen compounds with olefins and aromatic compounds were reported.^{38,39} The inexpensive, nontoxic, and environment-friendly iodine⁴⁰ is useful as electron acceptor which readily forms charge transfer complexes with aromatic hydrocarbons,⁴¹ heterocyclic compounds like pyridine⁴² and antipyrene⁴³ (Scheme 22).

Scheme 22

In the aromatic substitution reactions like halogenations of aromatic compounds, iodine undergoes electron transfer reaction followed by combination of the corresponding radical cation with iodine resulting in the formation of the substitution product (Scheme 23).³⁸

Recently, it was reported that *N*-aryltetrahydroisoquinoline **74** derivatives react with iodine to give the corresponding radical cation that forms the corresponding iminium ion under aerobic conditions leading to the nucleophilic addition products in good yields (Scheme 24).⁴⁴

Scheme 24

However, earlier it was reported that iodine forms charge transfer complex with triphenylamine **78** in solution followed by formation of the corresponding radical cation **80** with subsequent bimolecular coupling to give the product tetraphenyl benzidine **81** (Scheme 25). 45,46

Chapter 1 Section 2 21

It is of interest to us to further investigate such aromatic coupling reactions. A brief review of recent literature reports will facilitate the discussion.

Schneider *et al.* reported⁴⁷ that the 1,1'-binaphthyl-4,4'-diamines (naphthidines) **83** were formed when 1-naphthylamine **82** derivatives were reacted with the TiCl₄ reagent in DCM solvent (Scheme 26).

Scheme 26

$$R^{1}_{N}$$
, R^{2}
 R^{1}_{N} , R^{2}_{N}
 R^{1}_{N} , R^{2}_{N}
 R^{1}_{N} , R^{2}_{N}
 R^{1}_{N} , R^{2}_{N}
 R^{1}_{N} , R^{2}_{N}

83

up to 76% y

Yang *et al.* reported⁴⁸ FeCl₃ mediated oxidative coupling of naphthylamines **82** and **84** in DCE solvent (Scheme 27).

FeCl₃, K₂CO₃

R¹ N R²

S2

R¹ = R² = alkyl or aryl

R¹
$$R^2$$

83

up to 92% y

FeCl₃, K₂CO₃

CICH₂CH₂CI

rt, 1 h

R¹ R^2

83

up to 92% y

R¹ R^2

84

R¹ = R² = alkyl or aryl

85

up to 81% y

Gopidas *et al.* reported⁴⁹ the preparation of benzidine compounds 81-94% yield in the presence of Cu(II) catalyst in acetonitrile solvent (Scheme 28).

Scheme 28

$$R^{1}_{N}$$
, R^{2}

$$\frac{\text{Cu(CIO}_{4})_{2}, 0-25 \,^{\circ}\text{C}, 12 \,\text{h}}{\text{K}_{2}\text{CO}_{3}, \text{CH}_{3}\text{CN}} \stackrel{R^{1}}{\underset{R^{2}}{\longrightarrow}} \frac{R^{1}_{N}}{R^{2}}$$
86
87
 $R^{1} = R^{2} = \text{alky or aryl}$
81-94% y

Oxidative coupling of N,N'-dialkylarylamines was reported from this laboratory using TiCl₄ reagent in DCM solvent to obtain the corresponding N,N,N',N'-tetra alkylbenzidines in up to 92% yield (Scheme 29).⁵⁰

Scheme 29

We have investigated the oxidative coupling of 2-naphthol and N,N-dialkyl 1-naphthylamine derivatives using I_2 in DCM solvent. The results are described in the next section.

1.2.2.1 Reactions of Iodine with 2-Naphthol

As described in section 1, it was of interest to us to develop oxidative coupling reactions through electron transfer reactions. So, we became interested in examining the reaction of 2-naphthol **17a** with iodine. Accordingly, we have carried out the reaction of 2-naphthol **17a** with iodine. The resulting reaction mixture gave epr signal indicating that radical species are formed in the reaction. The epr signal intensity slowly decreases with time and it disappears in 24 h (figure 5).

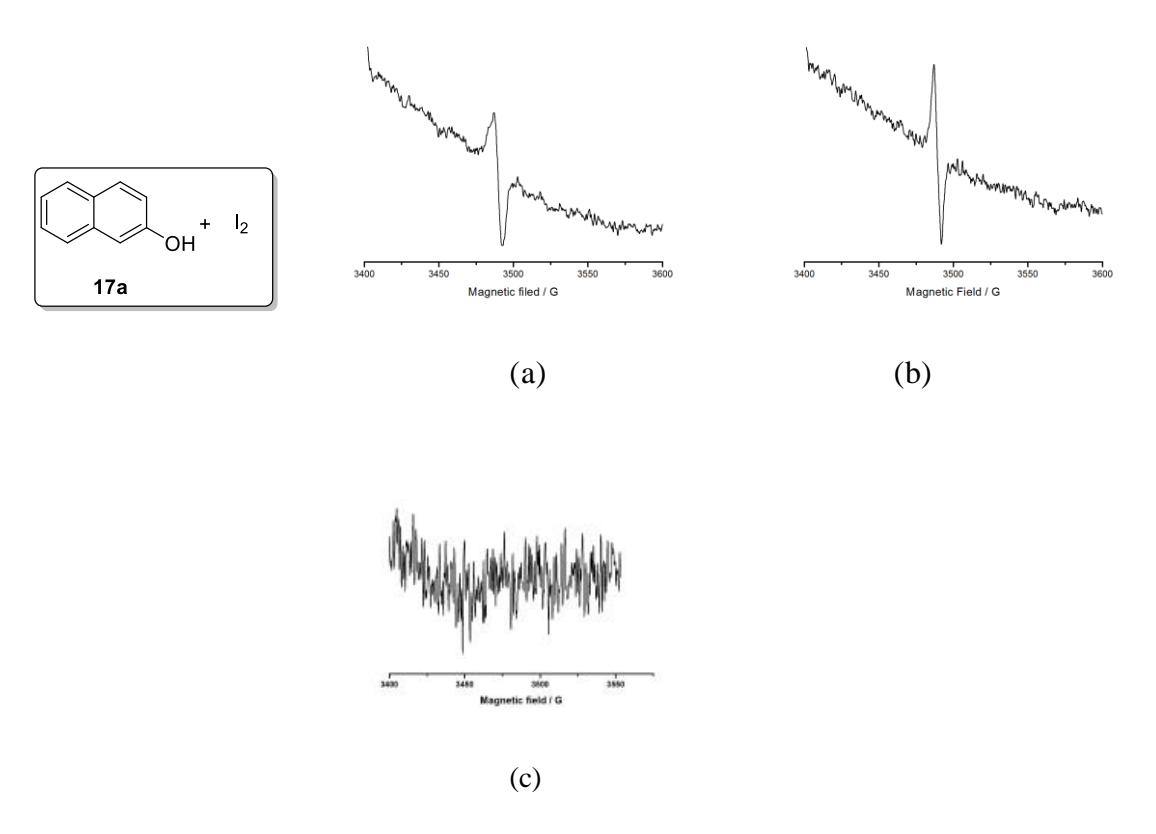


Figure. 5. EPR spectra of 2-naphthol 17a with iodine (a) at 5min (b) 12 h (c) 24 h.

24 Results and Discussion

Table 3. Screening of reaction conditions for I_2 mediated oxidative coupling of 2-naphthol.^a

Entry	2-naphthol	I ₂ (mmol)	Solvent (mL)	Product 1a
	17a			% yield ^b
	(mmol)			
1	2	5	DCM (10)	40
2	2	4	DCM (10)	35
3	2	3	DCM (10)	30
4	2	5	Toluene (10)	Trace
5	2	5	THF (10)	15
6	2	5	MeOH (10)	-
7°	2	1	DCM (5)	82
8	2	0.5	DCM (5)	55

^aThe reactions were carried out at 25 °C for 24 h. ^bIsolated yield. ^cThe reaction was carried out in presence of O_2 at 25 °C for 24 h.

We have carried out the reaction in different conditions under nitrogen atmosphere. The DCM solvent is found to be more effective in this transformation compared to other solvents like toluene, THF and MeOH (entries 1-6, Table 1). There was a dramatic increase in yield (88%, entry 7) when the reaction was carried out using only 0.5 equivalent of I_2 in the presence of O_2 . Further decrease in the amount of I_2 (0.25 equivalent) gave the bi-2-naphthol product $\mathbf{1a}$ in lower yield (55% yield, entry 8, Table 1).

The other derivatives of 2-naphthol **17** were also coupled under similar reaction conditions, and the products **1** were obtained in moderate to good yields (Table 4). The substituted derivatives of 2-naphthol **17b**, **17c**, and **17d** gave the corresponding coupling products **1b**, **1c** and **1d** in 75%, 65% and 63% yields, respectively (Table 4).

Table 4. Reaction of 2-naphthol derivatives with I₂/O₂.^a

We have observed that the reaction of 9-phenanthrol **90** with iodine under similar reaction conditions gave the coupled product [9, 9'-biphenanthrene]-10, 10'-diol **91** in 68% yield (Scheme 30).

Scheme 30

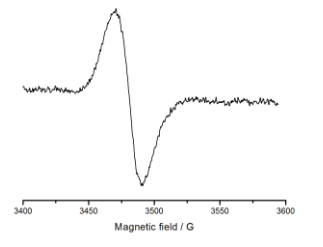
The oxidative coupling of bi-2-naphthol can be rationalized by considering the mechanism outlined in Scheme 31. Iodine could accept an electron from 2-naphthol 17a to

^aThe reactions were carried out by taking 2-naphthols (1 mmol), I_2 (0.5 mmol) in presence of oxygen in DCM solvent for 24 h.

form the corresponding radical cation **92**. After dimerization followed by aromatization and elimination of HI, the bi-2-naphthol **1a** would be formed (Scheme 31). The HI could react with molecular oxygen to regenerate iodine.⁴⁴

Scheme 31:

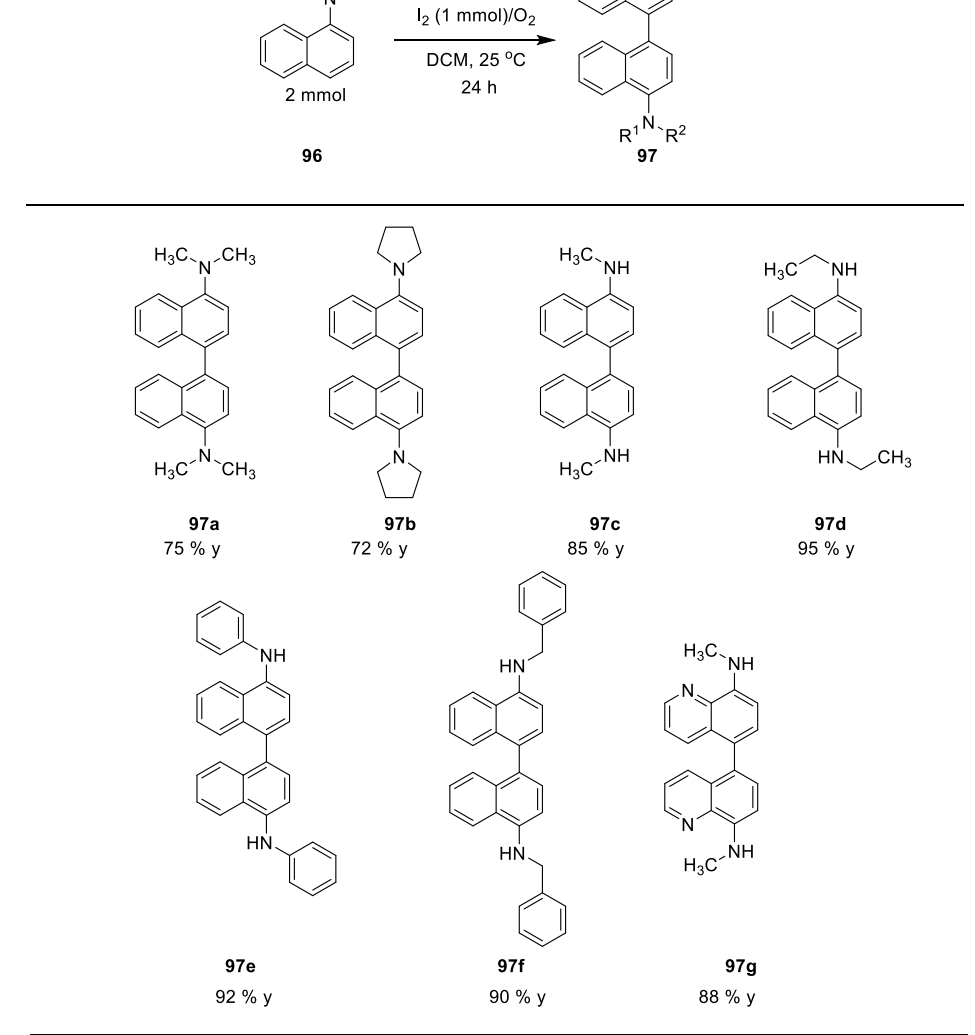
We have also carried out the coupling reaction of 1- naphthylamines **96** under similar reaction conditions. Initially, we have carried out reaction of *N*,*N*-dimethyl-1-naphthylamine **96a** with iodine in an EPR tube. The EPR signal was obtained upon mixing which disappeared after 24 h. We have also observed that *N*-methyl-1-naphthylamine **96c** gives epr signal which disappeared after 24 h (Figure 6).



(a) 5 min

Figure. 6. EPR spectra of (a) *N*,*N*-dimethyl-1-naphthylamine **96a** with iodine and (b) *N*-methyl-naphthylamine **96c** with iodine at 5min.

Table 5: Reaction of 1-alkylnaphthylamines with I₂/O₂.^a



 $[^]a\! T\! he$ reactions were carried out by taking naphthylamines (1 mmol), I_2 (0.5 mmol) in the presence of oxygen in DCM solvent for 24 h. $^b Isolated$ yield.

We have found that the reaction of *N*,*N*-dimethyl-1-naphthylamine **96a** with iodine in presence of O₂ at 25 °C in DCM for 12 h gave the coupled product naphthidine **97a** in 75% yield. The naphthylamine derivative **96b** gave the product **97b** in 72% yield. Further, we have carried out the reaction of 1-naphthylamines under similar conditions. The coupled product was isolated in 95% yield. 1-naphthylamine derivatives **96c**, **96d**, **96e**, **96f** also gave the products **97c**, **97d**, **97e** and **97f** in excellent yields (Table 5).

The reaction of *N*-methyl 8-aminoquinoline derivative **96g** gave the coupled product **97g** in 88% yield. The structure of the compound **97g** was further confirmed by single crystal X-ray data (Figure 7).

Figure. 7: X-ray crystal structure of compound 97g.

The oxidative coupling of 1-alkylnaphthylamines **96** can be explained by considering mechanism outlined in Scheme 32. Iodine could accept an electron from naphthylamine **96** to give the intermediate **99**, which upon dimerisation followed by aromatization and elimination of HI would give the product naphthidine **97**. The HI could react with molecular oxygen to regenerate iodine.⁴⁴

Scheme 32

Naphthidines are important compounds with potential for application in electronic devices as hole transporting materials.⁴⁸ Hence, the method described here has significant potential for further application.

We have also investigated the preparation and utilization of polypyrrole radical cation salts. The results are presented in the next section.

Table 1.Crystal data and structure refinement for compound 97g

Table 1. Crystal data and structure refinement for compound 9/g				
Identification code	Compound 97g			
Empirical formula	C20 H16 N4			
Formula weight	312.37			
Temperature	298(2) K			
Wavelength	0.71073 Å			
Crystal system	Monoclinic			
Space group	P 21/n			
Unit cell dimensions	a = 11.7100(12) Å	$\alpha = 90^{\circ}$.		
	b = 9.5335(9) Å	$\beta = 94.556(4)^{\circ}$.		
	c = 14.2691(14) Å	$\gamma = 90^{\circ}$.		
Volume	1587.9(3) Å ³			
Z	4			
Density (calculated)	1.307 Mg/m^3			
Absorption coefficient	0.080 mm ⁻¹			
F(000)	656			
Crystal size	0.36 x 0.24 x 0.12 mm ³			
Theta range for data collection	2.343 to 24.400°.			
Index ranges	-13<=h<=13, -11<=k<=11, -16<=l<=16			
Reflections collected	25273			
Independent reflections	2610 [R(int) = 0.1732]			
Completeness to theta = 24.400°	99.9 %			
Absorption correction	None			
Refinement method	Full-matrix least-squares	on F^2		
Data / restraints / parameters	2610 / 0 / 217			
Goodness-of-fit on F ²	1.069			
Final R indices [I>2sigma(I)]	R1 = 0.0730, wR2 = 0.1670			
R indices (all data)	R1 = 0.1388, $wR2 = 0.1937$			
Extinction coefficient	n/a			
Largest diff. peak and hole	0.456 and -0.208 e.Å- ³			

1.3 Studies on p-Doped N-methylpolypyrrole with Sodium borohydride

1.3.1 Introduction

Electroactive conducting polymers have proven applications in several technologies such as solar cells, display devices, gas sensors and actuators.⁵¹ It is relatively easy to process these polymers to make these devices and their chemically tunable property makes them useful in electronic devices.⁵² These polymers are redoxactive and their conductivity can be changed by doping the polymer. The physical properties of these conductive polymers depend on the type of doping and the dopant used.

Polypyrrole is one of the most intensively investigated electronically conductive polymers.⁵³ Polypyrrole exhibits good reversibility in doping and undoping. Therefore, polypyrrole is one of the most promising materials for use as positive electrodes in rechargeable batteries.⁵⁴ Polypyrroles can be prepared through electro polymerisation method and chemical oxidation methods. Roncali reported⁵⁵ the preparation of polypyrrole and polythiophene through electropolymerisation method (Scheme 33).

Scheme 33

Conductive polymers can be also prepared by using metal catalysts like $FeCl_3$, $Fe(ClO_4)_2$, and $(NH_4)_2S_2O_8$ in aqueous solvent (Scheme 34).⁵⁶

Scheme 34

We have prepared poly-N-methyl pyrrole salts for synthetic applications. The results are presented in the next section.

1.3.2.1 Synthesis of *p*-doped N-methylpolypyrrole (NMPPY)

We have prepared N-methylpolypyrrole **108** using FeCl₃ and N-methylpyrrole **107** in water following a reported method (Scheme 35).^{56a} We have confirmed the formation of NMPPY^{(.+)m} nCl⁻ **108** through IR spectroscopy and the presence of radical species was confirmed by epr spectroscopy (g value 2.0024).

Scheme 35

1.3.2.2 Preparation of Lewis base borane complexes using the NMPPY/NaBH₄ reagent system.

Earlier reports indicated that there are three different structures possible for N-methylpolypyrrole (Scheme 36).⁵⁷

Scheme 36

$$\begin{array}{c} H_3C \\ CH_3 \\ N \\ CH_3 \\ Neutral \ Polymer \\ \hline \\ H_3C \\ CH_3 \\ \hline \\ Neutral \ Polymer \\ \hline \\ CH_3 \\ CH_3 \\ \hline \\ CH_3 \\ CH_3 \\ \hline CH_3 \\ \hline \\ CH_3 \\ CH_3 \\ \hline \\ CH_3 \\ CH_3 \\ \hline \\ CH_3 \\ CH$$

The structure **109** is a neutral polymer. Removal of an electron from structure **109** leads to the radical cation polymer **111**. This radical cation polymer **111** is also called as

polaron. Removal of an electron from structure **111** gives a bipolaron **110** which is a dication. The polaron and bipolaron are formed directly through oxidation of the monomer. Previous reports reveal that the radical cation present in the polypyrrole could delocalize into the rings.⁵⁸ The repeating unit of cation radical in these polymers are approximately six monomer units. The planarity of these polymers gets twisted and decrease beyond six rings.

It was of interest to develop a method for estimating the doping levels in N-methylpolypyrrole by using NaBH₄ and Ph₃P based on the yield of Ph₃P:BH₃ complex formed (Scheme 37).

Scheme 37

A tentative mechanism for the formation of Ph₃P:BH₃ complexes can be considered involving the reduction of cation radical site by NaBH₄ through single electron transfer (SET) process to give neutral polymer and Ph₃P:BH₃. The possible mechanism is outlined in Scheme 38.

Scheme 38

1.3.3.3 Estimation of radical cation sites present in N-methylpolypyrrole

We have observed that the reaction of NMPPY^{(.+)n} nCl⁻ **108** (1g, 2.10 mmol, assuming that six repeating units contain one radical cation) of with NaBH₄ (1 mmol) and PPh₃ **58** (1 mmol) obtained the Ph₃P:BH₃ **59** in 0.62 mmol yield (Table 1, entry 1). When the reaction was carried out using higher amounts of NaBH₄/Ph₃P, higher yields of Ph₃P:BH₃ **59** was obtained (Table 1 entries 2-4).

There was no significant change observed, when the reaction was performed using more than 4 mmol each of NaBH₄ and Ph₃P. Accordingly, it can be concluded that a minimum of approximately 1.35 mmol of radical cation sites are present in the 1g of NMPPY^{(,+)n} nCl⁻ 108. However, the actual number of radical cations salts present is expected to be slightly more than this as the yields are of isolated yields and hence about 5% loss expected during workup.

The recovered NMPPY^{(.+)n} nCl⁻ **108** (1g), after oxidation with FeCl₃ (Scheme 35), reacts with NaBH₄ (1 mmol)/PPh₃ (1 mmol) to give the Ph₃P:BH₃ in 0.57 mmol of yield (Table 1, entry 5) without significant change from the freshly prepared sample, illustrating the recyclability of the polymer used.⁵⁹

Table 6. Reaction of NMPPY^{(.+)n} nCl⁻ radical cation **108** with NaBH₄ and PPh₃^a

Entry	NaBH4 108 (m mol)	PPh ₃ 58 (m mol)	H ₃ B:PPh ₃ 59 Yield(mmol) ^b
1	1	1	0.62
2	2	2	1.02
3	3	3	1.20
4	4	4	1.35
5°	1	1	0.57

^aThe reactions were performed with NMPPY radical cation salts **108** (1 g, 2.10 mmol), NaBH₄ and PPh₃ in THF at 25 °C. ^bIsolated H₃B:PPh₃ complex in mmol. ^cReaction was performed with re-oxidized polymer radical cation salts.

Similarly, when the reaction of NMPPY 108 was carried out with NaBH₄ and amines in THF solvent the corresponding amine:BH₃ complexes were attained in moderate yields (Table 7).

Table 7. Generation of Amine:Borane from NMPPY 108 Radical Cation^a

Entry	Amine 113	NaBH4 (mmol)	Polymer (g) (mmol radical cation sites)	Amine:BH3 114	Yield (%) ^b
1		5	NMPPY (4,8.2)	N: BH ₃	45
	113a			114a	
2	N H	5	NMPPY (4,8.2)	N. H BH ₃	40
	113b			114b	
3	N H 113c	5	NMPPY (4,8.2)	H N BH ₃ 114c	60
4	0 N H 113d	5	NMPPY (4,8.2)	O H N BH ₃ 114d	43
5	O N CH ₃ 113e	5	NMPPY (4,8.2)	O H ₃ C N BH ₃	40

^aThe reactions were carried out by using NMPPY (4 g), NaBH₄ (5 mmol) and amine (5 mmol) in dry THF (20 mL). ^bThe yields are of isolated products based on amine.

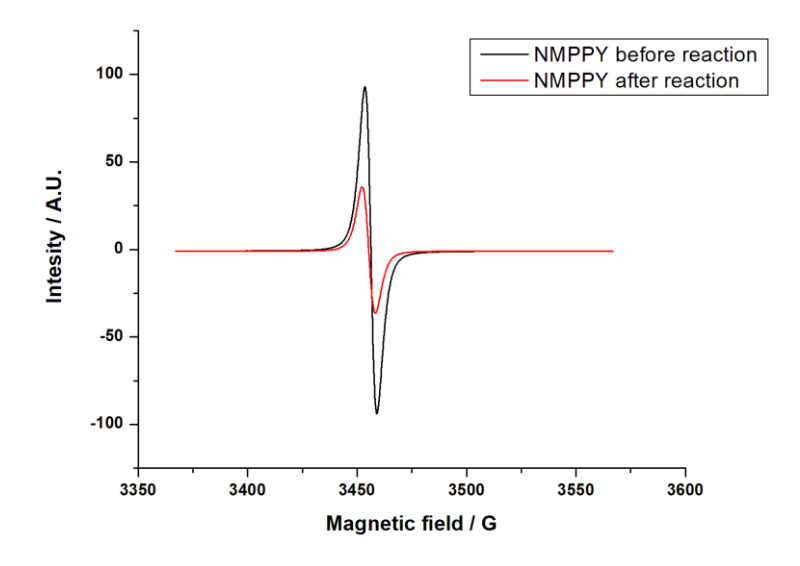


Figure 8: EPR of NMPPY 108 before and after reaction.

The epr studies also indicated that there was a decrease in the radical cation spin density present in the polymer salts after reaction with NaBH₄. The epr spectra of NMPPY **108** indicated that some radical cation sites remain after the reaction with NaBH₄ and PPh₃. The epr signals became weak but not totally absent (Figure 8). Earlier, it was reported that the neutral pyrrole polymers react with molecular oxygen to give paramagnetic species. ^{60,61} Therefore, formation of small amounts of paramagnetic species by the reaction of polymer with O₂ during the work up procedure cannot be ruled out in these cases.

We have analysed the NMPPY **108** by UV-Visible spectroscopy before and after the reaction with NaBH₄ and PPh₃. Broad absorptions at longer wavelength (red shift) was observed for the NMPPY before reaction with NaBH₄ and PPh₃. The wavelength of absorptione get decreased or move to shorter wavelength after reaction with NaBH₄ and PPh₃ (Figure 9). The color of the polymer also gets changed from black to green.

The shift in the UV-Visible absorptions in the spectra to lower wavelength (blue shift) after the reaction with NaBH₄ and PPh₃ may indicate that the effective conjugation

present in the polymer or in polymer cation radical sites present in the polymer gets lowered.

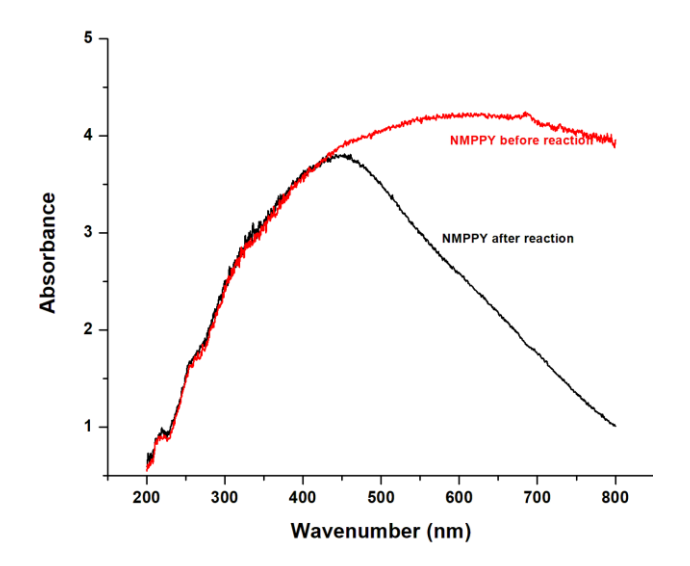


Figure 9. UV-Visible spectra of NMPPY **108** powder sample before (red line) and after (black line) reaction with NaBH₄ and PPh₃

The Ph₃P:BH₃ complex is very stable and hence it is not useful for synthetic applications. However, the amines like pyridine form relatively less stable complexes and they are useful for hydroboration of olefins at elevated temperatures or at room temperature under activation by I₂. Therefore, we have decided to investigate the reaction of NaBH₄ with the polymer radical cation salts in the presence of pyridine.

We have found that the reaction of NMPPY radical cation salt (1 g) with NaBH₄ and pyridine **115** in THF gives the pyridine:BH₃ **116** complex. The results are summarized in Table 8. In the reaction of 1 g of NMPPY radical cation **108**, which contain a minimum of approximately 1.35 mmol of radical cation sites, highest yield (74%) of pyridine:BH₃ **116** was obtained using 3 mmol each of NaBH₄ and PPh₃ (Table 8, entry 3).

Table 8. Reaction of NMPPY radical cation with NaBH4 and pyridine^a

Entry	Pyridine 115 (mmol)	NaBH4 (mmol)	Pyridine:BH ₃ 116 Yield ^b (mmol)	Pyridine:BH ₃ 116 Yield
1	1	1	0.53	39
2	2	2	0.89	66
3	3	3	1.00	74

^aThe reactions were performed with 1g NMPPY **108** radical cation salts, NaBH₄ and pyridine in THF at 25 °C. ^bIsolated pyridine:BH₃ complex in mmol.

We have also performed the hydroboration reaction using α -methyl styrene using polymers with NaBH₄ in THF at 25 °C for 24 h. There was no hydroboration observed. This indicates that the polymer-BH₃ complex product does not hydroborate olefin. The pyridine:BH₃ complex **116** is useful for hydroboration reaction at elevated temperatures.⁶² Recently, it was also reported that pyridine:BH₃ complex **116** hydroborates olefins at room temperature under activation by I_2 .⁶³ Hence, the pyridine-borane prepared in this way could be activated for the hydroboration reactions of olefins.

Diborane is one of most important reagent in organic synthesis. Diborane itself is difficult to handle and relatively inert towards olefins. So, it is normally utilized in the form of its complexes such as BH₃:THF, BH₃:SMe₂ and BH₃:NR₃. Many reagent systems have been developed for the generation of diborane gas.⁶⁴ Previously, simple methods for generation of diborane gas from I₂/NaBH₄, I₂/*n*-Bu₄NBH₄ and PhCH₂Cl/*n*-Bu₄NBH₄ regent system were reported from this laboratory (Scheme 39).⁶⁵

Scheme 39

We have undertaken the studies to estimate the doping level in N-methylpolypyrrole by using NaBH₄/Lewis base system. This simple method is also useful for the preparation of Lewis base-borane complexes (Table 7 and Table 8). The advantage of the present method is that the N-methylpolypyrrole can be recovered by simple filtration for reuse again for the preparation of the Lewis borane complexes.

It was also observed in this laboratory that the reaction of polymers such as polythiophene (PT^(.+)_m nCl⁻) **123** and poly(*N*-methylaniline) (PNMA^(.+)_m nCl⁻) **124** radical cation salts with NaBH₄ (1 mmol) and PPh₃ (1 mmol) gave the Ph₃P:BH₃ **59** in 0.72 mmol and 0.68 mmol (Scheme 18). The results indicate that a minimum of approximately 1.70 mmol of radical cation sites are present in 1 g PT^(.+)_m nCl⁻ **123** and also a minimum of 1.60 mmol of radical cation sites are present in 1 g of PNMA^(.+)_m nCl⁻ **124** (Scheme 40).^{34,66}

Scheme 40

NaBH₄ +
$$\begin{pmatrix} \cdot \cdot \cdot \end{pmatrix}$$
 m PPh₃ 58 Ph₃P:BH₃ THF 59 25 °C, 24 h up to 1.70 mmol PT radical cation salts

PNMA radical cation salts

Next, we have investigated the reactions of amine donors with quinone acceptors.

The results are discussed in chapter 2.

1.4 Conclusions

We have developed a simple method for the preparation of the bi-2-naphthol derivatives using activated charcoal and carbon materials.

We have also developed new synthetic methods for the preparation of bi-2-naphthol compounds and naphthidines using metal free I_2/O_2 system as oxidant.

$$R_{N}^{1}$$
 R^{2}
 R^{1}
 R^{2}
 R^{1}
 R^{2}
 R^{1}
 R^{2}
 R^{1}
 R^{2}

Simple and convenient method for estimating doping levels in NMPPY^{(.+)m} nCl⁻ and for the preparation of PPh₃:BH₃ and amine borane complexes were developed.

These methods have potential for large scale preparation as the polypyrrole derivatives can be isolated by filtration for reuse.

1.5 Experimental Section

1.5.1 General Informations

IR (KBr) and IR (neat) spectra were recorded on JASCO FT-IR spectrophotometer model-5300. The NMR spectra [1 H (400 MHz) and 13 C (100 MHz)] were recorded on Bruker-Avance-400 spectrometers chloroform-d as solvent. Chemical shifts are expressed in δ downfield with respect to the signal of internal standard tetramethylsilane ($\delta = 0$ ppm). Coupling constants J are in Hz. The mass spectral analyses were carried out using Chemical Ionization (CI) or Electro Spray Ionization (ESI) techniques. EPR spectra was recorded in a spectrometer equipped with an EMX micro X source for X band measurement using Xenon 1.1b.60 software provided by the manufacturer. Analytical thin layer chromatographic tests were carried out on glass plates (3 x 10 cm) coated with 250 m μ silica gel-G and GF₂₅₄ containing 13% calcium sulfate as binder. The spots were visualized by short exposure to iodine vapor or UV light. Column chromatography was carried out using silica gel (100-200 mesh).

All the glasswares were pre-dried at 100-120 °C in an air-oven for 4 h, assembled in hot condition and cooled under a stream of dry nitrogen. Unless otherwise mentioned, all the operations and transfer of reagent were carried out using standard syringe-septum technique recommended for handling air sensitive reagents and organometallic compounds.

In all experiments, a round bottom flask of appropriate size with a side arm, a side septum, a magnetic stirring bar, a condenser and a connecting tube attached to a mercury bubbler was used. The outlet of the mercury bubbler was connected to the atmosphere by a long tube. All dry solvents and reagents used were distilled from appropriate drying

agents. As a routine practice, all organic extracts were washed using saturated NaCl solution (brine) and dried over Na_2SO_4 or K_2CO_3 and concentrated on Heidolph-EL-rotary evaporator.

Activated carbon was heated at 200 °C under reduced pressure (0.001 mm Hg) in a vacuum oven and stored under dry nitrogen. Toluene and THF were freshly distilled over sodium-benzophenone ketyl before use. FeCl₃ and 2-naphthol supplied by E-Merck (India) was used as received. N-methylpyrrole, was purchased from Aldrich and used as received. NaBH₄, PPh₃ and NaOH were supplied by E-Merck (India) was used as received. 1.5.2 General Procedure for the reaction of molecular oxygen doped activated charcoal with 2-naphthol.

In a 50 mL RB flask 2-naphthol derivatives (**17a-17c**) (2 mmol) dissolved in THF (30 mL), under nitrogen atmosphere. To this add *t*-BuOK (2 mmol) and the contents were stirred for about 1h followed by addition of activated carbon (2 g). The reaction mixture further stirred for 48 h. The reaction mixtures were filtered, and wash several times with DCM and H₂O. The organic layer extracts with DCM, washes with brine and then dried over anhyd.Na₂SO₄. Evaporate solvent under vacuum and the crude mixture was chromatographed on silicagel using hexane:ethylacetate (85:15) as eluent to isolate the pure compound.

1.5.3 General Procedure for the reaction of 2-naphthol with I₂/O₂.

In a 50 mL RB flask 2-naphthol derivatives (**17a-17d**), 9-phenanthrol **90** (2 mmol) dissolved in DCM (5 mL) under nitrogen atmosphere. To this add Iodine (1 mmol) and the contents were stirred for 24 h under oxygen atmosphere by keeping oxygen balloon. The reaction mixture was quenched with sodiumthiosulphate. The organic layer extracts with DCM, washes with brine and then dried over anhyd. Na₂SO₄. Evaporate solvent under

ОН

OH.

ОН

.OH

1b

1a

vacuum and the crude mixture was chromatographed on silicagel using hexane:ethylacetate as eluent to isolate the pure compound.

1,1'-Bi-2,2'-naphthol 1a

Yield : 0.275 g (95%); Colorless solid.

mp : 217-219 °C; (lit. ¹⁰ mp. 216-218 °C)

IR (**KBr**) : (cm⁻¹) 3484, 3402, 3040, 1621, 1599,

1517, 1468, 1386, 1325, 1271, 1221, 1183, 1145.

¹**H NMR** : $(400 \text{ MHz, CDCl}_3, \delta \text{ ppm}) 7.96 \text{ (d, } J = 8\text{Hz, 2H), } 7.89 \text{(d, } J = 8\text{Hz, 2H)}$

2H), 7.39-7.33 (m, 4H) 7.33-7.29 (m, 2H), 7.16 (d, J = 8Hz, 2H),

5.09 (s, 2H)

¹³C NMR : (100 MHz, CDCl₃, δ ppm) 152.6, 133.4, 131.4, 129.4, 128.4, 127.5,

124.2, 124.0, 117.7, 110.8.

6,6'-Dibromo-1,1'-bi-2,2'-naphthol 1b

Yield : 0.372g (83%); Colorless solid.

mp : 198-200 °C; (lit. 10 mp. 200-202 °C)

IR (**KBr**) : (cm⁻¹) 3451, 1604, 1588, 1495, 1380, 1347,

1215, 1160, 1122.

¹**H NMR** : (400 MHz, CDCl₃, δ ppm) 8.06-8.04 (m, 2H), 7.91-7.87(m, 2H),

7.41-7.35 (m, 4H), 6.98-6.94 (m, 2H), 5.04 (s, 2H).

¹³C NMR : $(100 \text{ MHz}, \text{CDCl}_3, \delta \text{ ppm}) 152.9, 131.9, 130.8, 130.7, 130.5, 130.4,$

125.8, 118.9, 118.02, 110.6.

.COOMe

COOMe

HO HO

1c

Dimethyl 2,2'-dihydroxy-1,1'-binaphthyl-3,3'-dicarboxylate 1c

Yield: 0.275 g (68%); Yellow Color solid.

mp : 284-286 °C; (lit. 10 mp. 285-287 °C)

IR (KBr) : (cm⁻¹) 3183, 2947, 1676, 1506, 1441, 1326,

1293, 1221, 1150, 1084.

¹**H NMR** : (400 MHz, CDCl₃, δppm) 10.77 (s, 2H), 8.71(s, 2H), 7.95-7.93 (m,

2H), 7.37-7.35 (m, 4H), 7.20-7.18 (m, 2H), 4.06 (s, 6H).

¹³C NMR : $(100 \text{ MHz}, \text{CDCl}_3, \delta \text{ ppm}) 170.6, 154.0, 137.2, 132.9, 129.8, 129.5,$

127.2, 124.7, 124.0, 117.0, 114.1, 52.7.

6,6'-Dimethoxy-[1,1'-binaphthalene]-2,2'-diol 1d

Yield : 0.242 g (70%); Colorless solid

mp : 90-92 °C; (lit. 12 mp. 88.5-91 °C)

IR (KBr) : (cm⁻¹) 3357, 2931, 1624, 1588, 1449, 1218,

1083,1014, 810, 761.

¹**H NMR** : (400 MHz, DMSO-d₆, δ ppm) 9.48 (s, 2H), 8.10 (d. J = 9.04, 2H),

7.22 (d, J = 7.8, 2H), 7.02-7.0 (m, 2H), 6.84 (d, J = 7.84, 2H), 6.52

(d, J = 2.16, 2H), 3.99 (s, 6H).

¹³C NMR : $(100 \text{ MHz}, \text{ DMSO-d}_6, \delta \text{ ppm})$ 156.2, 155.0, 135.7, 129.4, 128.6,

119.6, 117.8, 108.1, 101.6, 55.9.

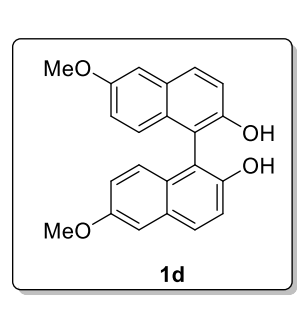
9,9'-Biphenanthrene-10,10'-diol 91

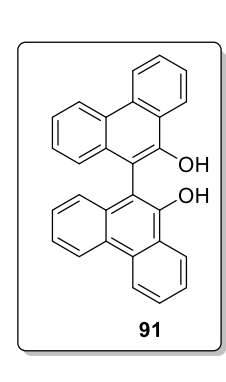
Yield : 0.289 g (75%), Colorless solid.

mp : 242-244 °C; (lit. ⁶⁷ mp. 240-242 °C)

IR (neat) : (cm⁻¹) 3514, 3437, 3074, 2982, 2920, 1688, 1589,

1490, 1448, 1400, 1291, 1193, 1152, 1111,





1074, 1039, 997, 859, 757, 723.

¹**H NMR** : (400 MHz, CDCl₃, δppm) 8.90-8.73 (m, 4H), 8.58-8.45 (m, 2H),

7.90-7.72 (m, 4H), 7.61-7.53 (m, 2H), 7.45-7.30 (m, 4H), 5.66-5.57

(t, J = 17.28, 2H).

¹³C NMR : $(100 \text{ MHz}, \text{CDCl}_3, \delta \text{ ppm}) 149.4, 132.0, 131.7, 128.2, 127.7, 127.1,$

126.9, 125.1, 124.8, 123.5, 122.9, 122.7, 107.1.

1.5.4 Typical procedure for the preparation of naphthidines 97.

In a 50 mL RB flask naphthylamine derivatives **96** (2 mmol) dissolved in DCM (5 mL) under nitrogen atmosphere. To this add Iodine (1 mmol) and the contents were stirred for about 24 h under oxygen atmosphere. The reaction mixture was quenched with sodiumthiosulphate. The organic layer extracts with DCM, washes with brine and then dried over anhyd. Na₂SO₄. Evaporate solvent under vacuum and the crude mixture was chromatographed on silicagel using hexane:ethylacetate as eluent to isolate the pure compound.

N, N, N', N'-Tetramethyl-[1,1'-binaphthalene]-4,4'-diamine 97a

Yield : 0.255 g (75%); Colorless solid.

mp : 126-127 °C (lit. 48 mp. 127-128 °C)

IR (**KBr**) : (cm⁻¹) 3416, 3061, 2979, 2934, 2865, 2830,

2786, 1861, 1732, 1577, 1500, 1452, 1419,

1375, 1320, 1199, 1143, 1040, 1020, 942, 841, 770.

¹**H NMR** : (400 MHz, CDCl₃, δ ppm) 8.46 (d, J = 8.32, 2H), 7.58-7.54 (m,

4H), 7.49 (d, J = 7.56, 2h), 7.37-7.33 (m, 2H), 7.26 (d, J = 7.6,

 H_3C_N C H_3

`CH₃ 97a

2H), 3.08 (s, 12H).

97b

H₃C NH

H₃C^{'NH}

97c

¹³C NMR : (100MHz, CDCl₃ δ ppm) 150.5, 134.4, 133.5, 128.8, 128.0, 127.3,

125.7, 125.0, 124.3, 113.6, 45.4.

4,4'-Di(pyrrolidin-1-yl)-1,1'-binaphthalene 97b

Yield : 0.282 g (72%); Colorless solid

mp : 185-187 °C (lit. 48 mp. 191-192 °C)

IR (KBr) : (cm⁻¹) 3407, 3034, 2931, 2827, 1856, 1721, 1572,

1504, 1450, 1422, 1378, 1318, 1158, 1124, 1065,

1027, 962, 824, 765.

¹**H NMR** : (400 MHz, CDCl₃, δ ppm) 8.35 (d, J = 8.44, 2H), 7.49-4.39 (m,

6H), 7.30-7.26 (t, J = 7.4, 2H), 7.12 (d, J = 7.72, 2H), 3.48 (d, J =

5.32, 8H), 2.12-2.09 (t, J = 12.0, 8H).

¹³C NMR : $(100MHz, CDCl_3 \delta ppm) 147.3, 134.5, 132.0, 128.2, 128.1, 127.2,$

125.4, 124.8, 124.1, 111.2, 52.8, 24.8.

N, N'-Dimethyl-[1,1'-binaphthalene]-4,4'-diamine 97c

Yield : 0.265 g (85%); Colorless solid.

mp : 126-127 °C (lit. 48 mp. 127-128 °C)

IR (**KBr**) : (cm⁻¹) 3437, 3065, 2920, 1727, 1582, 1525, 1489,

1376, 1329, 1267, 1035, 906, 813, 756, 735.

¹**H NMR** : (400 MHz, CDCl₃, δ ppm) 7.91 (d, J = 8.4, 2H), 7.47-7.40 (m, 6H),

7.29 (d, J=6.15Hz, 2H), 6.77 (d, J = 6.5Hz, 2H), 4.9 (brs, 2H), 3.12

(s, 6H).

¹³C NMR : (100MHz, CDCl₃ δ ppm) 143.9, 133.9, 129.0, 128.3, 127.6, 125.5,

124.5, 123.4, 119.9, 103.7, 31.1.

`NH

97d

N, N'-Diethyl-[1,1'-binaphthalene]-4,4'-diamine 97d

Yield: 0.323 g (95%); Pink color solid.

mp : 175-177 °C

IR (**KBr**) : (cm⁻¹) 3400, 3070, 3039, 2967, 2868, 1587, 1525,

1479, 1376, 1334, 1267, 1143, 1035, 808, 761.

¹**H NMR** : (400 MHz, CDCl₃, δ ppm) 7.95 (d, J = 8.4Hz, 2H), 7.53-7.42, (m,

6H), 7.33-7.29 (m, 2H), 6.79 (d, J = 7.76Hz, 2H), 4.4 (brs, 2H),

3.47-3.42 (m, 4H), 1.52-1.49 (t, J = 7.08, 6H).

¹³C NMR : (100MHz, CDCl₃ δ ppm) 143.0, 134.1, 129.0, 128.3, 127.7, 125.5,

124.4, 123.3, 119.9, 104.2, 38.9, 14.9.

HRMS : (ESI-TOF) m/z: [M+H⁺] Calcd for $C_{24}H_{24}N_2$: 341.2017; found:

341.2017.

N, N'-Diphenyl-[1,1'-binaphthalene]-4,4'-diamine 97e

Yield : 0.401 g (92%); Colorless solid.

mp : 180-182 °C (lit. ⁴⁸ mp. 181-182 °C)

IR (**KBr**) : (cm⁻¹) 3399, 3049, 1587, 1494, 1376, 1298, 1262,

1148, 1050, 828, 740.

¹**H NMR** : (400 MHz, CDCl₃, δ ppm) 8.19 (d, J=8.08, 2H), 7.58-7.46 (m, 8H),

7.39-7.35 (m, 6H), 7.16 (d, J = 7.44, 4H), 7.03-7.0 (t, J = 6.72,

2H), 6.10 (brs, 2H).

¹³C NMR : (100MHz, CDCl₃ δ ppm) 144.7, 138.6, 134.2, 133.4, 129.5, 128.3,

127.6, 127.4, 126.2, 125.6, 121.9, 120.7, 117.7, 115.2.

H₃C_{NH}

H₃C

N, N'-Dibenzyl-[1,1'-binaphthalene]-4,4'-diamine (97f)

Yield : 0.417 g (90%); Colorless solid.

mp : 173-174 °C (lit. 48 mp. 171-172 °C)

IR (**KBr**) : (cm⁻¹) 3441, 3059, 1582, 1520, 1478, 1380,

1339, 1267, 1106, 1034, 920, 807, 755, 735.

¹**H NMR** : $(400 \text{ MHz, CDCl}_3, \delta \text{ ppm})$

8.0 (d, J = 8.44 Hz, 2H), 7.69 - 7.64 (m, 6H), 7.57 - 7.47 (m, 10H),

7.42-7.38 (m, 2H), 6.89 (d, J = 7.76Hz, 2H), 4.9 (s, 2H), 4.67 (s,

4H).

¹³C NMR : (100MHz, CDCl₃ δ ppm) 142.9, 139.4, 134.2, 129.2, 128.9, 128.7,

128.0, 127.8, 127.6, 125.8, 124.7, 123.5, 120.2, 104.7, 48.8.

N, N'-Dimethyl-[5,5'-biquinoline]-8,8'-diamine 97g

Yield: 0.276 g (88%), Yellow color solid.

mp : 247-250 °C

IR (**KBr**) : (cm⁻¹) 3416, 3037, 2924, 2842, 1606, 1579, 1519,

1477, 1434, 1362, 1152, 1090, 818, 790, 656, 625.

¹**H NMR** : $(400 \text{ MHz, CDCl}_3, \delta \text{ ppm}) 8.72 \text{ (s, 2H)}. 7.75-7.72 \text{ (m, 2H)}, 7.43-$

7.41 (m, 2H), 7.26-.20 (m, 2H), 6.77-6.75 (m, 2H), 6.27 (s, 2H),

3.13 (s, 6H).

¹³C NMR : (100MHz, CDCl₃ δ ppm) 146.6, 145.3, 138.1, 134.7, 130.0, 128.5,

123.7, 121.2, 103.7, 30.1.

HRMS : (ESI-TOF) m/z: [M+H⁺] Calcd for C₂₀H₁₈N₄: 315.1609; found:

315.1608.

1.5.5 General procedure for the preparation of N-methyl polypyrrole:

In 250 mL RB anhydrous Fecl₃ (120 mmol) was dissolved in distilled water. Then add N-methylpyrrole (50 mmol) slowly through liquid addition funnel by keeping reaction at 5-7 °C. Stir the contents up to 4 h and keep the reaction flask unagitated for 24 h. The polymer was filtered and washes several times with methanol and water to remove impurities. The polymer powder was dried in a vacuum at 50 °C for 12 h.

Yield : 3.2 g

IR (**KBr**) : (cm⁻¹) 3432, 2920, 1633, 1507, 1310, 1055, 773.

N CI n CH₃

1.5.6 General procedure for the preparation of PPh₃:BH₃ complex from NMPPY 108

In a 50 mL RB flask, NMPPY cation radical **108** (1 g) and NaBH₄ (0.037 g, 1 mmol) in THF (20 mL) were added under N₂ atmosphere. To this reaction mixture PPh₃ (0.262 g, 1mmol) was added and the contents were stirred for 24 h. The reaction mixture was filtered and the organic layer was separated. The solvent was evaporated under reduced pressure and the crude product was subjected to chromatography on silica gel (100-200) using hexane/ethyl acetate (98:2) as eluent to isolate pure PPh₃:BH₃ as white solid.

Ph₃P:BH₃ complex

Yield : 0.151 g (55%), Colorless solid.

IR (Neat) : (cm⁻¹) 3046, 2378, 2345, 2246, 1435, 1183, 728.

¹**H NMR** : (400 MHz, CDCl₃, δ ppm) δ 6.85-6.79 (m, 6H), 6.75-6.65 (m, 9H)

¹³C NMR : $(100 \text{ MHz}, \text{CDCl}_3 \delta \text{ ppm}) 132.5, 132.4, 130.5, 128.7, 128.1, 127.9;$

¹¹**B NMR** : $(128.3 \text{ MHz, CDCl}_3 \delta \text{ ppm}) - 38.5.$

P³¹ **NMR** : (162 MHz, CDCl₃ δ ppm) 21.1

 $\cdot N' : BH_3$

1.5.7 General procedure for the preparation of amine: BH_3 complexes from NMPPY 108

In a 50 mL RB flask, NMPPY cation radical **108** (4 g) and NaBH₄ (5 mmol) in THF (20 mL) were added under N₂ atmosphere. To this reaction mixture amine (5mmol) was added and the contents were stirred for 24 h. The reaction mixture was filtered and the organic layer was separated. The solvent was evaporated under reduced pressure and the crude product was subjected to chromatography on silica gel (100-200) using hexane/ethyl acetate as eluent to isolate the corresponding amine:BH₃ complex.

Triethylamine borane complex 114a

Yield : 0.227 g (45%); Colorless solid.

IR (Neat) : (cm⁻¹) 2953, 2389, 2334, 2268, 1391, 1161, 800.

 $(400 \text{ MHz}, \text{CDCl}_3, \delta \text{ ppm}) 2.80-2.74 (q, J = 8 \text{ Hz}, 6\text{H}), 1.20-1.16 (t, S)$

J = 8 Hz, 9 H

¹³C NMR : $(100 \text{ MHz}, \text{CDCl}_3, \delta \text{ ppm}) 52.3, 8.59$

¹¹**B NMR** : (128.3 MHz, CDCl₃ δ ppm) -13.9

Piperidine:BH₃ complex 114b

¹H NMR

Yield : 0.196 g (40%); Colorless solid.

IR (Neat) : (cm⁻¹) 3189, 2936, 2383, 2339, 2317, 2257,

1452, 1172, 876.

¹**H NMR** : (400 MHz, CDCl₃, δ ppm) 3.80 (brs, 1H), 3.23 (d, J = 8 Hz, 2H),

2.53-2.47 (m, 2H), 1.78-1.48 (m, 6H)

¹³C NMR : $(100 \text{ MHz}, \text{CDCl}_3, \delta \text{ ppm}) 53.3, 25.3, 22.5$

¹¹**B NMR** : (128.3 MHz, CDCl₃ δ ppm) -15.0

Pyrrolidine: BH₃ complex 114c

Yield : 0.255 g (60%); Colorless solid.

IR (**KBr**) : (cm⁻¹) 3227, 2931, 2854, 2389, 2356, 2279,

1452, 1358, 1331, 1276, 1161, 1134, 1106.

¹**H NMR** : $(400 \text{ MHz}, \text{CDCl}_3, \delta \text{ ppm}) 3.28-3.25 \text{ (m, 2H)}, 2.74-2.70 \text{ (m, 2H)},$

2.0-1.97 (m, 2H), 1.86-1.81 (m, 2H)

¹³C NMR : $(100 \text{ MHz}, \text{CDCl}_3, \delta \text{ ppm}) 54.2, 24.6$

¹¹**B NMR** : $(128.3 \text{ MHz}, \text{CDCl}_3 \delta \text{ ppm}) - 16.3$

Morpholine: BH3 complex 114d

Yield: 0.217 g (43%); Colorless solid.

IR (**KBr**) : (cm⁻¹) 3194, 2969, 2854, 1419, 1369, 1254,

1139, 1041, 904, 843, 734.

¹**H NMR** : (400 MHz, CDCl₃, δ ppm) 4.36 (s, 1H), 3.97-3.94 (d, J = 12Hz,

2H), 3.62-3.55 (t, J = 4Hz, 2H), 3.11-3.08 (d, J = 12Hz, 2H), 2.85-

2.76 (m, 2H)

¹³C NMR : $(100 \text{ MHz, CDCl}_3, \delta \text{ ppm}) 65.7, 51.9$

¹¹**B NMR** : (128.3 MHz, CDCl₃ δ ppm) -16.1

N-methylmorpholine:BH₃ complex 114e

Yield : 0.230 g (40%); Colorless solid.

IR (**KBr**) : (cm⁻¹) 2969, 2876, 2372, 1452, 1304, 1227,

1178, 1117, 1063, 876, 827.

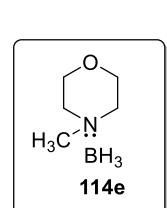
¹**H NMR** : (400 MHz, CDCl₃, δ ppm) 4.15-4.10 (m, 2H), 3.74-3.70 (m, 2H),

3.02-2.98 (m, 2H), 2.75-2.70 (m, 2H), 2.68 (s, 3H)

¹³C NMR : $(100 \text{ MHz, CDCl}_3 \delta \text{ ppm}) 62.0, 59.2$







116

¹¹**B NMR** : (128.3 MHz, CDCl₃ δ ppm) -11.3

Pyridine: BH₃ complex 116

Yield : 0.195 g (74%); Colorless liquid.

IR (Neat) : (cm⁻¹) 2964, 2389, 2334, 2268, 1391, 1161, 800.

¹**H NMR** : (400 MHz, CDCl₃, δ ppm) 8.51 (d, J = 4.28Hz, 2H),

7.60-7.56 (t, J = 7.64Hz 1H), 7.21-7.18 (m, 2H)

¹³C NMR : (100 MHz, CDCl₃ δ ppm) 149.7, 135.8, 123.6

¹¹**B NMR** : (128.3 MHz, CDCl₃ δ ppm) -12.0

1.6 References

- 1. Chen, Y.; Yekta, S.; Yudin, A. K. Chem. Rev. 2003, 103, 3155.
- a) Meca, L.; Reha, D.; Havlas, Z. J. Org. Chem. 2003, 68, 5677. b) Kyba, E. P.;
 Gokel, G. W.; Dejong, F.; Koga, K.; Sousa, L. R.; Siegel, M. G.; Kaplan, L.;
 Sogah, G. D. Y.; Cram, D. J. J. Org. Chem. 1977, 42, 4173.
- 3. Kagan, H. B.; *In Asymmetric Synthesis*; Morrison, J. D., Ed.; Academic press: NewYork, **1985**, *5*, 1.
- 4. Akimoto, H.; Yamada, S. *Tetrahedron* **1971**, *27*, 5999.
- a) Wang, J. T.; Fan, X.; Quian, Y. M. Synthesis, 1989, 292. b) Reetz, M. T.;
 Kyung, S. H.; Bolm, C.; Ziekre, T. Chem. Ind 1986, 824. c) Grubbs, R. H.;
 Devries, R. A. Tetrahedron Lett. 1977, 1879. d) Sakane, S.; Maruoka, K.;
 Yamamoto, H.; Tetrahedron 1986, 42, 2203.
- 6. Noyori, R.; Tomino, I.; Tanomoto, Y. J. Am. Chem. Soc. 1979, 101, 3129.
- 7. Ding, K.; Wang, Y.; Zhang, L.; Wu, Y.; Matsuura, T. *Tetrahedron*. **1996**, *52*, 1005.
- Brussee, J.; Groenendijk, J. L. G.; Koppele, J. M.; Jansen, A. C. A. *Tetrahedron*.
 1985, 41, 3313.
- 9. Doussot, j.; Guy, A.; Ferroud, C. *Tetrahedron:Lett.* **2000**, *41*, 2545.
- 10. Wang, K.; Lu, M.; Yu, A.; Zhu, X.; Wang, Q. J. Org. Chem. 2009, 74, 935.
- 11. Morioku, K.; Morimoto, N.; Takeuchi, Y.; Nishina, Y. Sci. Rep. 2016, 6, 25824.
- 12. Grant-Overton, S.; Buss, J. A.; Smith, E. H.; Gutierrez, E. G.; Moorhead, E. J.; Lin, v. S.; Wenzel, A. G. Synth. Commun. 2015, 45, 331.

58 References

a) Periasamy, M.; Prasad, A. S. B.; Kanth, J. V. B.; Reddy, Ch. K. Tetrahaedron: Asymmetry 1995, 6, 341. b) Venkatraman, L; Periasamy, M. Tetrahaedron: Asymmetry 1996, 7, 2471. c) Periasamy, M.: Venkatraman, L.; Thomas, K. R. J. J. Org. Chem. 1997, 62, 4302. d) Periasamy, M.: Venkatraman, L.; Kumar, S. S.; Kumar, N. S.; Ramanathan, C. R. J. Org. Chem. 1999, 64, 7643. e) Periasamy, M.; Reddy, M. N.; Anwar, S. Tetrahedron: Asymmetry 2004, 15, 1809.

- a) Periasamy, M.; Kumar, N. S.; Kumar, S. S.; Rao, V. D.; Ramanathan C. R.;
 Venkatraman, L. J. Org. Chem. 2001, 66, 3828. b) Periasamy, M.; Kumar, N. S.;
 Kumar, S. S.; Rao, V. D.; Ramanathan, C. R.; Tetrahedron: Asymmetry 1999, 10,
 2307. c) Periasamy, M.; Reddy, M. N.; Anwar, S. Tetrahedron: Asymmetry, 2004,
 15, 1809.
- 15. Rao, V. D.; Periasamy, M. Tetrahedron: Asymmetry 1999, 10, 2307.
- 16. Periasamy, M.; Seenivasaperumal, M.; Rao, V. D. *Tetrahedron:Asymmetry* **2004**, *15*, 3847.
- a) Srivastava, M.; Kumar, M.; Singh, R.; Agrawal, U. C.; Garg, M. O. *J. Sci. and Ind. Res.* 2009, 68, 93. b) Zhai, Y.; Dou, Y.; Zhao, D.; Fulvio, P.F.; Mayes, R.T.;
 Dai, S. *Adv. Mater.* 2011, 23, 4828. c) Chung, D. D. L. *J. Mat. Sci.* 2004, 39, 2645.
- 18. Srivastava, M.; Kumar, M.; Singh, R.; Agrawal, U. C.; Garg, M. O. *J. Sci. and Ind. Res.* **2009**, *68*, 93.
- 19. Chung, D. D. L. *J. Mat. Sci.* **2004**, *39*, 2645.
- 20. Franklin R. E. *Acta Crystallogr* **1950**, *3*, 107.
- 21. Franklin R. E. Acta Crystallogr **1951**, *4*, 252.
- 22. Jagtoyen, M.; Derbyshire, F.; Rimmer, S.; Rathbone, R. Fuel. **1995**, 74, 610.

- 23. a) Kastening, B.; Hahn, M.; Kremeskotter, J. J. Electroanal. Chem. 1994, 374, 159.
 - b) Müllier, M.; Kastening, B. J. Electroanal. Chem. 1994, 374, 149. c) Chung D.
 D. L; Wang, S. Smart Mater. Struct. 1999, 8, 161.
- a) Menendez, J. A.; Phillips, J.; Xia, B.; Radovic, L. R. *Langmuir* 1996, 12, 4404.
 b) Zhou, Y.; Wei, L.; Yang, J.; Sun, Y.; Zhou, L. *J. Chem. Eng. Data* 2005, 50, 1068. c) Hallum, J. V.; Drushel, H. V. *Phys. Chem.* 1958, 62, 110.
- 25. Sumanasekera, G. U.; Chen, G.; Takai, K.; Joly, J.; Kobayashi, N.; Enoki, T.; Eklund, P. C. *J. Phys. Condens. Matter.* **2010**, 22, 334208.
- Shin, D.; Jeong, B.; Mun, B. S.; Jeon, H.; Shin, H.-J.; Baik, J.; Lee, J. J. Phys.
 Chem. C 2013, 117, 11619.
- 27. Yeager E. Electrochem. Acta. 1984, 29, 1527.
- a) Giannozzi, P.; Car, R.; Scoles, G. J. Chem. Phy, 2003, 118. b) Su, C.; Loh, K.
 P. Acc. Chem. Res. 2013, 2275.
- a) Radovic, L. R.; Bockrath, B. J. Am. Chem. Soc. 2005, 127, 5917. b) Radovic, L.
 R. J. Am. Chem. Soc. 2009, 131, 17166. c) Hu, X.; Zhou, Z.; Lin, Q.; Wu,Y.;
 Zhang, Z. Chem. Phys. Lett. 2011, 503, 287.
- 30. Zhang, I.; Liu, X.; Blume, R.; Zhang, A.; Schlögl, R.; Su, D. S. *Science* **2008**, *322*, 53.
- a) Yeager E. J Mol Catal 1986, 38, 5. b) Wilshire, J.; Sawyer, D. T. Acc. Chem. Res. 1979, 12, 105. c) Sawyer, D. T.; Valentine, J. S. Acc. Chem. Res. 1981, 14, 393. d) Kim, S. U.; Liu, Y.; Nash, K. M.; Zweier, J. L.; Rockenbauer, A.; Villamena, F. A. J. Am. Chem. Soc. 2010, 132, 17157.
- 32. Reddy, P. O. Ph.D. Thesis **2014**, School of Chemistry, University of Hyderabad.

60 References

33. Re-use of oxidized activated carbon: After completion of the reaction using carbon material, the resulting carbon materials were filtered and washed several times with organic solvents (THF followed by acetone) to remove trace amount of organic products. Then, the sample was heated at 200 °C under high vacuum for 2 h and brought to rt under N₂. The dry oxygen was adsorbed by passing it through the carbon material for 1 h. This oxygen adsorbed activated carbon sample was reused for synthetic transformations.

- 34. Shanmugaraja, M. Ph.D. Thesis **2018**, School of Chemistry, University of Hyderabad.
- 35. Rao, A. G. Ph.D. Thesis **2018**, School of Chemistry, University of Hyderabad.
- 36. Benesi, H. A.; Hildebrand, J. H. J. Am. Chem. Soc. 1949, 71, 2703.
- a) Mulliken, R. S. J. Am. Chem. Soc. 1950, 72, 600. b) Mulliken, R. S. J. Am.
 Chem. Soc. 1952, 74, 811.
- 38. Eberson, L.; Hartshorn, M. P.; Radner, F.; Persson, O. J. Chem. Soc. Perkin.

 Trans. 2. 1998, 59.
- a) Bianchini, R.; Chiappe, C.; Lenoiv, D.; Lammen, P.; Herges, R.; Grunenberg, J. Angew. Chem. Int. Ed. Engl. 1997, 36, 1284. b) George, L.; Wittmann, L.; Llaume, A.; Reid, S. A. J. Phys. Chem. Lett. 2010, 1, 2618. c) Sun, D.; Rosokha, S. V.; Kochi, J. K. J. Am. Chem. Soc. 2004, 126, 1388. d) Cheng, P. Y.; Zhong, D.; Zewail, A. H. Chem. Phys. Lett. 1995, 242, 369.
- 40. a) Parvatkar, P. T.; Parameswaran, P. S.; Tilve, S. G. Chem. Eur. J. 2012, 18, 5460. b) Tago, H.; Iida, S. Synlett 2006, 2159.
- 41. Bhattacharya, R.; Basu, S. Trans. Faraday Soc. 1958, 54, 1286.
- 42. Aloisi, G.; Cauzzo, G.; Mazzucato, U. Trans. Faraday Soc. 1967, 63, 1858.

- 43. Hasani, M.; Rezaei, A. Spectrochim. Acta A. 2006, 65, 1093.
- 44. Dhineshkumar, J.; Lamani, M.; Alagiri, K.; Prabhu, K. R. Org. Lett. 2013, 15, 1092.
- 45. Stamires, D. N.; Turkevich, J. J. Am. Chem. Soc. 1963, 85, 2557.
- 46. Dollish, F. R.; Hall, W. K. J. Phys. Chem. 1965, 69, 2127.
- 47. Desmarets, C.; Champagne, B.; Walcarius, A.; Bellouard, C.; Omar-Amrani, R.; Ahajji, A.; Fort, Y.; Schneider, R. *J. Org. Chem.* **2006**, *71*, 1351.
- 48. Li, X-L.; Huang, J-H.; Yang, L-M. Org. lett. 2011, 13, 4950.
- 49. a) Kirchgessner, M.; Sreenath, K.; Gopidas, K. R. J. Org. Chem. 2006, 71, 9849. b)
 Sreenath, K.; Suneesh, C. V.; Kumar, V. K. R.; Gopidas, K. R. J. Org. Chem.
 2008, 73, 3245.
- 50. Periasamy, M.; Jayakumar, K. N.; Bharathl, P. J. Org. Chem. 2000, 65, 3548.
- 51. a) Hemandez, S. C.; Chaudhari, D.; Chen, W.; Myung, N.; Mulchandani, A. Interscience. 2007, 19, 2125. b) Mabrrok, M. F.; Person, C.; Petty, M. C. Sensors and Acuator B: chemical. 2006, 115, 547.
- 52. Novak, P. *Electrochimia Acta*. **1992**, 37, 1227.
- 53. Novak, P.; Santhanam, K. V.; Haas, O. Chem. Rev. 1997, 97, 207.
- 54. Belharouak, L. LithiumIonBatteries-Newdevelopments. 2012, 7, 173.
- 55. Roncali, J. Chem. Rev. 1992, 92, 711.
- a) Chitte, H. K.; Bhat, N. V.; Walunj, V. E..; Shind, G. N. Journal of Sensor Technology. 2011, 1, 47. b) Nishio, K.; Fujimoto, M.; Ando, O.; Ono, H.; Murayama, T. Journal of Applied electrochemistry. 1996, 26, 425.
- 57. a) Pron, A.; Rannou, P. *Prog. Polym. Sci.* 2002, 27, 135. b) Bredas, J. L.; Street, G.
 B. *Acc. Chem. Res.* 1985, 18, 309. c) Bertho, D.; Jouanin, C. *Physical Review B*.

References

1987, 35, 626. d) Bredas, J. L.; Wudl, F.; Heeger, A. J. Solid State Comm. 1987, 63, 577. e) Lazzaroni, R.; Logdlund, M.; Stafstrom, S.; Salaneck, W. R.; Bredas, J. L. J. Chem. Phy. 1990, 93, 4433.

- 58. Finchou, D.; Horowitz, G.; Garnier, F. Synthetic Metals. 1990, 39, 125.
- 59. Reuse of re-oxidized polymer: After the reaction, the resulting polymers were filtered and washed several times with organic solvents (THF followed by acetone) to remove trace amounts of organic products. Then, the polymer was dried under high vacuum. The recovered polymer was oxidized with FeCl₃, following the same procedure mentioned in the experimental section. This re-oxidized polymer was reused for the preparation of lewis base borane complexes.
- Abdou, M. S. A.; Ortino, F. P.; Son, Y.; Holdcroft, S. J. Am. Chem. Soc. 1997, 119, 4518.
- a) Kanemoto, K.; Yamauchi, J. J. Phy. Chem. B., 2001, 105, 2117. b) Maksymiuk,
 K. Electroanalysis. 2006, 18, 1537.
- a) Hawthorne, M. F. J. Org. Chem. 1958, 23, 1788. b) Brown, H. C.; Murray, K.
 J.; Murray, L. J.; Snover, J. A.; Zweifel, G. J. Am. Chem. Soc. 1960, 82, 4233.
- 63. Clay, J. M.; Vedejs, E. J. Am. Chem. Soc. 2005, 127, 5766.
- 64. Freeguard, G. F.; Long, L. H. Chem. Ind. 1965, 471.
- a) Narayana, C.; Periasamy, M. J. Organomet. Chem. 1987, 323, 145. b)
 Periasamy, M.; Muthukumaragopal, G. P.; Sanjeevakumar, N. Tetraheron Lett.
 2007, 48, 6966. c) Narayana, C.; Periasamy, M. Chem. Commun. 1987, 1857. d)
 Periasamy, M.; Kishan Reddy, Ch.; Bhaskar Kanth, J. V. J. Indian Inst. Sci. 1994, 74, 149. e) Anwar, S.; Periasamy, M. Tetraherdon: Asymmetry 2006, 17, 3244. f)
 Bhaskar Kanth, J, V.; Periasamy, M. J. Org. Chem. 1991, 56, 5964. g) Kanth, J. V.

- B.; Periasamy, M. *J. Chem. Soc. Chem. Commun.*, **1990**, 1145. h) Reddy, Ch. K.; Kanth, J. V. B.; Periasamy, M. *Synth. Commun.* **1994**, 243, 313. i) Reddy, Ch. K.; Periasamy, M. *Tetrahedron Lett.* **1990**, 31, 1919. j) Reddy, Ch. K.; Periasamy, M. *Tetrahedron Lett.* **1989**, 30, 5663. k) Reddy, Ch. K.; Periasamy, M. *Tetrahedron* **1992**, 48, 8329. l) Periasamy, M. *Current Science*. **1995**, 68, 883.
- 66. Suresh, S. Ph.D. Thesis **2016**, School of Chemistry, University of Hyderabad.
- 67. Yamamoto, K.; Fukushimi, H.; Okamoto, Y.; Hatada, K.; Nakazaki, M. *J. Chem. Soc. Chem. Commun.* **1984**, 1111.

Chapter 2
Electron Transfer Reactions of Amine Donors with
Quinone Acceptors

2.1 Introduction

2.1.1 Electron transfer (ET) reactions in organic donor and acceptor systems

The reactions involving formation of charges can go through polar mechanism or single electron transfer (SET) mechanism (Scheme 1).

Scheme 1

Electron donors (D) and electron acceptors (A) are the reactant pairs that can act as nucleophile and electrophile in bond formation, reductant or oxidant in electron transfer, base or acid in adduct formation.¹ These reactions are generally explained by the Mulliken's charge transfer concept,² Taube's outer sphere/inner sphere mechanism³ and Marcus's two state non adiabatic theory.⁴

Electron transfer reactions take place without covalent interactions. The nature of non-covalent molecular interactions may be like electrostatic, charge transfer, dispersion (Vander Walls) and hydrophobic interactions. In biological systems, aromatic rings play a major role through non-covalent interactions.

The charge transfer complexes are formed between two organic molecules in which electron transfer takes place from donor to the acceptor. These are also called as electron donor-acceptor complexes. The electron donors should have low ionization potential and electron acceptors should have high electron affinities. Charge transfer complexes involve partial electron transfer from donor to acceptor molecule which is neutral in ground state. The charge transfer complexes or electron transfer complexes can be formed when an electron is excited from highest occupied molecular orbital (HOMO)

68 Introduction

of a donor and transferred to the lowest unoccupied molecular orbital (LUMO) of an acceptor.

Mulliken *et al.* reported⁵ that electron rich donor (D) interact with electron poor acceptor (A) to form a charge transfer complex which forms an electron transfer complex upon photoexcitation (Scheme 2).

Scheme 2

$$D + A \stackrel{\text{diffuse}}{=} [D, A] \stackrel{\text{hv}_{CT}}{=} [D, A]$$

In electron transfer reactions involving HOMO and LUMO energy levels play a major role. For example, benzene reacts with NO_2^+ to form nitrobenzene 5 *via* the formation of the radical intermediate 3. In this electrophilic substitution reaction, the LUMO of electrophilic reagent NO_2^+ lower than HOMO of aromatic compound benzene (Scheme 3).⁶

Scheme 3

Taube proposed that electron transfer reactions take place by outer-sphere or inner-sphere mechanisms. Taube *et al.* reported⁷ that the reaction between chromium complex **6** with cobalt complex **7** goes through inner sphere mechanisms *via* a bridged intermediate **8** to give the chromium complex **9** and cobalt complex **10** (Scheme 4).

$$\left[\text{Cr}(H_{2}O)_{6} \right]^{2+} + \left[\text{Co}(NH_{3})_{5}CI \right]^{2+} \longrightarrow \left[\text{Cr}(H_{2}O)_{5}CI \right]^{2+} + \left[\text{Co}(NH_{3})_{5}H_{2}O \right]^{2+}$$

$$6 \qquad 7 \qquad \qquad 9 \qquad \qquad 10$$

$$\left[\text{(NH}_{3})_{5}Co \qquad \text{Co}(H_{2}O)_{5} \right]$$

In outer sphere electron transfer, there is loss of electron or gain of electron. In this electron transfer, the molecule can accept or lose electron without undergoing structural changes like bond cleavage or bond formation with parental organic compound. For example, nitrobenzene radical anion 12 forms when nitrobenzene 11 can accept one electron. In this transformation, there is no structural change which involves outer sphere mechanism (Scheme 5).8

Scheme 5

$$NO_2$$
 $+ \bar{e}$ NO_2

Marcus reported⁹ the outer-sphere electron transfer between an electron donor (D) and electron acceptor (A). In this mechanism, the donor and acceptor diffuse to form an outer- sphere charge transfer complex (D/A) 13 which upon reorganization gives the corresponding electron transfer complex 14 which after diffusion forms radical cation and radical anion pair 15 (Scheme 6).

Scheme 6

$$D + A \xrightarrow{\text{diffuse}} [D/A] \xrightarrow{\text{K}_{\text{ET}}} [D/A] \xrightarrow{\text{diffuse}} D + A$$

2.1.2 ET and polar process in quinone chemistry

In organic redox systems the quinone-hydroquinone redox couples were studied over many years.¹⁰ Quinone moiety also plays a major role in biological reactions.¹¹ In aqueos solutions, quinones undergoes $2H^+/2e^-$ reductions.¹² The quinone and hydroquinone are stabilized by resonance. From hydroquinone one proton loss gives to phenoxide ion and further loss of electron leads to phenoxy radical. The semiquinone

70 Introduction

anion radical is formed through the loss of proton from phenoxy radical and upon loss of one more electron benzoquinone **17a** is formed (Figure 1).

Figure 1. The redox process of hydroquinone-quinone system.

In aprotic conditions, the quinone reduction proceeds through two consecutive single electron reductions. Whereas one electron addition to benzoquinone forms semiquinone anion radical, further addition of one more electron leads to bezoquinone dianion **19** (Figure 2).

Figure 2. Quinone reduction in aprotic solvents.

2.1.3 Addition and substitution reaction of quinones with amines

Suida *et al.* reported¹³ the preparation of addition products of 1,4-benzoquinone **17a** using various substituted anilines **20** (Scheme 7).

Scheme 7

Nagakura and coworkers reported¹⁴ that the reaction of p-chloranil **17b** with various substituted anilines gave the corresponding amino quinones **25** products. They

have proposed the formation of outer (π) -complex 23 followed by inner (σ) -complex 24 in the reaction (Scheme 8).

Scheme 8

Yamaoka and Nagakura reported¹⁵ the reaction of p-chloranil **17b** with n-butyl amine **26**. They showed that the electron transfer from n-butylamine **26** to p-chloranil **17b** takes place prior to the substitution (Scheme 9).

Scheme 9

2.1.4 Charge transfer and electron transfer reactions of quinones

Amines are excellent electron donors and can strongly interact with electron acceptors. For example, DABCO 30 reacts with p-chloranil 17b in benzene solvent to give DABCO-chloranil 1:1 complex. The reaction of p-chloranil or p-bromanil with amines like DABCO give paramagnetic species 31 in benzene or in THF solvent (Scheme 10). 16

Scheme 10

Fukuzumi *et al.* reported¹⁷ the hydride transfer from dihydroflavins **32** to 2,3-dichloro-5,6-dicynao-*p*-benzoquinone (DDQ) **33**. In this case, the back electron transfer is

72 Introduction

relatively slow. The production of the radical ion pair **34** and the proton transfer take place within the radical ion pair complex (Scheme 11).

Scheme 11

Pezza *et al.* reported¹⁸ that the reaction between p-chloranil **17b** and diclofenac **38** leads to the formation of the charge transfer complex **39** which is readily converted to electron transfer complex **40** (radical ion pair) in methanol solvent (Scheme 12).

Scheme 12

Kochi and coworkers reported¹⁹ the reversible interchange charge transfer and electron transfer complexes in donor-acceptor systems. For example, the reaction of 2,2,6,6-tetramethylbenzo[1,2-*d*;4,5-*d*']bis[1,3]dioxole (TMDO) **41** with 2,3-dichloro-5,6-dicynao-*p*-benzoquinone (DDQ) **33** in dichloromethane gives a bright green complex **42** (Scheme 13).

Scheme 13

However, the reaction of 2,2,6,6-tetramethylbenzo[1,2-*d*;4,5-*d*']bis[1,3]dioxole (TMDO) **41** with 2,3-dichloro-5,6-dicynao-*p*-benzoquinone (DDQ) **33** in polar solvents like acetonitrile or propylene carbonate leads radical ion pairs **50** as the electron transfer from TMDO to DDQ is fast in polar solvents (Scheme 14).

74 Introduction

We have undertaken detailed studies on the electron transfer reaction between amines and p-chloranil. We have monitored the reactions by epr spectral analysis. We have also looked for the formation of new organic products. The results are described and discussed in the next section.

Previously, it was observed in this laboratory that secondary amines react with quinones to give epr signal corresponding to the initial formation of radical ion intermediates **54** followed by formation of charge transfer (CT) complex and finally the diaminoquinone product **56** (Scheme 15).²⁰

Scheme 15

It was also found that the tertiary amines react with quinone acceptors in a similar way. Here, electron transfer takes place with subsequent formation of charge transfer (CT1) complex. In the case of tertiary amines, no organic product was isolated. However, the amine and amine radical cation, the quinone radical anion and the corresponding radical anion are expected to undergo exchange processes rapidly to give the new donor-acceptor complexes as transient species (CT2 and CT3) (Scheme 16).²⁰

We have further investigated the electron transfer reactions of amines like piperazines, amides, and 2-naphthol systems with quinone acceptors.

2.2.1 Reaction of secondary amines with quinone acceptors

We have observed that the *N*-phenylpiperazine **62a** reacts with 1,4-benzoquinone **17a** in DCM solvent to give paramagnetic species *via* electron transfer from *N*-phenylpiperazine to 1,4-benzoquinone. The intensity of the epr signal decreased with time. We have carried out the epr studies of piperazines with different quinones and the spectra are given in Figure 3.

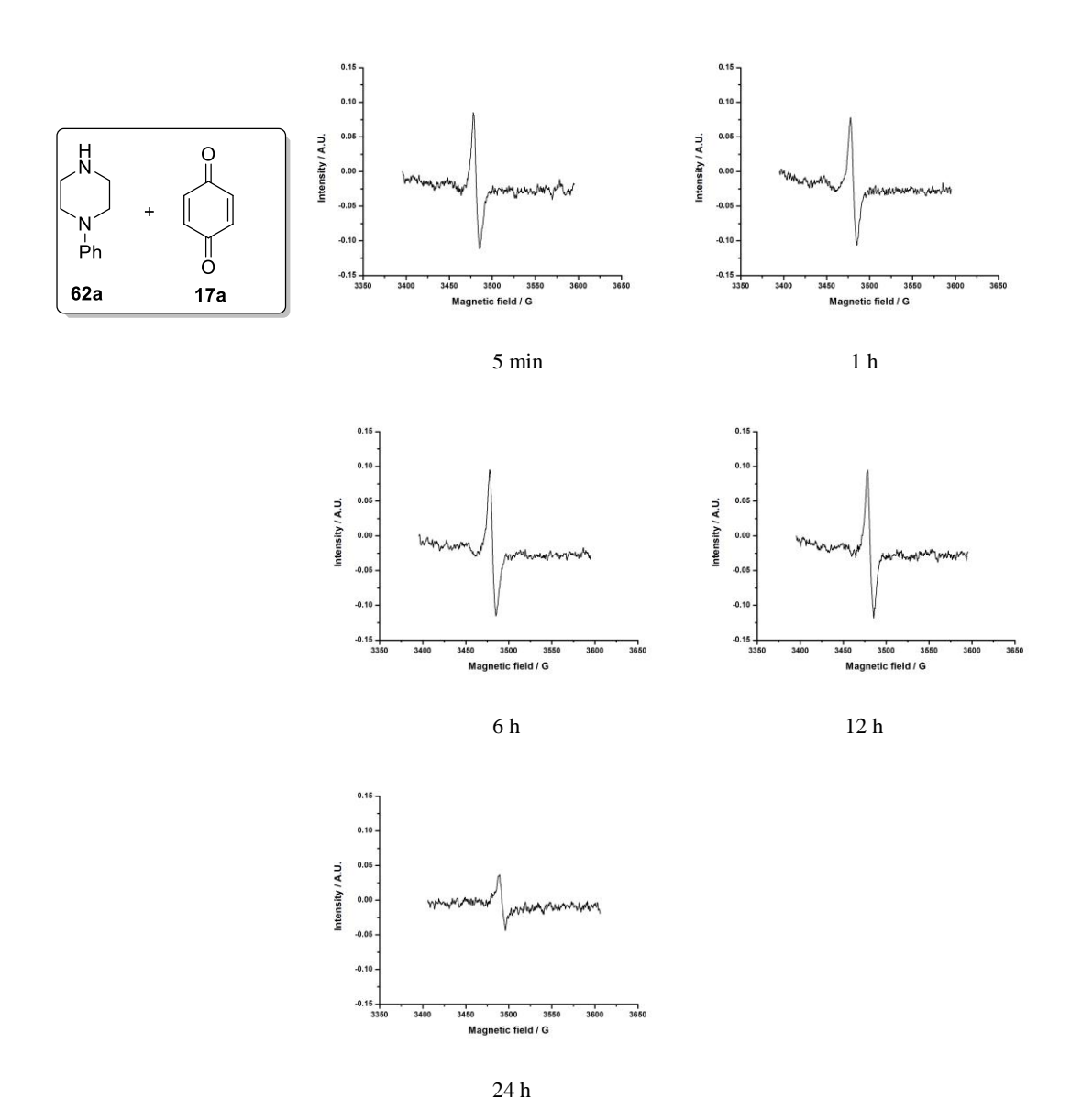
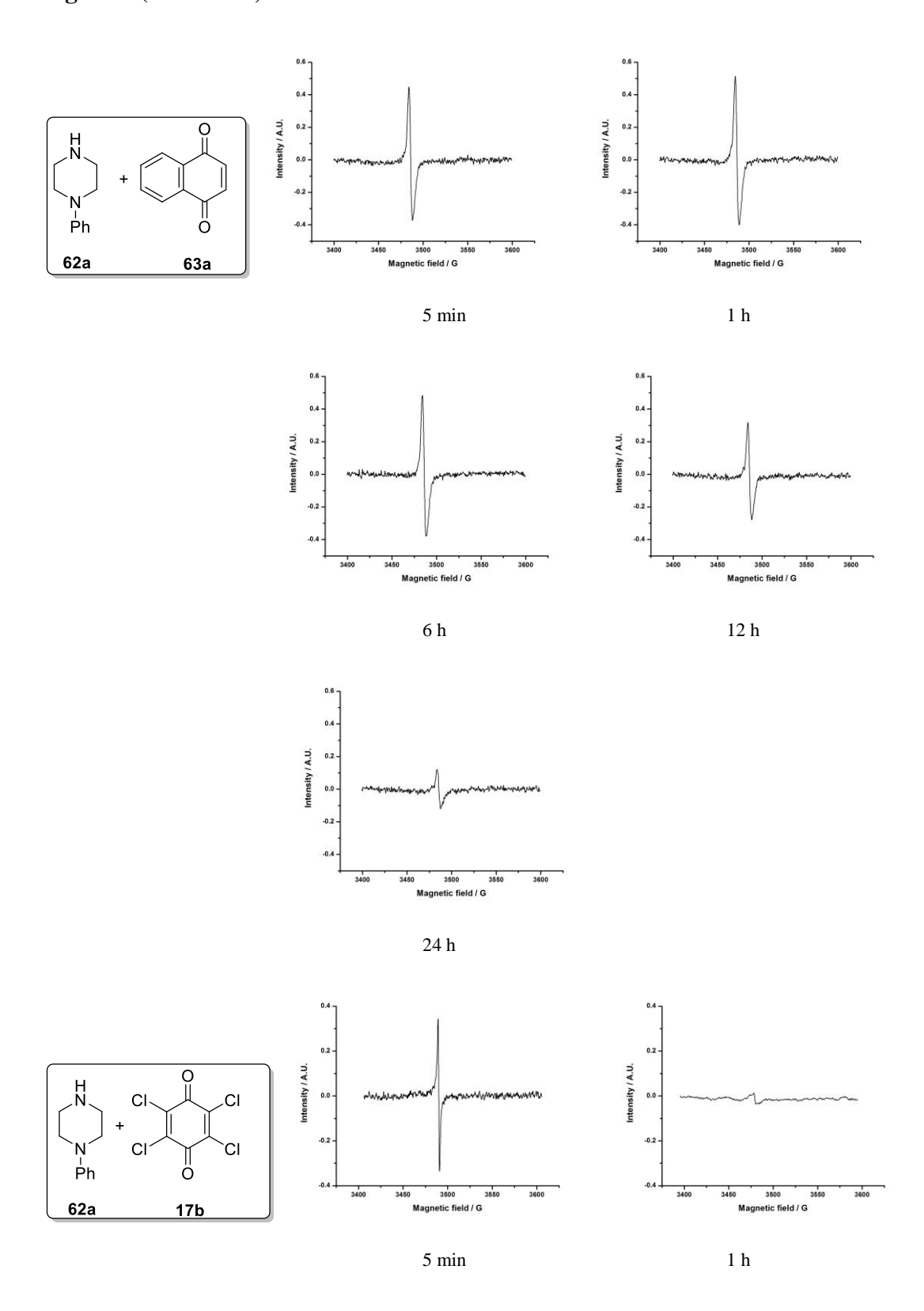


Figure 3 (continued)



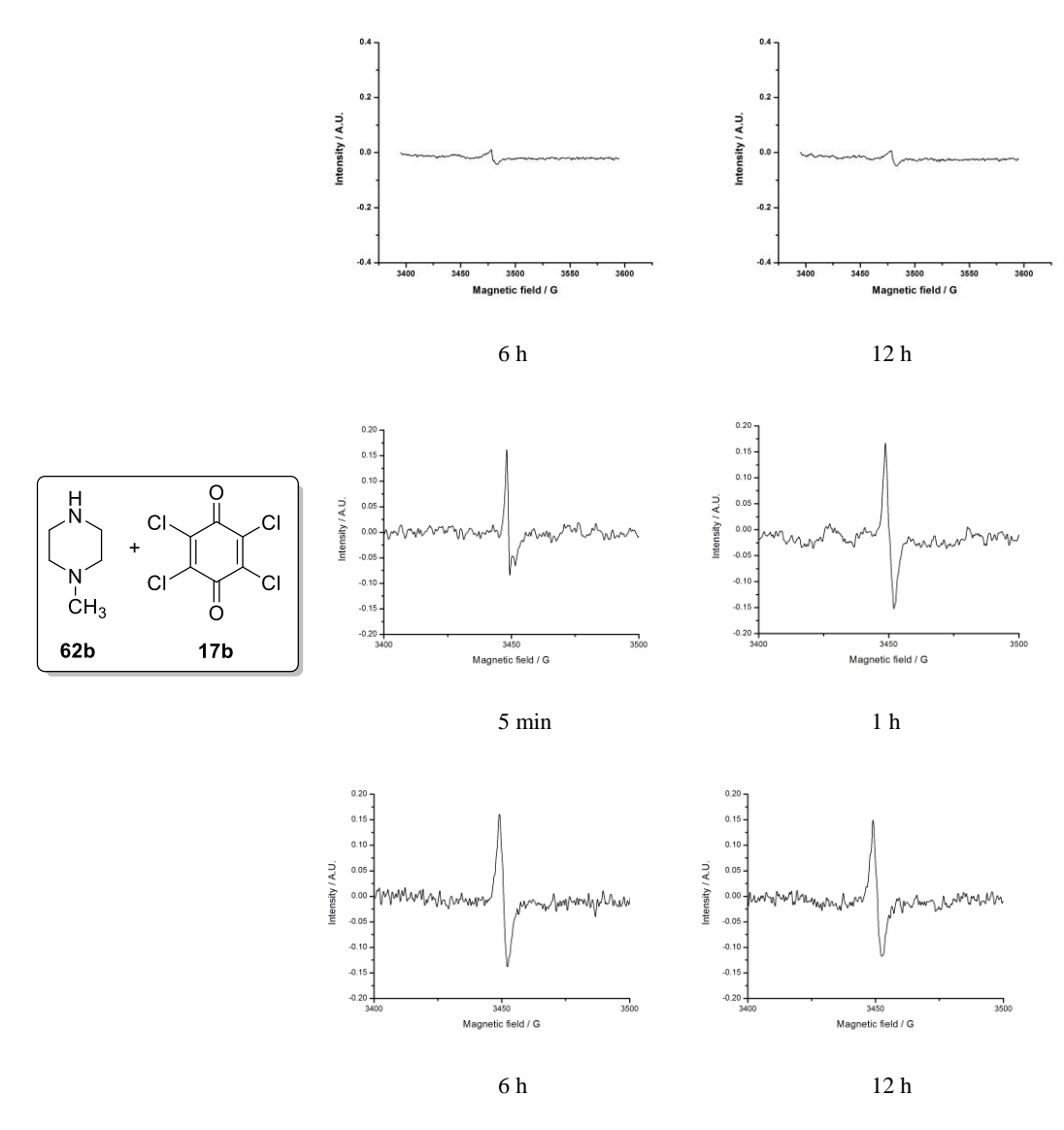


Figure 3. EPR studies of secondary amines **62** (0.05 mmol) with quinones **17** and **63a** (0.05 mmol) in DCM solvent at various time intervals.

Here, we have observed that compound N-phenylpiperazine **62a** reacts with 1,4-benzoquinone **17a** to give a weak epr signal stable up to 24 h. Similarly, in case of N-phenylpiperazine **62a** reaction with 1,4-naphthaquinone **63a** also the epr signal was observed and stable up to 24 h (Figure 3). When the reaction was performed with p-chloranil **17b** strong epr signal was observed and stable up to 12h. The strong epr signal may be due to greater electron affinity of p-chloranil (EA 2.78 eV).²¹

In all cases, we have observed singlet peak in the EPR spectra which corresponds to the quinone radical anion. The strength of the signals decreases with time as the covalent aminoquinone product or the diamagnetic charge transfer complex is formed.

Hence, we have performed reaction of *N*-phenylpiperazine **62a** with 1,4-benzoquinone **17a** in DCM solvent up to 12 h and after work up isolated a brown product identified as aminoquinone 2,5-bis(4-phenylpiperazin-1-yl)cyclohexa-2,5-diene-1,4-dione **64aa** in 60% yield (Table 1). In the case of 1,4-naphthaquinone **63a**, reaction with *N*-phenylpiperazine **62a** gave the product aminoquinone **65aa** in 53% yield (Table 1). The *N*-phenylpiperazine **62a** reaction with *p*-chloranil gave the product **64ab** in 78 % yield (Table 1). The yield was high in case of *p*-chloranill **17b** indicating that as stonger interactions are expected with *N*-phenylpiperazine **62a** compared to that with 1,4-benzoquinone **17a** and 1,4-naphthaquinone **63a**. Similraly we have perfomed reaction of *N*-methylpiperaze **62b** with *p*-chloranil **17b**. In this case the signal was observed up to 12 h and the aminoquinone product was obtained in **64bb** 80 % yield (Table 1).

In the case of reaction of 2,3-dichloronaphthaquinone **63b** with *N*-phenylpiperazine **62a** a weak epr signal was observed which disappeared within an hour with formation of the corresponding aminoquinone product **65ab** (Table 1). We have also carried out the reaction of piperazines **62** with different quinones **17** and **63**. The corresponding aminoquinone products were isolated in 53% to 85% yields (Table 1).

Table 1: Preparation of aminoquinone derivatives^a

^aThe reactions were carried out with quinones **17** (1 mmol), piperazines **62** (2 mmol) and quinones **63** (1 mmol), piperazines **63** (1 mmol) in DCM solvent for 12 h. ^bThe reaction was performed at 60 °C.

In the reaction of piperazine **62** with quinone **17**, two types of amine radical cations **66**a or **66b** are possible. After the formation of electron transfer complex, outersphere complex **67a** or inner-sphere complex **67b** is expected to be formed (Scheme 17).

Scheme 17

The formation of aminoquinone product **64aa** can be rationalized by initial formation of the amine radical cation and quinone radical anion **68** followed by inner sphere complex **69** as outlined in Scheme 18.

It was generally considered that initially an encounter complex would be formed before electron transfer takes place. However, the reaction could also take place through a cross exchange process, especially in polar solvents.²²

The epr results are in accordance with this mechanism (Scheme 19).

Scheme 19

2.2.2 EPR studies of aminoquinone in solid state

We have observed that the aminoquinone **64bb** and **65bb**, formed in the reaction of secondary amines with quinones, are an epr active compounds. Presumbly, this may be due to the intermolecular electron transfer between two molecules. When the aminoquinone was dissolved in DCM solvent, the solution did not give any epr signal indicating that electron transfer takes place between two aminoquinone compounds in close contact in the solid state (Figure 4).

Figure 4. EPR of aminoquinones in solid state

Very recently, Mayr and co-workers^{23,24} reported that the reaction of secondary amine with p-chloranil gives the corresponding products via a polar mechanism (Scheme 20).

Scheme 20

It was also suggested that the reaction of amine with quinone was several orders of magnitude faster than that expected for single electron transfer (SET) process. 23 However, these authors did not report any epr spectrum of the intermediate formed and the charge transfer complex formation was also not considered. We have observed epr signals for the paramagnetic intermediates upon mixing the secondary amine with p-chloranil. Hence, the formation of paramagnetic intermediates in aminoquinone formation through single electron transfer process cannot be ruled out.

2.2.3 Reaction of tertiary amines with quinone acceptors

We have also investigated the electron transfer reactions of the tertiary amines containing piperazine moieties with quinones. Thus, we have performed the reaction of 1-methyl-4-phenylpiperazine **76a** and 1,4-dimethylpiperazines **76b** with 1,4-benzoquinone **17a** and *p*-chloranil **17b** in DCM and PC solvents and monitored the reaction by epr spectral analysis (Figure 5).

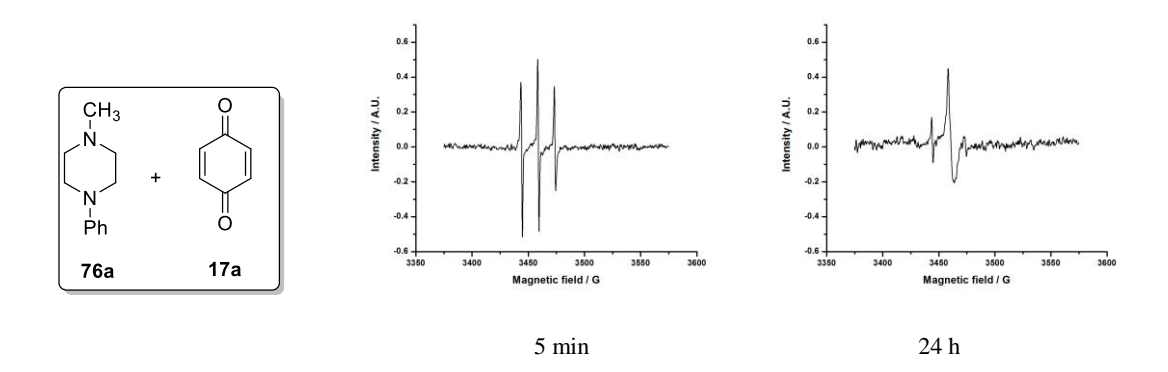
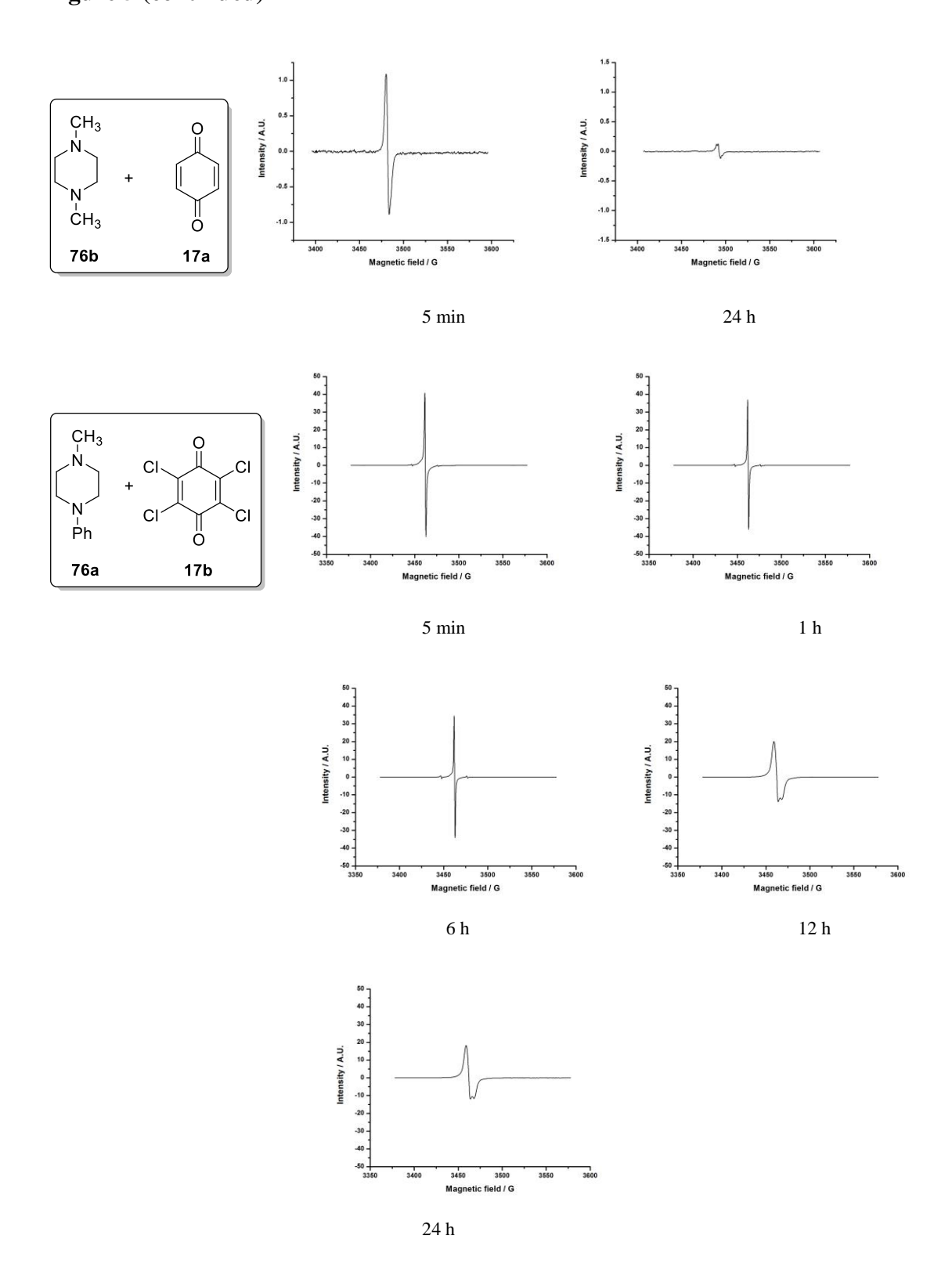


Figure 5 (continued)



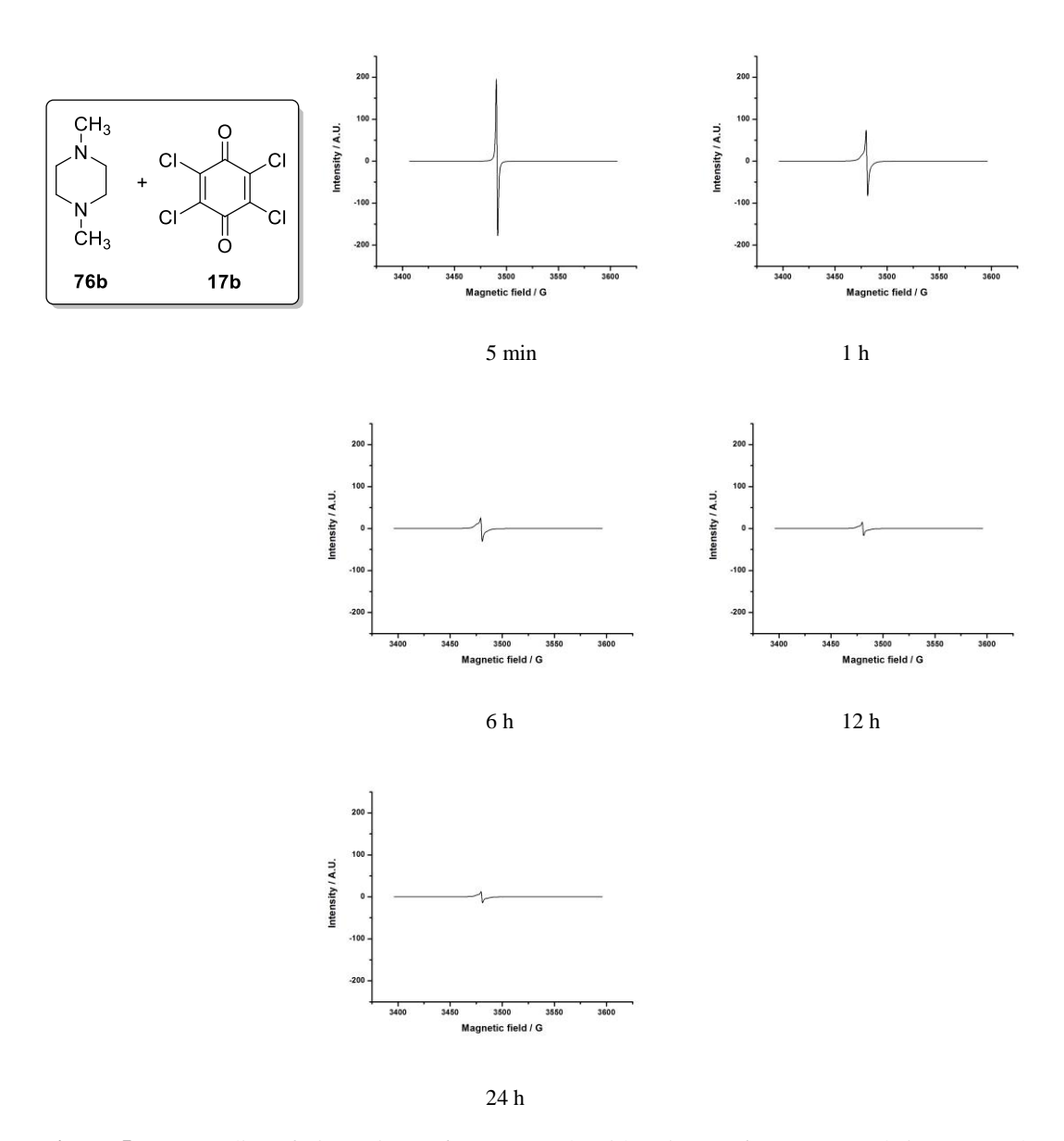


Figure 5. EPR studies of piperazines **76** (0.05 mmol) with quinones **17** (0.05 mmol) in DCM solvent with various time intervals.

We have observed that weak triplet epr signal observed for the reaction of 1-methyl, 4-phenylpiperazine **76a** with 1,4-benzoquinone **17a** in DCM solvent. However, in case of 1,4-dimethylpiperazine **76b** 1,4-benzoquinone **17a** singlet epr signal was observed. The signal was strong in case of reaction with 1,4-dimethylpiperazine **76b** with 1,4-benzoquinone **17a** as compared to reaction of 1-methyl, 4-phenylpiperazine **76a** with 1,4-benzoquinone **17a** (Figure 5). This may be because of the possibly of two types of amine

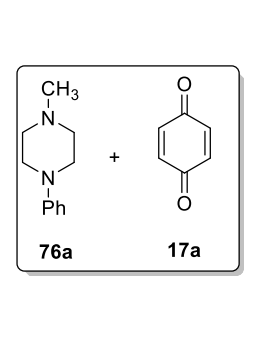
radical cations (**78a** or **78b**) in the reaction of 1-methyl, 4-phenylpiperazine **76a** with 1,4-benzoquinone **17a** whereas only one type of amine radical cation **79** is possible in the reaction 1,4-dimethyl piperazine **76b** with 1,4-benzoquinone **17a** (Scheme 21). The triplet signal corresponds to amine radical cation and the central peak corresponds to both amine radical cation and bezoquinone anion. The triplet epr signal was observed because of the relatively stable amine radical cation **78a** which may exchange with neutral amines in relatively slower rate (Scheme 21).

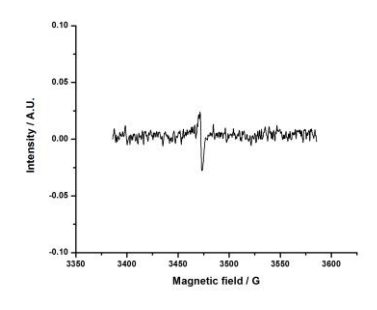
Scheme 21

As compared to 1,4-benzoquinone **17a**, *p*-chloranil **17b** is strong acceptor. Obviously, in the reactions of 1-methyl, 4-phenylpiperazine **76a** and 1,4-dimethylpiperazine **76b** with *p*-chloranil **17b** in DCM solvent, relatively strong epr signals

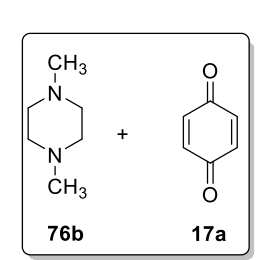
were observed (Figure 5). Here, the signal obtained with reaction of 1-methyl, 4-phenylpiperazine **76a** with *p*-chloranil **17b** the epr signal does not decrease that much with time but after 12 h line broadening of spectra take place, indicating that the more stable amine radical cation **78a** may be formed to more extent with time (Scheme 21). In the reaction of 1,4-dimethylpiperazine **76b** with *p*-chloranil **17b** the signal was strong compared to that obtained in the reaction of 1-methyl, 4-phenylpiperazine **76a** with *p*-chloranil **17b** but the strength decreases to more extent with time intervals, as the less sterically hindered amine may more easily for the corresponding charge transfer (CT) complex (Scheme 22).

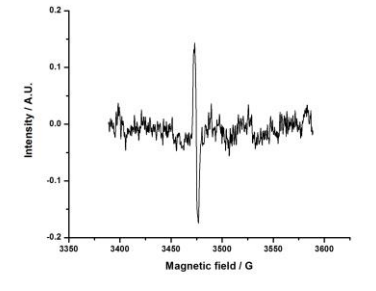
The epr spectra for the intermediates formed in the reaction of 1-methyl-4-phenylpiperazine **76a** and 1,4-dimethylpiperazines **76b** with benzoquinone **17a** and *p*-chloranil **17b** in PC solvent are shown in Figure 6.





12 h





5 min

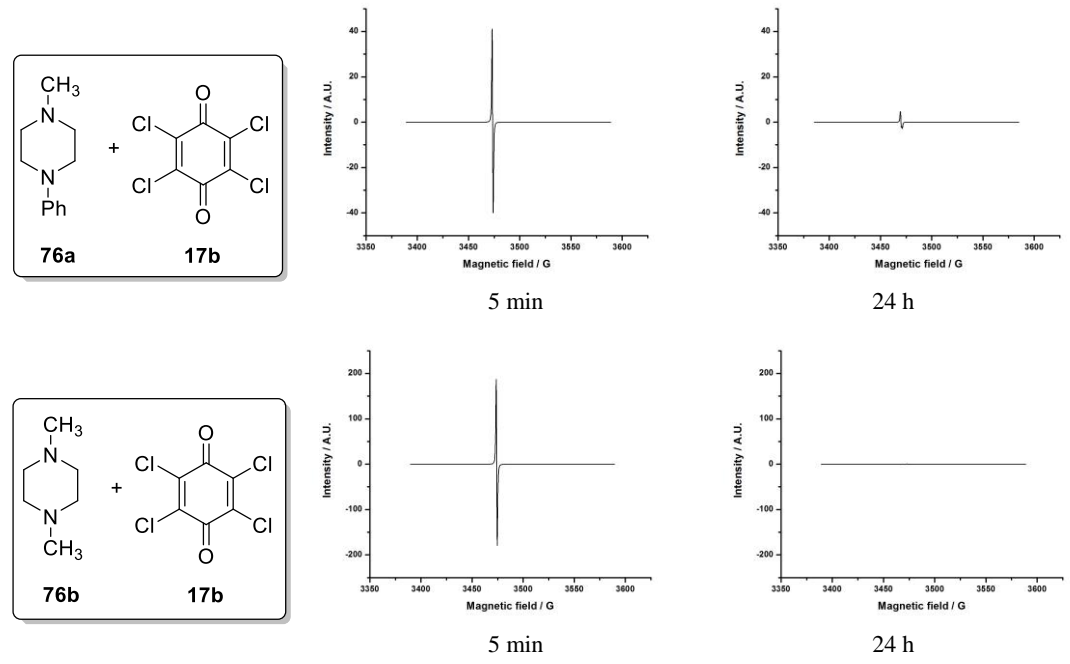


Figure 6. EPR studies of piperazines **76** (0.05 mmol) with quinones **17** (0.05 mmol) in PC solvent with various time intervals.

We have observed that the reaction of 1-methyl-4-phenylpiperazine **76a** with *p*-chloranil **17b** in DCM gave epr signal and the strength of the signal was observed even at 24 h (Figure 5). Interestingly, the epr signal intensity decrease with time indicating formation of the CT1, CT2 and CT3 complexes to more extent which may not exhibit epr signals for long time (Scheme 22).

$$\begin{array}{c} CH_3 \\ N \\ N \\ Ph \end{array}$$

In PC solvent, we have observed weak epr signals compared to DCM solvent (Figure 5). Also, in DCM solvent, the signals were stable up to 24 h but in PC solvent (Figure 6) the signals were observed only for a short time. Presumably, the radical ions may be present in more amounts and react faster to form charge transfer complexes (Scheme 23).

In the case of 1,4-dimethylphenylpiperazine **76b** reaction with 1,4-benzoquinone **17a** in DCM and PC solvents, we have observed weak singlet epr signals (Figure 5 and 6) as it is less electrophilic compared to p-chloranil. The formation of charge transfer complexes CT1, CT2 and CT3 may further weaken the signal strength (Figure 5 and Scheme 23).

Scheme 23

In summary, in the reactions of tertiary amines (piperazines) with quinones we have observed the epr signals strength decrease with time indicating formation of covalent products or charge transfer complexes. Since, we did not obtain any organic product formation in these cases the decrease in signal intensity may due to formation of charge transfer complex CT1 (Scheme 24).

Scheme 24

Ward *et al.* reported²⁵ that the line broadening was observed in the epr spectra of naphthalene negative ion by adding excess of naphthalene. They have reported rate constants for electron transfer between naphthalene negative ion and naphthalene are in the range 10⁷-10⁹ liter mole⁻¹sec.⁻¹ Such single line broadening was also reported²⁵ in the case of 2,3-dichloro-5,6-dicyano-1,4-benzoquinone (DDQ) radical anion **52** with DDQ **33** with fast exchange rate constant 2.5 x 10⁹ M⁻¹ S⁻¹ and activation energy of 1.6 kcal mol⁻¹ at 23 °C. The electron is transferred from HOMO of donor amine to the LUMO of *p*-chloranil acceptor. Electron transfer leads to the formation amine radical cation and quinone radical anion but in the epr spectrum, we have observed only one peak for the paramagnetic complex. This indicates that there is a fast self- exchange of electron between amine with amine radical cation.

Kochi *et al.* reported^{26,27} that the self-exchange and cross exchange between 2,2,6,6-tetramethylbenzo[1,2-d:4,5-d']bis[1,3]dioxole **41** (TMDO) donor with 2,3-dichloro-5,6-dicyano-*p*-benzoquinone **33** (DDQ) acceptor in dichloromethane (Scheme 25).

Scheme 25

(1) Cross exchange electron transfer process

TMDO + DDQ
$$\stackrel{ET}{\longleftarrow}$$
 TMDO + DDQ

41 33 51 52

(2) Self-exchange electron transfer process

TMDO + TMDO
$$\stackrel{\cdot +}{\longleftarrow}$$
 TMDO + TMDO + TMDO 41 51 51 41 ... $\stackrel{\cdot +}{\longleftarrow}$ DDQ + DDQ DDQ + DDQ 33 52 52 33

Similar cross exchange and self exchange reactions may also take place leading to CT1, CT2 and CT3 charge transfer complexes shown in Schemes 22, 23 and 24.

2.2.4 EPR studies of isopropyl amine and diisopropylamine with p-chloranil

We have performed reaction of the primary amine isopropylamine **84** with *p*-chloranil **17b** in DCM solvent and recorded epr spectra at various time intervals (Figure 7).

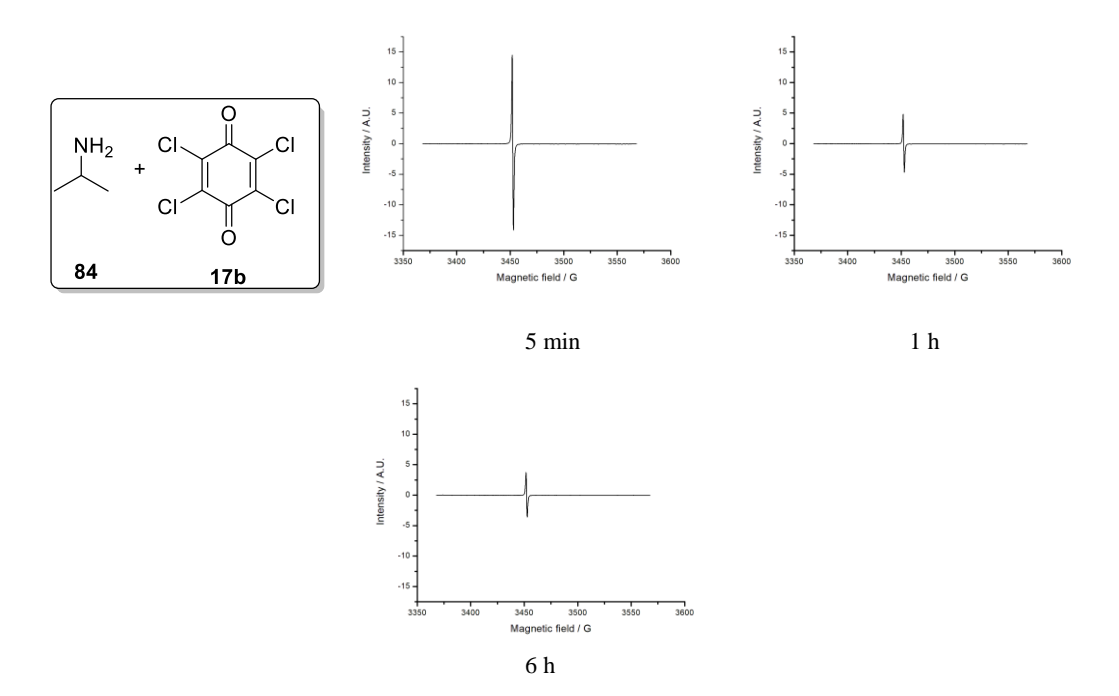
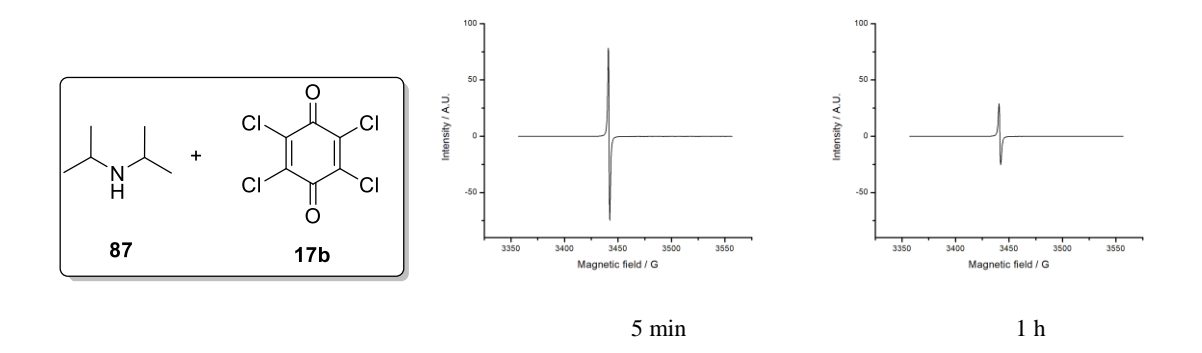


Figure 7. EPR studies of p-chloranil 17b (0.05 mmol) with isopropylamine 84 (0.05 mmol) in DCM solvent with time intervals.

We have observed that strong epr singlet signal was observed which disappears after 12 h (Figure 7). The decrease in epr signal with time indicates the formation of diamagnetic product but we did not obtain any aminoquinone product. Presumably, formation of inner-sphere complex (CT1) with time leads to weak epr signal (Scheme 26).

Scheme 26

Similarly, we have performed the reaction of the diisopropylamine **87** with *p*-chloranil **17b** in DCM solvent. In this case also, we have observed epr signal even at 24 h but the signal strength decreased with time (Figure 8).



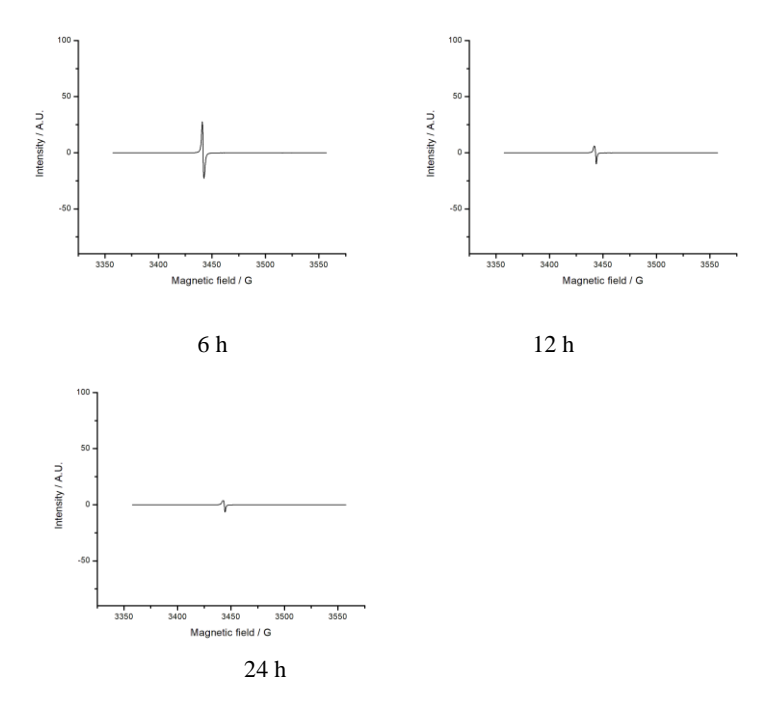


Figure 8. EPR studies of p-chloranil 17b (0.05 mmol) with diisopropylamine 87 (0.05 mmol) in DCM solvent with time intervals.

In this case also, we could not isolate any product as steric hindrance of the molecule **87** may not allow formation of the expected aminoquinone. The reaction may go through outer-sphere complex as shown in Scheme 27.

Scheme 27

Earlier, Sersen and co-workers reported 16 that the reaction of p-chloranil with 1, 4-diazabicyclo [2.2.2] octane DABCO gave 1:1 charge transfer complex. The absorption

band at 450 nm in UV spectra corresponds to p-chloranil anion radical. Andrews et~al. reported²⁸ that the certain donors like carbonyl compounds, amides, lactams and lactones forms weak 1:1 charge transfer complexes with the acceptors p-chloranil and p-fluoranil. Hence, we have decided to prepare different amides to investigate this reaction with the acceptor p-chloranil.

2.2.5 Preparation amide derivatives

We have prepared the *N*,*N*-diisopropyl amide derivatives **90** by the reaction of diisopropyl amine **87** with acid chloride in the presence of Et₃N as a base in DCM solvent following a reported procedure²⁹ (Scheme 28).

Scheme 28

We have also prepared *N*-acylpyrrolidine derivatives **91** by the reaction between pyrrolidine **73** and acid chloride in the presence of Et₃N as a base in DCM solvent following a reported procedure (Scheme 29).²⁹

Scheme 29

Also, the *N*-acylpiperazine derivatives **92** were prepared by the reaction between N-phenylpiperazine **62a** and acid chloride in the presence of Et₃N as a base in DCM solvent (Scheme 30).

Scheme 30

Similarly, the *N*-ethylanilide derivatives **94** were prepared by the reaction between *N*-ethylaniline **93** and acid chloride in presence of Et₃N as a base in DCM solvent (Scheme 31)

Scheme 31

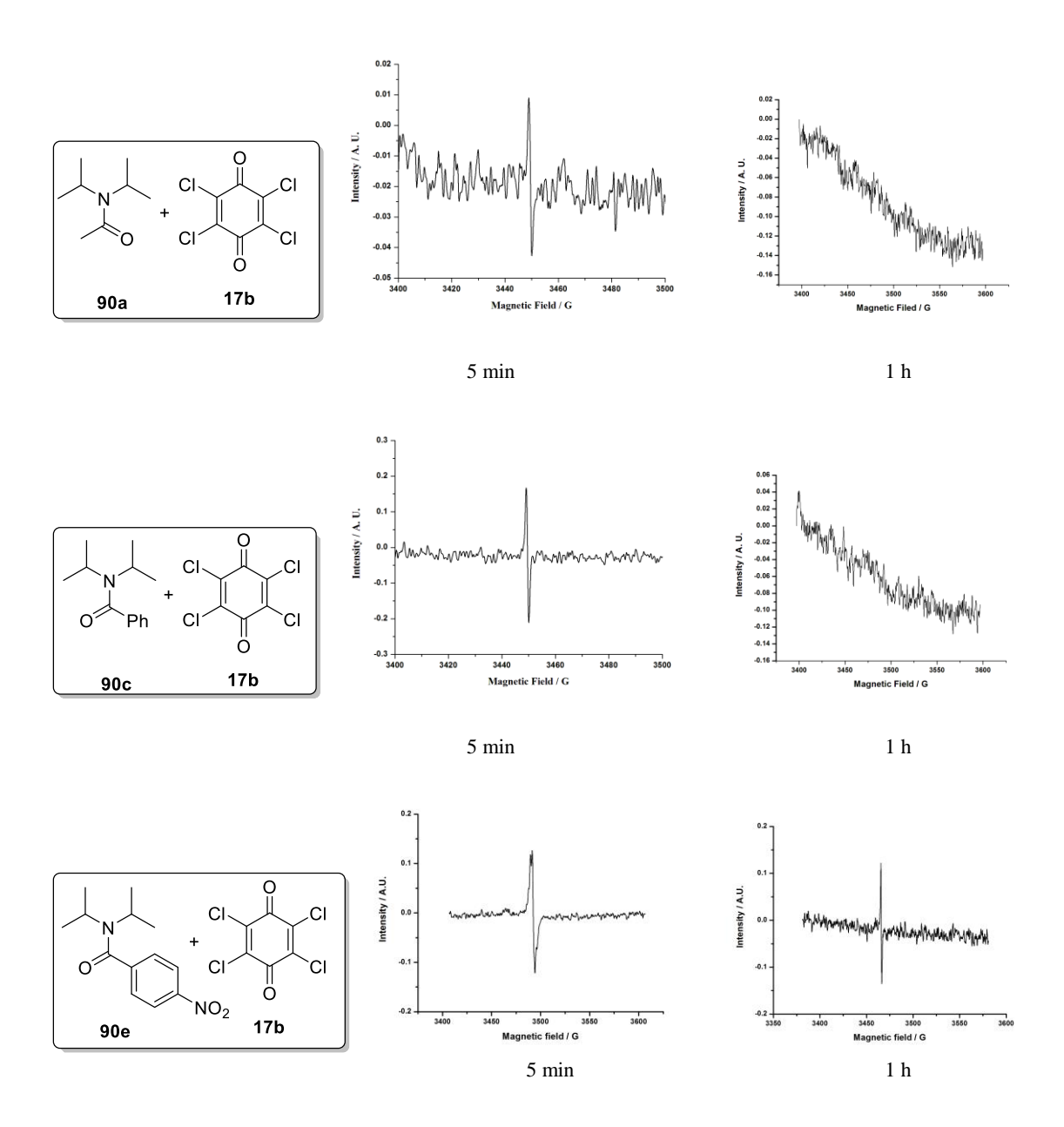
We have also developed a simple method to prepare polymers **97** containing amine as a pendant group by using PMMA (poly methyl methacrylate) **96** in THF solvent (Scheme 32).

2.2.6 EPR studies of amides with p-chloranil

We have carried out the EPR studies to investigate the electron transfer from amides to *p*-chloranil in PC (propylene carbonate) solvent. Amides are weak donors and it was of interest to us to investigate whether *p*-chloranil could accept electron from amides.

2.2.6.1 EPR studies of N,N-diisopropylamides with p-chloranil

We have carried out the reaction of N,N-diisopropylamide derivatives **90a** with p-chloranil **17b** in PC solvent (Figure 9).



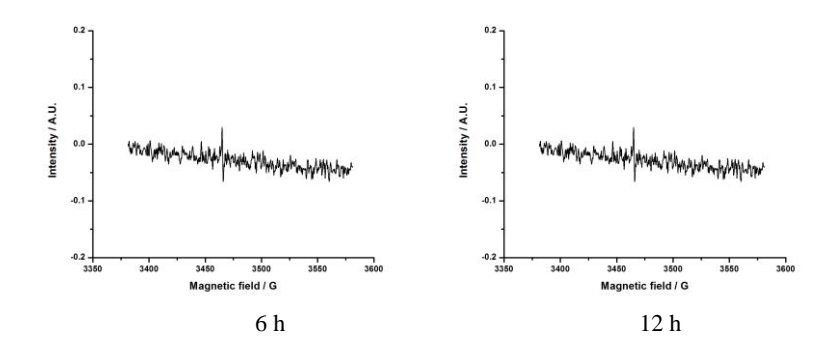


Figure 9. EPR studies of N,N-diisopropylamide derivatives **90** (0.05 mmol) with p-chloranil **17b** (0.05 mmol) 1ml PC solvent with time intervals.

We have observed that the *N*,*N*-diisopropylacetamide **90a** and *N*,*N*-diisopropylbenzamide **90c** react with *p*-chloranil **17b** to give epr signals which disappeared after 1 hour (Figure 9). Surprisingly, the reaction of *N*, *N*-diisopropyl-4-nitrobenzamide **90e** with *p*-chloranil **17b** gave weak epr signal but the signal disappeared only after 24 h. In the reactions using *N*,*N*-diisopropylpivalamide **90b**, *N*,*N*-diisopropyl-4-methoxybenzamide **90d** and *N*,*N*-diisopropyl-4-trifluoromethylbenzamide **90f** no epr signal was observed (Figure 9). The results are summarised in Scheme 33.

Presumably, the radical cations and radical anions formed may give the CT complexes CT1, CT2 and CT3, especially the CT1 complex faster (Scheme 34).

Scheme 34

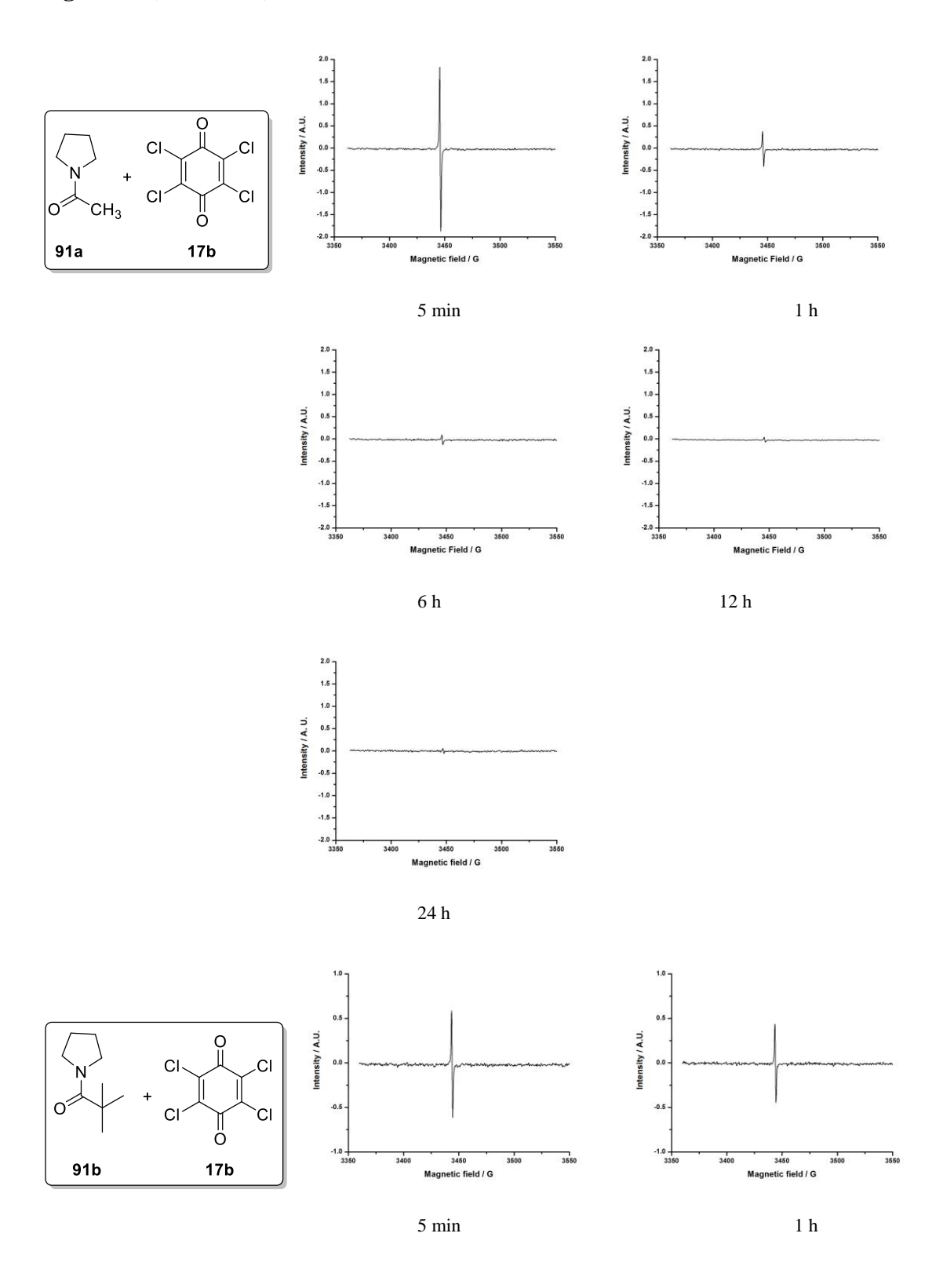
In the case of the *p*-nitro substituted amide **90e** the radical cation formed expected to be less stable but the delocated hindered radical ions would make the formation of CT1 complex slower and hence the epr signal may be stable for more time (Scheme 35).

Scheme 35

2.2.6.2 EPR studies of acylpyrrolidine derivatives with *p*-chloranil

In a similar way, we have performed EPR studies of the reaction of acylpyrrolidine derivatives **91** with *p*-chloranil **17b** in PC solvent and monitored the epr signals at different time intervals (Figure 10).

Figure 10 (continued)



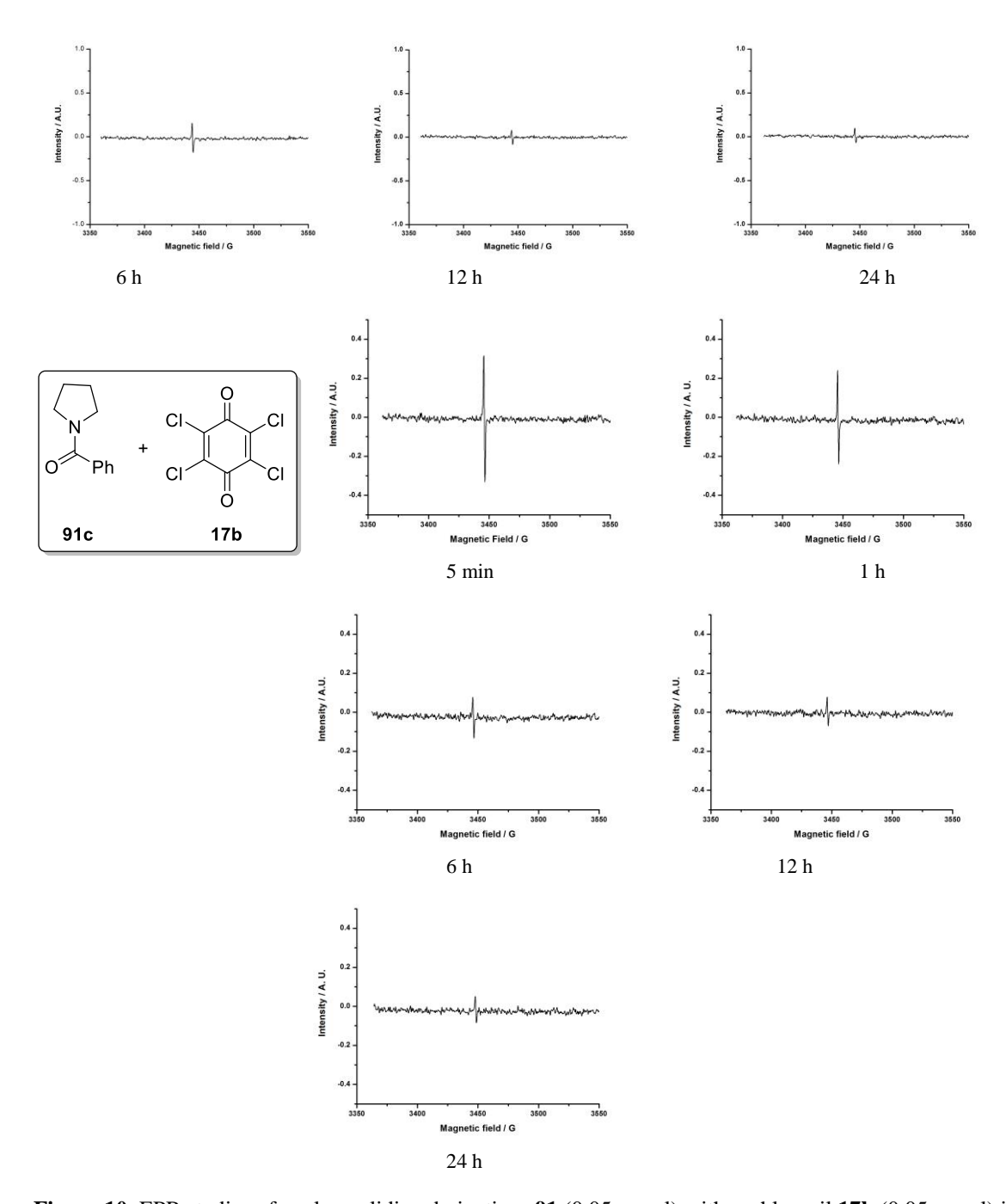


Figure 10. EPR studies of acylpyrrolidine derivatives **91** (0.05 mmol) with p-chloranil **17b** (0.05 mmol) in 1 mL PC solvent with time intervals.

As expected, the reaction using 1-(pyrrolidin-1-yl)ethanone **91a** and *p*-chloranil **17b** gave strong epr signals, compared to signals obtained using 2,2-dimethyl-1-(pyrrolidin-1-yl)propan-1-one **91b** and phenyl(pyrrolidin-1-yl)methanone **91c** (Figure 10).

Presumably, in the case of sterically hindered amides **91b** and **91c** the electron transfer would take place to lesser extent and hence weak epr signals were obtained (Scheme 36).

Scheme 36

Again, the formation of CT1 and CT2 complexes may also play a role in the decrease in the strength of epr signals with time (Scheme 37).

Scheme37

2.2.6.3 EPR studies of N-acylpiperazine derivatives with p-chloranil

Similarly, we have carried out EPR studies of the reaction of *N*-acylpiperazine derivatives **92** with *p*-chloranil **17b** in PC solvent (Figure 11).

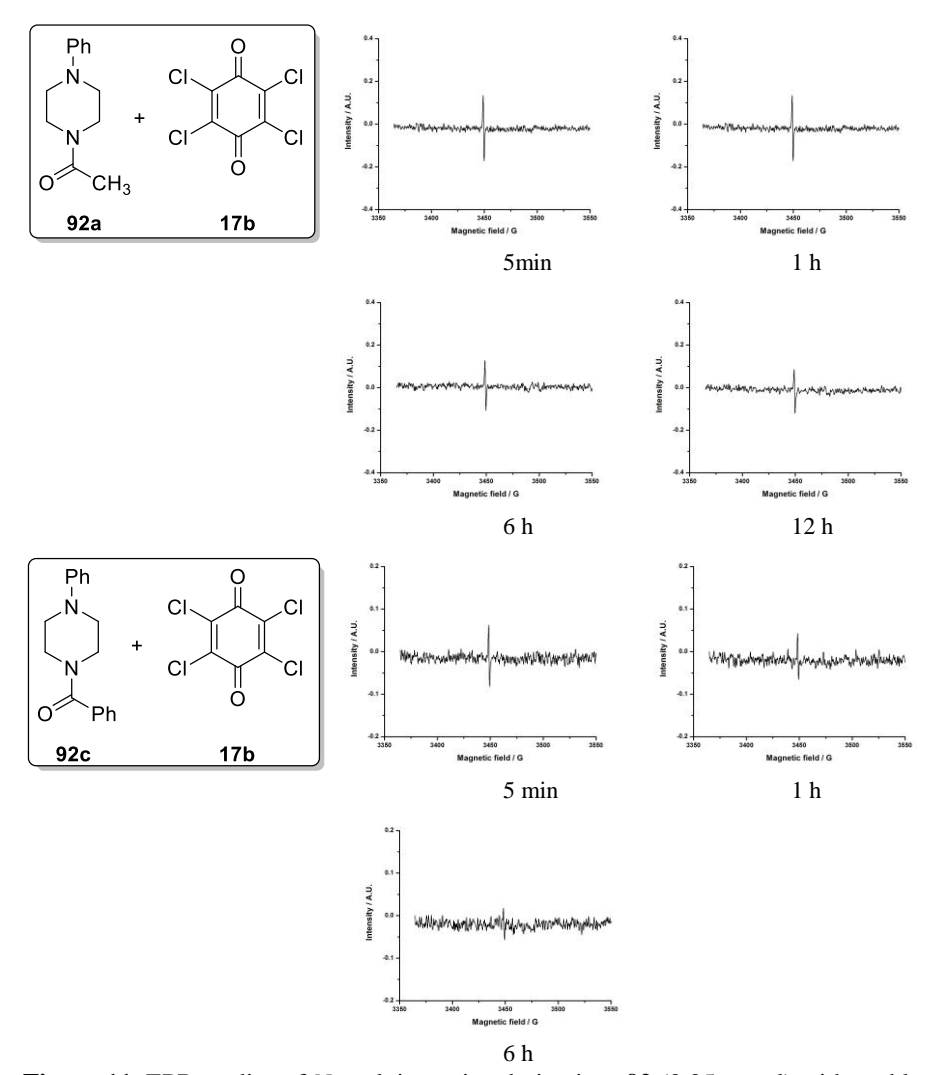


Figure 11. EPR studies of *N*-acylpiperazine derivatives **92** (0.05 mmol) with *p*-chloranil **17b** (0.05 mmol) in 1 mL PC solvent with time intervals.

Again, the steric hindrance in the compounds **92b** is expected to make the interaction with *p*-chloranil **17b** very weak and hence no epr signal observed in this case (Figure 11 and Scheme 38). Also, the epr signal observed in the reaction using **92c**, was

relatively weak compared to that observed in the case of **92a** due to steric hindrance expected for the amide **92c**.

Scheme 38

EPR signal observed

The epr signal strength decreased with time due to formation of charge transfer complexes CT1 and CT2 (Scheme 39).

Scheme 39

2.2.6.4 EPR studies of *N*-ethylanilides with *p*-chloranil

Similarly, we have carried out EPR studies of *N*-ethylanilide derivatives **94** with *p*-chloranil **17b** in PC solvent (Figure 12).

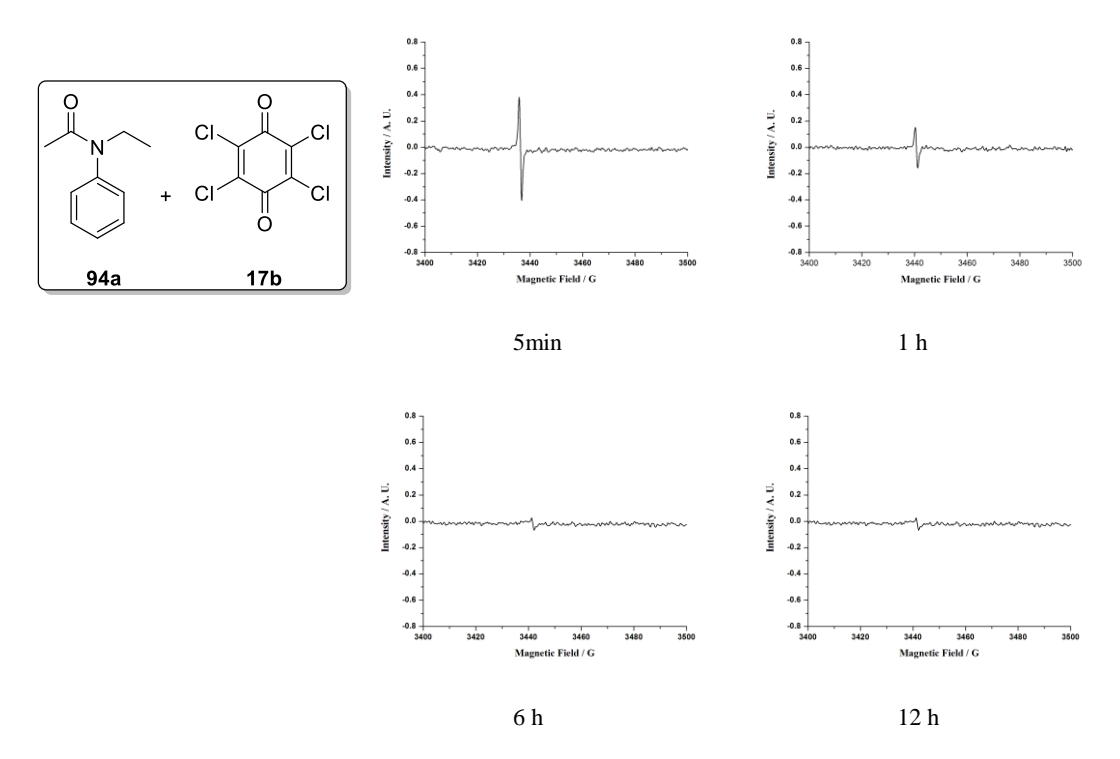


Figure 12. EPR studies of N-ethyl-N-phenyl acetamide 94a (0.05 mmol) with p-chloranil 17b (0.05 mmol) in 1 mL PC solvent with time intervals.

We have observed epr signal in the reaction of *N*-ethyl-*N*-phenyl acetamide **94a** with *p*-chloranil **17b** which decreased with time (Figure 12). In the reaction of *N*-ethyl-*N*-phenyl pivalamide **94b** and *N*-ethyl-*N*-phenyl benzamide **94c** with *p*-chloranil **17b**, we did not observe epr signals, presumably due to steric hindrance, thereby not allowing electron transfer from the amides to *p*-chloranil **17b** (Scheme 40).

Scheme 40

106

Presumably, the reaction of *N*-ethyl-*N*-phenyl acetamide **94a** with *p*-chloranil **17b**, the signal strength decrease with time due to the formation of charge transfer complexes CT1, CT2 and CT3 (Scheme 41).

Scheme 41

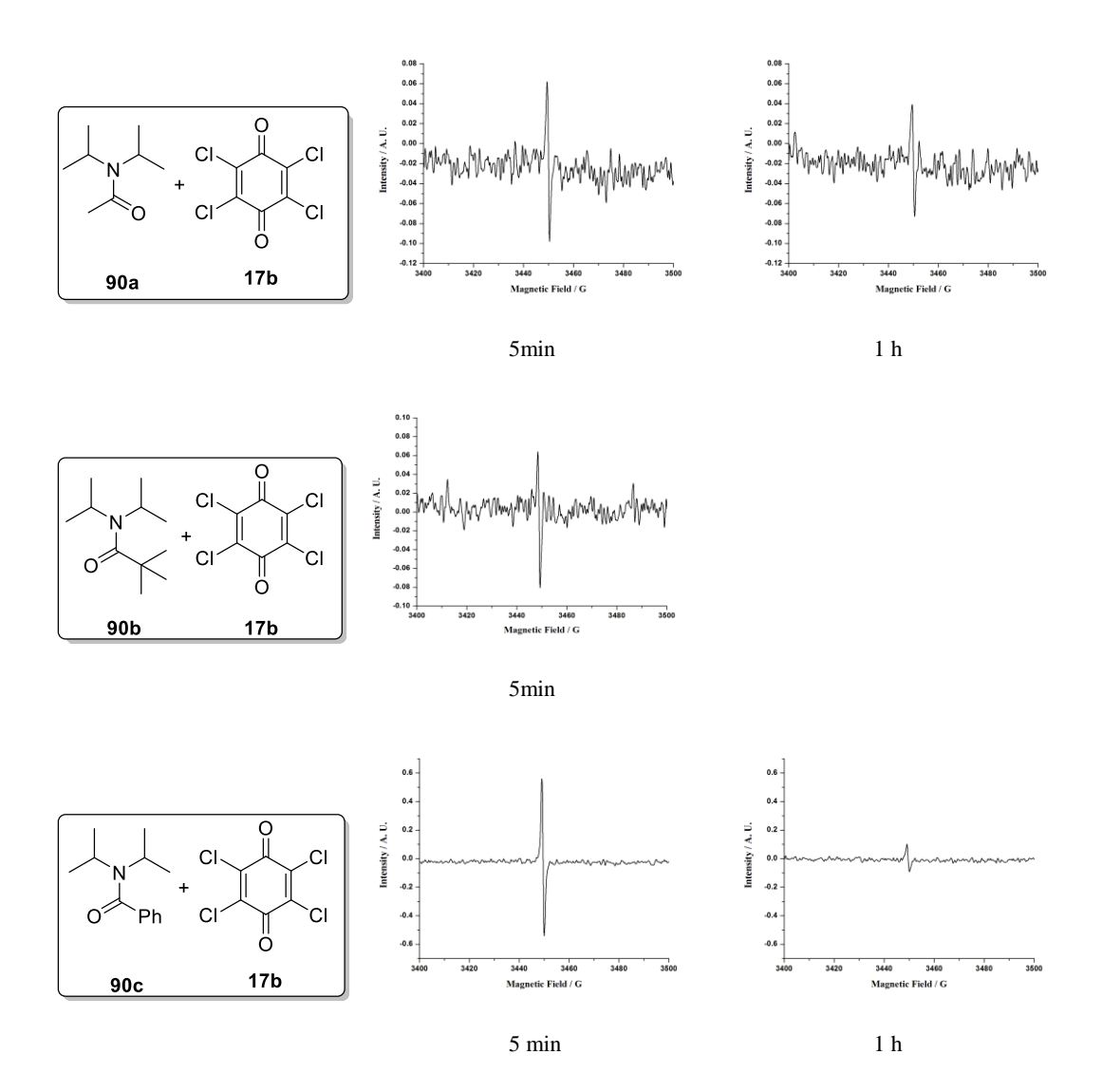
2.2.7 Effect of TiO₂ on EPR studies of amides with *p*-chloranil

We have observed that the reaction of amide derivatives with p-chloranil **17b** in presence of TiO₂ gives epr signal appears for a longer time. Previously, there were reports

on the formation paramagnetic intermediates when p-chloranil was adsorbed on the surface of TiO_2 .³⁰ Although, we have observed that the TiO_2 sample used in this laboratory did not give epr signal with p-chloranil,²⁰ we have decided to perform the electron transfer reactions of amides with p-chloranil in the presence of TiO_2 .

2.2.7.1 Effect of TiO₂ on EPR studies of N,N-diisopropyl amides with p-chloranil

We have carried out the reaction of N,N-diisopropylamide derivatives **90** with p-chloranil **17b** in the presence of TiO₂ in PC solvent (Figure 13).



108 Results and Discussion

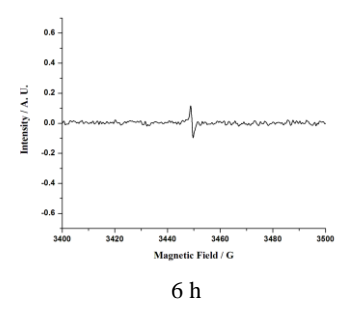


Figure 13. EPR studies of N,N-diisopropyl amide derivatives **90** (0.05 mmol) with p-chloranil **17b** (0.05 mmol) and TiO₂ in 1mL PC solvent with time intervals.

We have observed that the epr signal observed was weaker and disappeared 12 h in the reaction of N,N-diisopropylacetamide **90a** with p-chloranil **17b** (Figure 13), whereas in the reaction without TiO₂, the epr signal was observed only for 5 min and disappeared after 1 h (Figure 9). The reaction of N,N-diisopropylpivalamide **90b** with p-chloranil **17b** (Figure 13) the epr signal was observed for only 5 min in the presence of TiO₂ but the epr signal was not observed without TiO₂ (Figure 9). In the case of reaction using N,N-diisopropylbenzamide **90b** and p-chloranil **17b**, the epr signal (Figure 13) appeared up to 6 h but without TiO₂, the epr signal was observed only for 5 min (Figure 9).

Presumably, the epr signals appear for more time as the quinone radical ions may get adsorbed on the surface of the TiO_2 (Scheme 42).

Scheme 42

2.2.7.2 Effect of TiO₂ on EPR studies of acylpyrrolidines with p-chloranil

We have also performed EPR studies for the acylpyrrolidine derivatives 91 with p-chloranil 17b in the presence of TiO_2 in PC solvent and monitored the epr signals at different time intervals as shown in Figure 14.

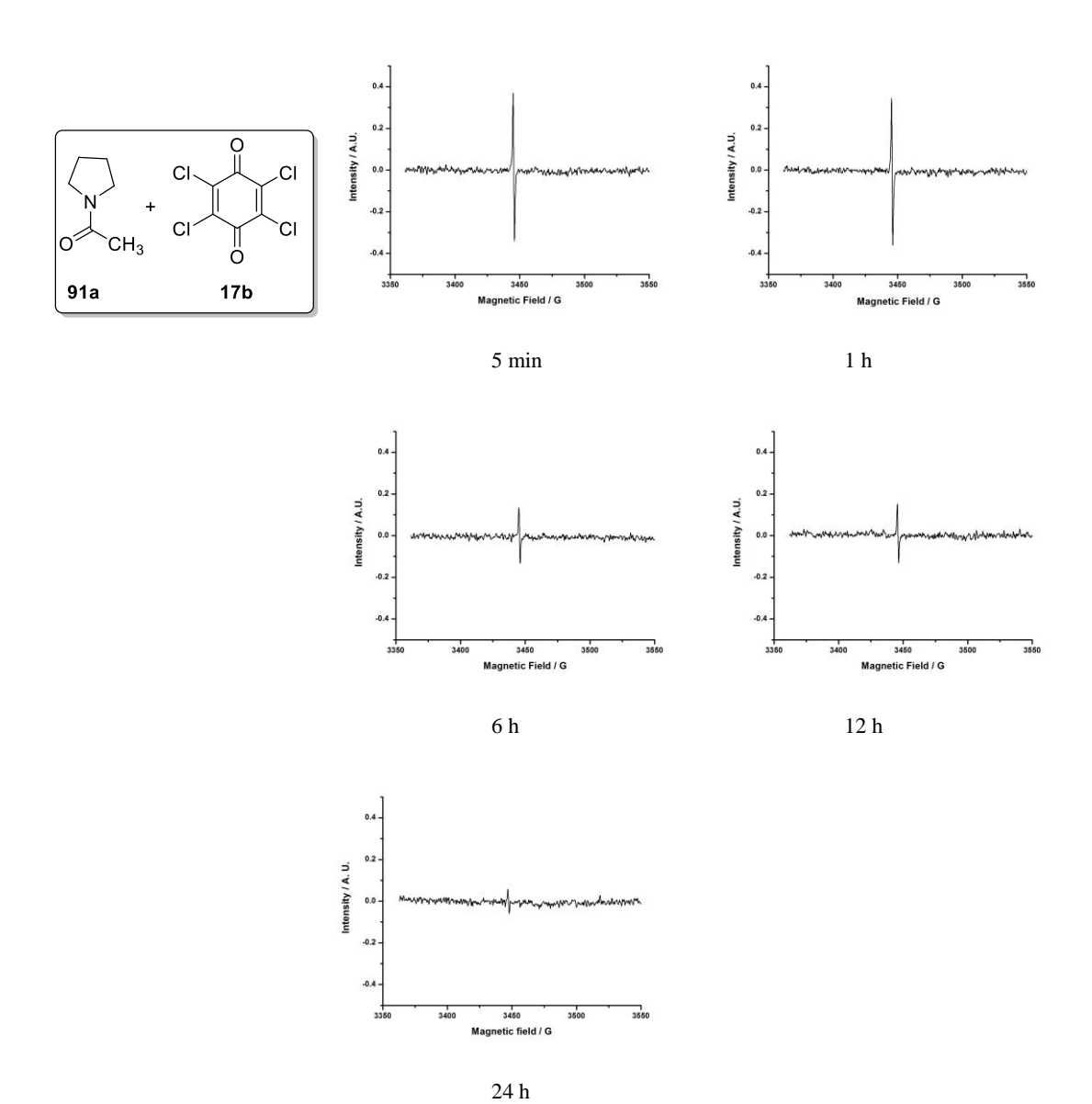
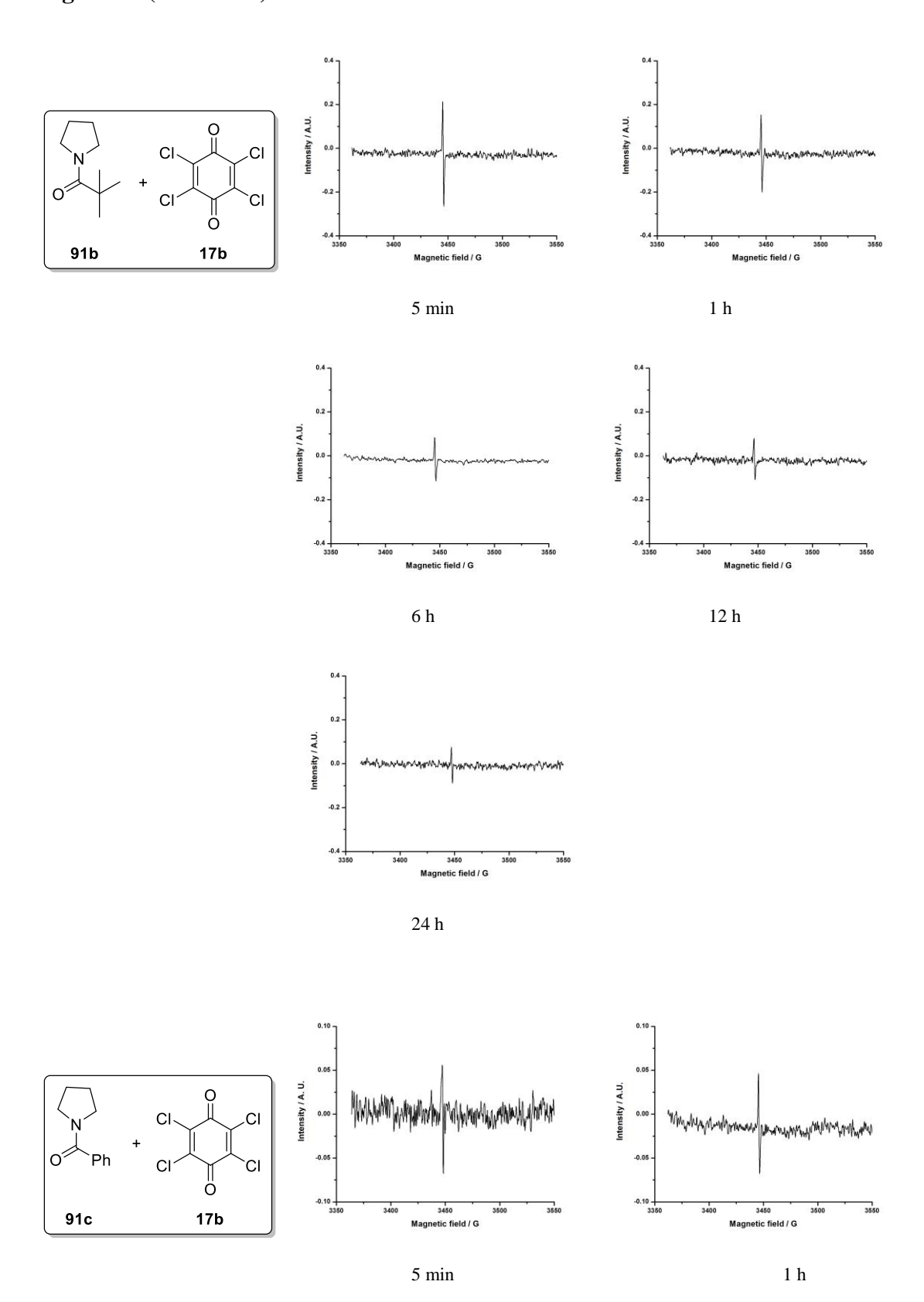


Figure 14 (continued)



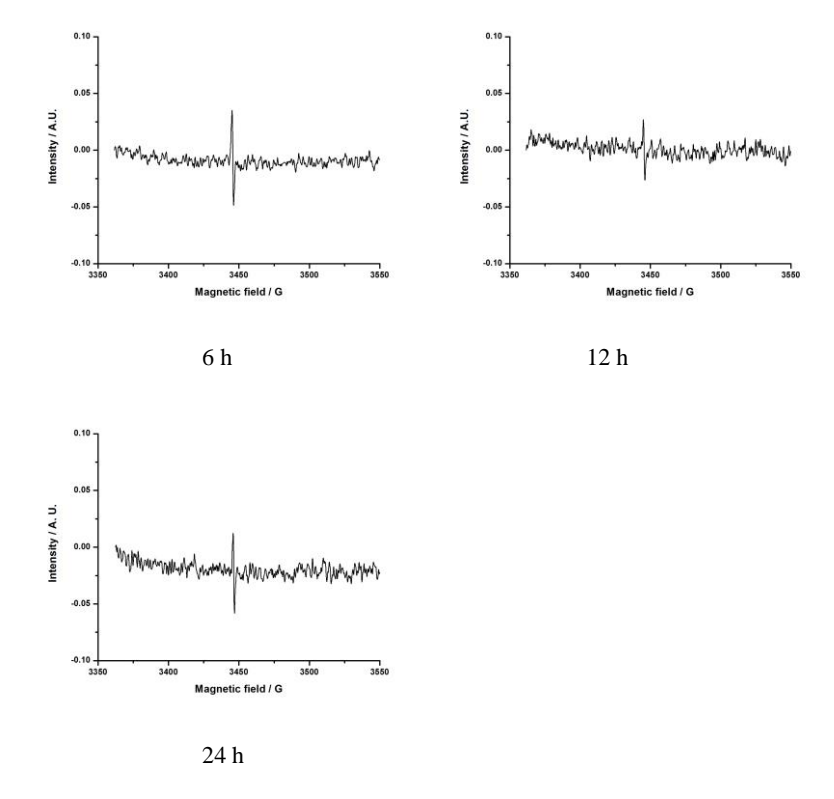


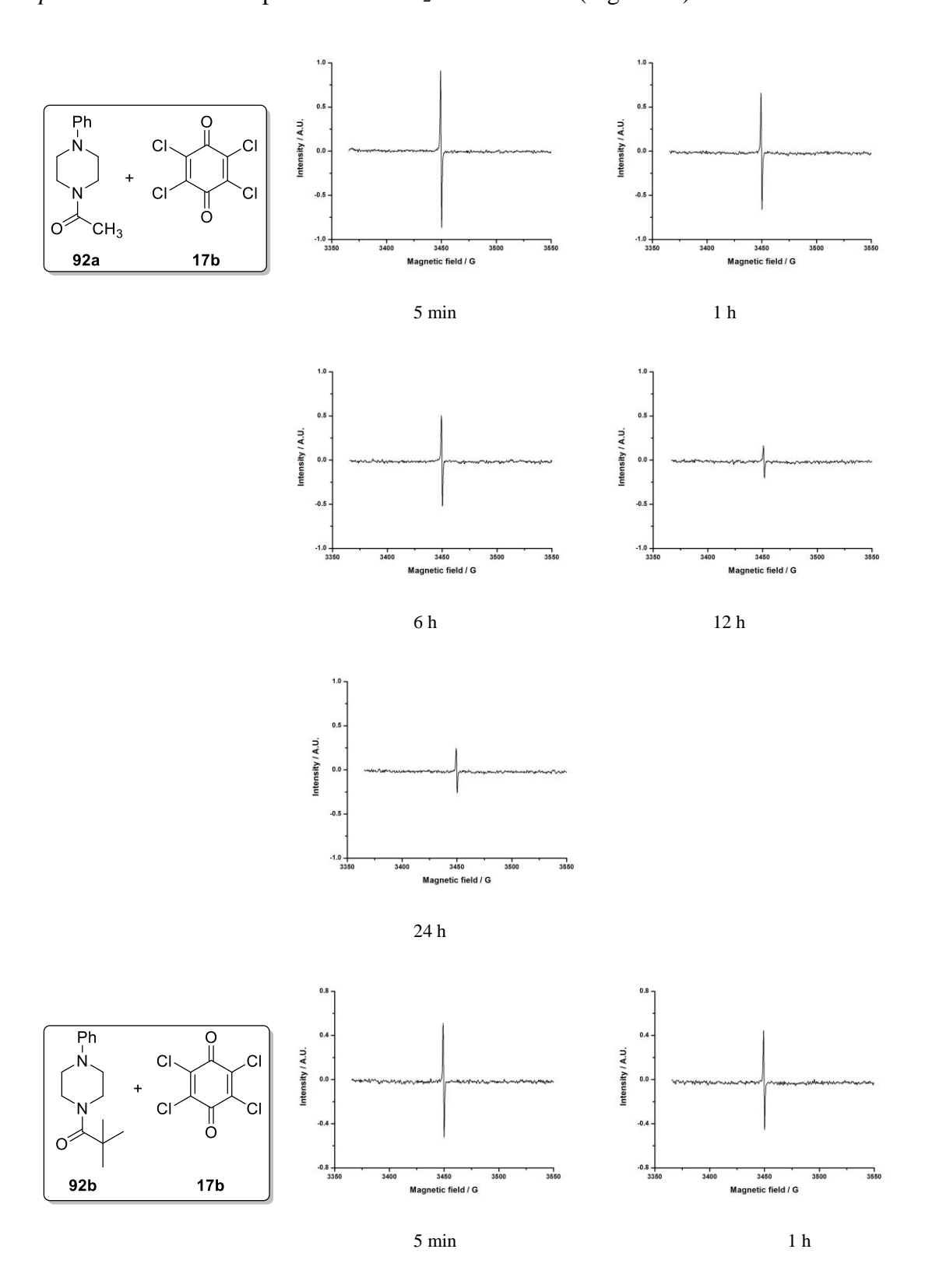
Figure 14. EPR studies of acylpyrrolidine derivatives **91** (0.05 mmol) with p-chloranil **17b** (0.05 mmol) and TiO₂ in 1 mL PC solvent with time intervals.

We have observed epr signals appear up to 24 h in the reactions of acyl pyrrolidine derivatives **91** with *p*-chloranil **17b** in presence of TiO₂ (Figure 14). Without TiO₂, reactions the epr signals are decreased fast with time (Figure 10). The signal intensities are relatively weaker compared to signals observed without TiO₂ but the signal intensity decreased at slower rate indicating that the radical cations and radical anions in the presence of TiO₂, are stabilised on the surface of the TiO₂ (Scheme 43).

Scheme 43

2.2.7.3 Effect of TiO₂ on EPR studies of N-acylpiperazine amides with p-chloranil

Similarly, we have carried out EPR studies of N-acylpiperazine derivatives **92** with p-chloranil **17b** in the presence of TiO₂ in PC solvent (Figure 15).



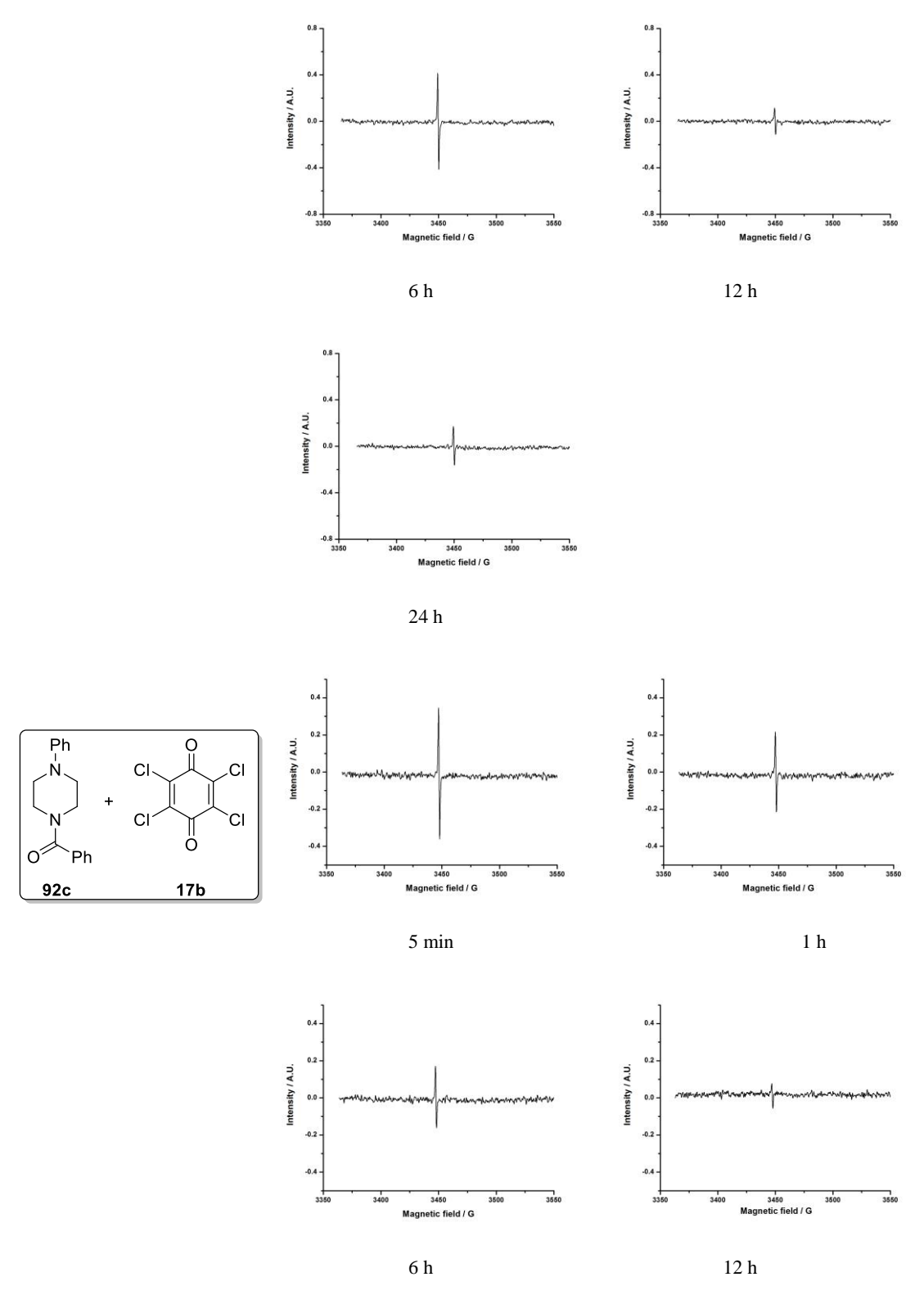


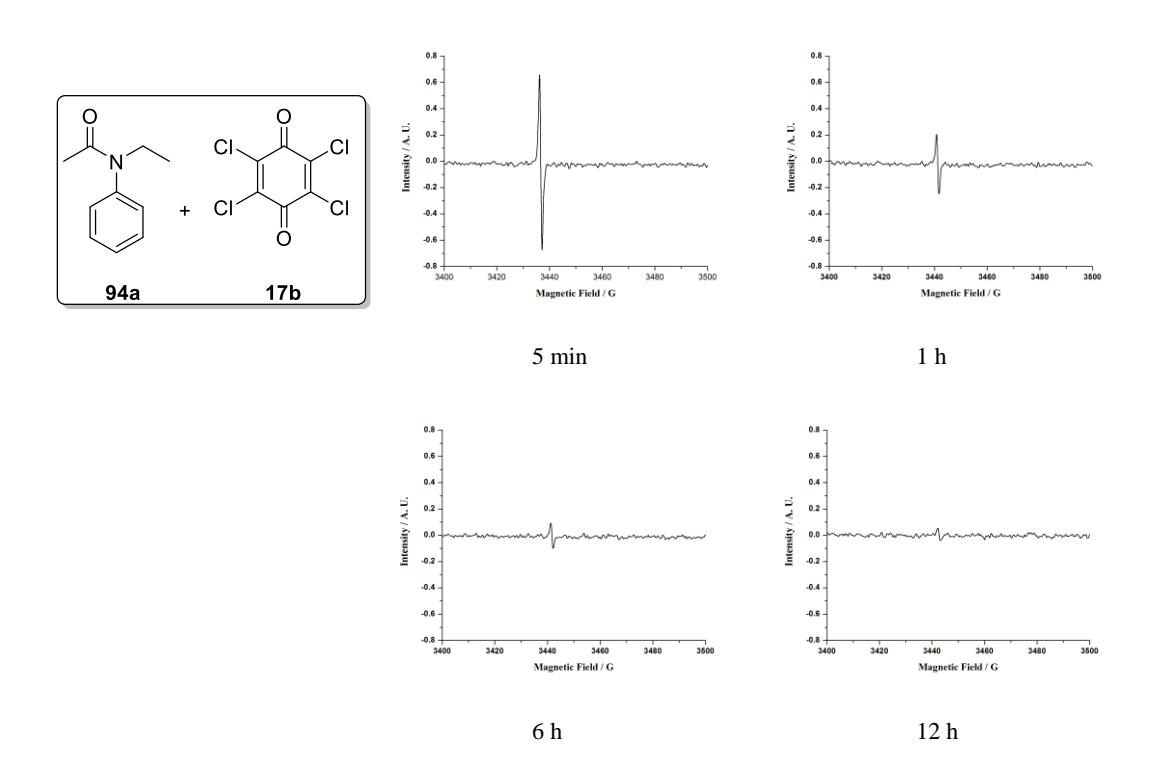
Figure 15. EPR studies of *N*-acylpiperazine derivatives **92** (0.05 mmol) with *p*-chloranil **17b** (0.05 mmol) and TiO_2 in 1 mL PC solvent with time intervals.

Again, the epr signals appeared for more time in the presence of TiO_2 , indicating that the radical ions formed in the reaction (Scheme 44).

Scheme 44

2.2.7.4 Effect of TiO₂ on EPR studies of N-ethylanilides with p-chloranil

We have carried out EPR studies of N-ethylanilide derivatives **94** with p-chloranil **17b** in presence of TiO₂ in PC solvent (Figure 16).



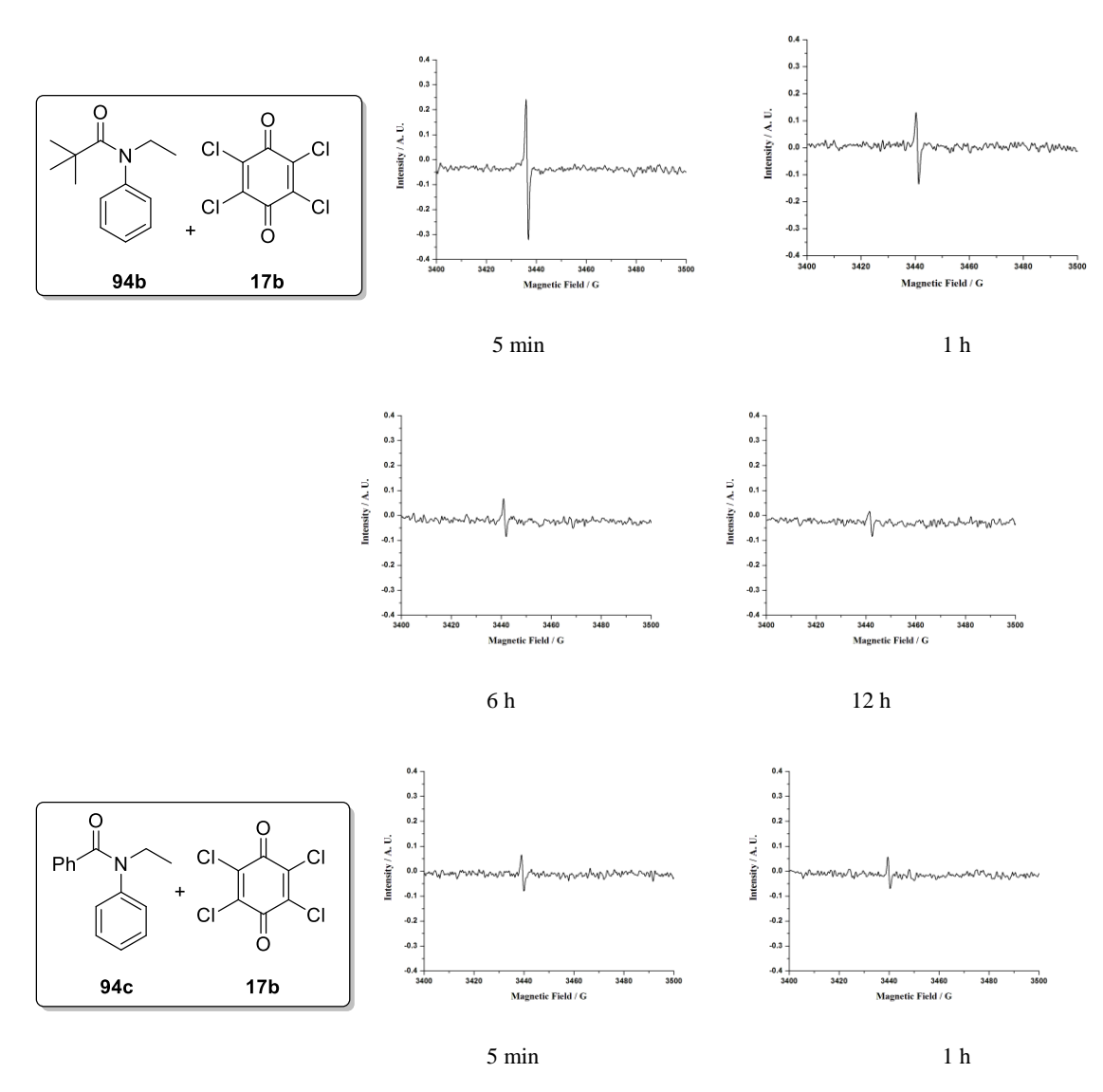


Figure 16. EPR studies of *N*-ethylanilide derivatives **94** (0.05 mmol) with *p*-chloranil **17b** (0.05 mmol) and TiO_2 in 1 mL PC solvent with time intervals.

Again, the TiO_2 plays a role in stabilizing the radical cation and radical anion pair on the surface of TiO_2 (Scheme 45).

Scheme 45

116 Results and Discussion

In all cases, we found that EPR signal strength decreases with time indicating the formation of charge transfer complexes as discussed in earlier sections. We have also examined the reaction of p-chloranil with tertiary amides by UV-Visible spectroscopy. The results are presented in the next section.

2.2.7.5 UV-Visible spectral studies of amides and *p*-chloranil

We have observed that when p-chloranil (10^{-4} M) and the corresponding amides (10^{-4} M) were mixed in PC solvent there was no color change. However, the formation a weak charge transfer complex band was observed at around 500-600 nm. This band corresponds to charge transfer complex in accordance with the data reported in the literature. The UV-Visible spectra of p-chloranil-amide systems are shown in Figure 17. The epr results are also given in Figure 17.

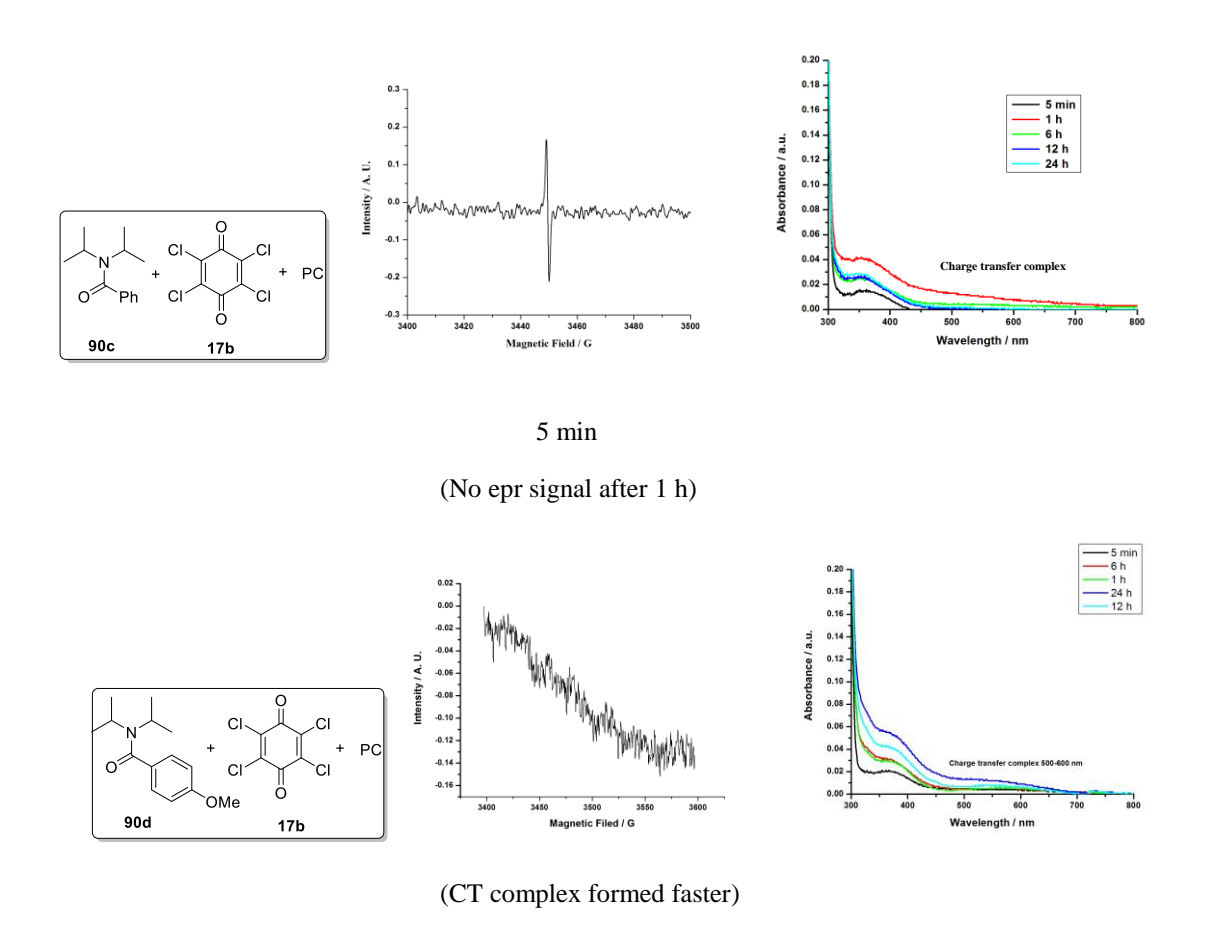
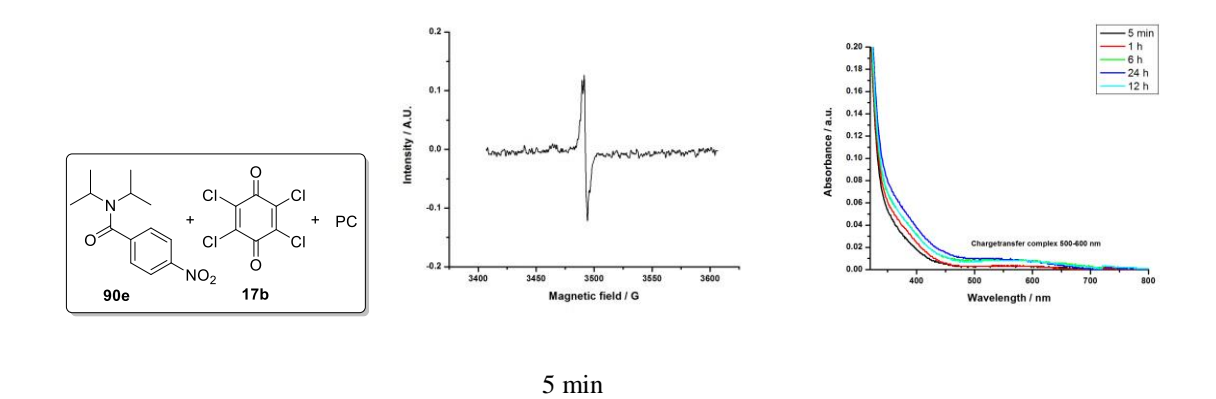
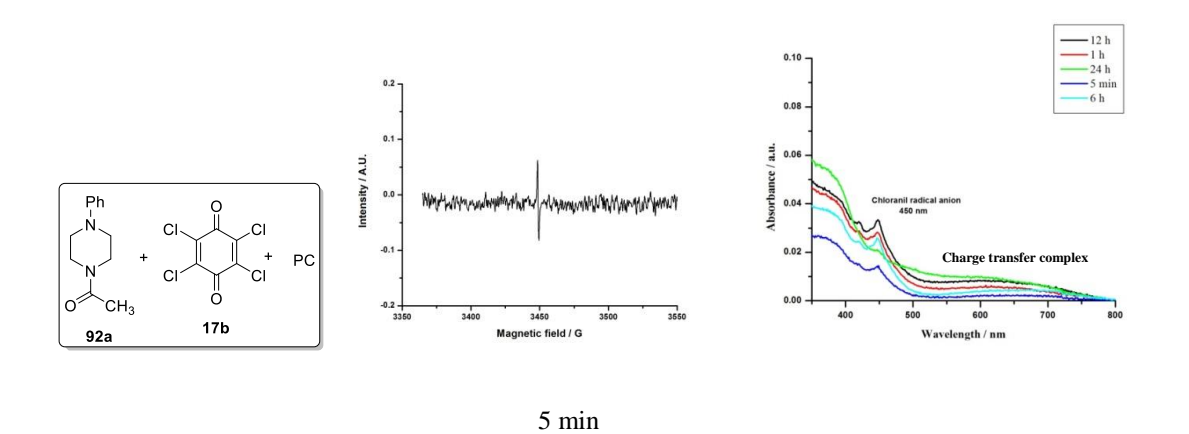


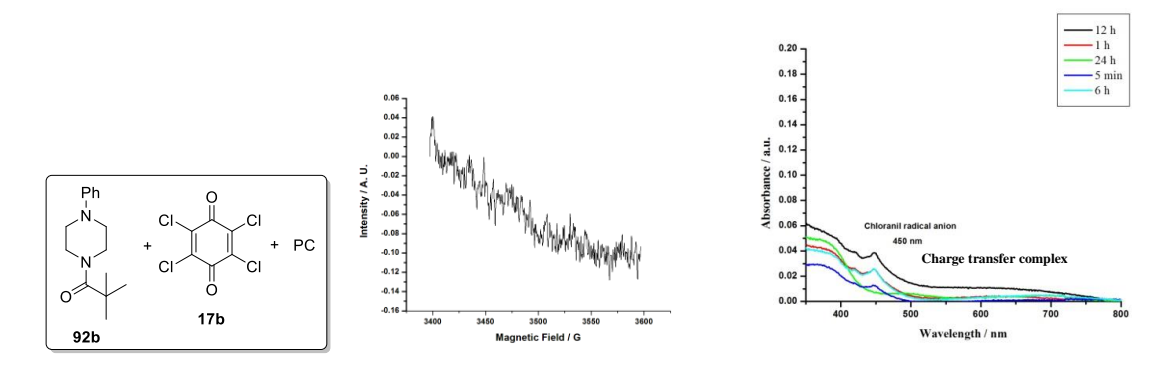
Figure 17 (continued)



(EPR signal observed up to 12 h)

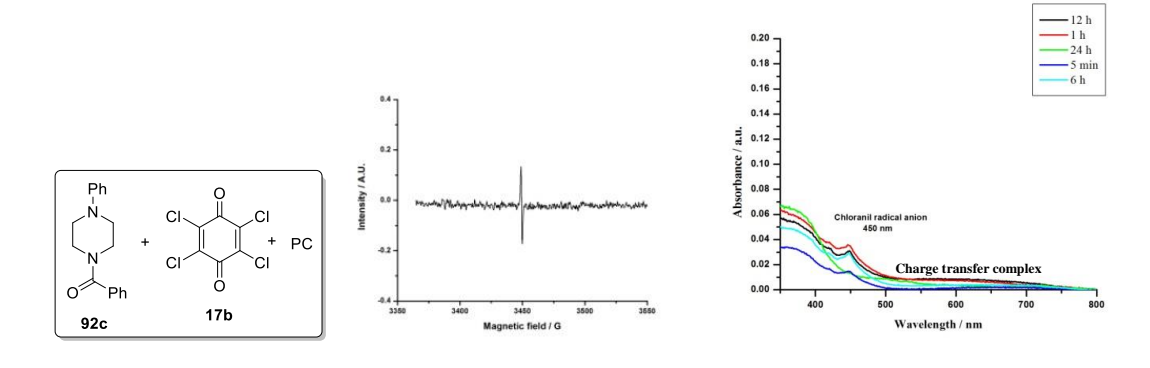


(No epr signal after 24 h)



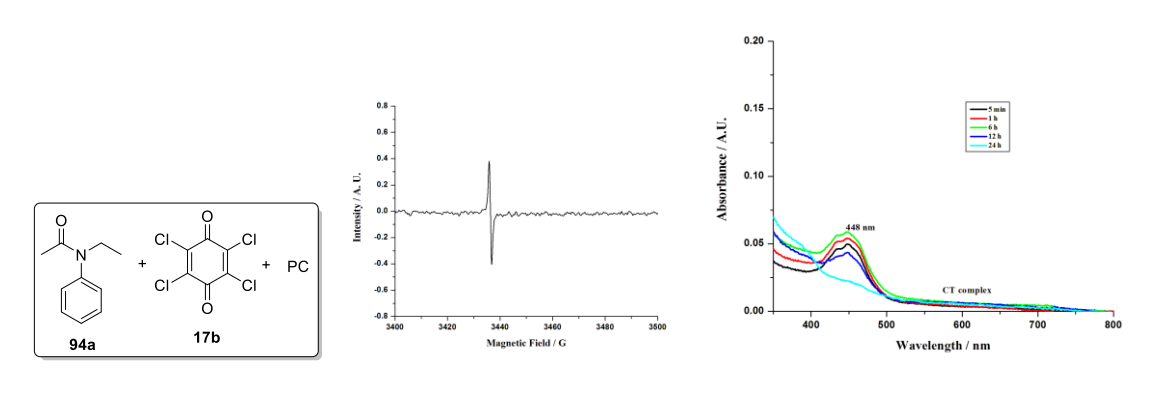
(CT complex formed faster)

Figure 17 (continued)



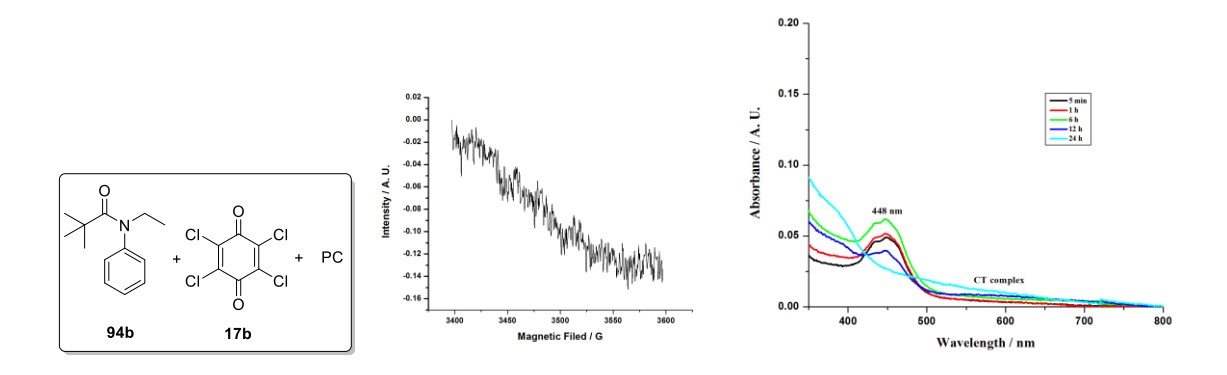
5 min

(No epr signal after 12 h)

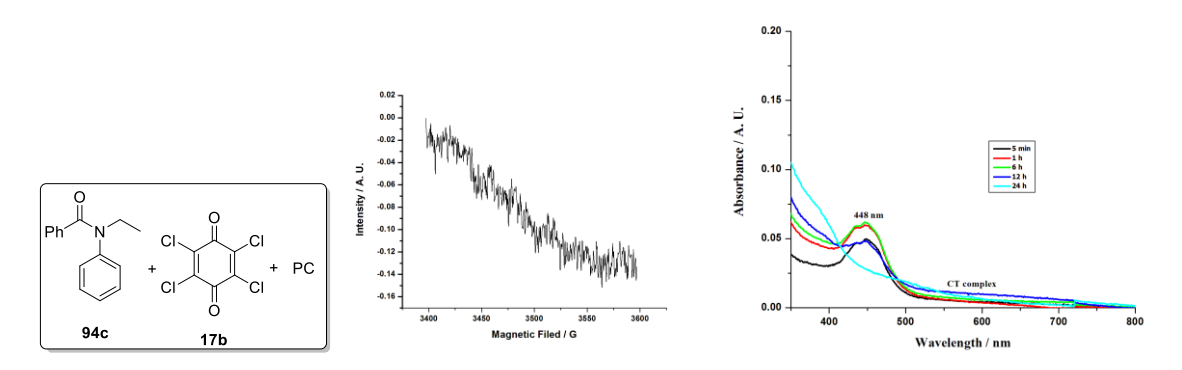


5 min

(No epr signal after 24 h)



(CT complex formed faster)



(Steric hindrance to the reaction)

Figure 17: Comparision of UV-Visible spectra of a mixture of p-chloranil 17b (1x10⁻⁴) and amide derivatives 90, 92 and 94 (1x10⁻⁴) in PC solvent at different time intervals with corresponding EPR studies.

The *p*-chloranil anion radical absorption absorbed at 440-450 nm. The absorption beyond 500 nm corresponds to the charge transfer complex.¹⁶ In the reaction of *N*,*N*-diisopropyl benzamide **90c** with *p*-chloranil **17b**, a weak charge transfer complex was observed. The epr signal for *N*,*N*-diisopropyl benzamide **90c** with *p*-chloranil **17b** observed only short time the charge transfer complex formed faster (Figure 17). The UV-visible spectra for the reaction of compound **90d** with *p*-chloranil are due to charge transfer complex and the intensity increases with time. We have noted that in the reaction of compound **90e** with *p*-chloranil **17b** the epr signls observed for 12 h but the UV-Visible spectral studies indicates that very little or no charge transfer complex formed, in accordance with stability of the radical anion as discussed earlier (Scheme 33).

Also, UV-Visible spectra for the reaction of other amides (92 and 94) with *p*-chloranil, when the epr signal disappears due to formation of charge transfer complexes, and this was confirmed by the UV-Visible specral analysis (Figure 17).

The charge-transfer complex **112** of *N*,*N*,*N'*,*N'*-tetramethyl-*p*-phenylenediamine (TMPD) **111** and *p*-chloranil **17b** was reported.³¹ It was proposed that such complexes interchanged reversibly (Scheme 46).³² The TMPD-chloranil system was also reported to give ionic diamagnetic complexes in solid state.³³

Scheme 46

Earlier, it was observed in this laboratory that the tertiary amines react with *p*-chloranil to give the radical cation and radical anions with subsequent formation of diamagnetic CT complexes lending to decrease in the strength of epr signals (Scheme 47).

Scheme 47

In the case of amides, the epr signal intensities decreased with time but we did not observe any product formation upon reaction of amides with *p*-chloranil. Presumably, the epr signal strength decreased due to formation of charge transfer complexes CT1, CT2 and CT3 (Scheme 48).

Scheme 48

2.2.8 Reaction of 2-naphthol and bi-2-naphthol with *p*-chloranil

As we have discussed in chapter 1, the reaction of 2-naphthol with oxygen adsorbed activated carbon and I_2/O_2 systems gives bi-2-naphthol through electron transfer mechanism. Accordingly, it was of interest to us to investigate the reaction of 2-naphthol with *p*-chloranil. We have observed that the reaction of 2-naphthol **121** with *p*-chloranil **17b** in DCM solvent gave a weak epr signal which also decreased with time (Figure 18).

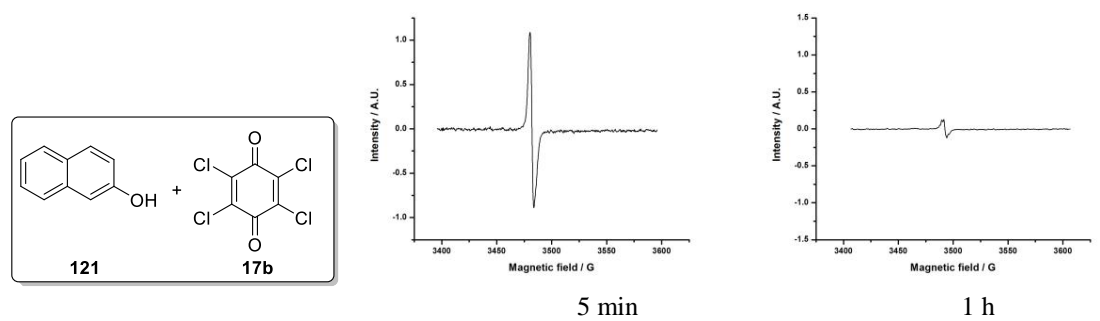


Figure 18. EPR studies of *p*-chloranil **17b** (0.05 mmol) with 2-naphthol **121** (0.05 mmol) in DCM (1 mL) solvent with time intervals.

After 12 h reaction of 2-naphthol **121** with *p*-chloranil **17b** in DCM solvent, the product **123** was obtained in 75% yield and the expected bi-2-naphthol **122** was not formed (Scheme 49).

122 Results and Discussion

Scheme 49

The formation of the product **123** can be explained by considering a tentative mechanism outlined in Scheme 50. The 2-naphthol could react with *p*-chloranil to give the electron transfer complex **124**. The cation radical could combine with chloranil anion radical to give the species **125** which after HCl elimination could give the product **123**.

Scheme 50

In the case of bi-2-naphthol 122, the reaction with p-chloranil 17b in DCM solvent did not give epr signal. After workup of the reaction only the starting materials were recovered (Scheme 51).

Scheme 51

However, it was observed in this laboratory that when bi-2-napthol was reacted with p-chloranil in the presence of K_2CO_3 in acetone solvent, the corresponding benzoquinone derivative **126** was obtained in 65% yield (Scheme 52).³⁴

Scheme 52

We have carried out the reaction of phenol (1 mmol) with p-chloranil (1 mmol) under similar reaction conditions to isolate the product **128** in 67% yield (Scheme 53).

Scheme 53

The aryloxy benzoquinone derivatives 126 and 128 have potential for use in electron transfer reactions.

2.2.9. Reaction of N-methylpyrrolidone (NMP) with p-chloranil

As discussed earlier, amides react with *p*-chloranil to give weak charge transfer complexes. We have also reacted *p*-chloranil with *N*-methylpyrrolidone (NMP) **129** in neat condition and also in PC solvent. A weak charge transfer complex formed was

124 Results and Discussion

identified by UV-Visible spectral studies but there was no epr signal observed. However, a weak epr signal was observed in the presence of titanium dioxide (TiO₂). The signal persisted up to 2 h (Figure 19).

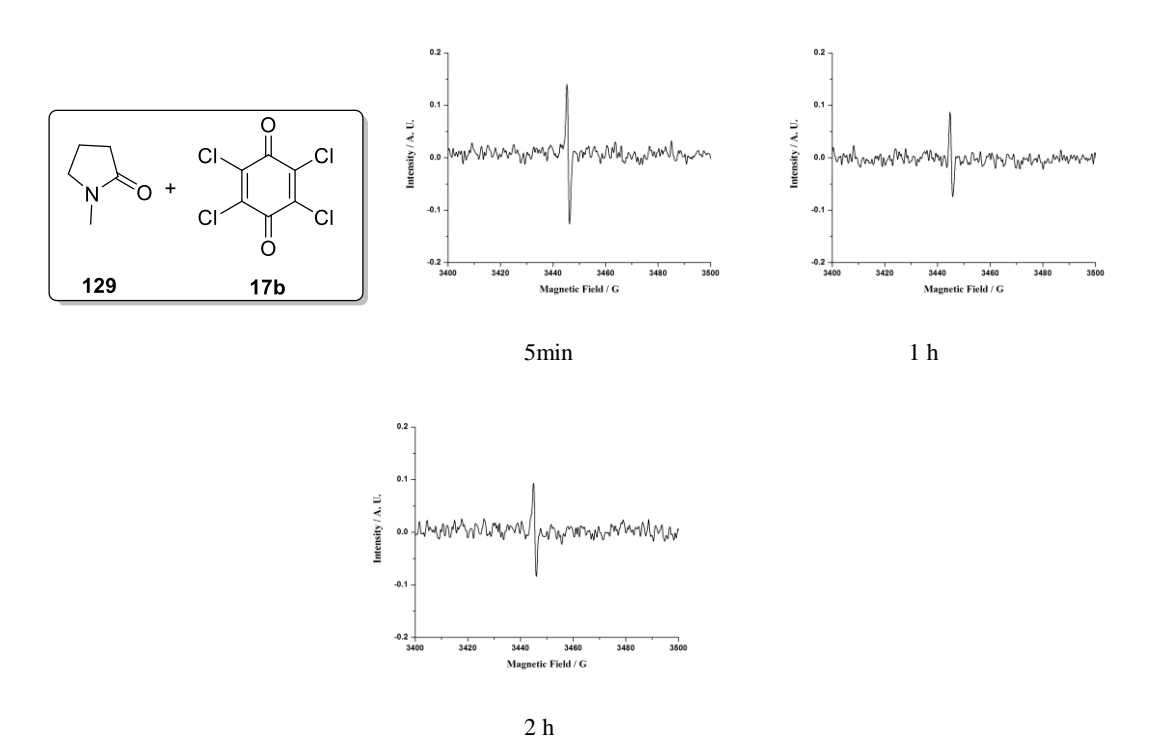


Figure 19. EPR studies of NMP **129** (0.05 mmol) with p-chloranil **17b** (0.05 mmol) and TiO₂ (10 mg) in 1ml PC solvent with time intervals.

The TiO₂ is an electron acceptor and also it has high electron affinity (EA=4.8 eV).³⁵ Accordingly, it was thought that it would interact with the radical anion species formed insitu. Presumably, the radical ion pairs formed is stabilized on the surface of TiO₂ as discussed earlier (Schemes 42-45). The charge transfer complex formed in the reaction of *p*-chloranil **17b** with NMP **129** in PC solvent was also confirmed by UV-Visible spectral studies (Figure 20).

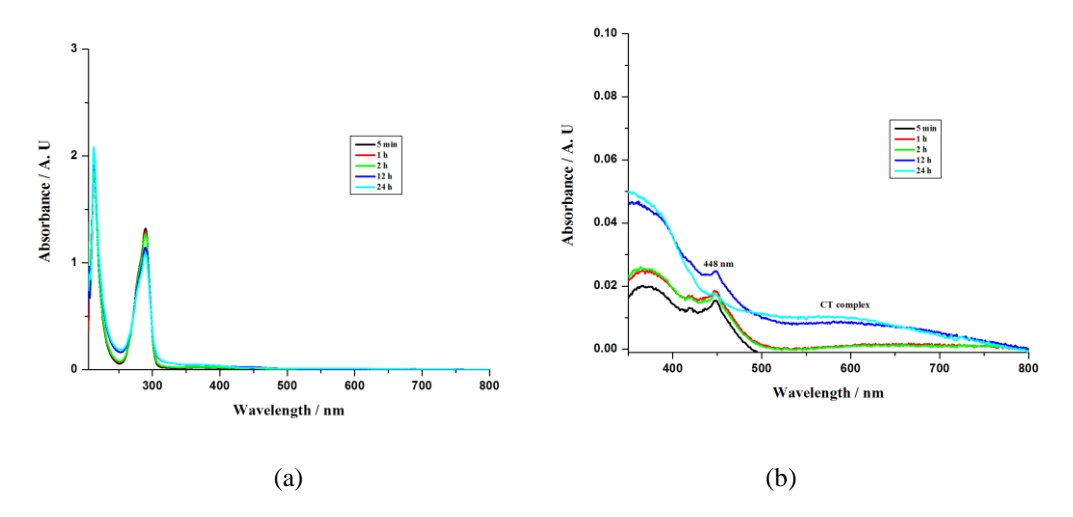


Figure 20. a) UV-Vis spectra of a mixture of NMP **129** (1 x 10^{-3} mol L⁻¹) and *p*-chloranil **17b** (1 x 10^{-4} mol L⁻¹) in PC at 25 °C. b) Expanded UV-Visible spectra.

The UV-Visible spectral measurements of solution of NMP **129** with p-chloranil **17b** were carried out in PC solvent at 25 °C (Figure 20). The absorption at 448 nm corresponds to p-chloranil radical anion. The charge transfer complex absorption was observed beyond 500 nm. The intensity of absorption bands indicates the weak nature of NMP **129** donor.

It was observed that *p*-chloranil (1 mmol) reacts with excess of NMP (5 mL) to give some unidentified products.³⁶ Accordingly, we have carried out the reaction of 2-naphthol in the presence of NMP. Surprisingly, the substitution product **130** was isolated in 63% yield (Scheme 54).

Scheme 54

The formation of the product **130** can be rationalised by the mechanism involving interaction of NMP with the 2-naphthol-*p*-chloranil electron transfer complex and

subsequent coupling of the *p*-chloranil radical anion with the keto radical **132** followed by elimination of HCl could result in the product **130** (Scheme 55).

Scheme 55

Clearly, NMP and other tertiary amides play an important role in the electron transfer reactions with *p*-chloranil. Accordingly, we have investigated the construction of organic electrochemical cells using amides and *p*-chloranil. The results are discussed in chapter 3.

2.3 Conclusions

We have observed that the reaction of quinones with secondary amine donors gave corresponding aminoquinones via electron transfer reaction through initial formation of radical cation and anion pair intermediates. The reaction of tertiary amine with quinone acceptor can be rationalized by initial electron transfer reaction followed by formation of outer-sphere π complex or inner-sphere σ complex.

The diisopropyl amides, N-ethyl anilides, acyl pyrrolidine derivatives and acyl piperazine derivatives react with p-chloranil to give weak epr signals. UV-Visible spectral studies indicate the weak donor nature of the amides.

Charge transfer complex

128 Conclusions

Whereas the reaction of 2-naphthol with *p*-chloranil gave 2-naphthoxy chloranil product in DCM, in the presence of NMP C-arylation of 2-naphthol takes place. These reactions have potential for further exploitation in organic synthesis.

Since NMP seems to give electron transfer reaction and charge transfer complexes, we have investigated the construction of organic electrochemical cells using NMP and *p*-chloranil. The results are discussed in chapter 3.

2.4 Experimental Section

2.4.1 General Information

The information given in the experimental section 1.4 are also applicable for the experiments outlined in this section.

DIPEA, N-ethyl aniline and trimethylamine were supplied by E-Merck (India) was used as received. Diisopropylamine, pyrrolidine, *N*-phenylpiperazine were purchased from AVRA (India). 1, 4-benzoquione, 1,4-naphthaquinone, chloranil, 2,3-dichloro-1,4-naphthaquinone, NMP, PC, PMMA were purchased from Aldrich and used as received.

2.4.2 General procedure for the preparation of aminoquinones 64

In a 50 mL RB flask, corresponding quinones (5 mmol) was dissolved in DCM (30 mL) solvent and amine (10 mmol) was slowly added for 5 min. The reaction mixture was stirred at room temperature for 12 h. Then the reaction mixture was concentrated under reduced pressure and 100 mL of ether was added to precipitate out the polar impurities and it was removed by filtration. Water was added to the filtrate and the organic layer was separated. The organic layer was washed with saturated NaCl solution and the solvent was evaporated under reduced pressure. The residue was chromatographed on a silica gel (100-200) column to isolate the corresponding aminoquinones.

2,5-bis(4-phenylpiperazin-1-yl)cyclohexa-2,5-diene-1,4-dione 64aa

Yield : 1.28 g (60%); Brown solid.

mp : 210-215 °C.

IR (**KBr**) : (cm⁻¹) 3023, 2946, 2830, 1634, 1598,

1567, 1499, 1442, 1369, 1299, 1219,

1135, 1028, 941, 824, 756, 690.

¹**H NMR** : (400 MHz, CDCl₃, δ ppm) 7.33-7.28 (m, 4H), 6.94 (d, J = 7.7 6Hz,

6H) 5.62 (s, 2H), 3.78 (s, 8H), 3.36-3.35 (t, *J* = 4.16 Hz, 8H).

¹³C NMR : $(100 \text{ MHz}, \text{CDCl}_3 \delta \text{ ppm}) 182.5, 152.5, 150.5, 129.2, 120.1, 115.9,$

106.4, 48.6, 48.5.

2,5-dichloro-3,6-bis(4-phenylpiperazin-1-yl)cyclohexa-2,5-diene-1,4-dione 64ab

Yield : 1.93 g (78%); Green solid.

IR (**KBr**) : (cm⁻¹) 2915, 2837, 2357, 1644, 1598,

1556, 1494, 1438, 1360, 1272, 1216, 1169,

1143, 1040, 993, 952, 916, 761, 689.

Ph\N\O\CI\O\N\N\Ph\

64ba

¹**H NMR** : (400 MHz, CDCl₃, δ ppm) .31 (brs, 4H), 6.71 (brs, 4H) 3.77(s,

8H), 3.35(s, 8H).

¹³C NMR : $(100 \text{ MHz}, \text{CDCl}_3 \delta \text{ ppm}) 176.0, 150.9, 148.2, 129.2, 120.4, 116.5,$

116.3, 113.1, 51.5, 50.2.

2,5-bis(4-methylpiperazin-1-yl)cyclohexa-2,5-diene-1,4-dione 64ba

Yield : 0.836 g (55%); Green solid.

mp : 201-203 °C.

IR (**KBr**) : (cm⁻¹) 2933, 2848, 2804, 2765, 1634, 1568,

1444, 1300, 1233, 1199, 1141, 1076, 1004,

931, 826, 756.

¹**H NMR** : $(400 \text{ MHz}, \text{CDCl}_3, \delta \text{ ppm}) 5.50 \text{ (s, 2H)}, 3.54-3.52 \text{ (t, } J=9.36 \text{ Hz,}$

8H), 2.48-2.46 (t, J = 9.92 Hz, 8H), 2.27(s, 6H).

¹³C NMR : $(100 \text{ MHz, CDCl}_3 \delta \text{ ppm}) 182.6, 152.5, 106.8, 54.6, 48.6, 45.9.$

2,5-dichloro-3,6-bis(4-methylpiperazin-1-yl)cyclohexa-2,5-diene-1,4-dione 64bb

Yield : 1.48 g (80%); Brown solid.

mp : 208-210 °C.

IR (**KBr**) : (cm⁻¹) 2936, 1654, 1579, 1291, 735.

CI CI N CH₃

¹**H NMR** : $(400 \text{ MHz, CDCl}_3, \delta \text{ ppm}) 3.58 \text{ (s, 8H), } 2.54 \text{ (s, 8H), } 2.31 \text{ (s, 6H).}$

¹³C NMR : $(100 \text{ MHz}, \text{CDCl}_3, \delta \text{ ppm}) 175.9, 148.3, 115.9, 55.6, 51.6, 46.0.$

2.4.3 Procedure for the preparation of 2,5-dichloro-3,6-bis(diphenylamino)cyclohexa-2,5-diene-1,4-dione 64d

In a 50 mL RB flask, corresponding p-chloranil (5 mmol) was dissolved in DCM (30 mL) solvent and diphenylamine (5 mmol) was slowly added for 5 min. The reaction mixture was stirred at 60 °C for 12 h. Then the reaction mixture was cooled and concentrated under reduced pressure. To this 100 mL of ether was added to precipitate out the polar impurities and it was removed by filtration. Water was added to the filtrate and the organic layer was separated. The organic layer was washed with saturated NaCl solution and the solvent was evaporated under reduced pressure. The residue was chromatographed on a silica gel (100-200) column to isolate the corresponding aminoquinones.

2,5-dichloro-3,6-bis(diphenylamino)cyclohexa-2,5-diene-1,4-dione 64d

Yield : 0.562 g (80%); Violet solid.

mp : 220-222 °C.

IR (**KBr**) : (cm⁻¹) 2910, 2844, 1668, 1640, 1594, 1556,

Ph CI N Ph O Ph

1497, 1326, 1282, 1231, 1128, 1050, 982, 916, 851, 792, 759, 720.

¹**H NMR** : (500 MHz, DMSO-d₆, δ ppm) 7.47-7.44 (t, J = 8 Hz, 4H), 7.41-7.39

(d, J = 8.85 Hz, 4H) 7.37-7.35 (d, J = 7.65 Hz, 4H), 7.25-7.19 (m,

8H).

¹³C NMR : (125 MHz, DMSO-d₆, δ ppm) 177.9, 153.3, 140.7, 139.5, 130.1,

129.0, 125.1, 122.3, 115.3.

2.4.4 General procedure for the preparation of aminoquinones 65

In a 50 mL RB flask, corresponding quinones (5 mmol) was dissolved in DCM (30 mL) solvent and amine (5 mmol) was slowly added for 5 min. The reaction mixture was stirred at room temperature for 12 h. Then the reaction mixture was concentrated under reduced pressure and 100 mL of ether was added to precipitate out the polar impurities and it was removed by filtration. Water was added to the filtrate and the organic layer was separated. The organic layer was washed with saturated NaCl solution and the solvent was evaporated under reduced pressure. The residue was chromatographed on a silica gel (100-200) column to isolate the corresponding aminoquinones.

2-(4-methylpiperazin-1-yl)naphthalene-1,4-dione 65aa

Yield : 0.84 g (53%); Brown solid.

mp : 142-145 °C.

IR (KBr) : (cm⁻¹) 3059, 2842, 1672, 1633, 1593, 1563, 1499, 1389. 1327,

1303, 1231, 1209, 1154, 1123, 984, 880, 757, 726, 693.

¹**H NMR** : $(400 \text{ MHz, CDCl}_3, \delta \text{ ppm}) 8.04-7.73 \text{ (m, 2H), } 7.10-7.63 \text{ (m, 2H),}$

7.32-7.26 (m, 2H), 6.96-6.07 (m, 3H), 6.06 (s, 1H), 3.7-3.6 (m,

4H), 3.4-3.3 (m, 4H).

¹³C NMR : $(100 \text{ MHz}, \text{CDCl}_3 \delta \text{ ppm}) 180.6, 180.0, 153.4, 150.7, 133.9, 132.7,$

132.5, 132.3, 129.3, 126.7, 125.6, 120.3, 116.1, 111.6, 49.7.

2-(4-methylpiperazin-1-yl)naphthalene-1,4-dione 65ab

Yield : 1.16 g (66%); Red solid.

mp : 108-110 °C.

IR (**KBr**) : (cm⁻¹) 2909, 2853, 2332, 1675, 1645, 1594,

1556, 1497, 1324, 1282, 1230, 1128, 1049, 992,

916, 851, 792, 759, 719.

¹**H NMR** : $(400 \text{ MHz, CDCl}_3, \delta \text{ ppm}) 8.13 \text{ (dd, } J = 7.56 \text{ Hz, } 1.4 \text{ Hz, } 1\text{H}), 8.0$

(dd, J = 7.28 Hz, 1.2 Hz, 1H) 7.74-7.66 (m, 2H), 7.34-7.30 (m, 2H)

2H), 7.02-6.9 (m, 3H), 3.8-3.78 (t, J = 4.72 Hz,4H), 3.39-3.37 (t, J

= 4.96 Hz, 4H).

¹³C NMR : $(100 \text{ MHz}, \text{CDCl}_3 \delta \text{ ppm}) 181.8, 178.0, 151.1, 149.8, 134.1, 133.5,$

131.5, 131.4, 129.2, 126.9, 126.6, 123.3, 116.5, 51.2, 50.3.

2-(4-methylpiperazin-1-yl)naphthalene-1,4-dione 65ba

Yield : 0.74 g (58%); Brown solid.

mp : 118-120 °C.

IR (**KBr**) : (cm⁻¹) 2960, 2930, 2843, 2804, 2755, 1672,

1641, 1592, 1561, 1438, 1338, 1292, 1241,

1207, 1145, 1076, 981, 839, 777, 725.

O N N CH₃

¹**H NMR** : $(400 \text{ MHz}, \text{CDCl}_3, \delta \text{ ppm}) 8.0-7.94 \text{ (m, 2H)}, 7.68-7.58 \text{ (m, 2H)},$

5.99 (s, 1H), 3.52-3.49 (t, J = 9.76 Hz, 4H), 2.56-2.53 (t, J = 4.88

Hz, 4H), 2.32 (s, 3H).

¹³C NMR : $(100 \text{ MHz}, \text{CDCl}_3 \delta \text{ ppm}) 183.5, 183.0, 153.7, 133.8, 132.7, 132.4,$

132.2, 126.6, 125.5, 111.7, 54.5, 48.8, 45.9.

65bb

90a

2-chloro-3-(4-methylpiperizin-1-yl)naphthalene-1,4-dione 65bb

Yield : 1.23 g (85%); Violet solid.

mp : 200-205 °C.

IR (**KBr**) : (cm⁻¹) 2933, 1645, 1557, 1276, 717.

¹**H NMR** : $(400 \text{ MHz}, \text{CDCl}_3, \delta \text{ ppm}) 8.10-8.12 \text{ (m, 1H)}, 8.0-8.02 \text{ (m, 1H)},$

7.67-7.71 (m, 2H), 3.67 (s, 4H), 2.67 (s, 4H), 2.40 (s, 3H).

¹³C NMR : $(100 \text{ MHz}, \text{CDCl}_3 \delta \text{ ppm}) 181.8, 178.0, 149.8, 134.1, 133.1, 131.5,$

131.4, 126.5, 123.2, 55.4, 51.0, 45.9.

2.4.5 Procedure for preparation of N,N-diisopropyl amide derivatives 90

In an oven dried 250 mL RB flask, the diisopropyl amine (20 mmol) was added in dichloromethane (60 mL) solvent. To this solution triethylamine (2.1 mL, 21 mmol) was added slowly at room temperature with constant stirring. Then the reaction mixture was stirred for 1 h and corresponding acid chloride (20 mmol) was added at 0° C. Then the reaction mixture was brought to room temperature and it stirred for 8 h. The mixture was quenched with saturated ammonium chloride solution and the organic layer was separated. The organic layer was extracted with dichloromethane (2 x 50 mL). The combined organic extracts were washed with saturated NaCl solution (15 mL) and dried over anhydrous Na₂SO₄. Then the solvent was evaporated to get the crude product. The corresponding crude amide product was purified by column chromatography on silica gel (100-200) using hexane and ethyl acetate as eluent to isolate pure amide product.

N, N-diisopropylacetamide 90a

Yield : 2.43 g (85%); Colorless liquid.

IR (neat) : (cm⁻¹) 2964, 2931, 1638, 1446, 1375, 1331, 1222,

1134, 1046, 734.

90c

¹**H NMR** : (400 MHz, CDCl₃, δ ppm): 3.83 (m, 1H), 3.46 (s, 1H), 1.99 (s, 3H),

1.24 (d, J = 8 Hz, 6H), 1.13 (s, 6H).

¹³C NMR : $(100 \text{ MHz}, \text{CDCl}_3, \delta \text{ ppm}) 169.4, 49.2, 45.3, 23.8, 20.8, 20.5.$

N, N-diisopropylpivaloylamide 90b

Yield : 3.07 g, (83%); Colorless solid.

mp : 49-50 °C.

IR (neat) : 2970, 2931, 1622, 1479, 1425, 1359, 1222,

1145, 1046, 756 cm⁻¹.

¹**H NMR** : (400 MHz, CDCl₃, δ ppm): 4.26 (s, 1H), 3.22 (s, 1H), 1.33 (s, 6H),

1.19 (s, 9H), 1.14 (s, 6H).

¹³C NMR : (100 MHz, CDCl₃, δ ppm) 176.3, 48.1, 46.5, 39.3, 28.4, 27.0, 20.5.

N, N-diisopropylbenzamide 90c

Yield : 3.48 g (85%); Colorless solid.

mp : 68-70 °C.

IR (**KBr**) : (cm⁻¹) 2970, 2937, 1627, 1446, 1342, 1222, 1156, 1041, 739.

¹**H NMR** : $(400 \text{ MHz}, \text{CDCl}_3, \delta \text{ ppm}): 7.36 \text{ (m, 3H)}, 7.31 \text{ (m, 2H)},$

3.75 (s, 2H), 1.35 (s, 12H).

¹³C NMR : $(100 \text{ MHz}, \text{CDCl}_3, \delta \text{ ppm}) 171.0, 138.9, 128.5, 128.4, 125.5, 50.8,$

45.7, 20.7.

N, N-diisopropyl-4-methoxy-benzamide 90d

Yield: 4.2 g (90%); Colorless liquid.

IR (Neat) : 2969, 2935, 1779, 1771, 1609, 1512, 1440, 1371,

1340, 1297, 1251, 1160, 1031, 764 cm⁻¹.

90e

¹**H NMR** : (400 MHz, CDCl₃, δ ppm): 8.10-7.97 (m, 1H), 7.26 (s, 1H), 6.98-

6.87 (m, 2H), 5.28 (s, 3H), 3.80 (s, 2H), 1.33 (s, 12H).

¹³C NMR : $(100 \text{ MHz}, \text{CDCl}_3, \delta \text{ ppm})$ 171.1, 159.9, 132.8, 127.4, 113.4, 55.2,

53.4, 20.7.

N, N-diisopropyl-4-nitro-benzamide 90e

Yield: 4.4 g (88%); Yellow color solid.

mp : 134-136 °C.

IR (**KBr**) : (cm⁻¹) 2976, 2931, 1634, 1598, 1521, 1492, 1345, 1211, 1192,

1161, 1136, 1036, 758, 714.

¹**H NMR** : $(400 \text{ MHz}, \text{CDCl}_3, \delta \text{ ppm}): 8.30-8.23 \text{ (m, 2H)}, 7.52-7.45 \text{ (m, 2H)},$

3.68-3.57 (m, 2H), 1.55-1.17 (m, 12H).

¹³C NMR : (100 MHz, CDCl₃, δ ppm) 168.6, 147.7, 144.8, 126.5, 124.0, 51.1,

46.1, 20.5.

N, N-diisopropyl-4-trifluoromethyl-benzamide 90f

Yield: 4.6 g (85%); Colorless liquid.

IR (Neat) : (cm⁻¹) 2972, 2935, 1634, 1518, 1442, 1372,

1323, 1165, 1127, 1064, 1017, 854, 834, 765, 749.

¹**H NMR** : (400 MHz, CDCl₃, δ ppm): 7.66 (d, J = 8.04 Hz, 2H), 7.43

(d, J = 7.8Hz, 2H), 3.74-3.56 (m, 2H), 1.56-1.16 (m, 12H).

¹³C NMR : $(100 \text{ MHz}, \text{CDCl}_3, \delta \text{ ppm}) 169.4, 142.3, 125.9, 125.6, 125.5, 51.0,$

46.0, 20.6.

2.4.6 Procedure for preparation of acyl pyrrolidine derivatives 91

In an oven dried 250 mL RB flask, the pyrrolidine (20 mmol) was added in dichloromethane (60 mL) solvent. To this solution triethylamine (2.1 mL, 21 mmol) was added slowly at room temperature with constant stirring. Then the reaction mixture was stirred for 1 h and corresponding acid chloride (20 mmol) was added at 0° C. Then the reaction mixture was brought to room temperature and it stirred for 8 h. The mixture was quenched with saturated ammonium chloride solution and the organic layer was separated. The organic layer was extracted with dichloromethane (2x50 mL). The combined organic extracts were washed with saturated NaCl solution (15 mL) and dried over anhydrous Na₂SO₄. Then the solvent was evaporated to get the crude product. The corresponding crude amide product was purified by column chromatography on silica gel (100-200) using hexane and ethyl acetate as eluent to isolate pure amide product.

1-(pyrrolidin-1-yl)ethanone 91a

¹H NMR

Yield: 1.92 g (90%); Yellow color liquid.

IR (neat) : (cm⁻¹) 2980, 2876, 1627, 1452, 734.

(400 MHz, CDCl₃, δ ppm): 3.30 (d, 2H), 1.92 (s,3H), 1.83 (d, 2H),

1.74 (s, 2H)

¹³C NMR : $(100 \text{ MHz}, \text{CDCl}_3, \delta \text{ ppm}) 165.1, 43.3, 22.0, 20.5, 18.4.$

2,2-dimethyl-1-(pyrrolidin-1-yl)propan-1-one 91b

Yield: 2.48 g (80%); Yellow color liquid.

IR (neat) : (cm⁻¹) 2964, 2865, 1616, 1480, 756.

¹**H NMR** : (400 MHz, CDCl₃, δ ppm): 3.46 (s, 4H), 1.78 (s, 4H), 1.17(d, 9H)

¹³C NMR : (100 MHz, CDCl₃, δ ppm) 176.3, 47.7, 38.8, 27.4

Phenyl(pyrrolidin-1-yl)methanone 91c

Yield: 2.97 g (85%); Yellow color liquid.

IR (neat) : (cm⁻¹) 2969, 2871, 1627, 1424, 717.

N O Ph 91c

¹**H NMR** : $(400 \text{ MHz}, \text{CDCl}_3, \delta \text{ ppm}): 7.5 \text{ (s, 2H)}, 7.4 \text{ (s, 3H)}, 3.65 \text{ (s, 2H)},$

3.42 (s, 2H), 1.96 (s, 2H), 1.87 (d, 2H).

¹³C NMR : $(100 \text{ MHz}, \text{CDCl}_3, \delta \text{ ppm}) 169.7, 137.2, 129.7, 128.2, 127.0, 49.6,$

46.1, 26.3, 24.4.

2.4.7 Procedure for preparation of acyl piperazine derivatives 92

In an oven dried 250 mL RB flask, piperazine (20 mmol) was dissolved in dichloromethane (60 mL) solvent. To this solution triethylamine (2.1 mL, 21 mmol) was added slowly at room temperature with constant stirring. Then the reaction mixture was stirred for 1 h and corresponding acid chloride (20 mmol) was added at 0° C. Then the reaction mixture was brought to room temperature and it stirred for 8 h. The mixture was quenched with saturated ammonium chloride solution and the organic layer was separated. The organic layer was extracted with dichloromethane (2x50 mL). The combined organic extracts were washed with saturated NaCl solution (15 mL) and dried over anhydrous Na₂SO₄. Then the solvent was evaporated to get the crude product. The corresponding crude amide product was purified by column chromatography on silica gel (100-200) using hexane and ethyl acetate as eluent to isolate pure amide product.

1-(4-phenylpiperazin-1-yl)ethanone 92a

Yield : 3.67 g (90%); Brown color solid.

mp : 95-96 °C.

IR (**KBr**) : (cm⁻¹) 3063, 2821, 1632, 1441, 1227, 1002, 772.

¹**H NMR** : $(400 \text{ MHz}, \text{CDCl}_3, \delta \text{ ppm}): 7.26-7.28 \text{ (m, 2H)},$

6.9 (s, 3H), 3.74 (s, 2H), 3.57 (s, 2H), 3.14 (s, 4H), 2.11 (s, 3H)

¹³C NMR : $(100 \text{ MHz}, \text{CDCl}_3, \delta \text{ ppm}) 168.9, 150.9, 129.2, 120.4, 116.6, 49.6,$

49.2, 46.1, 41.3, 21.3

2,2-dimethyl-1-(4-phenylpiperazin-1-yl)propan-1-one 92b

Yield: 3.92 g (85%); Brown color solid.

mp : 75-77 °C.

IR (**KBr**) : (cm⁻¹) 3058, 2986, 1638, 1501,1375, 1013, 761.

¹**H NMR** : (400 MHz, CDCl₃, δ ppm): 7.32-7.28 (m, 2H), 6.9 $\overline{\text{6-6.90}}$ (m, 3H),

3.84-3.81 (m, 4H), 3.20-3.17 (m, 4H), 1.31-1.33 (m, 9H).

¹³C NMR : $(100 \text{ MHz}, \text{CDCl}_3, \delta \text{ ppm}) 176.4, 151.0, 129.2, 120.4, 49.5, 45.0,$

38.6, 28.4

Phenyl(4-phenylpiperazin-1-yl)methanone 92c

Yield: 5.05 g (95%); Brown color solid.

mp : 95-97 °C.

IR (neat) : (cm⁻¹) 3063, 2816, 1709, 1600,1435,1232, 1019, 761.

¹**H NMR** : (400 MHz, CDCl₃, δ ppm): 7.46 (s, 3H), 7.31-7.33 (m, 3H), 6.97-

6.92 (m, 3H), 3.96 (s, 2H), 3.63 (s, 2H), 3.21-3.22 (m, 4H)

¹³C NMR : (100 MHz, CDCl₃, δ ppm) 170.4, 150.9, 135.6, 129.8, 129.2,

128.5,127.1, 120.6, 116.7, 49.8.

2.4.8 Procedure for preparation of *N*-ethylanilide derivatives 94

In an oven dried 250 mL RB flask, the diisopropyl amine (20 mmol) was added in dichloromethane (60 mL) solvent. To this solution triethylamine (2.1 mL, 21 mmol) was added slowly at room temperature with constant stirring. Then the reaction mixture was

94b

stirred for 1 h and corresponding acid chloride (20 mmol) was added at 0° C. Then the reaction mixture was brought to room temperature and it stirred for 8 h. The mixture was quenched with saturated ammonium chloride solution and the organic layer was separated. The organic layer was extracted with dichloromethane (2x50 mL). The combined organic extracts were washed with saturated NaCl solution (15 mL) and dried over anhydrous Na₂SO₄. Then the solvent was evaporated to get the crude product. The corresponding crude amide product was purified by column chromatography on silica gel (100-200) using hexane and ethyl acetate as eluent to isolate pure amide product.

N-ethyl-N-phenylacetamide 94a

Yield : 2.61 g (80%); Colorless solid.

mp : 54-55 °C.

IR (KBr) : (cm⁻¹) 2970, 2926, 1660, 1495, 1408, 1298,

1139, 767, 706.

¹**H NMR** : $(400 \text{ MHz, CDCl}_3, \delta \text{ ppm}): 7.42-7.35 \text{ (m, 3H)}, 7.15-7.17 \text{ (m, 2H)},$

3.73 (q, J = 8 Hz, 2H), 1.82 (s, 3H), 1.11 (t, J = 8 Hz, 3H).

¹³C NMR : $(100 \text{ MHz}, \text{CDCl}_3, \delta \text{ ppm}) 169.9, 142.9, 126.6, 128.2, 127.8, 43.8,$

22.8, 13.0.

N-ethyl-*N*-phenylpivalamide 94b

Yield : 2.87 g (70%); Colorless solid.

mp : 55-56 °C.

IR (**KBr**) : (cm⁻¹) 2986, 2953, 1627, 1490, 1375, 1293,

1200, 1134, 750, 717.

¹**H NMR** : $(400 \text{ MHz}, \text{CDCl}_3, \delta \text{ ppm}): 7.36-7.34 \text{ (m, 3H)}, 7.17-7.15 \text{ (m, 2H)},$

3.64-3.62 (m, 2H), 1.09-1.06 (m, 3H), 0.98 (s, 9H).

Chapter 2

141

¹³C NMR : $(100 \text{ MHz}, \text{CDCl}_3, \delta \text{ ppm}) 169.9, 142.9, 126.6, 128.2, 127.8, 43.8,$

22.8, 13.0.

N-ethyl-N-phenylbenzamide 94c

Yield: 3.28 g (73%); Yellow color solid.

mp : 65-67 °C.

IR (**KBr**) : (cm⁻¹) 3068, 2975, 1649, 1594, 1490, 1391,

1298, 767, 701.

¹**H NMR** : $(400 \text{ MHz}, \text{CDCl}_3, \delta \text{ ppm}): 7.31-7.29 \text{ (m, 2H)}, 7.21-7.19 \text{ (m, 3H)},$

7.15-7.13 (m, 3H), 7.04-7.02 (m, 2H), 3.95 (q, J = 8 Hz, 2H),

1.22 (t, J = 8 Hz, 3H)

¹³C NMR : $(100 \text{ MHz}, \text{CDCl}_3, \delta \text{ ppm}) 170.0, 136.3, 129.4, 129.0, 128.6, 127.9,$

127.6, 126.

2.4.9 Procedure for the preparation of polymers 106

In an oven dried RB flask, PMMA **75** (10 mmol, 1 g) was dissolved in THF solvent. Then, amine **104** (12 mmol) was added to the dissolved polymer. Then the mixture was heated to around 70 °C for 2 h. Then the reaction was distilled out to get a crude polymer. The polymer was dissolved in DCM and water was added to the reaction mixture. After work up, the organic layer was separated, dried over Na₂SO₄ and evaporated to give the polymer **106**.

2.4.10 Procedure for preparation of 2,3,5-trichloro-6-(naphthalen-2-yloxy)cyclohexa-2,5-diene-1,4-dione 123

In an oven dried 50 mL RB flask, 2-naphthol (1 mmol) was dissolved in dichloromethane (15 mL) solvent. To this solution add p- chloranil (1 mmol) at room

temperature with constant stirring. Then the reaction mixture was allowed to stir for 12 h. The reaction mixture was quenched with H_2O . The organic layer was extracted with dichloromethane (2 x 50 mL). The combined organic extracts were washed with saturated NaCl solution (15 mL) and dried over anhydrous Na_2SO_4 . Then the solvent was evaporated to get the crude product. The corresponding crude product was purified by column chromatography on silica gel (100-200) using hexane and ethyl acetate as eluent to isolate the compound.

2,3,5-trichloro-6-(naphthalen-2-yloxy)cyclohexa-2,5-diene-1,4-dione 123

Yield: 0.263 g (75%); Reddish brown color solid.

mp : 320-325 °C.

IR (neat) : (cm⁻¹) 3411, 3057, 1673, 1659, 1622, 1583,

1511, 1434, 1271, 1117, 1048, 955, 738.

¹**H NMR** : $(500 \text{ MHz}, \text{CDCl}_3, \delta \text{ ppm}): 7.29-7.59 \text{ (m, 4H)}, 7.75-7.91 \text{ (m, 3H)}.$

¹³C NMR : (125 MHz, CDCl₃, δ ppm) 174.7, 171.4, 150.9, 143.4, 141.9, 141.5,

132.0, 131.2, 128.7, 128.5, 127.6, 127.5, 123.1, 117.4, 111.4.

2.4.11 Procedure for preparation of 2,5-dichloro-3,6-diphenoxycyclohexa-2,5-diene-1,4-dione 128

In an oven dried 50 mL RB flask, Phenol (1 mmol) was dissolved in acetone (15 mL) solvent. To this solution add K₂CO₃ (2 mmol) and stir for 30 min. To the reaction mixture add *p*-chloranil (1 mmol) slowly at room temperature with constant stirring. Then the reaction mixture was allowed to stir for 12 h. After completion of reaction the solvent was evaporated on rotary vapor, and add H₂O to the crude solid and stir for some time. To this add dichloromethane (2 x 50 mL) to extract the organic product. The combined organic extracts were washed with saturated NaCl solution (15 mL) and dried over

128

anhydrous Na₂SO₄. Then the solvent was evaporated to get the crude product. The corresponding crude product was purified by column chromatography on silica gel (100-200) using hexane and ethyl acetate as eluent to isolate the compound.

2,5-dichloro-3,6-diphenoxycyclohexa-2,5-diene-1,4-dione 128

Yield : 0.230 g (63%); Red solid.

IR (**neat**) : (cm⁻¹) 3232, 1663, 1579, 1511, 1420,

1252, 1111, 1028, 975, 728.

¹**H NMR** : (400 MHz, DMSO-d₆, δ ppm): 7.42-7.38 (m,4H), 7.28-7.14 (m,

6H).

¹³C NMR : $(100 \text{ MHz}, \text{DMSO-d}_6, \delta \text{ ppm}) 173.9, 156.5, 15.09, 130.3, 130.0,$

124.1, 116.6.

2.4.12 Procedure for preparation of 2,3,5-trichloro-6-(2-hydroxynaphthalen-1-yl)cyclohexa-2,5-diene-1,4-dione 130

In an oven dried 50 mL RB flask, 2-naphthol (1 mmol) was dissolved in NMP (5 mL) solvent. To this solution add *p*- chloranil (1 mmol) at room temperature with constant stirring. Then the reaction mixture was allowed to stir for 12 h. The reaction mixture was quenched with H₂O. The organic layer was extracted with dichloromethane (2 x 50 mL). The combined organic extracts were washed with saturated NaCl solution (15 mL) and dried over anhydrous Na₂SO₄. Then the solvent was evaporated to get the crude product. The corresponding crude product was purified by column chromatography on silica gel (100-200) using hexane and ethyl acetate as eluent to isolate the compound.

2,3,5-trichloro-6-(2-hydroxynaphthalen-1-yl)cyclohexa-2,5-diene-1,4-dione 130

Yield : 0.221 g (63%); Blue color solid.

mp : 290-293 °C.

 IR (neat) : (cm⁻¹) 3324, 2870, 1672, 1644, 1583, 1546,

1480, 1315, 1294, 1215, 1138, 1050, 981, 918, 852, 793, 759, 721.

¹**H NMR** : (500 MHz, CDCl₃, δ ppm): 7.86 (t, J = 8.75 Hz, 2H), 7.48-7.45

(m, 1H), 7.41-7.38 (m, 1H), 7.32 (d, J = 8.25 Hz 1H), 7.10 (d, J =

8.25 Hz, 1H), 5.77 (s, 1H).

¹³C NMR : (125 MHz, CDCl₃, δ ppm) 174.6, 171.4, 150.5, 143.3, 142.0, 141.4,

140.5, 132.0, 128.7, 127.7, 124.1, 123.2, 117.3, 111.5.

- Foster, R. Organic Charge-Transfer Complexes. Academic Press, New York,
 1969.
- a) Mulliken, R. S. J. Chem. Phys. 1955, 23, 397. b) Mulliken, R. S. J. Am. Chem. Soc. 1950, 72, 600. c) Mulliken, R. S. J. Phys. Chem. 1952, 56, 801. d) Reid, C.; Mulliken, R. S. J. Am. Chem. Soc. 1956, 76, 3869.
- a) Taube, H. J. Am. Chem. Soc. 1942, 64, 161. b) Taube, H. J. Am. Chem. Soc. 1943, 65, 1876. c) Hochhauser, I. L.; Taube, H. J. Am. Chem. Soc. 1947, 69, 1582.
 d) Taube, H. J. Am. Chem. Soc. 1947, 69, 1418. e) Taube, H. J. Am. Chem. Soc. 1948, 70, 1216 f) Taube, H. J. Am. Chem. Soc. 1948, 70, 3928. g) Rich, R. L.; Taube, H. J. Phys. Chem. 1954, 58, 6. h) Rich, R. L.; Taube, H. J. Am. Chem. Soc. 1954, 76, 2608. i) Taube, H.; Myers, H.; Rich, R. L. J. Am. Chem. Soc. 1953, 75, 4118. j) Taube, H.; Myers, H. J. Am. Chem. Soc. 1954, 76, 2103. k) Saffir, P.; Taube, H. J. Am. Chem. Soc. 1960, 82, 13. l) Taube, H.; Gould, E. S. Acc. Chem. Res. 1969, 2, 321. m) Nordmeyer, F. R.; Taube, H. J. Am. Chem. Soc. 1968, 90, 1162. n) French, J. E.; Taube, H. J. Am. Chem. Soc. 1969, 91, 6951. o) Endicott, J. F.; Taube, H. Inorg. Chem. 1965, 4, 437. p) Stritar, J. A.; Taube, H. Inorg. Chem. 1969, 8, 2281. q) Hammershoi, A.; Geselowitz, D.; Taube, H. Inorg. Chem. 1984, 23, 979. r) Ford, P. C.; Rudd, D. P.; Gaunder, R.; Taube, H. J. Am. Chem. Soc. 1968, 90, 1187.
- a) Marcus, R. A. J. Chem. Phys. 1952, 20, 359. b) Marcus, R. A. J. Chem. Phys. 1957, 26, 872. c) Marcus, R. A. Can. J. Chem. 1959, 37, 155. d). Marcus, R. A. Annu. Rev. Phys. Chem. 1964, 15, 155. e) Marcus, R. A. J. Chem. Phys. 1965, 43,

146 References

- 2654. f) Marcus, R. A. J. Chem. Phys. **1965**, 43, 3477. g) R. A. Electrochim. Acta **1968**, 13, 995. h) Marcus, R. A. J. Chem. Phys. **1984**, 81, 5613.
- 5. Mulliken, R. S. J. Am. Chem. Soc. 1952, 74, 811.
- 6. Nagakura, S. Mol. Cryst. Liq. Cryst. 1985, 126, 9.
- 7. Taube, H.; Mayers, H.; Rich, R. L. J. Am. Chem. Soc. 1953, 75, 4118.
- 8. Wagenknecht, J. H. J. Org. Chem. 1977, 42, 1836.
- a) Marcus, R. A. J. Chem. Phys. 1956, 24, 966. b) Marcus, R. A. Angew. Chem.
 Int. Ed. 1993, 32, 1111.
- Guin, P. S.; Das, S.; Mandal, P. C. International journal of Electrochemistry. 2011,
 2011, 1.
- a) Efremov, R. G.; Baradaran, R.; Sazanov, L. A. *Nature*. **2010**, *465*, 441. b) Nohl,
 H.; Jordan, W.; Youngman, R. J. *Adv. Free. Radical. Biol.* **1986**, *2*, 211.
- 12. Patai, S.; Rappoport, Z.; Eds. *Electrochemistry of Quinones*. Wiley: New York, **1988**, 2, 719.
- 13. Suida, H. and Suida, W. *Justus Liebigs Ann. Chem.* **1918**, *416*, 113.
- Nogami, T.; Yoshihara, K.; Hosoya, H.; Nagakura, S. J. Phys. Chem. 1969, 73, 2670.
- 15. Yamaoka, T.; Nagakura, S. Bull. Chem. Soc. Japan 1971, 44, 2971.
- Sersen, F.; Koscal, S.; Banacky, P.; Krasnec, L. Coll. Czech. Chem. Comm. 1977,
 42, 2173.
- 17. Fukuzumi, S.; Kitano, T. *Chemical Physics*. **1993**, *176*, 337.
- Ciapina, E. G.; Santini, A. O.; Weinert, P. L.; Gofardo, M. A.; Pezza, H. R.; Pezza,
 L. Ecl. Quim. 2005, 30, 29.
- 19. Sun, D.; Rosokha, S. V.; Kochi, J. K. J. Phys. Chem. B. 2007, 111, 6655.

- Shanmugaraja, M. Ph.D. Thesis. 2018, School of chemistry, University of Hyderabad.
- a) Shalev, H.; Evans, D, H. J. Am. Chem. Soc. 1989, 111, 2667. b) Kebarle, P.;
 Chowdhury, S. Chem. Rev. 1987, 87, 513.
- 22. Brunschwig, B. S.; Sutin, N. Coord. Chem. Rev. 1999, 187, 233.
- 23. Guo, X.; Mayr, H. J. Am. Chem. Soc. 2014, 136, 11499.
- 24. Guo, X.; Mayr, H. J. Am. Chem. Soc. 2013, 135, 12377.
- 25. Ward, R. L.; Weissman, S. I. J. Am. Chem. Soc. 1957, 79, 2086.
- a) Rosokha, S. V.; Kochi, J. K. Acc. Chem. Res. 2008, 41, 641. b) Rosokha, S. V.;
 Kochi, J. K. J. Am. Chem. Soc. 2007, 129, 3683. c) Rosokha, S. V.; Newton, M.
 D.; Jalilov, A. S.; Kochi, J. K. J. Am. Chem. Soc. 2008, 130, 1944.
- 27. Sun, D.; Rosokha, S. V.; Kochi, J. K. J. Phys. Chem. B. 2007, 111, 6655.
- 28. Andrews, L. J.; Keefer, R. M. J. Org. Chem. 1988, 53, 2163.
- 29. John, J. H.; Loorthuraia, R.; Antoniuk, E.; Bergens, S. H. Catalysis Science and Technology. 2015, 5, 1181.
- 30. Davidson, R. S.; Slater, M. R. J. Chem. Soc. Faraday. Trans. 1. 1976, 72, 2416.
- a) Nagakura, S. *Mol. Cryst. Liq. Crtst.* 1985, 126, 9. b) Nogami, T.; Yamaoka, T.;
 Yoshihara, K.; Nagakura, S. *Bull. Chem. Soc. Japan.* 1971, 44, 380. c) Sato, Y.;
 Kinoshita, M.; Sano, M.; Akamatu, H. *Bull. Chem. Soc. Japan.* 1970, 43, 2370. d)
 Foster, R.; Thomson, J. *Trans. Faraday. Soc.* 1962, 58, 860.
- a) Lu, J. M.; Rosokha, S. V.; Lindeman, S. V.; Neretin, I. S.; Kochi, J. K. J. Am. Chem. Soc. 2005, 127, 1797.
 b) Lu, J. M.; Rosokha, S. V.; Lindeman, S. V.; Neretin, I. S.; Kochi, J. K. J. Am. Chem. Soc. 2006, 128, 16708.

148 References

Soos, Z.G.; Keller, H. J.; Ludolf, K.; Queckborner, J.; Wehe, D. J. Chem. Phys.
 1981, 74, 5287.

- 34. Venkanna, B.: Periasamy, M. unpublished results.
- a) Scanlon, D. O.; Dunnill, C. W.; John Buckeridge, J.; Shevlin, S. A; Logsdail, A. J.; Woodley, M. C.; Catlow, R. A.; Powell, M. J.; Palgrave, R. G.; Parkin, I. P.; Watson, G.W.; Keal, T. W.; Sherwood, P.; Walsh, A.; Sokol, A. A. *Nat. Mater.*,
 2013, 12, 798. b) Xiong, G; Shao R., Droubay T. C.; Joly, A. G; Beck K. M.; Chambers, S. A; Hess W. P. *Adv. Funct. Mater.* 2007, 17, 2133.
- 36. Ramesh, E.: Periasamy, M. unpublished results.

Chapter 3

Electricity Harvesting Organic Electrochemical
Cell Exploiting Reversible Electron Transfer
Reaction between Tertiary Amine Donors and
Quinone Acceptors.

3.1 Introduction

Electron-transfer reactions are of great importance in chemistry and biology. Many biological processes, like photosynthesis and oxygen transfer in living cells involve reactions that are governed by electron transfer processes. Over the years, there have been numerous reports that several popular organic reactions go through single electron transfer (SET) mechanism. These reactions take place in the ground state of the molecules. Since our interest is to construct an electrochemical cell device based on ground state reactions, a brief review on this topic reaction would facilitate the discussion.

3.1.1 Electron transfer (ET) mechanism for Birch reduction

Birch *et al.* discovered that the reduction of substituted benzene derivatives to the corresponding gave unconjugated cyclohexadienes by using Na metal in liquid ammonia (Scheme 1).²

Scheme 1

Birch reduction occurs through a SET process. The electron from Na in liquid ammonia is transferred to the benzene ring **5** to give the radical anion **6** which abstracts a proton from alcohol. Subsequent electron transfer and protonation lead to the formation of 1, 4-cyclohexadiene **7** (Scheme 2).

Scheme 2

Birch reduction is also regioselective. Whereas electron withdrawing (W) groups promote *ipso* and *para* reduction, electron donating (D) groups promote *ortho* and *meta* reduction (Scheme 3).

Scheme 3

$$N_{a} \xrightarrow{NH_{3}(liq)} N_{a}^{+} + e^{-}$$

$$D = OR, NR_{2}$$

$$W = \frac{e^{-}}{SET}$$

$$W = CO_{2}H, CO_{2}R, COR, CONR_{2}, Ar$$

$$W_{a}^{+} + e^{-}$$

$$R = \frac{e^{-}}{H}$$

$$W_{a}^{+} + e^{-}$$

$$R = \frac{e^{-}}{H}$$

$$R = \frac{e^{-}}$$

3.1.2 ET mechanism in Acyloin condensation

Acyloin condensation involves the reaction of two equivalents of carboxylic ester **12** with two equivalent of sodium metal to give the radical anion **13**. Subsequent dimerization leads to the formation of the 1,2-diketone **14** which undergoes further SET reaction to give the acyloin product **17** (Scheme 4).³

Scheme 4

3.1.3 ET mechanism in Grignard reaction

Grignard reaction is one of the most important and synthetically useful carbon-carbon bond forming reaction in organic chemistry. Grignard reactions can go through polar or single electron transfer (SET) pathway. Some representative Grignard reactions and SET intermediates are shown in Chart 1.4-7

Chart 1(Continued)

3.1.4 ET mechanism in Aldol Condensation

Aldol condensation is an important synthetic reaction involving condensation of aldehyde or ketone in the presence of a base. Generally, the reaction mechanism was considered to be in polar nature. However, Ashby *et al.*⁸ gave evidence that the Aldol reaction goes through SET pathway in some cases (Scheme 5).

Scheme 5

3.1.5 ET mechanism in Cannizzaro reaction

Cannizzaro reaction involves the reaction of an aldehyde, in the presence of a strong base (e.g. NaOH) to give an equimolar mixture of the corresponding primary

alcohol and carboxylic acid. Ashby *et al.* gave evidence for single electron transfer mechanism for Cannizzaro reaction with some aldehydes.⁹ For example, the reaction of two molecules of substituted benzaldehyde **42** with sodium hydroxide gave the benzylalcohol **44** and benzoic acid **43** along with a cyclized product **45** (Scheme 6).

Scheme 6

In the above reaction, evidence for paramagnetic intermediates was obtained by EPR spectral analysis. Hence, the mechanism outlined in Scheme 7 involving formation of radical intermediates was proposed.⁹

Scheme 7

2 CHO
2 CH3 +
$$\overline{O}$$
H OH

CH3 CH3 CH3 CH3

42 46 SET

CH3 CH3 OH

HOH

CH3 OH

CH4 OH

CH3 OH

CH4 OH

CH3 OH

CH4 OH

CH4 OH

CH4 OH

CH4 OH

CH5 OH

CH5 OH

CH5 OH

CH5 OH

CH6 OH

CH7 OH

CH7 OH

CH7 OH

CH7 OH

CH8 OH

CH9 OH

3.1.6 ET mechanism in Meerwein-Pondorf-Verley (MPV) reduction

Asbhy *et al.* also provided evidence that the MPV reduction of benzophenone **18** with lithium isopropoxide **51** proceeded *via* single electron transfer (SET) mechanism (Scheme 8). They confirmed the formation of benzophenone ketyl radical by ESR experiments.¹⁰

Scheme 8

3.1.7 ET mechanism for nucleophilic substitution reactions

In 1970, Bunnett discovered the single electron transfer pathway in nucleophilic aromatic substitution (Scheme 9).¹¹

Scheme 9

$$RX + Y^{-} \longrightarrow R\vec{X} + Y$$

$$\downarrow$$

$$RX + RY \stackrel{RX}{\longleftarrow} R\vec{Y} \stackrel{Y^{-}}{\longleftarrow} \vec{R} + X^{-}$$

Some of the S_{RN}^{-1} reactions involving SET mechanism are shown in Chart 2.¹²⁻¹⁴

Chart 2(continued)

CI NH2 MeOH, CH3CN HN HN HCI SET HN
$$NO_2$$
 NO_2 NO_2

3.1.8 Electron transfer (ET) reactions in electrochemical processes

Faraday first reported the electrochemical production of ethane by electrolysis of aqueous acetate solution in the year 1834. Kolbe reported that the anodic oxidation of carboxylate leads the decarboxylation and formed radical formed insitu combine to form a hydrocarbon (Scheme 10).¹⁵

Scheme 10

Kolbe electrolysis was applied in the synthesis of some useful organic compounds like α -Onocerin (Scheme 11).¹⁶

Scheme 11

The electrochemical oxidation is an important tool for C-H functionalization and nucleophilic functionalization of arenes (Chart 3). 17-20

Chart 3 (continued)

Also, anodic oxidation was widely used for the preparation of allylic systems. Highly reactive intermediate radical ion species were generated in the anodic oxidation (Chart 4).²¹⁻²³

Chart 4 (continued)

Similarly, the cathodic reduction also plays an important role in the reduction of organic compounds in organic synthesis (Chart 5).^{24,25}

Chart 5 (continued)

3.2 **Electron transfer in photochemical reactions**

Ме

In recent years, photochemistry of visible light active metal complexes were widely reported. For example, the metal complex Ru(bpy)₃Cl₂ has high molar extinction coefficient ($\varepsilon = 14,600 \text{ M}^{-1} \text{ cm}^{-1}$) and absorbs at 452nm. It is widely used as a photocatalyst in organic synthesis. Some of the important photochemical reactions are shown in Chart 6.26-31

Chart 6 (continued)

Chart 6 (continued)

$$R^{1} \longrightarrow N_{Ar} \qquad \frac{Ir(bpy)_{2}(dtbbpy)PF_{6} (1.0 \text{ mol}\%)}{R^{2}CH_{2}NO_{2}, 15 \text{ W CFL}}$$

$$rt, 10-18 \text{ h}$$

$$R^{2} \longrightarrow N_{2}$$

$$R^{2} \longrightarrow N_$$

In all these electron transfer reactions, organic compounds are obtained as end products. However, our interest is on the development of organic electrochemical cells to produce electricity from radical ion intermediates before they give organic products. Accordingly, methods to produce electricity through donor-acceptor solar cells are briefly reviewed in the next section.

3.3 Organic solar cells

The organic photovoltaics or solar cells are flexible devices with low manufacturing cost compared to inorganic solar cells. A brief review on reports on the construction of various types of organic solar cells including donor/acceptor organic photovoltaic cells would facilitate discussion of present studies involving radical cation and radical anion formed in ground state electron transfer reactions.

In organic solar cells, upon excitation of organic active materials the holes (positive charges) are created in the donor layer and electron (negative charges) in the acceptor layer. The electron-hole pair (exciton) is produced upon photo excitation of the light harvesting organic material. In the presence of electric field, the exciton splits into charge carriers (separated electron and hole) which move to the respective electrodes.

Some donor polymers and acceptors used in the heterojunction organic solar cells are shown in Figure 1.

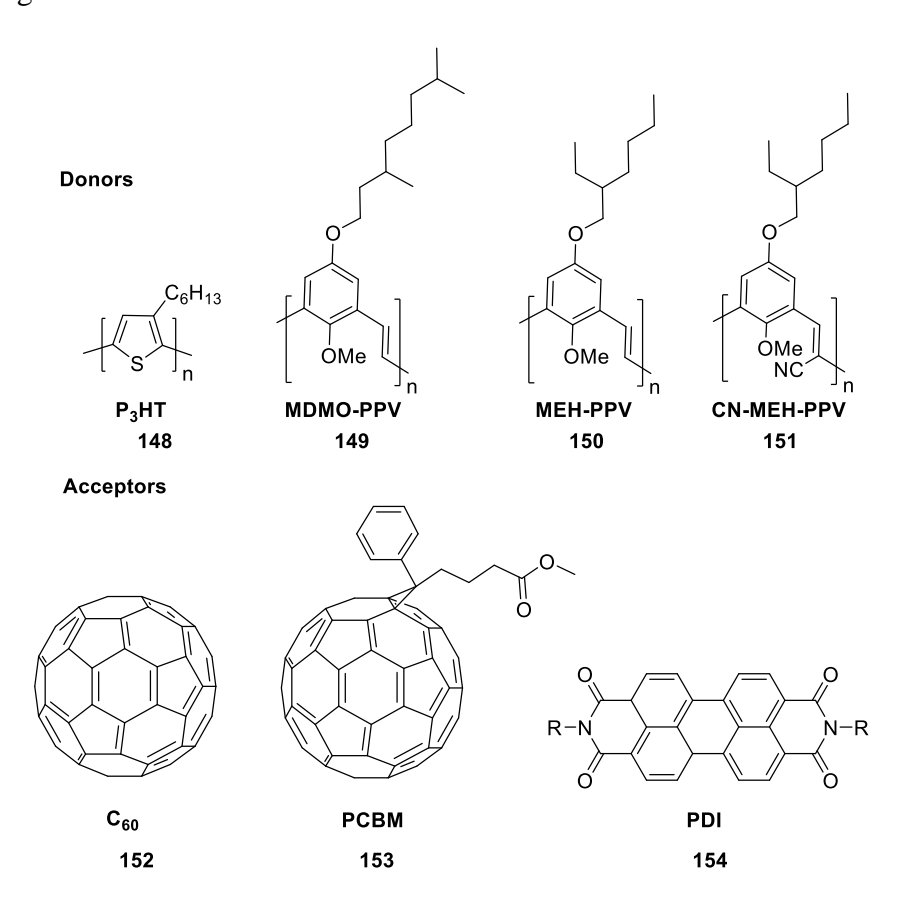


Figure 1. Major donor polymers and acceptors used in the organic solar cells.

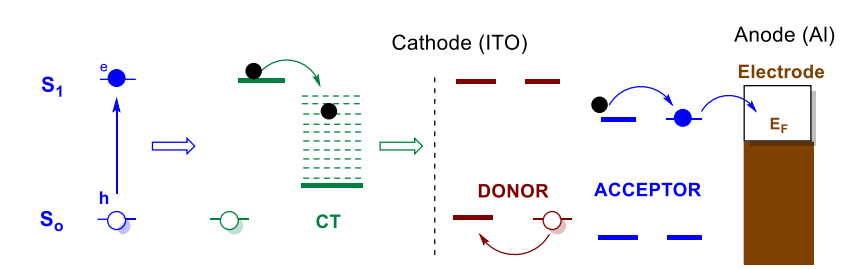


Figure 2. Energy diagram in the organic solar cells.

3.3.1 Single layer organic cells

The conducting indium tin oxide (ITO) with work function (4.4-4.5 eV) is used as ITO cathode and the low work function metals such as aluminum (4.06-4.26 eV), magnesium (3.66 eV) or calcium (2.87 eV) are used as anode in organic solar cells.³² The

cell was made by sandwiching the organic donor and acceptor materials between the ITO and the metal (Figure 3).

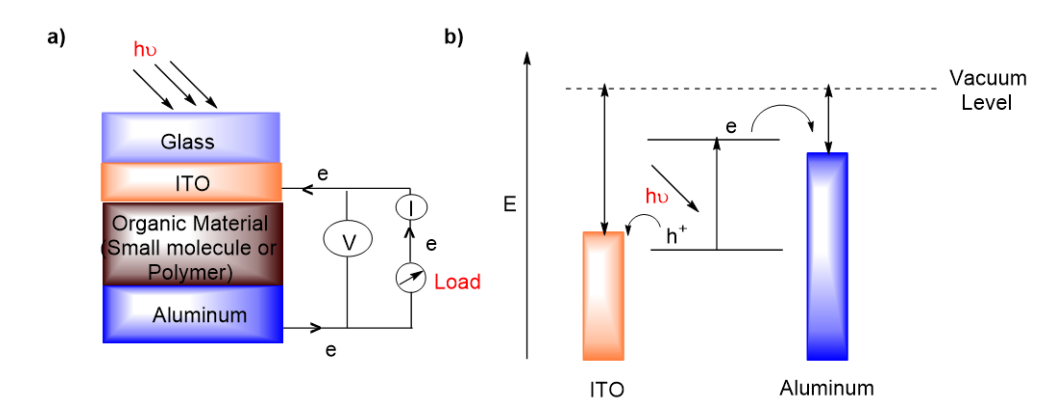


Figure 3. (a) Schematic diagram for single layer organic solar cell (b) Energy level diagram for organic solar cell.

When the organic material absorbs the sun light, the electrons are excited to the LUMO and holes are in the HOMO. Thus, the potential created by the different work functions of the metals splits the exciton pair. The electrons move to the anode and holes to the cathode. Ghosh and co-workers reported³³ that magnesium phthalocyanine (MgPc) in the single layer solar cell (Al/MgPc/Ag) produce power with conversion efficiency 0.01%. Glenis and co-workers reported³⁴ 0.15% power conversion efficiency in the single layer cell using poly-3-methyl thiophene. In the case of single layer cell using the conjugated polymer polyacetylene 0.3% conversion efficiency was reported.³⁵ These types of cells produce less than 1% power conversion efficiency.

3.3.2 Bilayer donor-acceptor solarcells

Bilayer cells are constructed by sandwiching two different donor and acceptor layers between the ITO and metal conductors (Figure 4 (a)).

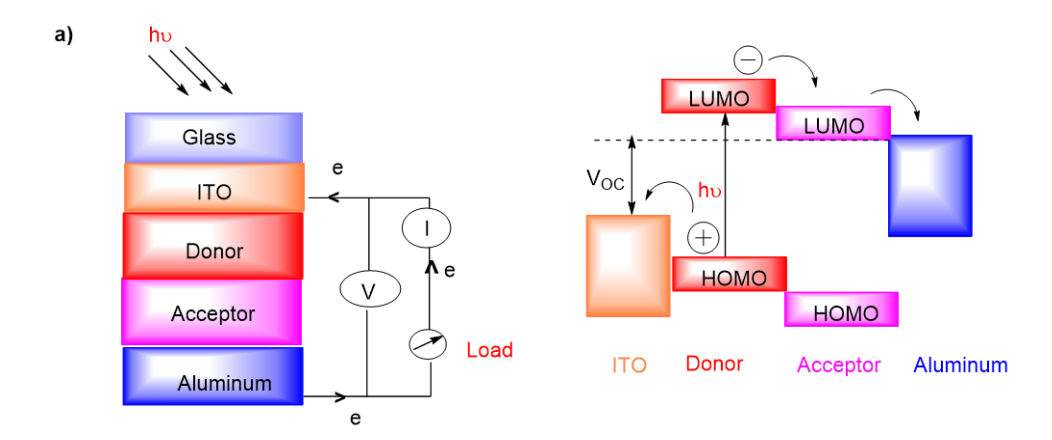


Figure 4. (a) Schematic diagram for bilayer organic solar cell (b) Energy level diagram for bilayer organic solar cell.

As the electron affinity and ionization energy of the donor and acceptor layers are different, electrostatic forces are generated at the interface. Hence, in this cell the exciton splits efficiently compared to the single layer cell. The layer having high electron affinity is called as electron acceptor and the layer with low ionization energy acts as electron donor. It was reported³⁶ that C₆₀ acts as an acceptor and poly (2-methoxy-5-(2'-ethylhexyloxy- 1,4-phenylene-vinylene), MEH-PPV acts as a donor. Perylene amide derivatives which earn high electron affinity can be also used as acceptor.

Tang *et al.* reported³⁷ cells with copper phthalocyanine (CuPc) acts as electron donor and perylene tetracarboxylic amide derivative acts as acceptor in two layer organic solar cell. This cell gave 1% power conversion efficiency. Halls *et al.* reported³⁸ that bilayer cell with donor polymer poly (p-phenylenevinylene) PPV and acceptor C_{60} . This PPV/ C_{60} cell produced 9% power conversion efficiency.

3.3.3 Bulk heterojunction (BHJ) solar cell

In organic solar cells, the layer thickness is important for the effective absorption of light. If the layer thickness increases, there is increase in the exciton diffusion pathway in the donor-acceptor interface. Exciton has shorter life time and it can recombine before reaching the electrodes. The light absorption efficiency increases when the exciton

diffusion pathway is minimized by placing a mixture of donor-acceptor blend as in bulk heterojunction solar cell. The light absorbing layer of bulk heterojunction solar cell consists of a blend of donor and acceptor materials. In these cells, the donor and acceptor were mixed together and deposited over the ITO electrode (Figure 5 (a)).

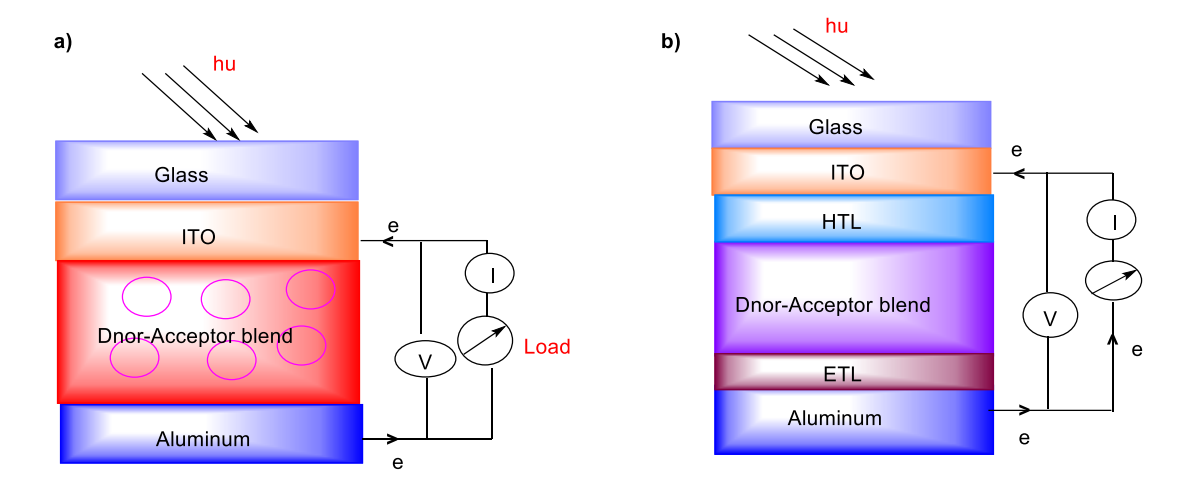


Figure 5. (a) Schematic diagram for Bulk heterojunction solar cell (b) Use of buffer HTL (hole transport layer) and ETL (electron transport layer) layers.

In bulk heterojunction solar cells, the active layer consists of conjugated donor and fullerene type acceptor. The efficiency of the polymer photovoltaic (single layer) cell was improved by the introduction of fullerene based derivatives. Yu *et al.* reported³⁹ that the cell with a blend of polymer MEH-PPV donor and fullerene based acceptor as the heterojunction. The device using Ca/MEH-PPV/PCBM/ITO gave 2.9% power conversion efficiency. Yu and co-workers⁴⁰ replaced MEH-PPV polymer with poly 3-octylthiophen (P3OT) polymer which improved the power conversion efficiency.

3.3.4 Electricity harvesting cells based on ground state electron transfer reactions

As described in Chapter 2, amines readily undergo electron transfer reactions to give the corresponding radical cation—anion pair in dipolar aprotic solvent like PC (propylene carbonate). The esr signal strength decreases with time indicating that the

initially formed paramagnetic radical ion intermediates may combine to form charge transfer (CT) complexes but in equilibrium with the charged species (Scheme 12).

Scheme 12

$$R_3N + Q \longrightarrow R_3N + Q \longrightarrow \begin{bmatrix} R_3N, Q \end{bmatrix}$$
155 156 157 158 159
CT complex

An interesting possibility is development of an electrochemical cell device based on transport of charges in these radical cation and anion species to the electrodes to complete the circuit. If the electron transfer from the amine donor to the quionone acceptor could happen reversibly, then the device would be useful for continuously converting the heat around it to electricity (Figure 6).

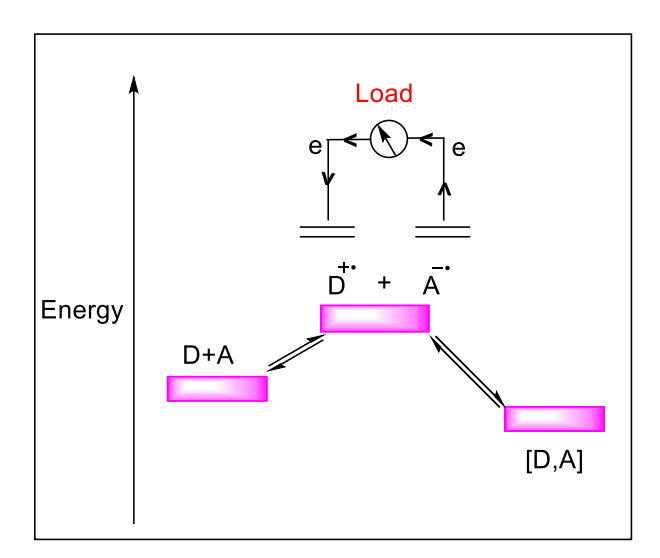


Figure 6. Ground state electron transfer between organic electron donor (D) and acceptor (A)-construction of an electricity harvesting cell.

The difference between such ground state electron transfer process and the electron transfer involved in donor/acceptor photovoltaic or solar cells is that in the later case the electron transfer from a donor to an acceptor takes place after photoexcitation of the electron in the ground state to excited state. The results on the construction of an electricity harvesting cell based on ground state electron transfer reaction (Scheme 12) are described and discussed in the next section.

3.4 Results and Discussion

We have selected the readily accessible quinones and amines listed in Figure 7 for studies on the construction of organic electrochemical cell. We have selected the highly electron deficient *p*-chloranil **167** (CA) as acceptor for detailed studies as it acts as an electron acceptor even with tertiary amides. The phthalimide **168** and N-methylphthalimide (MeN-phthalimide) **169** were selected as electron transporters for our studies. Also, we have selected the donors *N*,*N*-diethylaniline (PhNEt₂) **160**, *N*,*N*'-tetramethyl-1,4-phenylenediamine (TMPDA) **161**, triphenylamine (TPA) **162**, 1,4-diazabicyclo[2.2.2]octane (DABCO) **163**, *N*, *N*-diisopropylethylamine (DIPEA) **164** and *N*,*N*-diisopropylbenzamide (DiPrBA) **165** for the construction of the electrochemical cell.

Figure 7: Eelectron donors and acceptors for use in electrochemical cells.

3.4.1 Construction of energy harvesting electrochemical cell.

3.4.1.1 Two layer cell configuration

Previously, it was observed in this laboratory⁴¹ that the cells can be easily constructed by making donor and acceptor pastes using TiO₂, polyethylene oxide (PEO)

170 Results and discussion

and propylene carbonate (PC) and coating on commercially available Al (0.2mm x 5cm x 5cm) and SS (SS 304, 0.05mm x 5cm x 5cm) foils or graphite sheet (0.4mm x 5cm x 5cm). The configuration of two layer cell was constructed as shown in Figure 8.

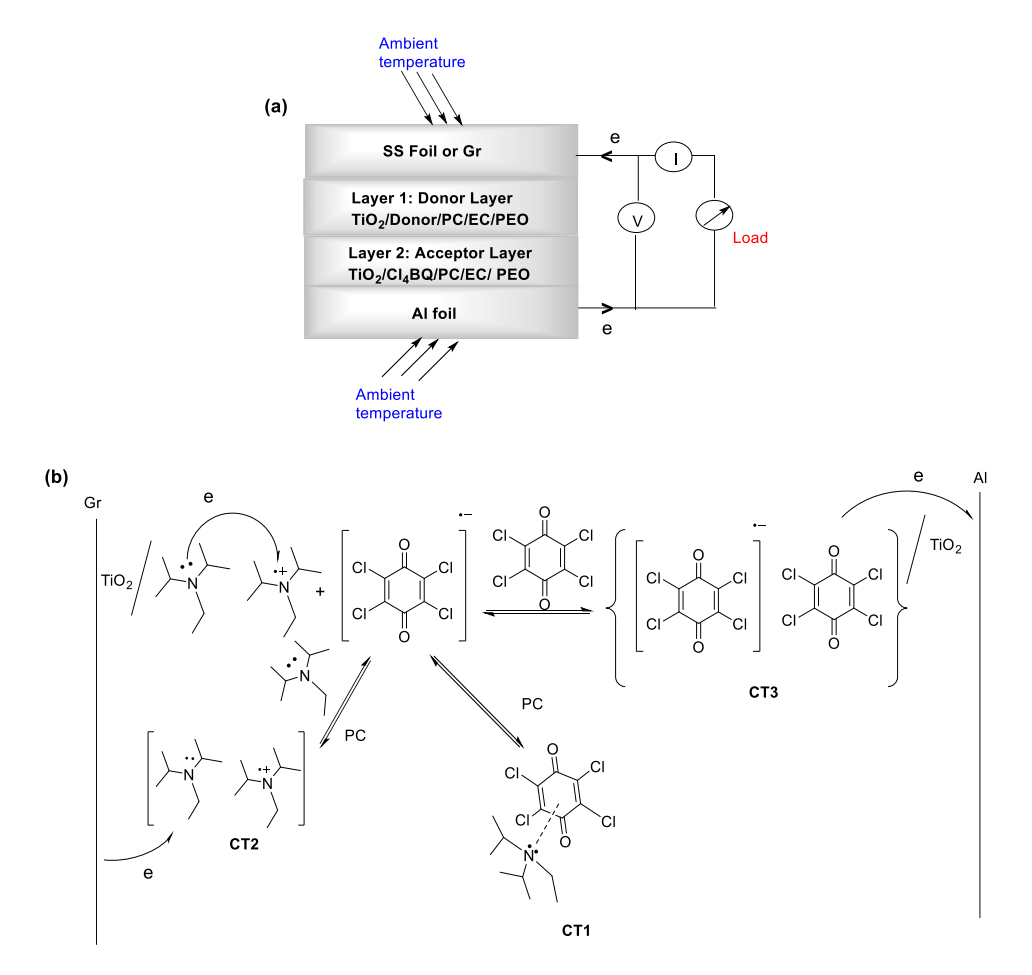


Figure 8. (a) Schematic diagram of cell with two layer configuration (b) Tentative mechanism for electron transport via D/D^{-+} and A^{-}/A exchange reactions.

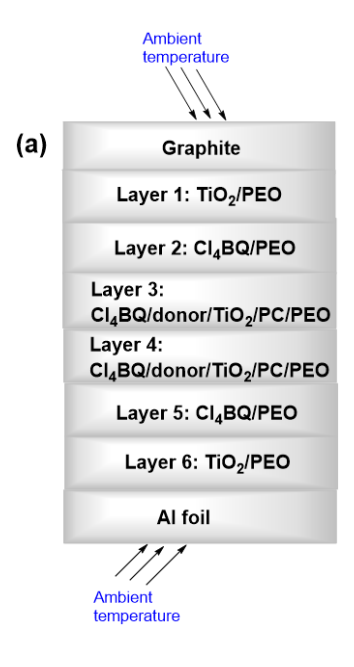
The acceptor layer was coated on Al foil and the donor layer was coated on SS foil or Graphite sheet. The foils were then sandwiched to construct the electrochemical cell. Initially, we have used SS foils but visible holes were formed indicating corrosion and hence later graphite sheets were used. The configuration of two layers electrochemical cell are almost similar to the bi-layer in organic solar cell⁴² but the electron transport would

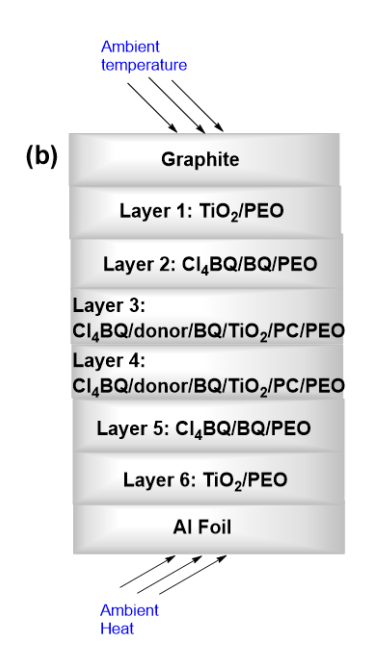
have contributions from both ionic conduction and also through exchange reactions involving D/D^{-+} and A^{--}/A .

It was observed that the two layer cells did not produce power after 24 h. Hence, multilayer cells were constructed which gave better results.

3.4.1.2 Multi-layer Cell Configuration

The multilayer cells constructed in this laboratory⁴¹ as shown in Figure 9.





1 h after packing

Donor	Pmax/mW/FF(40 °C)	Donor	Pmax/mW/FF(40 °C)
TMPDA	3.099/0.261	TMPDA	1.614/0.282
TPA	0.375/0.245	TPA	0.939/0.219
DABCO	6.155/0.206	DABCO	4.806/0.432
DIPEA	8.147/0.347	DIPEA	11.74/0.296
DiPrBA	4.193/0.295	DiPrBA	1.871/0.232

48 h after packing

Donor	Pmax/mW/FF(40 °C)	Donor	Pmax mW/FF(40°C)
TMPDA	1.822/0.250	TMPDA	1.299/0.263
TPA	0.142/0.256	TPA	0.728/0.219
DABCO	1.216/0.249	DABCO	3.776/0.434
DIPEA	2.057/0.334	DIPEA	8.338/0.394
DiPrBA	2.969/0.273	DiPrBA	1.411/0.243

...Figure 9 (continued)

Figure 9. (a) Schematic diagram of multi-layer with Cl₄BQ/Donor/PC/TiO₂/PEO configuration and (b) Schematic diagram of multi-layer with Cl₄BQ/Donor/BQ/TiO₂/PC/PEO configuration packing (c) Tentative mechanism for electron transport to the electrodes *via* D/D.+ and A-/A exchange reactions.

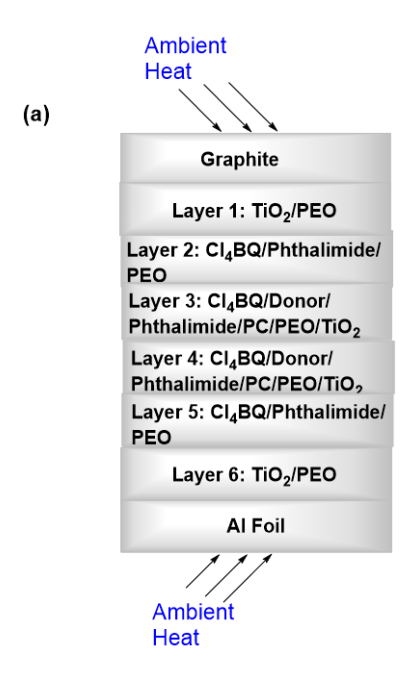
The multilayer cells with different configurations were made by coating TiO₂/PEO on both electrodes, followed by coating of Cl₄BQ/PEO on TiO₂/PEO/Al and TiO₂/PEO/Gr. Then, the Cl₄BQ/donor/PC/PEO pastes were coated above the Cl₄BQ/PEO layers as shown in Figure 9.

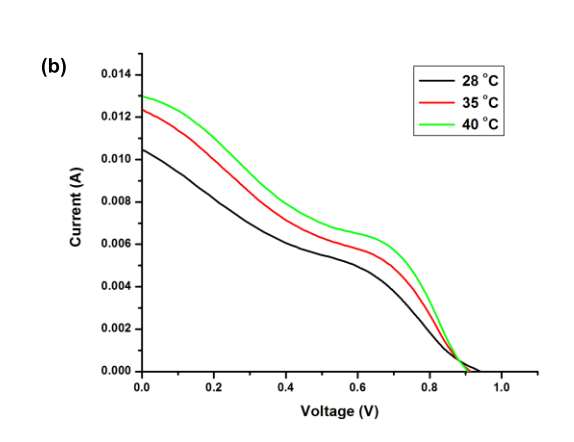
In these configurations the solvent PC (propylene carbonate) was used for dissolving the donor and acceptor to facilitate the electron transfer reaction. The IV curves are recorded at 28 °C, 35 °C and 40 °C after 1 h and 48 h after packing. The higher power outputs presented (Pmax) observed at 1 h after packing and that observed after 48 h.

The epr studies indicated that the initially formed radical ions are transformed to charge transfer complexes with time as discussed in chapter 2. This could account for the reduction of current and Pmax values with time as the concentration of radical ions would be lesser with time. It was reported that radical anions of compounds with lesser electron affinity are stabilized to more extent in polar solvents. Since, benzoquinone (BQ) has lesser electron affinity (EA 1.91 eV) accompared to *p*-chloranil (EA 2.78 ev), the BQ could accept electron from *p*-chloranil radical anion and hence the *p*-chloranil will be

available for reversible electron transfer from the amines. Indeed, the Pmax values were higher in reactions using BQ for electron transport (Figure 9).

The electron affinity of phthalimides⁴⁴ are about EA=1.015 eV compared to that of benzoquinone (EA=1.91 eV) and p-chloranil (EA=2.78 eV). Therefore, we have constructed the cell with phthalimide in 4 layers with different donors using PC as solvent (Figure 10).





1	h	after	packing

Donor	Pmax/mW/FF(28 °C)	Donor	$Pmax/mW/FF(35~^{\circ}C)$	Donor	$Pmax/mW/FF(40~^{\circ}C)$
TMPDA	1.509/0.427	TMPDA	1.903/0.449	TMPDA	2.107/0.428
TPA	0.795/0.254	TPA	0.921/0.254	TPA	0.921/0.25
DABCO	3.834/0.25	DABCO	4.9/0.256	DABCO	5.62/0.249
DIPEA	5.495/0.242	DIPEA	8.473/0.337	DIPEA	9.596/0.4
DiPrBA	2.612/0.255	DiPrBA	2.706/0.251	DiPrBA	2.779/0.257
48 h afte	r packing				
Donor	Pmax/mW/FF(28 °C)	Donor	Pmax/mW/FF(35 °C)	Donor	Pmax/mW/FF(40 °C)
TMPDA	0.713/0.25	TMPDA	0.854/0.236	TMPDA	0.974/0.237
TPA	0.311/0.255	TPA	0.384/0.248	TPA	0.418/0.256
DABCO	1.32/0.188	DABCO	1.835/0.205	DABCO	2.284/0.223
DIPEA	2.972/0.302	DIPEA	3.55/0.315	DIPEA	4.082/0.347
DiPrBA	1.274/0.277	DiPrBA	1.532/0.282	DiPrBA	1.641/0.296

...Figure 10 (continued)

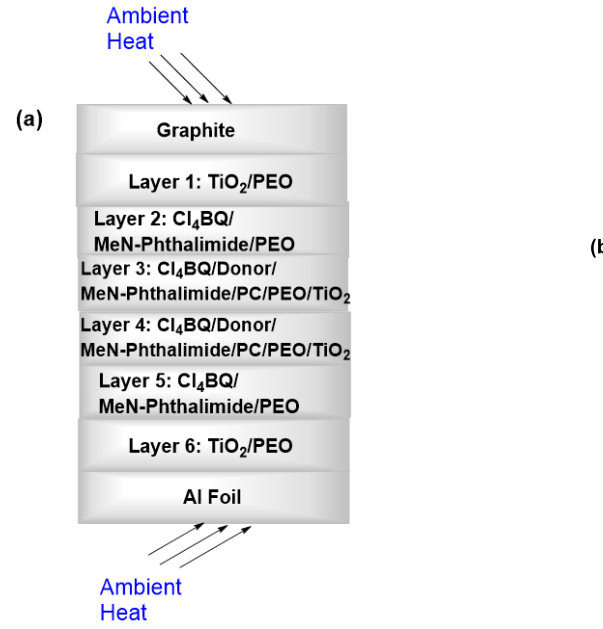
Figure 10. (a) Schematic diagram of multi-layer with Cl₄BQ/Phthalimide/Donor/PC/TiO₂/PEO configuration. (b) Representative IV for the cell (Table ES 1, entry 4, DIPEA donor). (c) Tentative mechanism for electron transport to the electrodes via D/D.+ and A-/A exchange reactions.

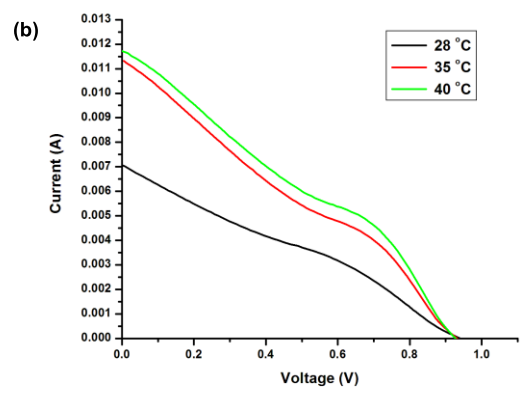
We have recorded IV-data after 1 h and 48 h after packing as outline in Figure 10. The 1 h IV-data values are high compared to 48 h, as initially more number of radical ions will be present leading to better conduction. The power output becomes less with time indicating that the amine radical cations and *p*-chloranil anions are converted to charge transfer complexes (CT1, CT2 and CT3). The conduction will decrease with formation of CT complexes, as little conduction can be expected with these CT complexes, especially formation of CT1 complex.

Among various donors TMPDA, TPA, DABCO, DIPEA and DiPrBA, the donor DIPEA gave better results at 28 °C, 35 °C, and 40 °C (Figure 10). The recorded IV data of cell Figure 10a (after 1 h packing) the power maximum (Pmax) and Fill factor (FF) values for DIPEA at 28 °C (Pmax=5.495 mW, FF=0.242) at 35 °C (Pmax=8.473 mW, FF=0.337) and at 40 °C (Pmax=9.596 mW, FF=0.4) (Table ES1 entry 4). While increasing temperature we have observed that the Pmax and FF values increase and higher values are obtained at 40 °C. This may be due to the increase in rate of electron transport and also

dissociation of charge transfer complexes (CT1, CT2 and CT3) to the radical ions. The increase in the temperature may also induce the ions to cross the activation energy barrier to reach the electrode for conduction. The power output is less even at 40 °C after 48 h (Pmax=4.082 mW) compared with 1 h recorded values (Table ES1 entry 4). The decrease in Pmax due to formation of charge transfer complexes (CT1, CT2, CT3 and CT4) which will decrease the conduction with time, especially in the case of CT1 complex.

Surprisingly, the Pmax values obtained using the phthalimide in 4 layers (Figure 10) are much lower compared to those obtained using benzoquinone (Figure 9). Presumably, the phthalimide radical anions may be more stable and hence lead to poor conduction (Figure 10c). Hence, we have constructed the cell using the MeN-phthalimide in the place of phthalimide (Figure 11).





1 h after packing

Donor	Pmax/mW/FF(28 °C)	Donor	$Pmax/mW/FF(35 \ ^{\circ}C)$	Donor	Pmax/mW/FF(40 °C)
TMPDA	1.582/0.227	TMPDA	1.961/0.238	TMPDA	2.009/0.217
TPA	0.490/0.247	TPA	0.605/0.246	TPA	0.648/0.254
DABCO	2.372/0.218	DABCO	3.329/0.224	DABCO	3.805/0.239
DIPEA	4.616/0.223	DIPEA	6.353/0.326	DIPEA	6.41/0.355
DiPrBA	1.495/0.242	DiPrBA	1.533/0.253	DiPrBA	1.689/0.248

...Figure 11(continued)

48 h after packing

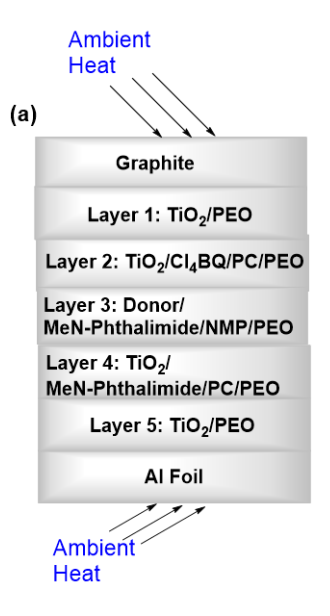
Donor	$Pmax/mW/FF(28~^{\circ}C)$	Donor	$Pmax/mW/FF(35~^{\circ}C)$	Donor	$Pmax/mW/FF(40~^{\circ}C)$
TMPDA	0.946/0.292	TMPDA	1.257/0.285	TMPDA	1.302/0.295
TPA	0.167/0.254	TPA	0.214/0.257	TPA	0.254/0.265
DABCO	1.581/0.2	DABCO	2.239/0.203	DABCO	2.662/0.214
DIPEA	1.917/0.289	DIPEA	2.908/0.276	DIPEA	3.313/0.305
DiPrBA	0.468/0.244	DiPrBA	0.519/0.25	DiPrBA	0.527/0.245

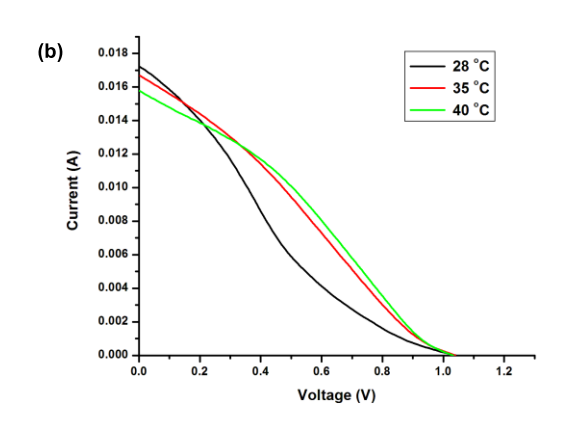
$$\begin{array}{c} \text{Gr} \\ \text{(c)} \\ \text{TiO}_2 \\ \text{CI} \\ \text{$$

Figure 11. (a) Schematic diagram of multi-layer with Cl₄BQ/MeN-Phthalimide/Donor/PC/TiO₂/PEO configuration. (b) Representative IV for the cell (Table ES 1, entry 9, DIPEA donor). (c) Tentative mechanism for electron transport.

In this cell configuration also, DIPEA gave better results compared to other donors (Figure 11). The Pmax and FF values (Pmax=3.313 mW, FF=0.313) at 40 °C after 48 h (Figure 11) were less compared to the Pmax and FF values (Pmax=4.082 mW, FF=0.347) realized using phthalimide (Figure 10). Clearly, the conduction was better with phthalimide compared to MeN-phthalimide as electron transporter in PC solvent.

As discussed in chapter 2, NMP forms charge transfer complex with p-chloranil. Also, p-chloranil is soluble in NMP solvent to more extent compared to solubility in PC. For instance, whereas only 0.03 g of p-chloranil is soluble in 1 mL PC, 0.1 g is soluble in 1 mL NMP. Hence, we have chosen NMP as solvent along with PC (Figure 12) and constructed the cell using MeN-phthalimide as (Figure 12a).





1 h after packing

Donor	Pmax/mW/FF(28 °C)	Donor	Pmax/mW/FF(35 °C)	Donor	Pmax/mW/FF(40 °C)
TPA	1.915/0.208	TPA	2.322/0.22	TPA	2.378/0.218
DABCO	1.82/0.158	DABCO	2.962/0.205	DABCO	4.166/0.24
DIPEA	0.811/0.137	DIPEA	1.362/0.163	DIPEA	1.723/0.179
DiPrBA	1.042/0.155	DiPrBA	1.591/0.176	DiPrBA	1.872/0.185
48 h afte	r packing				
Donor	Pmax/mW/FF(28 °C)	Donor	$Pmax/mW/FF(35~^{\circ}C)$	Donor	Pmax/mW/FF(40 °C)
TPA	2.635/0.203	TPA	2.868/0.221	TPA	3.035/0.233
DABCO	3.563/0.199	DABCO	4.729/0.273	DABCO	5.051/0.311
DIPEA	2.369/0.178	DIPEA	3.117/0.213	DIPEA	3.785/0.233

Figure 12. (a) Schematic diagram of multi-layer with Cl₄BQ/PC/Donor/MeN-phthalimide/NMP/TiO₂/PEO configuration. (b) Representative IV for the cell (Table ES2, entry 12, DABCO donor).

The performance of the cell improved when NMP was used (Figure 12). In the cell configuration as in Figure 11, the DIPEA donor gave higher Pmax (Pmax=3.785 mW) value. In the cell configuration as in Figure 12, the DABCO gave higher power (Pmax=5.051 mW) as shown in Table ES2, entry 12. Also, the shapes of the IV-curve (Figure 12b) are also better compared to the IV-curve shown in Figure 11b.

We have also constructed the cell by using only NMP as solvent. Accordingly, a cell with similar configuration was constructed using N-methylphthalimide in NMP solvent without PC (Figure 13).

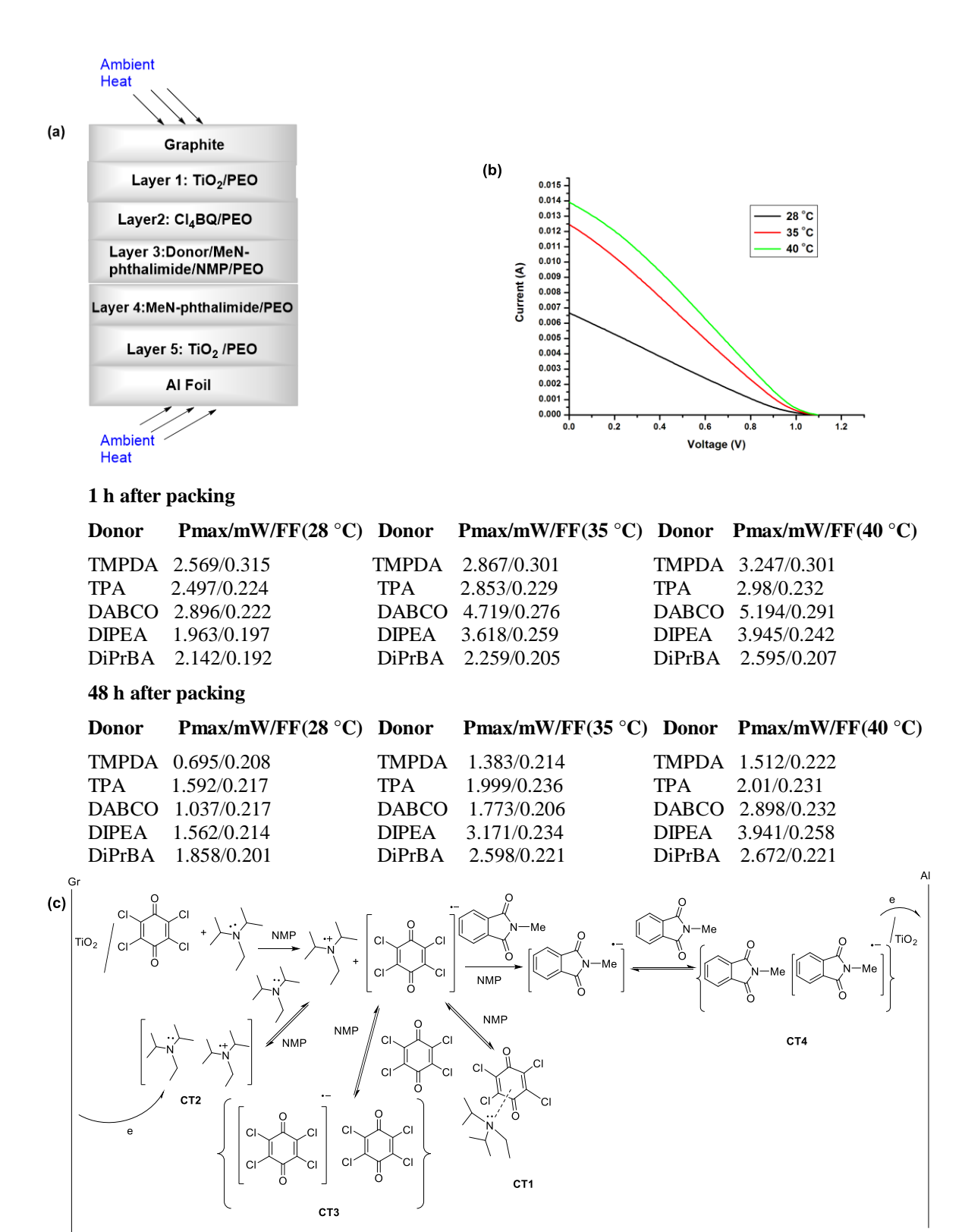


Figure 13. (a) Schematic diagram of multi-layer with Cl₄BQ/Donor/MeN-Phthalimide/NMP/TiO₂/PEO configuration. (b) Representative IV for the cell (Table ES3, entry 18, DIPEA donor). (c) Tentative mechanism for electron transport to the electrodes via D/D.+ and A-/A exchange reactions.

DABCO 3.28/0.23

DiPrBA 2.719/0.313

In this configuration DIPEA gave better results than other donors (Figure 13a). However, the Pmax values obtained for the donor DIPEA in the configurations in Figure 12 and 13 were almost the same Pmax(mW)/FF=3.785/0.233 and Pmax(mW)/FF=3.941/0.258.

We have then constructed the 7 layer configuration using MeN-phthalimide and NMP solvent (Figure 14a).

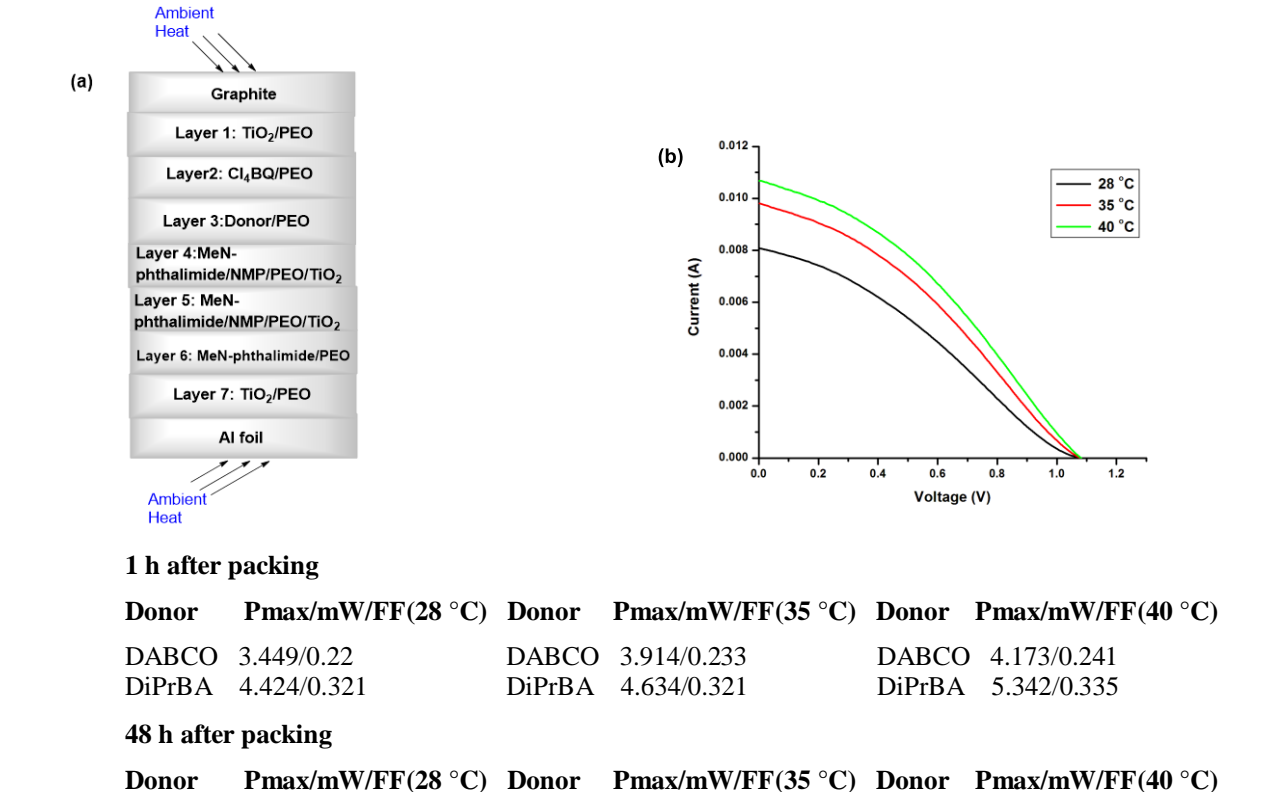


Figure 14. (a) Schematic diagram of multi-layer with Cl₄BQ/Donor/MeN-phthalimide/NMP/TiO₂/PEO configuration. (b) Representative IV for the cell (Table ES3, entry 21, DiPrBA donor).

3.566/0.336

DABCO 3.622/0.246

DiPrBA 4.032/0.349

DABCO 3.457/0.246

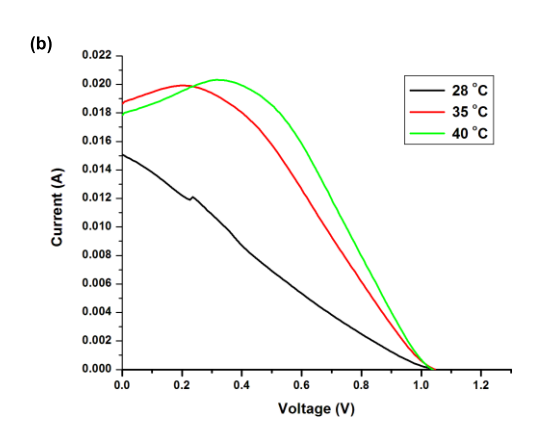
DiPrBA

The cell configuration Figure 14a gave better results with the electron transporter MeN-phthalimide using donors DABCO and DIPEA. There is also increase in the Pmax values and improvement in the shape of the IV-curve for the configuration as in Figure 14.

Among the two donors studied, the relatively weak donor DiPrBA gave better results, Pmax=4.032 mW for the amide donor DiPrBA compared to DABCO Pmax=3.622 mW.

Earlier the BQ was used as electron transporter as the corresponding radical anion is expected to interact better with the PC solvent compared to *p*-chloranil radical anion (Figure 10). Hence, we have also carried out experiments using BQ as electron transporter and NMP as solvent. The results are presented in Figure 15.





1 h after packing

Donor	Pmax/mW/FF(28 °C)	Donor	$Pmax/mW/FF(35~^{\circ}C)$	Donor	$Pmax/mW/FF(40~^{\circ}C)$
TMPDA	2.998/0.239	TMPDA	4.069/0.287	TMPDA	4.191/0.266
TPA	2.123/0.181	TPA	3.346/0.188	TPA	4.123/0.203
DABCO	7.082/0.175	DABCO	13.03/0.242	DABCO	13.67/0.3
DIPEA	6.266/0.184	DIPEA	12.88/0.282	DIPEA	14.01/0.317
48 h after	r packing				
Donor	Pmax/mW/FF(28 °C)	Donor	Pmax/mW/FF(35 °C)	Donor	Pmax/mW/FF(40 °C)
Donor	Pmax/mW/FF(28 °C) 1.436/0.262	Donor TMPDA	· · ·		Pmax/mW/FF(40 °C) 1.849/0.306
Donor	· · · · ·		· · ·		
Donor TMPDA TPA	1.436/0.262	TMPDA	1.605/0.277 3.505/0.302	TMPDA TPA	1.849/0.306

(c)

Gr

$$TIO_2$$
 CI
 CI

Figure 15. (a) Schematic diagram of multi-layer with Cl₄BQ/Donor/BQ/NMP/TiO₂/PEO configuration. (b) Representative IV for the cell (Table ES4, entry 25, DIPEA donor) (c) Tentative mechanism for electron transport.

Indeed, the performance of the cells improved and higher Pmax and FF values were realized in this cell configuration. The cell using DABCO gave higher Pmax 6.394 mW with FF 0.353 and the cell using DIPEA gave Pmax 9.579 mW and FF 0.516 (Figure 15). The solubility of *p*-chloranil and bezoquinone are high in NMP which may contribute to higher current and power realized.

Since, the use of NMP solvent gave higher Pmax values, we have constructed double cells coating TiO_2/PEO on two Al foils and both sides of graphite sheet (Al/Gr/Al configuration) using only NMP solvent and p-chloranil (Figure 16).

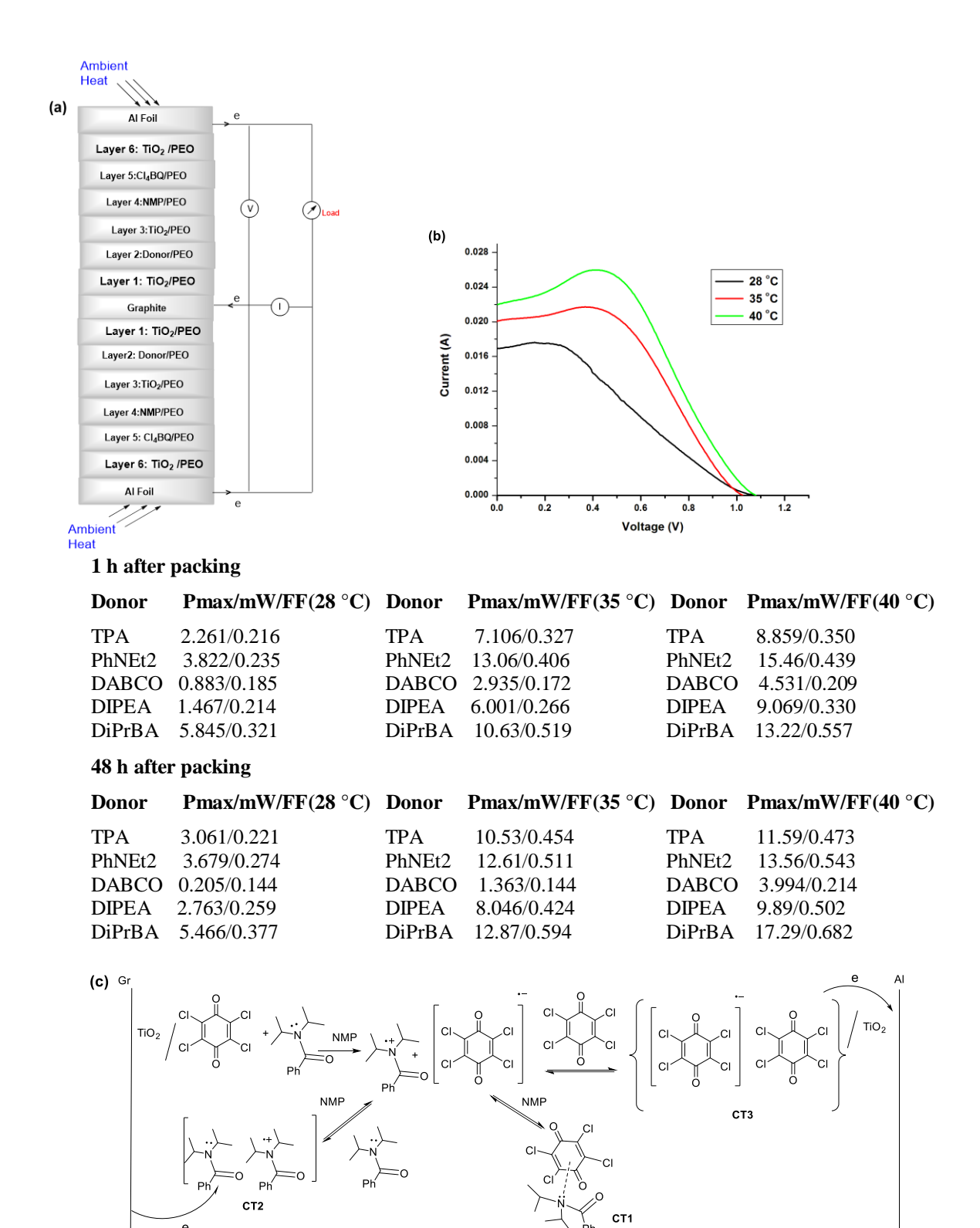
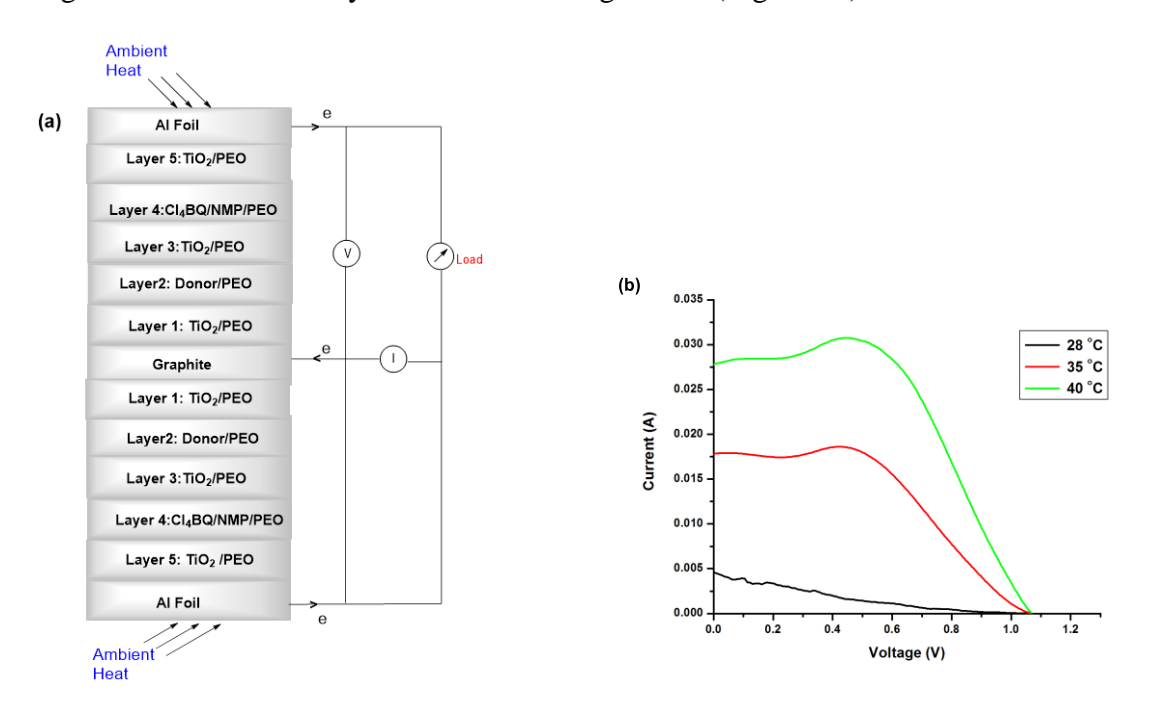


Figure 16. (a) Schematic diagram of multi-layer with Donor/Cl₄BQ/NMP/TiO₂/PEO configuration. (b) Representative IV for the cell (Table ES5, entry 30, DiPrBA donor). (c) Tentative mechanism for electron transport to the electrodes via D/D.+ and A-/A exchange reactions.

In this double cell configuration, the Pmax and FF values were higher at 40 °C compared to the power obtained with other configurations. For example, in the case of the *N*,*N*-diisopropyl benzamide the fill factor (FF) was 0.682 compared to other fill factor values, FF=0.296, Figure 10, FF=0.245, Figure 11, FF=0.23, Figure 12, FF=0.207, Figure 13 and FF=0.335, Figure 14. Also, the amide donor DiPrBA, gave higher Pmax values compared to the other donors used in the cell configuration Figure 16a.

As discussed earlier (chapter 2), the DiPrBA gave weak DiPrBA epr signals and weak charge transfer complexes with *p*-chloranil which could be reason for lower Pmax/FF values at 28 °C (Figure 16). Presumably, the radical ions are likely to be formed in more amounts and the mobility of ions also will be better leading to higher current and power (Figure 16).

We have also constructed the double cell with p-chloranil and NMP solvent together in the middle layer in another configuration (Figure 17).



...Figure 17 (continued)

1 h after packing

 Donor
 Pmax/mW/FF(28 °C)
 Donor
 Pmax/mW/FF(35 °C)
 Donor
 Pmax/mW/FF(40 °C)

 DiPrBA
 0.867/0.173
 DiPrBA
 9.374/0.493
 DiPrBA
 17.24/0.582

 48 h after packing

 Denor
 Pmax/mW/FF(28 °C)
 Ponor
 Pmax/mW/FF(35 °C)
 Ponor
 Pmax/mW/FF(40 °C)

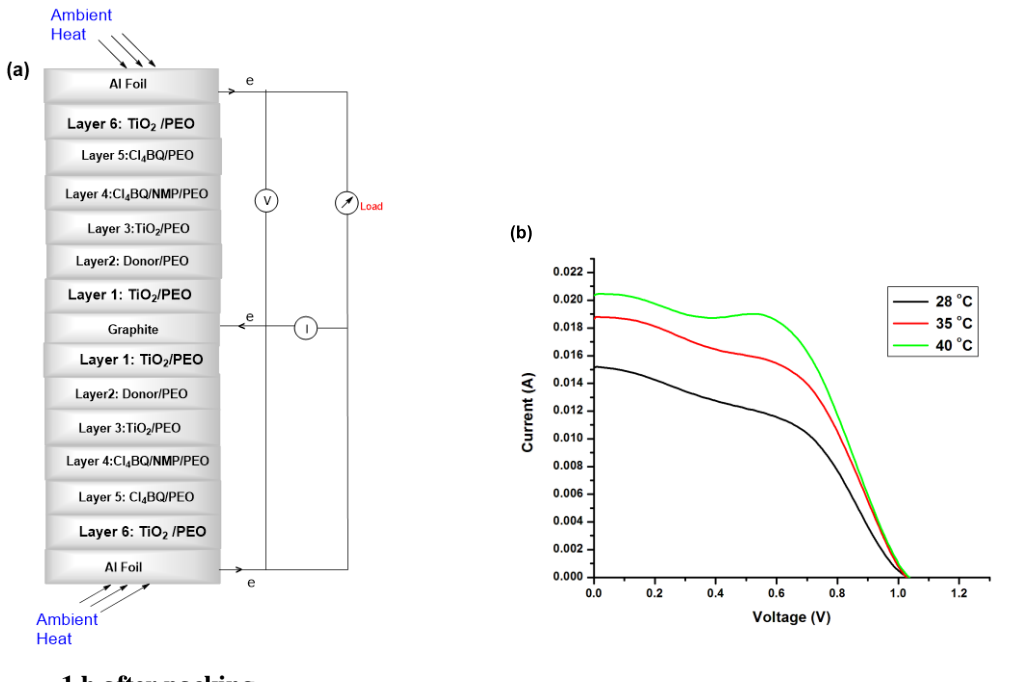
 Donor
 Pmax/mW/FF(28 °C)
 Donor
 Pmax/mW/FF(35 °C)
 Donor
 Pmax/mW/FF(40 °C)

 DiPrBA
 0.457/0.242
 DiPrBA
 13.47/0.632
 DiPrBA
 15.54/0.688

Figure 17. (a) Schematic diagram of multi-layer with Donor/Cl₄BQ/NMP/TiO₂/PEO configuration. (b) Representative IV for the cell (Table ES5, entry 31, DiPrBA donor).

In this case also, higher power outputs were realized, (after 1 h Pmax 17.24 mW/FF 0.582 and after 48 h Pmax 15.59 mW/FF 0.688). The shape of the IV-curve also improved at higher temperatures.

We have also constructed the cell by introducing additional acceptor layer (*p*-chloranil) as shown in Figure 18.



1 h after packing

 Donor
 Pmax/mW/FF(28 °C)
 Donor
 Pmax/mW/FF(35 °C)
 Donor
 Pmax/mW/FF(40 °C)

 DiPrBA
 7.283/0.465
 DiPrBA
 9.781/0.51
 DiPrBA
 11.31/0.545

 48 h after packing

 Donor
 Pmax/mW/FF(40 °C)

 DiPrBA
 20.07/0.566

Figure 18. (a) Schematic diagram of multi-layer with Donor/TiO₂/Cl₄BQ/NMP/PEO configuration. (b) Representative IV for the cell (Table ES 6, entry 32, DiPrBA donor).

In this configuration (Figure 18), there is improvement in the shape of the IV-curve at 28 °C (Figure 18b). The performance of the cell after 48 h was also very good Pmax 20.07 mW with FF 0.566 (Table ES 6, entry 32). We have also constructed the cell in a 8 layer configuration as shown in Figure 19.

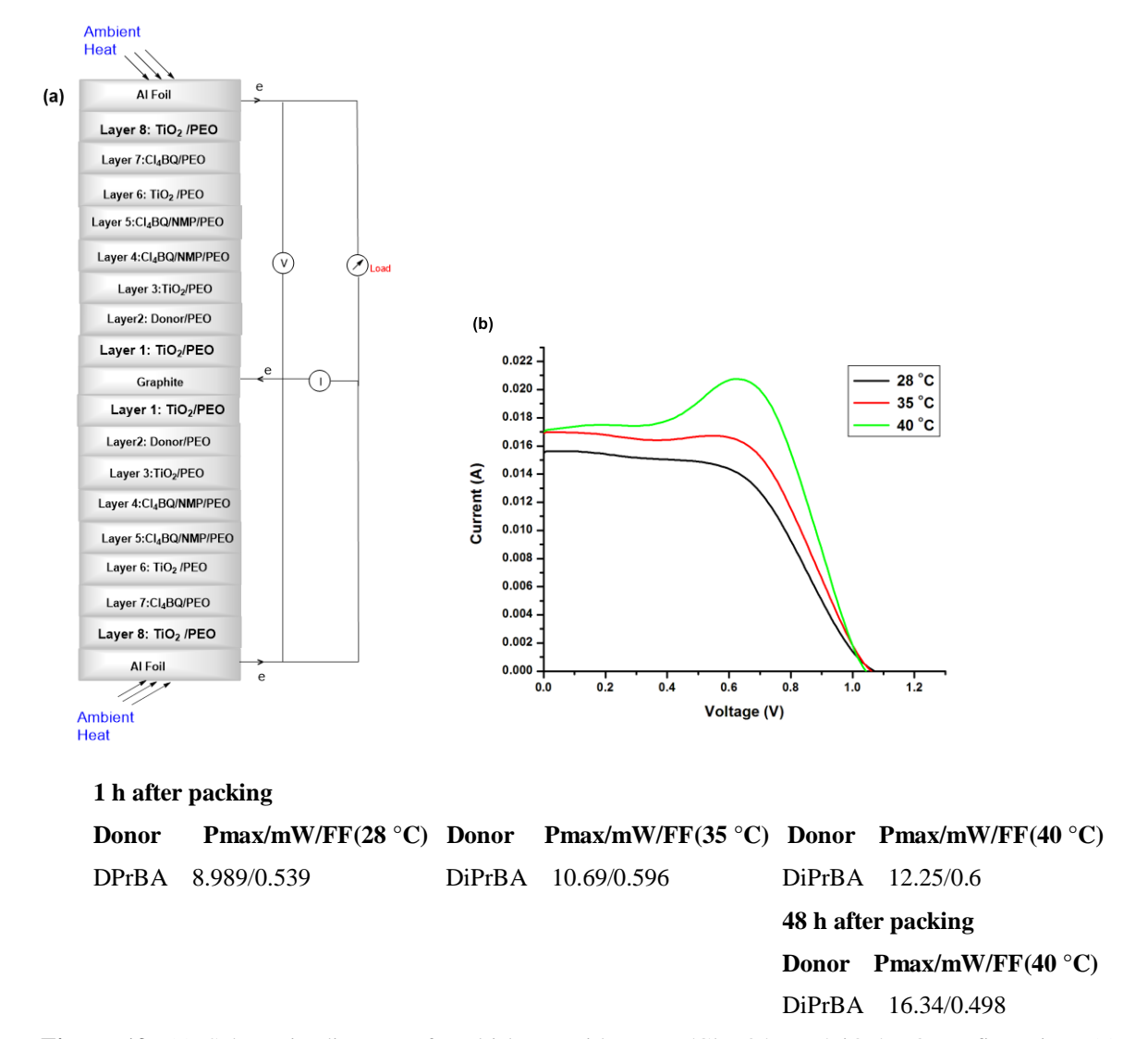


Figure 19. (a) Schematic diagram of multi-layer with Donor/Cl₄BQ/NMP/TiO₂/PEO configuration. (c) Representative IV for the cell (Table ES 6, entry 33).

In this cell configuration, the shape of the IV-curve was good at 28 °C, but higher temperature lead to hump in the curve (Figure 19b) presumably, due to side reactions at the higher temperature. Accordingly, it is advisable to construct the cell at lower

temperatures. The performance of the cells at 28 °C and 40 °C are listed in Table 1. The results should be useful for further research work to come up with practical electricity harvesting devices.

Table 1. Long performance of the cells at 28 °C and 40 °C.^a

Entry	Configuration	Donor	Pmax/mW	Pmax/mW at
	/Figure		at	$40~^{0}\text{C}/48~\text{h}$
			28 °C/48 h	
1 ^b	7/16	TPA	3.061	11.59
2 ^b	7/16	PhNEt ₂	3.679	13.56
3 ^b	7/16	DABCO	0.205	3.994
4 ^b	7/16	DIPEA	2.763	9.89
5 ^b	7/16	DiPrBA	5.466	17.29
6 ^c	8/17	DiPrBA	0.457	15.54
7 ^b	9/18	DiPrBA	-	20.07
8 ^d	10/19	DiPrBA	-	16.34

^aDouble cell configurations monitored for long time. ^bSix layer cell configurations. ^cFivelayer cell configuration. ^dEight layer cell configuration

Methods are available for storing solar heat in simple chemicals like aq. NaOH and CaCl₂ for regenerating heat (40 °C to 60 °C) when required.⁴⁵ Therefore, the ambient heat harvesting device reported here has the potential for developing devices that could produce electricity 24x7, day and night, rainy or cloudy atmospheric conditions. These low/ambient heat harvesting electricity producing cells can be readily stacked, thus suitable for putting up units for large-scale applications. However, long term performance of this cell device remains to be established. Since, these cells utilize readily accessible

inexpensible materials, there is plenty of scope for further research and development to improve the performance of the devices.

3.5 Conclusions

We have developed a simple electrochemical cell device based on electron transfer in ground state with readily available amine or amide as donors and *p*-chloranil as electron acceptor at ambient temperatures. In these electrochemical cell devices, the donors react with acceptors to give radical ions and produce electricity in the ground state. Ambient temperature is enough to induce the electron transfer from donor to acceptor for generation of electric current.

The advantage of this method is that number of cells can be stacked by parallel or series connections to increase the current or voltage. Also, the devices utilized inexpensive materials already manufactured in large scale and hence it will be suitable in bulk-scale power generation units. Further, systematic investigations on the development of these electrochemical cells have potential to come up with devices for practical applications for the generation of electricity for household, grid and automobile applications.

3.6 Experimental Section

3.6.1 General Information

P-Chloranil, N, N-diisopropylethylamine (DIPEA), 1,4-diazabicyclo[2.2.2]octane (DABCO) and TiO₂ were purchased from Avra chemicals (India). p-benzoquinone (BQ), triphenylamine (TPA), N,N'-tetramethyl-1,4-phenylenediamine (TMPDA), N,N-diethyl aniline (PhNEt₂), propylene carbonate (PC), ethylene carbonate (EC) and polyethylene oxide (PEO) were purchased from Sigma Aldrich. Netural alumina (Al₂O₃) was purchased from SRL chemicals, India. Zinc oxide (ZnO) was purchased from E-Merck, India. The metal oxides were heated at 150 °C in a vacuum oven for 2 h before use. PC and EC were always kept under molecular sieves. N, N-diisopropylbenzamide was prepared from the literature procedure. Graphite sheet (0.4mm thickness, 5cm x 5cm, Resistivity, $\rho = 2x10^{-1}$ ⁴Ω.m) was purchased from Falcon Graphite Industries, Hyderabad, India. Aluminium Foil (0.2mm thickness, 5cm x 5cm, Resistivity, $\rho = 2x10^{-5}\Omega$.m) and Stainless steel (0.4mm thickness, 5cm x 5cm, Resistivity, $\rho = 5x10^{-4}\Omega$.m) were purchased from Aluminium Enterprises and Rasik Metals, Hyderabad, India. EPR spectra was recorded on a Bruker-ER073 instrument equipped with an EMX micro X source for X band measurement using Xenon 1.1b.60 software provided by the manufacturer. Electrical measurements were carried out by ZAHNER instrument using CIMPS software. The current-voltage curve was drawn using Origin software.

3.6.2 Preparation of Electrochemical Cells

Simple solution processing and casting techniques were followed for the construction of the cell device.

Table ES1

Configuration 1

The PEO (0.05 g) was dissolved in dichloromethane and mixed with TiO₂ (0.5 g) powder. DCM was removed to obtain a paste for coating on Al and Graphite foils. After 1 h, Cl₄BQ (0.1g)/Phthalimide (1 mmol)/PEO (0.05 g) in DCM was coated on TiO₂/PEO/Al and on TiO₂/PEO/Gr and dried. Cl₄BQ (0.025 g)/Donor (1 mmol)/PC (0.5 g)/Phthalimide (1 mmol)/PEO (0.1 g)/TiO₂ (0.5 g) in DCM was coated on coated coated Al and coated on coated Gr and dried in air at room temperature overnight. The cell was prepared by sandwiching the coated Al/Gr layers. The rim of the cell prepared in this way was sealed all around using TiO₂/PEO paste, then with commercial adhesive Bondfix (India) and covered with cellophane tape.

Configuration 2

The PEO (0.05 g) was dissolved in dichloromethane and mixed with TiO₂ (0.5 g) powder. DCM was removed to obtain a paste for coating on Al and Graphite foils. After 1 h, Cl₄BQ (0.1g)/MeN-Phthalimide (1 mmol)/PEO (0.05 g) in DCM was coated on TiO₂/PEO/Al and on TiO₂/PEO/Gr and dried. Cl₄BQ (0.025 g)/Donor (1 mmol)/PC (0.5 g)/ MeN-Phthalimide (1 mmol)/PEO (0.1 g)/ TiO₂ (0.5 g) in DCM was coated on coated coated Al and coated Gr and dried in air at room temperature overnight. The cell was prepared by sandwiching the coated Al/Gr layers. The rim of the cell prepared in this way was sealed all around using TiO₂/PEO paste, then with commercial adhesive Bondfix (India) and covered with cellophane tape.

Table ES2

Configuration 3

The PEO (0.05 g) was dissolved in dichloromethane and mixed with TiO₂ (0.5 g) powder. DCM was removed to obtain a paste for coating on Al and Graphite foils. After 1 h, TiO₂ (0.5 g)/MeN-Phthalimide (2 mmol)/ PC (0.5 g)/PEO (0.05 g) in DCM was coated on TiO₂/PEO/Al and TiO₂ (0.5 g)/ Cl₄BQ (0.25 g)/PC (0.5 g)/PEO (0.05 g) in DCM was coated on TiO₂/PEO/Gr and dried in air at room temperature overnight. Donor (1 mmol)/MeN-Phthalimide (1 mmol)/ NMP (0.5 g)/PEO (0.1 g) was heat coat before packing on dried coated Al foil. The cell was packed immediately by sandwiching the coated Al/Gr layers. The rim of the cell prepared in this way was sealed all around using TiO₂/PEO paste, then with commercial adhesive Bondfix (India) and covered with cellophane tape.

Table ES3

Configuration 4

The PEO (0.05 g) was dissolved in dichloromethane and mixed with TiO₂ (0.5 g) powder. DCM was removed to obtain a paste for coating on Al and Graphite foils. After 1 h, MeN-Phthalimide (2 mmol)/PEO (0.05 g) in DCM was coated on TiO₂/PEO/Al and Cl₄BQ (0.25 g)/PEO (0.05 g) in DCM was coated on TiO₂/PEO/Gr and dried in air at room temperature overnight. Donor (1 mmol)/MeN-Phthalimide (1 mmol)/ NMP (1 g)/PEO (0.1 g) was heat coat before packing on dried coated Al foil. The cell was packed immediately by sandwiching the coated Al/Gr layers. The rim of the cell prepared in this way was sealed all around using TiO₂/PEO paste, then with commercial adhesive Bondfix (India) and covered with cellophane tape.

Configuration 5

The PEO (0.05 g) was dissolved in dichloromethane and mixed with TiO₂ (0.5 g) powder. DCM was removed to obtain a paste for coating on Al and Graphite foils. After 1 h, Amide /PEO (0.05 g) in DCM was coated on TiO₂/PEO/Al and Cl4BQ (0.25 g)/PEO (0.05 g) in DCM was coated on TiO₂/PEO/Gr and dried. Donor (2 mmol)/PEO (0.05 g) in DCM was coated on coated Gr. MeN-phthalimide (1 mmol)/NMP (0.5 g)/PEO (0.05 g)/TiO₂ (0.25g) in DCM was coated on coated Al and coated on coated Gr layers and dried in air at room temperature overnight. The cell was prepared by sandwiching the coated Al/Gr layers. The rim of the cell prepared in this way was sealed all around using TiO₂/PEO paste, then with commercial adhesive Bondfix (India) and covered with cellophane tape.

Table ES4

Configuration 6

The PEO (0.05 g) was dissolved in dichloromethane and mixed with TiO₂ (0.5 g) powder. DCM was removed to obtain a paste for coating on Al and Graphite foils. After 1 h, BQ (0.2 g)/PEO (0.05 g) in DCM was coated on TiO₂/PEO/Al and Cl₄BQ (0.25 g)/PEO (0.05 g) in DCM was coated on TiO₂/PEO/Gr and dried. Donor (1 mmol)/PEO (0.05 g) in DCM was coated on coated Gr. The BQ (0.11 g)/NMP (0.5 g)/ PEO (0.05 g)/TiO₂ (0.25 g) slurry was prepared and casted above the coated Al and coated on coated Gr layers and dried in air at room temperature overnight. The cell was prepared by sandwiching the coated Al/Gr layers. The rim of the cell prepared in this way was sealed all around using TiO₂/PEO paste, then with commercial adhesive Bondfix (India) and covered with cellophane tape.

Table ES5

Configuration 7

The PEO (0.05 g)was dissolved in dichloromethane and mixed with TiO₂ (0.5 g) powder. DCM was removed to obtain a paste for coating on two Al foils and both sides on Graphite foil. After 1 h, Cl₄BQ (0.1 g)/PEO (0.05 g) in DCM was coated on TiO₂/PEO/Al and Donor (1 mmol)/PEO (0.05g) in DCM was coated on TiO₂/PEO/Gr. The NMP (0.025 g)/PEO (0.05 g) was coated on coated Al. TiO₂ (0.5g)/PEO (0.05g) was dissolved in DCM and coated on coated Graphite and dried in air at room temperature overnight. The cell was prepared by sandwiching the coated Al/Gr/Al layers. The rim of the cell prepared in this way was sealed all around using TiO₂/PEO paste, then with commercial adhesive Bondfix (India) and covered with cellophane tape.

Configuration 8

The PEO (0.05 g) was dissolved in dichloromethane and mixed with TiO₂ (0.5 g) powder. DCM was removed to obtain a paste for coating on two Al foils and both sides on Graphite foil. After 1 h, Cl₄BQ (0.1 g)/NMP(1 g)/PEO (0.1 g) in DCM was coated on TiO₂/PEO/Al and Donor (1 mmol)/PEO (0.05g) in DCM was coated on TiO₂/PEO/Gr. TiO₂ (0.5g)/PEO (0.05g) was dissolved in DCM and coated on coated Graphite and dried in air at room temperature overnight. The cell was prepared by sandwiching the coated Al/Gr/Al layers. The rim of the cell prepared in this way was sealed all around using TiO₂/PEO paste, then with commercial adhesive Bondfix (India) and covered with cellophane tape.

Table ES6

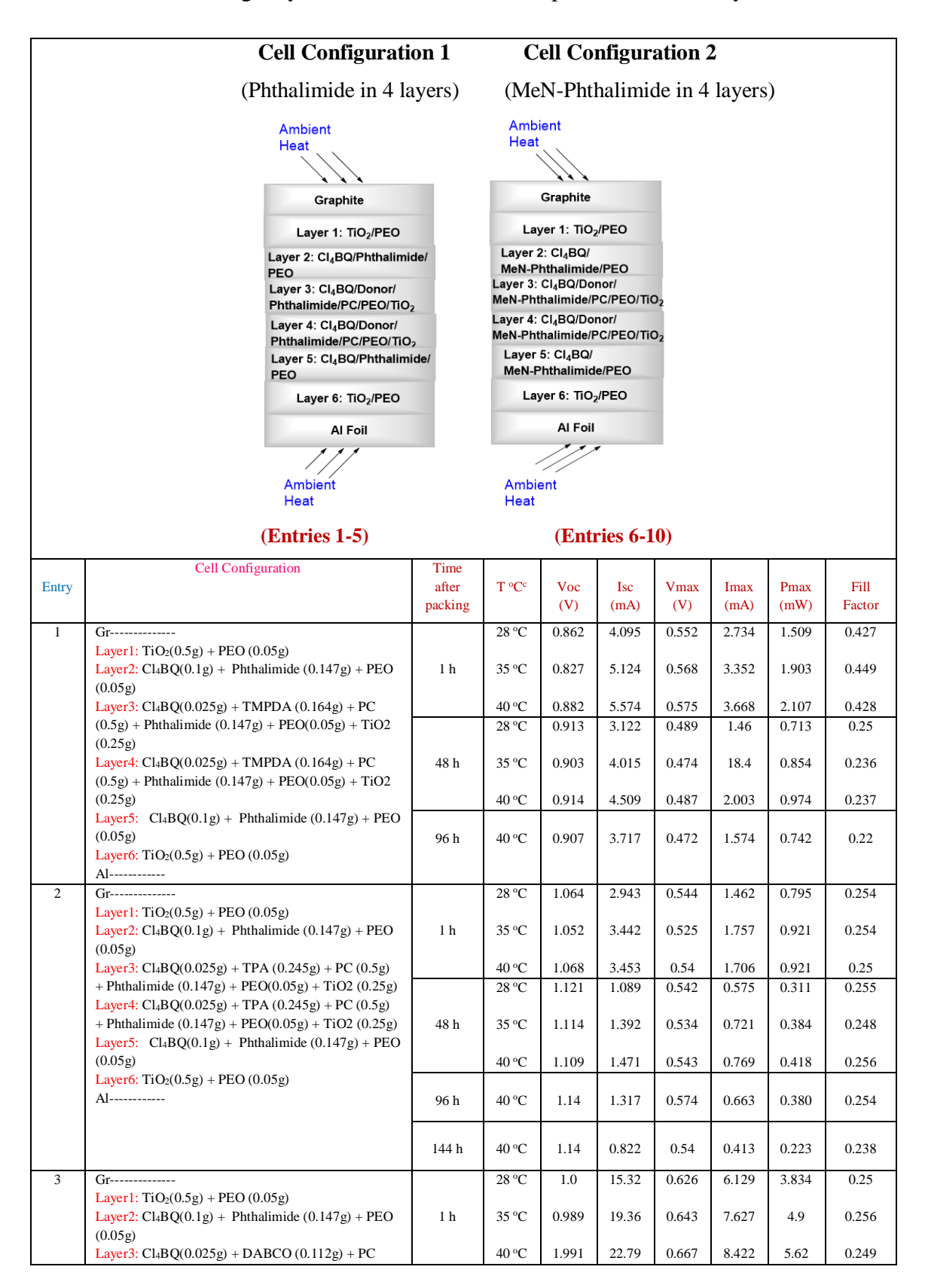
Configuration 9

The PEO (0.05 g)was dissolved in dichloromethane and mixed with TiO₂ (0.5 g) powder. DCM was removed to obtain a paste for coating on two Al foils and both sides on Graphite foil. After 1 h, Cl₄BQ (0.15 g)/PEO (0.05 g) in DCM was coated on TiO₂/PEO/Al and Donor (0.5 g)/PEO (0.05g) in DCM was coated on TiO₂/PEO/Gr. The Cl₄BQ (0.1 g)/NMP (1 g)/PEO (0.05 g) was coated on coated Al. TiO₂ (0.5g)/PEO (0.05g) was dissolved in DCM and coated on coated Graphite and dried in air at room temperature overnight. The cell was prepared by sandwiching the coated Al/Gr/Al layers. The rim of the cell prepared in this way was sealed all around using TiO₂/PEO paste, then with commercial adhesive Bondfix (India) and covered with cellophane tape.

Configuration 10

The PEO (0.05 g) was dissolved in dichloromethane and mixed with TiO₂ (0.5 g) powder. DCM was removed to obtain a paste for coating on two Al foils and both sides on Graphite foil. After 1 h, Cl₄BQ (0.15 g)/PEO (0.025 g) in DCM was coated on TiO₂/PEO/Al and Donor (0.5 g)/PEO (0.05g) in DCM was coated on TiO₂/PEO/Gr. TiO₂ (0.5g)/PEO (0.05g) was dissolved in DCM and coated on coated Al and coated Graphite. Cl₄BQ (0.05 g)/NMP (0.5 g)/PEO (0.025 g) in DCM was coated on both coated Al and coated Graphite and dried in air at room temperature overnight. The cell was prepared by sandwiching the coated Al/Gr/Al layers. The rim of the cell prepared in this way was sealed all around using TiO₂/PEO paste, then with commercial adhesive Bondfix (India) and covered with cellophane tape.

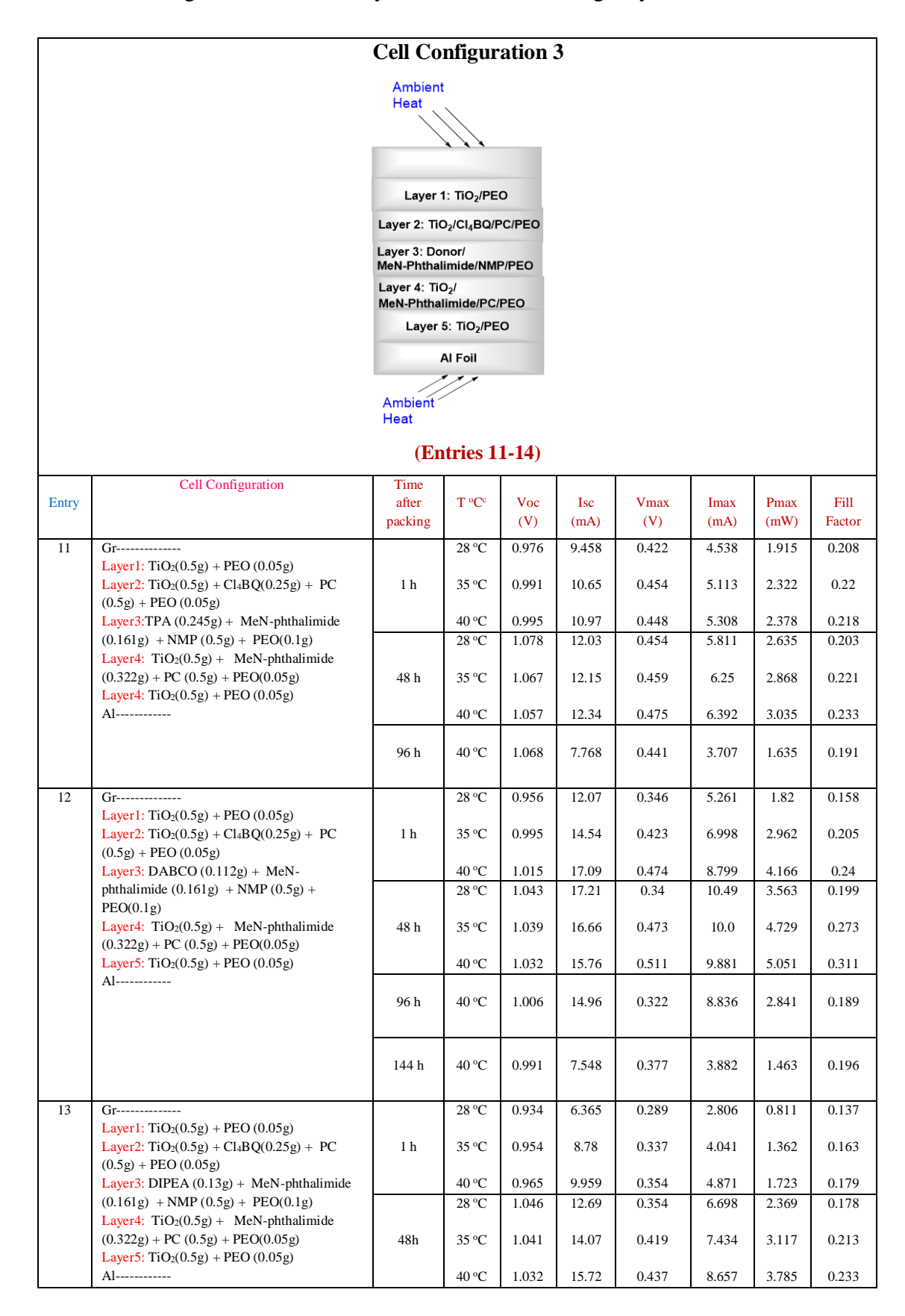
Table ES1. TiO₂ in edge layer, Phthalimide and MeN-phthalimide in 4 layers PC as solvent.



	(0.5g) + Phthalimide (0.147g) + PEO(0.05g) + TiO2		28 °C	0.928	7.564	0.453	2.914	1.32	0.188
	(0.25g) Layer4: Cl ₄ BQ(0.025g) + DABCO (0.112g) + PC	48 h	35 °C	0.909	9.852	0.388	4.726	1.835	0.205
	(0.5g) + Phthalimide (0.147g) + PEO(0.05g) + TiO2 (0.25g)		40 °C	0.899	11.38	0.367	6.233	2.284	0.223
	Layer5: Cl ₄ BQ(0.1g) + Phthalimide (0.147g) + PEO (0.05g) Layer6: TiO ₂ (0.5g) + PEO (0.05g)	96 h	40 °C	0.938	10.51	0.505	4.257	2.151	0.218
	Al	144 h	40 °C	0.953	6.878	0.5	3.235	1.617	0.247
4	Gr Layer1: TiO ₂ (0.5g) + PEO (0.05g)		28 °C	1.061	21.4	0.575	9.552	5.495	0.242
	Layer2: Cl ₄ BQ(0.1g) + Phthalimide (0.147g) + PEO (0.05g)	1 h	35 °C	1.021	24.61	0.63	13.44	8.473	0.337
	Layer3: Cl ₄ BQ(0.025g) + DIPEA (0.13g) + PC (0.5g)		40 °C	1.016	23.61	0.636	15.1	9.596	0.4
	+ Phthalimide (0.147g) + PEO(0.05g) + TiO2 (0.25g) Layer4: Cl ₄ BQ(0.025g) + DIPEA (0.13g) + PC (0.5g)		28 °C	0.942	10.45	0.597	4.976	2.972	0.302
	+ Phthalimide (0.147g) + PEO(0.05g) + TiO2 (0.25g) Layer5: Cl ₄ BQ(0.1g) + Phthalimide (0.147g) + PEO	48 h	35 °C	0.914	12.32	0.642	5.529	3.55	0.315
	(0.05g) Layer6: TiO ₂ (0.5g) + PEO (0.05g)		40 °C	0.907	12.97	0.662	6.166	4.082	0.347
	Al	96 h	40 °C	0.903	11.22	0.531	5.006	2.658	0.263
		144 h	40 °C	0.855	6.426	0.393	2.979	1.169	0.213
5	Gr		28 °C	1.088	9.399	0.549	4.797	2.612	0.255
	Layer1: TiO ₂ (0.5g) + PEO (0.05g) Layer2: Cl ₄ BQ(0.1g) + Phthalimide (0.147g) + PEO (0.05g)	1 h	35 °C	1.102	9.781	0.54	5.009	2.706	0.251
	Layer3: Cl ₄ BQ(0.025g) + DiPrBA (0.205g) + PC		40 °C	1.058	10.21	0.539	5.159	2.779	0.257
	(0.5g) + Phthalimide (0.147g) + PEO(0.05g) + TiO2 (0.25g)		28 °C	1.068	4.31	0.54	2.357	1.274	0.277
	Layer4: Cl ₄ BQ(0.025g) + DiPrBA (0.205g) + PC (0.5g) + Phthalimide (0.147g) + PEO(0.05g) + TiO2	48 h	35 °C	1.047	5.186	0.532	2.878	1.532	0.282
	(0.25g) Layer5: Cl ₄ BQ(0.1g) + Phthalimide (0.147g) + PEO		40 °C	1.033	5.36	0.53	3.095	1.641	0.296
	(0.05g) Layer6: TiO ₂ (0.5g) + PEO (0.05g) Al	96 h	40 °C	0.963	3.792	0.486	2.378	1.156	0.317
		144 h	40 °C	0.923	2.056	0.498	1.229	0.612	0.322
6	Gr		28 °C	0.861	8.094	0.46	3.436	1.582	0.227
	Layer1: TiO ₂ (0.5g) + PEO (0.05g) Layer2: Cl ₄ BQ(0.1g) + MeN-phthalimide (0.161g) + PEO (0.05g)	1 h	35 °C	0.812	10.13	0.394	4.976	1.961	0.238
	Layer3: Cl ₄ BQ(0.025g) + TMPDA (0.164g) + PC		40 °C	0.831	11.17	0.411	4.895	2.009	0.217
	(0.5g) + Phthalimide (0.147g) + PEO(0.05g) + TiO2 (0.25g)		28 °C	0.83	3.9	0.495	1.913	0.946	0.292
	Layer4: Cl ₄ BQ(0.025g) + TMPDA (0.164g) + PC (0.5g) + Phthalimide (0.147g) + PEO(0.05g) + TiO2	48 h	35 °C	0.836	5.271	0.51	2.467	1.257	0.285
	(0.25g)		40 °C	0.814	5.418	0.512	2.641	1.302	0.295
	Layer5: Cl ₄ BQ(0.1g) + MeN-phthalimide (0.161g) + PEO (0.05g) Layer6: TiO ₂ (0.5g) + PEO (0.05g)	96 h	40 °C	0.851	4.951	0.474	2.574	1.22	0.29
7	Al Gr		28 °C	1.069	1.859	0.54	0.908	0.490	0.247
	Layer1: TiO ₂ (0.5g) + PEO (0.05g) Layer2: Cl ₄ BQ(0.1g) + MeN-phthalimide (0.161g) +	1 h	35 °C	1.051	2.399	0.518	1.168	0.605	0.246
	PEO (0.05g) Layer3: Cl ₄ BQ(0.025g) + TPA (0.245g) + PC (0.5g)		40 °C	1.051	2.427	0.52	1.248	0.648	0.254
	+ Phthalimide (0.147g) + PEO(0.05g) + TiO2 (0.25g)		28 °C	1.06	0.622	0.518	0.323	0.167	0.254
	Layer4: Cl ₄ BQ(0.025g) + TPA (0.245g) + PC (0.5g) + Phthalimide (0.147g) + PEO(0.05g) + TiO2 (0.25g) Layer5: Cl ₄ BQ(0.1g) + MeN-phthalimide (0.161g)	48 h	35 °C	1.011	0.824	0.516	0.414	0.214	0.257
	+ PEO (0.05g)		40 °C	1.053	0.911	0.516	0.493	0.254	0.265

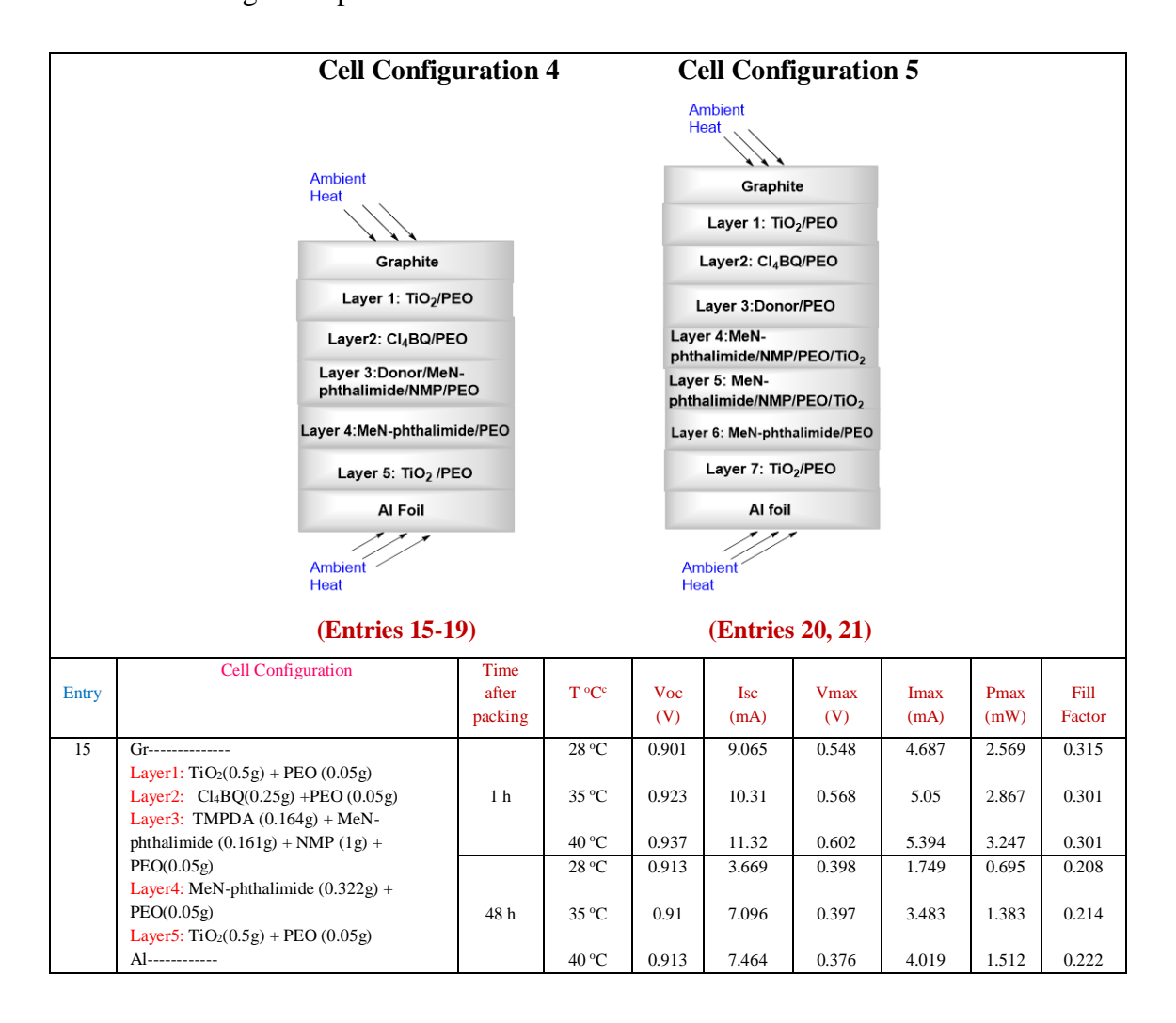
				•	•	•	•		
	Layer6: TiO ₂ (0.5g) + PEO (0.05g) Al	96 h	40 °C	1.062	0.555	0.525	0.272	0.143	0.243
8	Gr		28 °C	0.995	10.96	0.521	4.552	2.372	0.218
	Layer1: TiO ₂ (0.5g) + PEO (0.05g) Layer2: Cl ₄ BQ(0.1g) + MeN-phthalimide (0.161g) + PEO (0.05g)	1 h	35 °C	0.985	15.12	0.555	5.998	3.329	0.224
	Layer3: Cl ₄ BQ(0.025g) + DABCO (0.112g) + PC		40 °C	0.979	16.28	0.617	6.169	3.805	0.239
	(0.5g) + Phthalimide $(0.147g)$ + PEO $(0.05g)$ + TiO2		28 °C	1.0	7.898	0.498	3.176	1.581	0.2
	(0.25g) Layer4: Cl ₄ BQ(0.025g) + DABCO (0.112g) + PC (0.5g) + Phthalimide (0.147g) + PEO(0.05g) + TiO2	48 h	35 °C	0.992	11.14	0.513	4.369	2.239	0.203
	(0.3g) + Pitthanninge $(0.147g)$ + PEO $(0.03g)$ + 1102 $(0.25g)$		40 °C	0.983	12.64	0.609	4.374	2.662	0.214
	Layer5: $Cl_4BQ(0.1g) + MeN$ -phthalimide (0.161g)		40 C	0.963	12.04	0.009	4.374	2.002	0.214
	+ PEO (0.05g) Layer6: TiO ₂ (0.5g) + PEO (0.05g) Al	96 h	40 °C	0.972	7.506	0.491	3.274	1.607	0.22
9	Gr		28 °C	1.054	19.62	0.615	7.502	4.616	0.223
	Layer1: TiO ₂ (0.5g) + PEO (0.05g) Layer2: Cl ₄ BQ(0.1g) + MeN-phthalimide (0.161g) + PEO (0.05g)	1 h	35 °C	1.009	19.35	0.61	10.42	6.353	0.326
	Layer3: $C1_4BO(0.025g) + DIPEA(0.13g) + PC(0.5g)$		40 °C	0.993	18.18	0.619	10.36	6.41	0.355
	+ Phthalimide (0.147g) + PEO(0.05g) + TiO2 (0.25g)		28 °C	0.941	7.065	0.578	3.32	1.917	0.289
	Layer5: Cl ₄ BQ(0.025g) + DIPEA (0.13g) + PC (0.5g) + Phthalimide (0.147g) + PEO(0.05g) + TiO2 (0.25g) Layer4: Cl ₄ BQ(0.1g) + MeN-phthalimide (0.161g)	48 h	35 °C	0.932	11.32	0.644	4.516	2.908	0.276
	+ PEO (0.05g)		40 °C	0.928	11.71	0.657	5.042	3.313	0.305
	Layer6: TiO ₂ (0.5g) + PEO (0.05g) Al	96 h	40 °C	0.904	7.085	0.49	3.2	1.566	0.244
10	Gr		28 °C	1.113	5.545	0.547	2.731	1.495	0.242
	Layer1: TiO ₂ (0.5g) + PEO (0.05g) Layer2: Cl ₄ BQ(0.1g) + MeN-phthalimide (0.161g) +	1 h	35 °C	1.081	5.603	0.538	2.851	1.533	0.253
	PEO (0.05g) Layer3: Cl ₄ BQ(0.025g) + DiPrBA (0.205g) + PC		40 °C	1.086	6.281	0.536	3.15	1.689	0.248
	(0.5g) + Phthalimide $(0.147g)$ + PEO $(0.05g)$ + TiO2		28 °C	1.132	1.695	0.555	0.844	0.468	0.244
	(0.25g) (0.25g) Layer4: Cl ₄ BQ(0.025g) + DiPrBA (0.205g) + PC	48 h	35 °C	1.132	1.849	0.554	0.937	0.519	0.25
	(0.5g) + Phthalimide (0.147g) + PEO(0.05g) + TiO2 (0.25g)		40 °C	1.123	1.914	0.551	0.957	0.527	0.245
	Layer5: Cl ₄ BQ(0.1g) + MeN-phthalimide (0.161g) + PEO (0.05g) Layer6: TiO ₂ (0.5g) + PEO (0.05g) Al	96 h	40 °C	1.077	2.637	0.515	1.379	0.710	0.25

Table ES2. Using NMP in middle layer as solvent PC in edge layers.



		96 h	40 °C	1.071	18.65	0.402	9.387	3.769	0.189
		144 h	40 °C	1.069	12.89	0.459	7.172	3.288	0.239
14	Gr		28 °C	0.978	6.888	0.33	3.161	1.042	0.155
	Layer1: TiO ₂ (0.5g) + PEO (0.05g) Layer2: TiO ₂ (0.5g) + Cl ₄ BQ(0.25g) + PC (0.5g) + PEO (0.05g)	1 h	35 °C	0.978	9.223	0.385	4.133	1.591	0.176
	Layer3:DiPrBA (0.205g) + MeN-phthalimide		40 °C	0.981	10.33	0.389	4.817	1.872	0.185
	(0.161g) + NMP(0.5g) + PEO(0.1g)		28 °C	1.052	10.49	0.363	5.441	1.974	0.179
	Layer4: TiO ₂ (0.5g) + MeN-phthalimide (0.322g) + PC (0.5g) + PEO(0.05g) Layer5: TiO ₂ (0.5g) + PEO (0.05g)	48 h	35 °C	1.044	11.18	0.414	6.036	2.499	0.214
	Al		40 °C	1.04	10.9	0.444	5.865	2.604	0.23
		96 h	40 °C	1.072	11.11	0.397	5.842	2.316	0.195
		144 h	40 °C	1.063	6.4	0.471	3.615	1.701	0.25

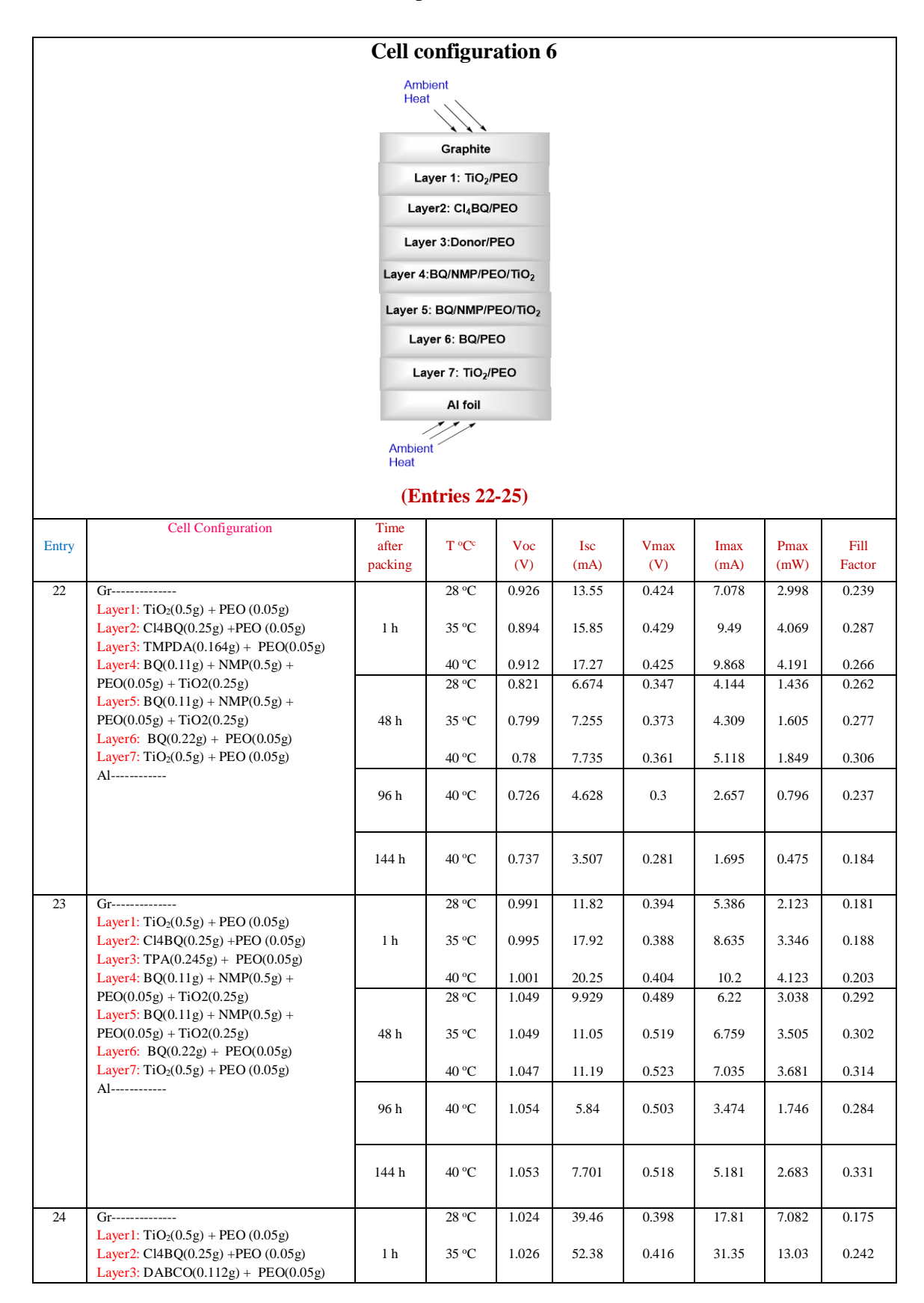
Table ES3. Using MeN-phthalimide in NMP solvent



		96 h	40 °C	0.889	3.516	0.34	1.722	0.585	0.187
16	Gr		28 °C	1.043	10.68	0.47	5.319	2.497	0.224
	Layer1: TiO ₂ (0.5g) + PEO (0.05g) Layer2: Cl ₄ BQ(0.25g) +PEO (0.05g) Layer3: TPA (0.245g) + MeN-phthalimide	1 h	35 °C	1.048	11.88	0.468	6.099	2.853	0.229
	(0.161g) + NMP (1g) + PEO(0.05g)		40 °C	1.064	12.06	0.498	5.991	2.98	0.232
	Layer4: MeN-phthalimide (0.322g) +		28 °C	1.094	6.705	0.476	3.346	1.592	0.217
	PEO(0.05g) Layer5: TiO ₂ (0.5g) + PEO (0.05g) Al	48 h	35 °C	1.093	7.764	0.492	4.067	1.999	0.236
	-		40 °C	1.12	7.786	0.496	4.057	2.01	0.231
		96 h	40 °C	1.08	6.096	0.472	3.256	1.537	0.233
		144 h	40 °C	1.059	4.534	0.468	2.665	1.242	0.259
17	Gr		28 °C	1.038	12.54	0.445	6.512	2.896	0.222
	Layer1: TiO ₂ (0.5g) + PEO (0.05g) Layer2: Cl ₄ BQ(0.25g) +PEO (0.05g)	1 h	35 °C	1.049	16.31	0.494	9.547	4.719	0.276
	Layer3: DABCO (0.112g) + MeN- phthalimide (0.161g) + NMP (1g) +		40 °C	1.061	16.8	0.509	10.2	5.194	0.291
	PEO(0.05g)		28 °C	1.084	4.412	0.487	2.129	1.037	0.217
	Layer4: MeN-phthalimide (0.322g) + PEO(0.05g) Layer5: TiO ₂ (0.5g) + PEO (0.05g)	48 h	35 °C	1.083	7.96	0.467	3.802	1.773	0.206
	Al		40 °C	1.085	11.49	0.479	6.053	2.898	0.232
		96 h	40 °C	1.081	3.849	0.459	1.709	0.784	0.189
		144 h	40 °C	1.085	3.2	0.493	1.5	0.739	0.213
18	Gr		28 °C	1.067	9.338	0.48	4.087	1.963	0.197
	Layer1: TiO ₂ (0.5g) + PEO (0.05g) Layer2: Cl ₄ BQ(0.25g) +PEO (0.05g) Layer3: DIPEA (0.13g) + MeN-	1 h	35 °C	1.061	13.18	0.428	8.463	3.618	0.259
	phthalimide (0.161g) + NMP (1g) +		40 °C	1.057	15.4	0.449	8.787	3.945	0.242
	PEO(0.05g)		28 °C	1.094	6.681	0.465	3.357	1.562	0.214
	Layer4: MeN-phthalimide (0.322g) + PEO(0.05g) Layer5: TiO ₂ (0.5g) + PEO (0.05g)	48 h	35 °C	1.093	12.42	0.474	6.693	3.171	0.234
	Al		40 °C	1.096	13.91	0.509	7.738	3.941	0.258
		96 h	40 °C	1.103	5.923	0.451	2.895	1.305	0.2
		144 h	40 °C	1.105	4.917	0.45	2.319	1.044	0.192
19	Gr		28 °C	1.036	10.75	0.421	5.09	2.142	0.192
	Layer1: TiO ₂ (0.5g) + PEO (0.05g) Layer2: Cl ₄ BQ(0.25g) +PEO (0.05g)	1 h	35 °C	1.038	10.63	0.444	5.091	2.259	0.205
	Layer3:DiPrBA (0.205g) + MeN- phthalimide (0.161g) + NMP (1g) +		40 °C	1.051	11.94	0.447	5.806	2.595	0.207
	PEO(0.05g)		28 °C	1.090	8.413	0.458	4.062	1.858	0.201
	Layer4: MeN-phthalimide (0.322g) + PEO(0.05g) Layer5: TiO ₂ (0.5g) + PEO (0.05g)	48 h	35 °C	1.090	10.78	0.493	5.296	2.598	0.221
	Al		40 °C	1.113	10.84	0.488	5.473	2.672	0.221
		96 h	40 °C	1.1	5.635	0.484	2.702	1.308	0.211

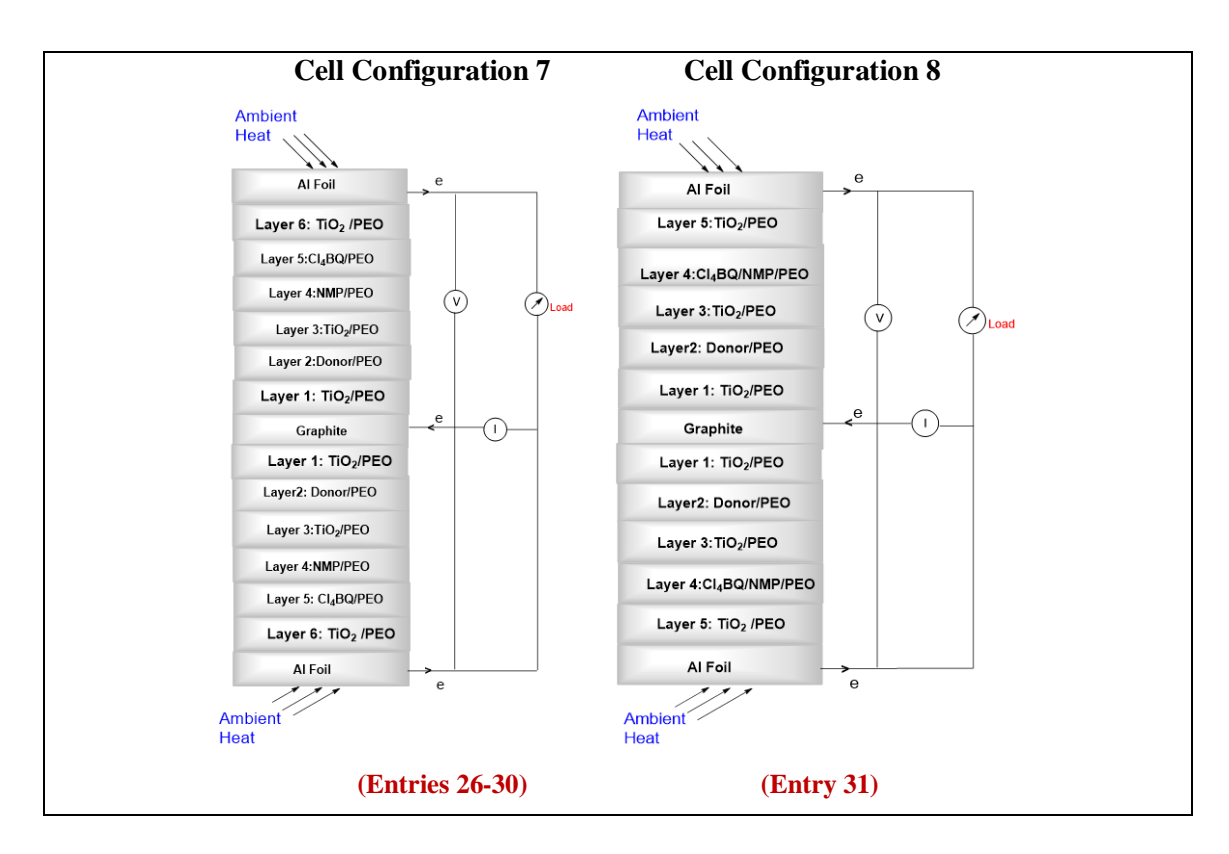
		144 h	40 °C	1.103	6.941	0.476	3.478	1.655	0.216
20	Gr		28 °C	0.941	16.64	0.499	6.918	3.449	0.22
	Layer1: TiO ₂ (0.5g) + PEO (0.05g) Layer2: Cl ₄ BQ (0.25g) +PEO (0.05g) Layer3: DABCO(0.224g) + PEO(0.05g)	1 h	35 °C	0.944	17.82	0.528	7.409	3.914	0.233
	Layer4: MeN-phthalimide(0.161g)+		40 °C	0.93	18.61	0.518	8.065	4.173	0.241
	NMP(0.5g) + PEO(0.05g) + TiO2(0.25g)		28 °C	0.998	14.31	0.551	5.95	3.28	0.23
	Layer5: MeN-phthalimide(0.161g)+ NMP(0.5g) + PEO(0.05g) + TiO2(0.25g) Layer6: MeN-phthalimide(0.322g) +	48 h	35 °C	0.963	14.6	0.598	5.781	3.457	0.246
	PEO(0.05g)		40 °C	0.978	15.08	0.58	6.251	3.622	0.246
	Layer7: TiO ₂ (0.5g) + PEO (0.05g) Al	96 h	40 °C	1.018	9.517	0.503	4.542	2.284	0.236
		144 h	40 °C	0.816	6.17	0.336	3.046	1.023	0.203
21	Gr		28 °C	1.055	13.06	0.583	7.595	4.424	0.321
	Layer1: TiO ₂ (0.5g) + PEO (0.05g) Layer2: Cl ₄ BQ (0.25g) +PEO (0.05g) Layer3: Diisopropylbenzamide(0.410g) +	1 h	35 °C	1.072	13.46	0.589	7.868	4.634	0.321
	PEO(0.05g)		40 °C	1.047	15.23	0.569	9.393	5.342	0.335
	Layer4: MeN-phthalimide(0.161g)+		28 °C	1.076	8.085	0.537	5.064	2.719	0.313
	NMP(0.5g) + PEO(0.05g) + TiO2(0.25g) Layer5: MeN-phthalimide(0.161g)+ NMP(0.5g) + PEO(0.05g) + TiO2(0.25g)	48 h	35 °C	1.08	9.814	0.561	6.354	3.566	0.336
	Layer6: MeN-phthalimide(0.322g) +		40 °C	1.082	10.68	0.588	6.863	4.032	0.349
	PEO(0.05g) Layer7: TiO ₂ (0.5g) + PEO (0.05g) Al	96 h	40 °C	1.099	4.871	0.561	2.984	1.675	0.313
		144 h	40 °C	1.083	9.831	0.55	6.771	3.721	0.35

Table ES4. Effect of BQ as second acceptor and NMP as solvent.



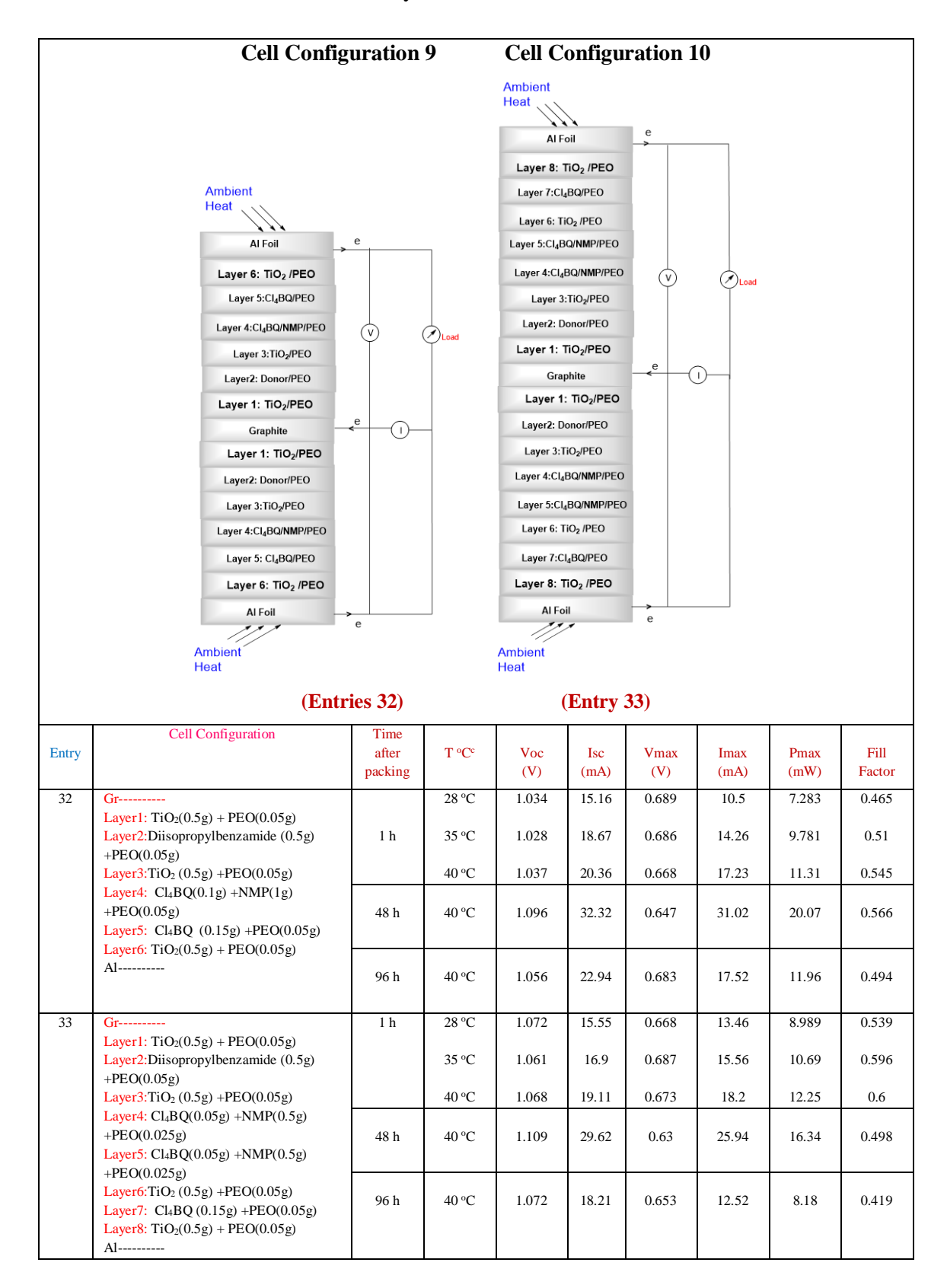
	Layer4: BQ(0.11g) + NMP(0.5g) + PEO(0.05g) + TiO2(0.25g) Layer5: BQ(0.11g) + NMP(0.5g) +		40 °C	1.025	44.45	0.467	29.27	13.67	0.3
	PEO(0.05g) + TiO2(0.25g) Layer6: BQ(0.22g) + PEO(0.05g) Layer7: TiO ₂ (0.5g) + PEO (0.05g) Al		28 °C	1.039	16.32	0.53	10.13	5.367	0.316
		48 h	35 °C	1.044	16.55	0.487	11.18	5.445	0.315
			40 °C	1.039	17.41	0.554	11.54	6.394	0.353
		96 h	40 °C	1.019	15.66	0.526	11.73	6.171	0.387
		144 h	40 °C	1.009	13.06	0.486	8.649	4.199	0.319
25	Gr		28 °C	1.034	32.98	0.391	16.02	6.266	0.184
	Layer1: TiO ₂ (0.5g) + PEO (0.05g) Layer2: Cl4BQ(0.25g) +PEO (0.05g) Layer3: DIPEA(0.13g, 0.17ml) + PEO(0.05g)	1 h	35 °C	1.031	44.35	0.434	29.71	12.88	0.282
			40 °C	1.027	38.2	0.464	30.17	14.01	0.317
	Layer4: BQ(0.11g) + NMP(0.5g) + PEO(0.05g) + TiO2(0.25g)		28 °C	1.049	15.07	0.436	8.012	3.491	0.221
	Layer5: BQ(0.11g) + NMP(0.5g) + PEO(0.05g) + TiO2(0.25g) Layer6: BQ(0.22g) + PEO(0.05g) Layer7: TiO ₂ (0.5g) + PEO (0.05g) Al	48 h	35 °C	1.047	18.65	0.517	15.28	7.9	0.405
			40 °C	1.04	17.86	0.567	16.89	9.579	0.516
		96 h	40 °C	1.041	13.39	0.531	11.44	6.074	0.436
		144 h	40 °C	1.021	9.827	0.515	7.007	3.61	0.36

Table ES5. Double cells



		Cell Configuration	Time							
Layer1: Tr0:(0.5p) + PEO(0.05p)	Entry	200. 200	after	T °C°						
Layer2TPA(0.5g) +PEQ00.5g)	26	Layer1: TiO ₂ (0.5g) + PEO(0.05g) Layer2:TPA(0.25 g) +PEO(0.05g)		28 °C	1.084	9.68	0.493	4.592	2.261	0.216
Layer's NMP(la) = PEO(0.05g)			1 h	35 °C	1.089	19.96	0.492	14.450	7.106	0.327
Layer's ClaBQ(0.25g) + PEO(0.05g)				40.°C	1 100	23 030	0.513	17 270	8 850	0.350
Al		Layer5: Cl ₄ BQ(0.25g) + PEO(0.05g) Layer6: TiO ₂ (0.5g) + PEO(0.05g)								
28 C			48 h							
Common				40 °C	1.145	21.380	0.632	18.350	0	0.473
28										
Layer2 PNNEq.(0.16 mt) +PEO(0.05g)	27	Gr		28 °C	1.079	15.06	0.489	7.823		0.235
Layers: NAP(1g) + PEQ(0.05g) 28 °C 1.117 12.04 0.577 6.375 3.679 0.274		Layer2:PhNEt ₂ (0.0.16 ml) +PEO(0.05g) Layer3: TiO ₂ (0.5g) + PEO(0.05g)	1 h	35 °C	1.087	29.60	0.579	22.56	13.06	0.406
LayerS: CLBQ(0.25g) + PEO(0.05g)				40 °C	1.076	32.76	0.593	26.09	15.46	0.439
Al										
28 Gr		Layer6: TiO ₂ (0.5g) + PEO(0.05g)	48 h	35 °C	1.115	22.13	0.646	19.51	12.61	0.511
28 Gr										
Layer1: TiO ₂ (0.5g) + PEO(0.05g)	20	C								
Layer3: TiO(0.5g) + PEO(0.05g)	28			28°C	1.044	4.383	0.468	1.89	0.883	0.185
Layer5: ClaBQ(0.25g) + PEO(0.05g)		Layer2:DABCO(0.11 g) +PEO(0.05g)	1 h	35 °C	1.058	16.15	0.408	7.203	2.935	0.172
Layer6: TiO ₂ (0.5g) + PEO(0.05g)		· · · · · · · · · · · · · · · · · · ·		40 °C	1.069	20.77	0.442	10.26	4.531	0.209
Al				28 °C	1.043	1.368	0.400	0.514	0.205	0.144
28 °C 1.055 6.506 0.475 3.092 1.467 0.214		• , , , , ,	48 h	35 °C	1.077	8.786	0.374	3.649	1.363	0.144
Layer1: TiO ₂ (0.5g) + PEO(0.05g) Layer2:DIPEA(0.17 ml) +PEO(0.05g) Layer3: TiO ₂ (0.5g) + PEO(0.05g) Layer4: NMP(1g) + PEO(0.05g) Layer4: NMP(1g) + PEO(0.05g) Layer6: TiO ₂ (0.5g) + PEO(0.05g) Layer6: Cid ₂ B(0.5g) + PEO(0.05g) Layer6: TiO ₂ C(0.5g) + PEO(0.05g) Layer6: Cid ₂ B(0.5g) + PEO(0.05g) Layer6: TiO ₂ C(0.5g) + PEO(0.05g) Layer6: TiO ₂ C(0				40 °C	1.122	16.63	0.490	8.15	3.994	0.214
Layer2:DIPEA(0.17 ml) +PEO(0.05g)	29			28 °C	1.055	6.506	0.475	3.092	1.467	0.214
Layer4: NMP(1g) + PEO(0.05g)	L	Layer2:DIPEA(0.17 ml) +PEO(0.05g) Layer3: TiO ₂ (0.5g) + PEO(0.05g)	1 h	35 °C	1.073	21.02	0.472	12.71	6.001	0.266
Layer6: TiO ₂ (0.5g) + PEO(0.05g)				40 °C	1.095	25.06	0.507	17.90	9.069	0.330
Al		•		28 °C	1.092	9.772	0.525	5.262	2.763	0.259
30 Gr		, , ,	48 h	35 °C	1.128	16.61	0.604	13.33	8.046	0.424
30 Gr				40 °C	1.141	17.28	0.638	15.51	9.89	0.502
Layer2:Diisopropylbenzamide (0.25g)	30	Gr								
Layer3: TiO ₂ (0.5g) + PEO(0.05g)		Layer2:Diisopropylbenzamide (0.25g)	1 h	35 °C	1.024	20.03	0.573	18.58	10.63	0.519
Layer4: NMP(1g) + PEO(0.05g) Layer5: Cl ₄ BQ(0.25g) + PEO(0.05g) Layer6: TiO ₂ (0.5g) + PEO(0.05g) Al 10				40 °C	1.08	22.0	0.572	23.13	13.22	0.557
Layer6: TiO ₂ (0.5g) + PEO(0.05g) Al 10		Layer4: NMP(1g) + PEO(0.05g)								
Au °C 1.119 22.65 0.705 24.54 17.29 0.682		Layer6: $TiO_2(0.5g) + PEO(0.05g)$	48 h	35 °C	1.11	19.52	0.614	20.97	12.87	0.594
31 Gr Layer1: TiO ₂ (0.5g) + PEO(0.05g) Layer2: Diisopropylbenzamide (0.25g) +PEO(0.05g) Layer3: TiO ₂ (0.5g) + PEO(0.05g) Layer4: Cl ₄ BQ(0.25g) + NMP(1g) +PEO(0.1g) Layer5: TiO ₂ (0.5g) + PEO(0.05g) Al 48 h 35 °C 1.083 4.621 0.344 2.522 0.867 0.173 0.493 9.374 0.493 9.374 0.493 9.374 0.493 9.374 0.493 9.374 0.493 9.374 0.582 1.066 1.767 0.539 0.849 0.457 0.242 0.658 20.47 13.47 0.632				40 °C	1.119	22.65	0.705	24.54	17.29	0.682
Layer2:Diisopropylbenzamide (0.25g) 1 h 35 °C 1.069 17.78 0.573 16.36 9.374 0.493 +PEO(0.05g) 40 °C 1.067 27.77 0.640 26.95 17.24 0.582 Layer4: Cl₄BQ(0.25g) +NMP(1g) 28 °C 1.068 1.767 0.539 0.849 0.457 0.242 +PEO(0.1g) 48 h 35 °C 1.114 19.14 0.658 20.47 13.47 0.632 Al	31	Layer1: TiO ₂ (0.5g) + PEO(0.05g) Layer2: Diisopropylbenzamide (0.25g) +PEO(0.05g) Layer3: TiO ₂ (0.5g) + PEO(0.05g) Layer4: Cl ₄ BQ(0.25g) + NMP(1g) +PEO(0.1g) Layer5: TiO ₂ (0.5g) + PEO(0.05g)								
Layer3: TiO ₂ (0.5g) + PEO(0.05g)			1 h	35 °C	1.069	17.78	0.573	16.36	9.374	0.493
Layer4: Cl ₄ BQ(0.25g) +NMP(1g) +PEO(0.1g) Layer5: TiO ₂ (0.5g) + PEO(0.05g) Al				40 °C	1.067	27.77	0.640	26.95	17.24	0.582
Layer5: TiO ₂ (0.5g) + PEO(0.05g) 48 h 35 °C 1.114 19.14 0.658 20.47 13.47 0.632										
			48 h	35 °C	1.114	19.14	0.658	20.47	13.47	0.632
		·		40 °C	1.123	20.13	0.688	22.58	15.54	0.688

Table ES6. Double cells with more layers



3.7 References

- a) Kornblum, N.; Michel, R. E.; Kerber, R. C. J. Am. Chem. Soc. 1966, 88, 5662.
 b) Kerober, R. C.; Urry, G. W.; Kornblum, N. J. Am. Chem. Soc. 1965, 87, 4520.
 c) Russell, G. A.; Danen, W. C. J. Am. Chem. Soc. 1966, 88, 5663. d) Marcus, R. A.; Sutin, N. Biochim. Biophys. Acta. 1985, 811, 265. e) Marcus, R. A. J. Chem. Phys. 1957, 26, 867. f) Marcus, R. A. Discuss. Faraday Soc. 1960, 29, 21. g) Marcus, R. A. J. Chem. Phys. 1965, 43, 679. h) Marcus, R. A. J. Phys. Chem. 1968, 72, 891. i) Marcus, R. A. Ann. Rev. Phys. Chem. 1964, 15, 155. j) Newton, M. D.; Sutin, N. Ann. Rev. Phys. Chem. 1984, 35, 437. k) Miller, J. R.; Calcaterra, L. T.; Closs, G. L. J. Am. Chem. Soc. 1984, 106, 3047. l) Eberson, L. J. Am. Chem. Soc. 1983, 105, 3192. m) Panteleeva, E. V.; Vaganova, T. A.; Shteiogarts, V. D. Tetrahedron Lett. 1955, 36, 8465. n) Rossi, R. A.; Pierini, B. A.; Penenory, A. B. Chem. Rev. 2003, 103, 71 and references cited therein.
- 2. a) Birch, A. J. J. Chem. Soc. **1944**, 430. b) Birch, A. J. J. Chem. Soc. **1945**, 809.
- 3. Finley, K. T. Chem. Rev. 1964, 64, 573.
- 4. Blicke, F. F.; Powers, L. D. J. Am. Chem. Soc. 1929, 51, 3378.
- 5. Blomberg, C.; Mosher, H. S. J. Organometal. Chem. 1968, 13, 519.
- 6. Ashby, E. C.; Bowers, J.; Depriest, R. Tetrahendron Letters. 1980, 21, 3541.
- 7. Uchiyama, N.; Shirakawa, E.; Hayashi, T. Chem. Commun. 2013, 49, 364.
- 8. Ashby, E. C.; Argyropoulos, J. N. J. Org. Chem. **1986**, *51*, 472.
- 9. Ashby, E. C.; Coleman, D.; Gamasa, M. J. Org. Chem. **1987**, 52, 4079.
- 10. Ashby, E. C.; Argyropoulos, J. N. J. Org. Chem. **1986**, *51*, 3593.
- 11. Kim, J. K.; Bunnett, J. F. J. Am. Chem. Soc. **1970**, 92, 7463.

210 References

- 12. Chatgilialoglu, C.; Asmus, K. D. Plenum Press, Newyork, 1990.
- 13. Ashby, E. C.; Sun, X.; Duff, J. L. J. Org. Chem. 1994, 59, 1270.
- 14. Choi, H.; Yang, K.; Lee, S.G.; Lee, J. P.; Koo, I. S. Bull. Korean Chem. Soc. **2010**, 31, 2801.
- 15. Kolbe, H. Annalen der chemie und pharmacie. **1848**, 64, 339.
- 16. Stork, G.; Davies, J. E.; Meisels, A. J. Am. Chem. Soc. 1959, 5516.
- 17. Morofuji, T.; Shimizu, A.; Yoshida, J. I. J. Am. Chem. Soc. 2014, 136, 4496.
- 18. Morofuji, T.; Shimizu, A.; Yoshida, J. I. J. Am. Chem. Soc. 2013, 135, 5000.
- Kirste, A.; Elsler, B.; Schnakenburg, G.; Waldvogel, S. R. J. Am. Chem. Soc. 2012, 134, 3571.
- 20. Mihelcic, J.; Moeller, K. D. J. Am. Chem. Soc. 2004, 126, 9106.
- 21. Shono, T.; Ikeda, A. J. Am. Chem. Soc. 1972, 7892.
- Masui, M.; Hara, S.; Ueshima, T.; Kawaguchi, T.; Ozaki, S. *Chem. Pharm. Bull.* 1983, 31, 4209.
- 23. Yoshida, J. I.; Kataoka, K.; Horcajada, R.; Nagaki, A. Chem. Rev. 2008, 108, 2265.
- 24. Shono, T.; Mitani, M. J. Am. Chem. Soc. 1971, 5284.
- a). Shono, T.; Kashimura, S.; Mori, Y.; Hayashi, T.; Soejima, T.; Yamaguchi, Y. J.
 Org. Chem. 1989, 54, 6001. b). Shono, T. Tetrahedron. 1984, 40, 811.
- 26. Nagib, D. A.; MacMillan, D. W. C. Nature. 2011, 480, 224.
- Furst, L.; Matsuura, B. S.; Narayanam, J. M. R.; Tucker, J. W.; Stephenson, C. R.
 J. Org. Lett. 2010, 12, 3104.
- 28. Nicewicz, D. A.; MacMillan, D. V. C. Science. 2008, 322, 77.
- Tucker, J. W.; Nguyen, J. D.; Narayanam, J. M. R.; Krabbe, S. W.; Stephenson, C.
 R. J. Chem. Commun. 2010, 46, 4985.

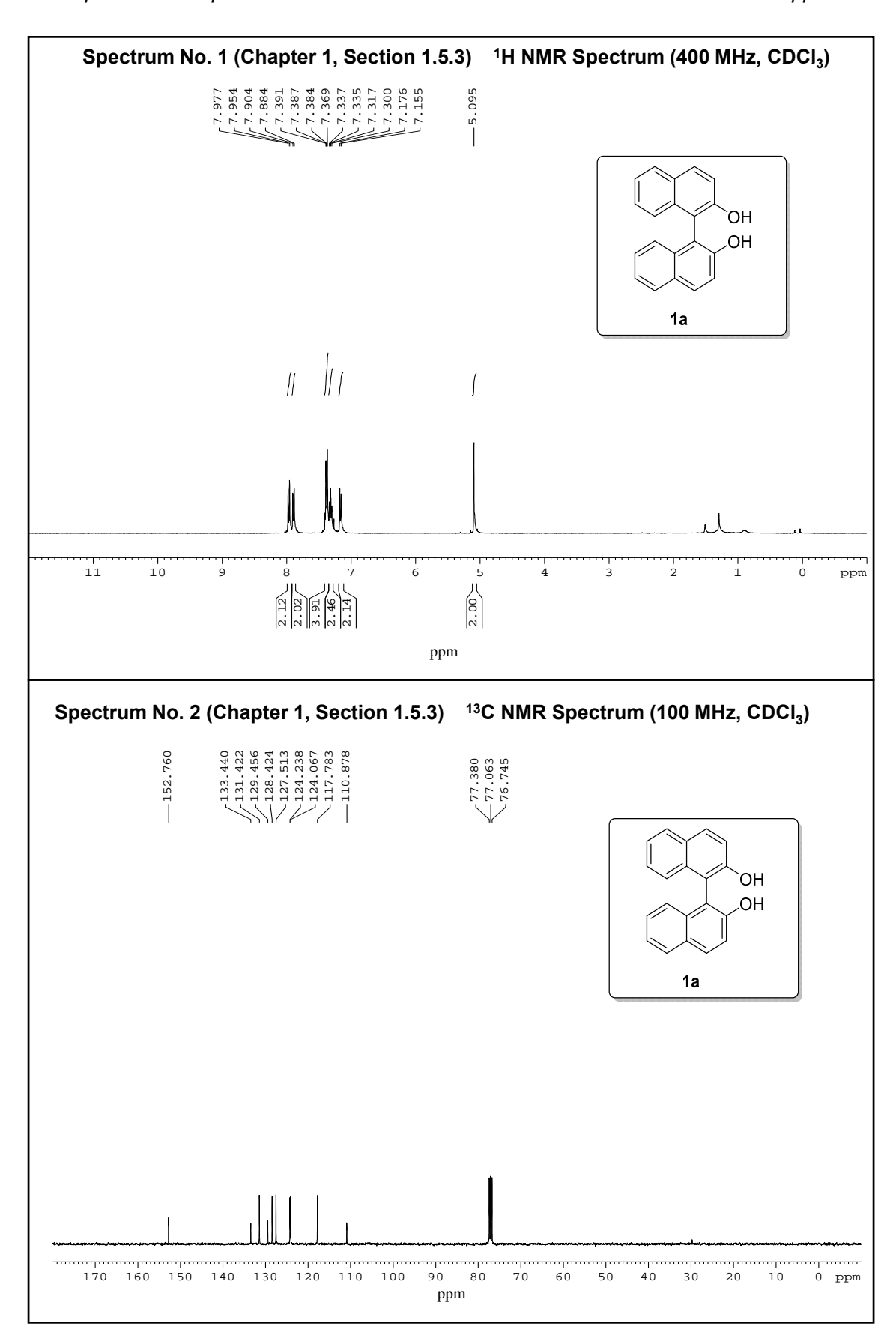
- Condie, A. G.; Gonzalez-Gomez, J. C.; Stephenson, C. R. J. J. Am. Chem.Soc.
 2010, 132, 1464.
- 31. Lin, S.; Ischay, M. A.; Fry, C. G.; Yoon, T. P. J. Am. Chem. Soc. 2011, 133, 19350.
- a) Park, Y.; Choong, V.; Gao, Y.; Hsich, B. R.; Tang, C. W. Appl. Phys. Lett.
 1996, 68, 2699. b) Michaelson, H. B. J. Appl. Phys. 1977, 48, 4729.
- 33. Ghosh, A. K.; Morel, D. L.; Feng, T.; Shaw, R. F.; Rowe Jr, C. A. *Journal of Applied Physics.* **1974**, *45*, 230.
- 34. Gelenis, S.; Tourillon, G.; Granier, F. *Thin Solid Films.* **1986**, *139*, 221.
- 35. Weinberger, B. R.; Akhtar, M.; Gau, S. C. Synthetic Metals. 1982, 4, 187.
- Sariciftci, N. S.; Braun, D.; Zhang, C.; Srdanov, V. I.; Heeger, A. J.; Stucky, G.;
 Wudl, F. Appt. Phys. Lett. 1993, 62, 585.
- 37. Tang, C. W. Appl. Phy. Lett. 1986, 48, 183.
- 38. Halls, J. J. M.; Pichler, K.; Friend, R. H.; Moratti, S. C.; Holmes, A. B. *Appt. Phys. Lett.* **1996**, *68*, 3120.
- 39. Yu, G.; Gao, J.; Hummelen, J. C.; Wudl, F.; Heeger, A. J. Science. 1995, 270, 1789.
- 40. Yu, G.; Wang, J.; McElvain, J.; Heeger, A. J. Adv. Mater. 1998, 10, 1431.
- 41. Shanmugaraja, M. Ph.D. Thesis. **2018**, School of Chemistry, University of Hyderabad.
- 42. a) Lee, K. H.; Schwenn, P. E.; Smith, A. R. G.; Cavaye, H.; Shaw, P.W.; James, M.; Krueger, K. B.; Gentle, I. R.; Meredith, P.; Burn, P. L. Adv. Mater. 2011, 23, 766. b) Hoppea, H.; Sariciftci, N. S. J. Mater. Res. 2004, 19, 1924.
- 43. a) Shalev, H.; Evans, D, H. J. Am. Chem. Soc. 1989, 111, 2667. b) Kebarle, P.;Chowdhury, S. Chem. Rev. 1987, 87, 513.

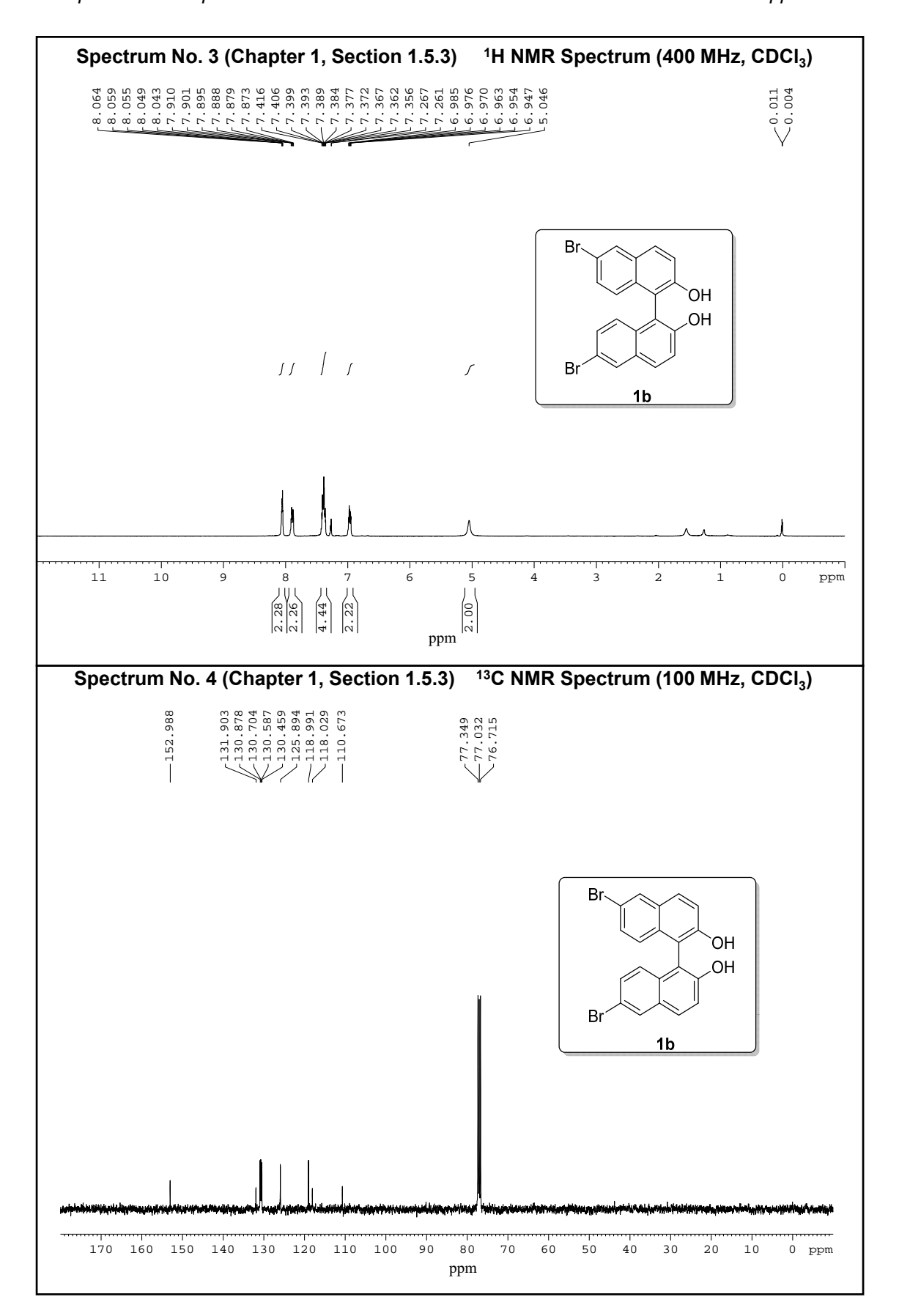
212 References

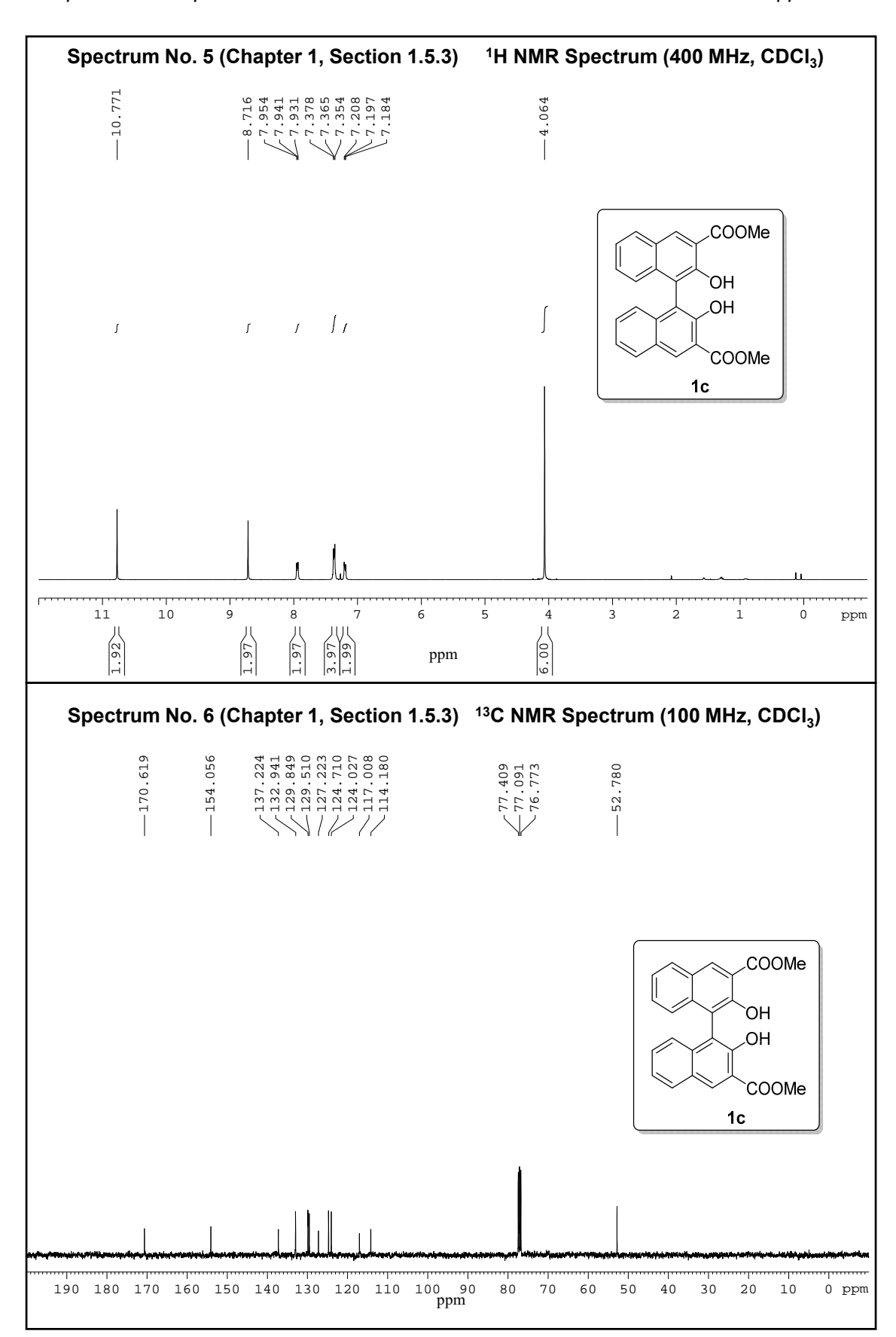
- 44. Paul, G.; Kebale, P. J. Am. Chem. Soc. 1989, 111, 464.
- 45. a) Fumey, F.; Weber, R.; Gatenbein, P.; Daguenet-Frick, X.; Williamson, T.; Dorer, V. Energy Procedia. 2014, 46, 134. b) Yu, N.; Wang, R. Z.; Wang, L. W. Progress in Energy and Combustion Science. 2013, 39, 489.

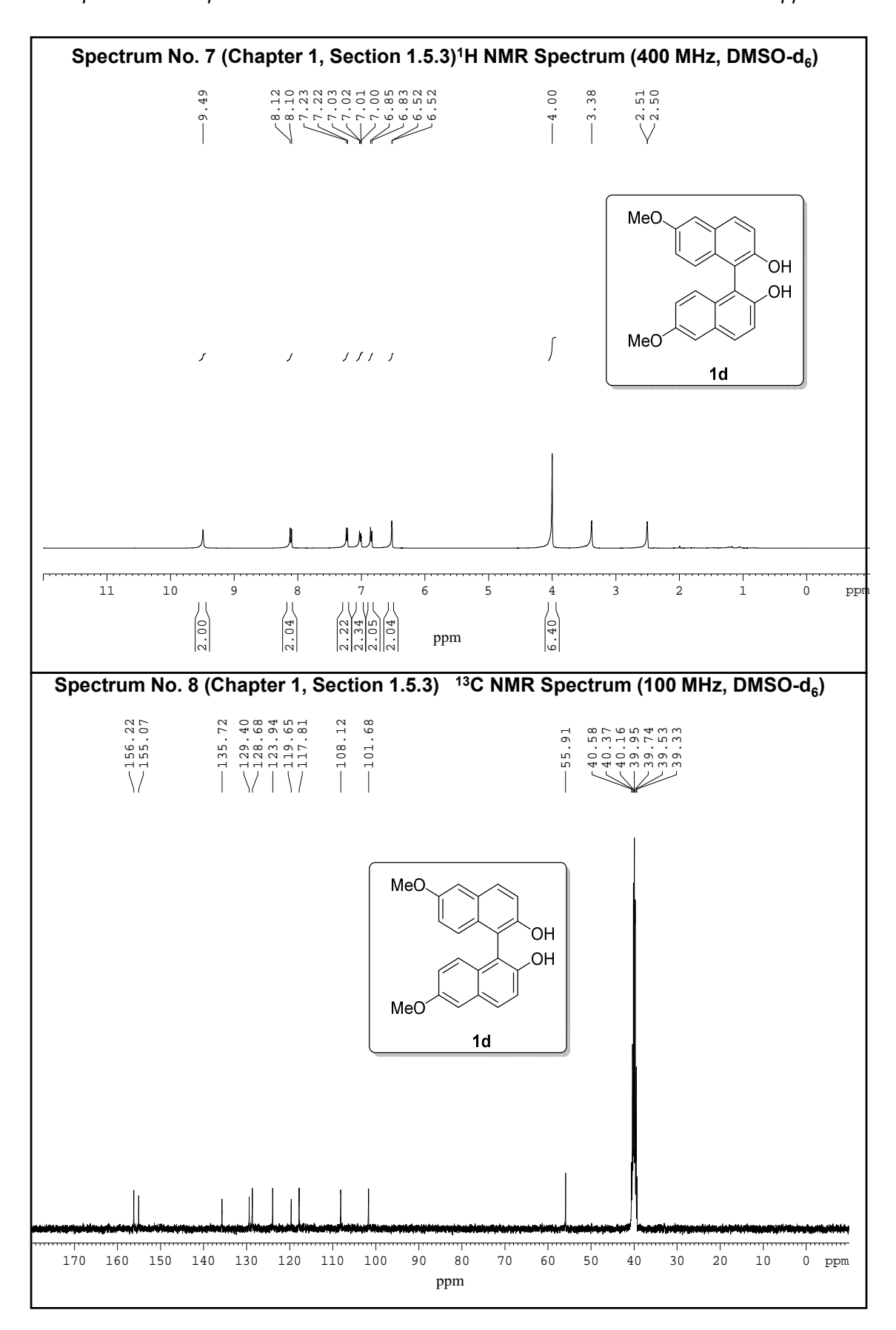
Appendix I

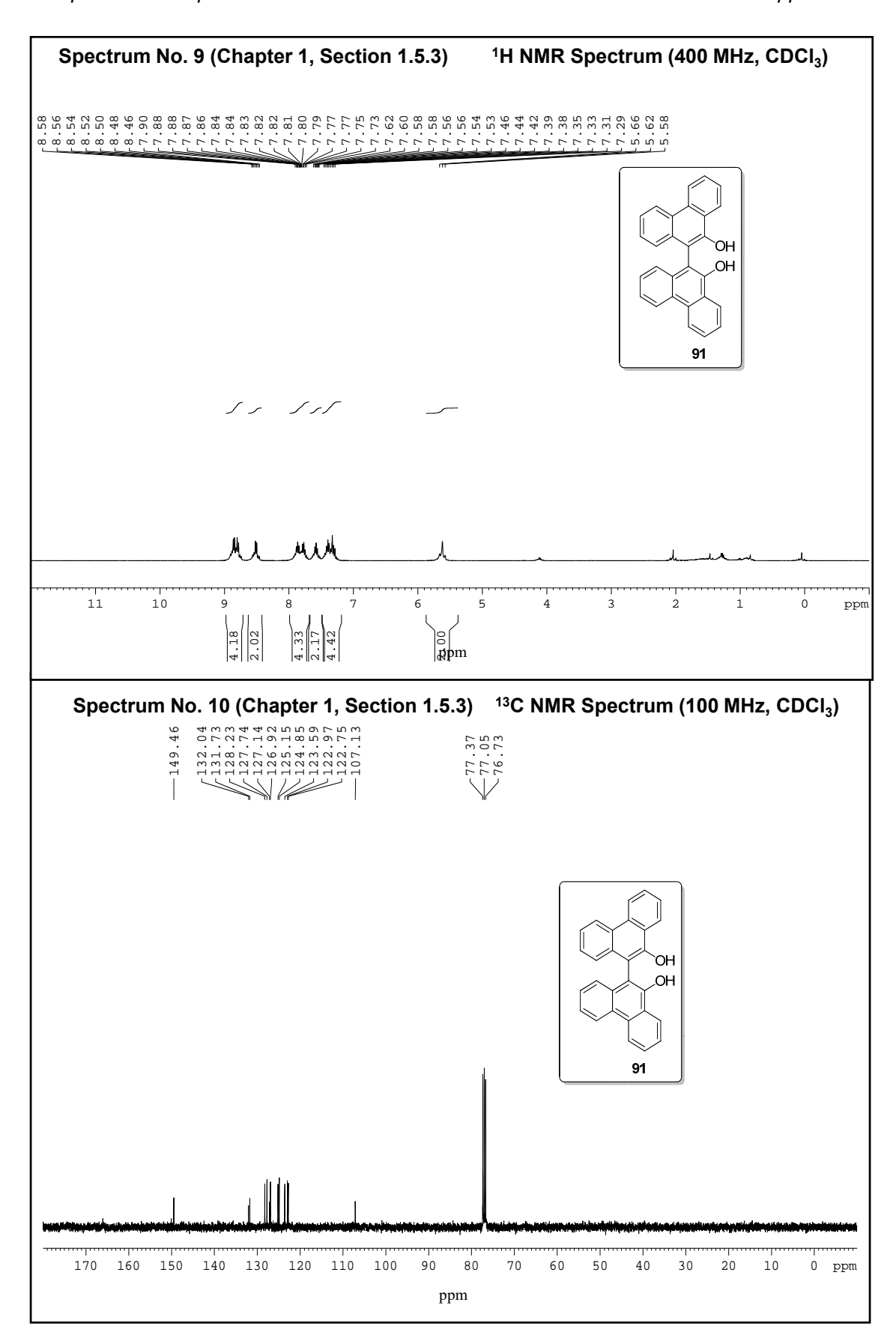
(Representative Spectra)

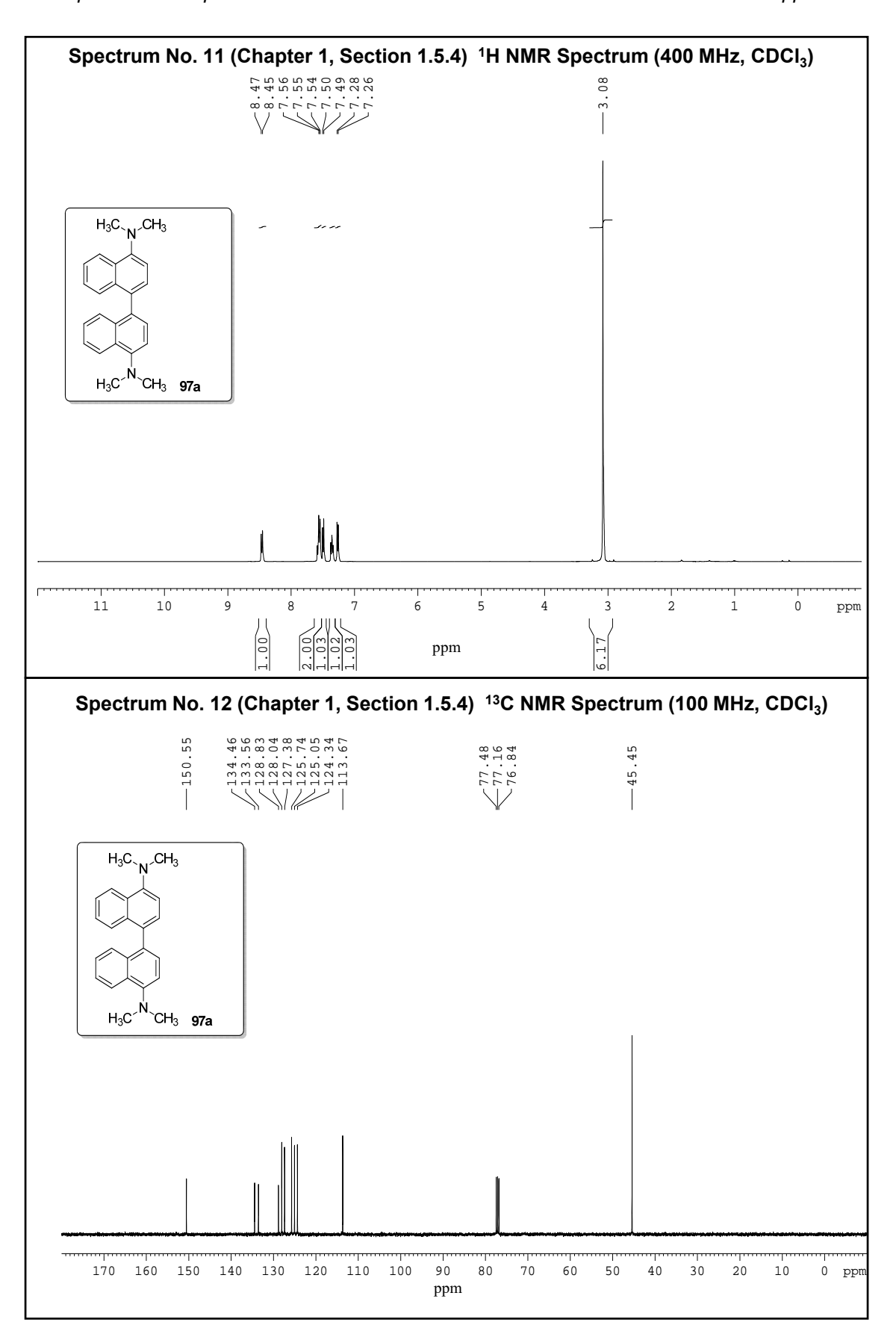


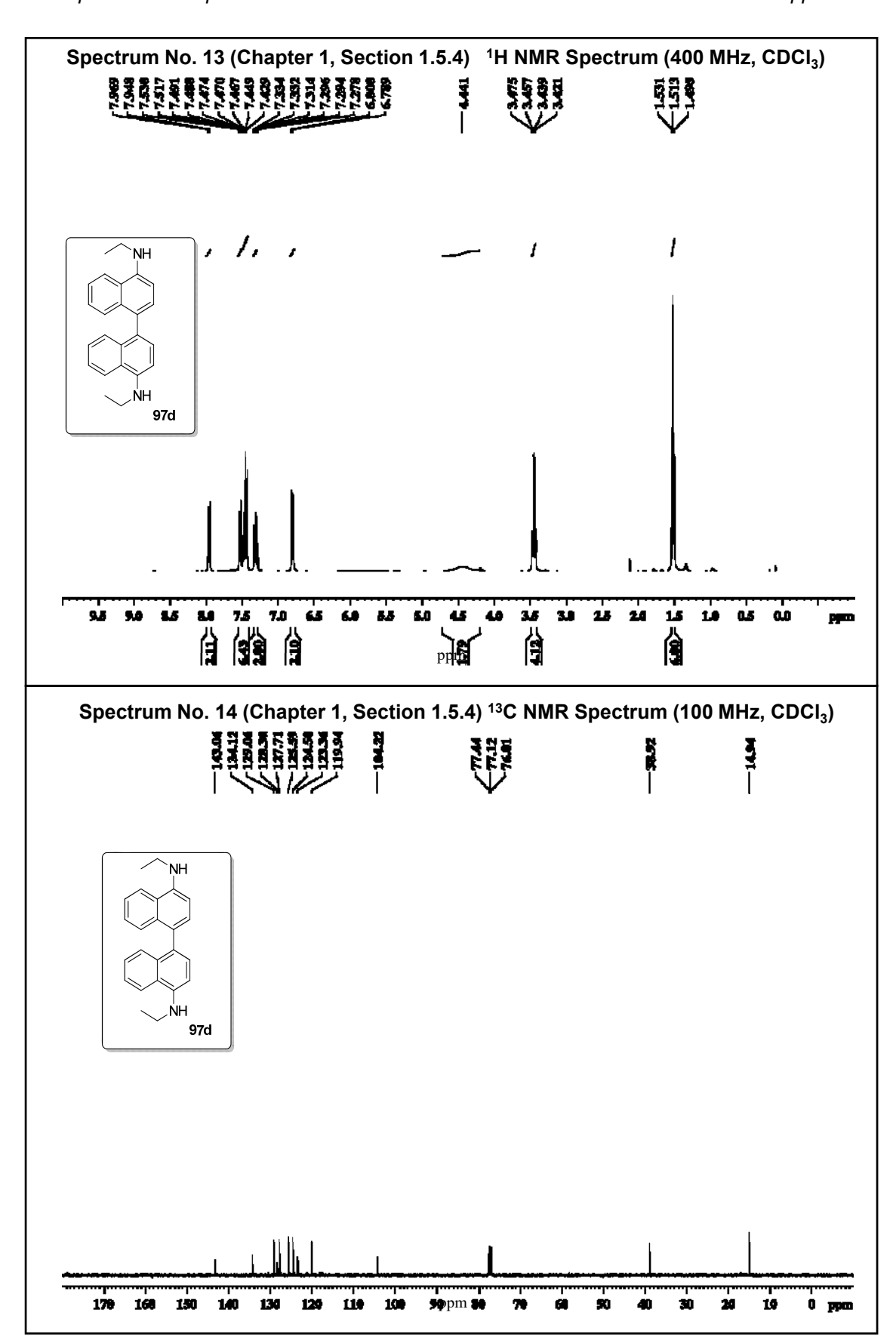


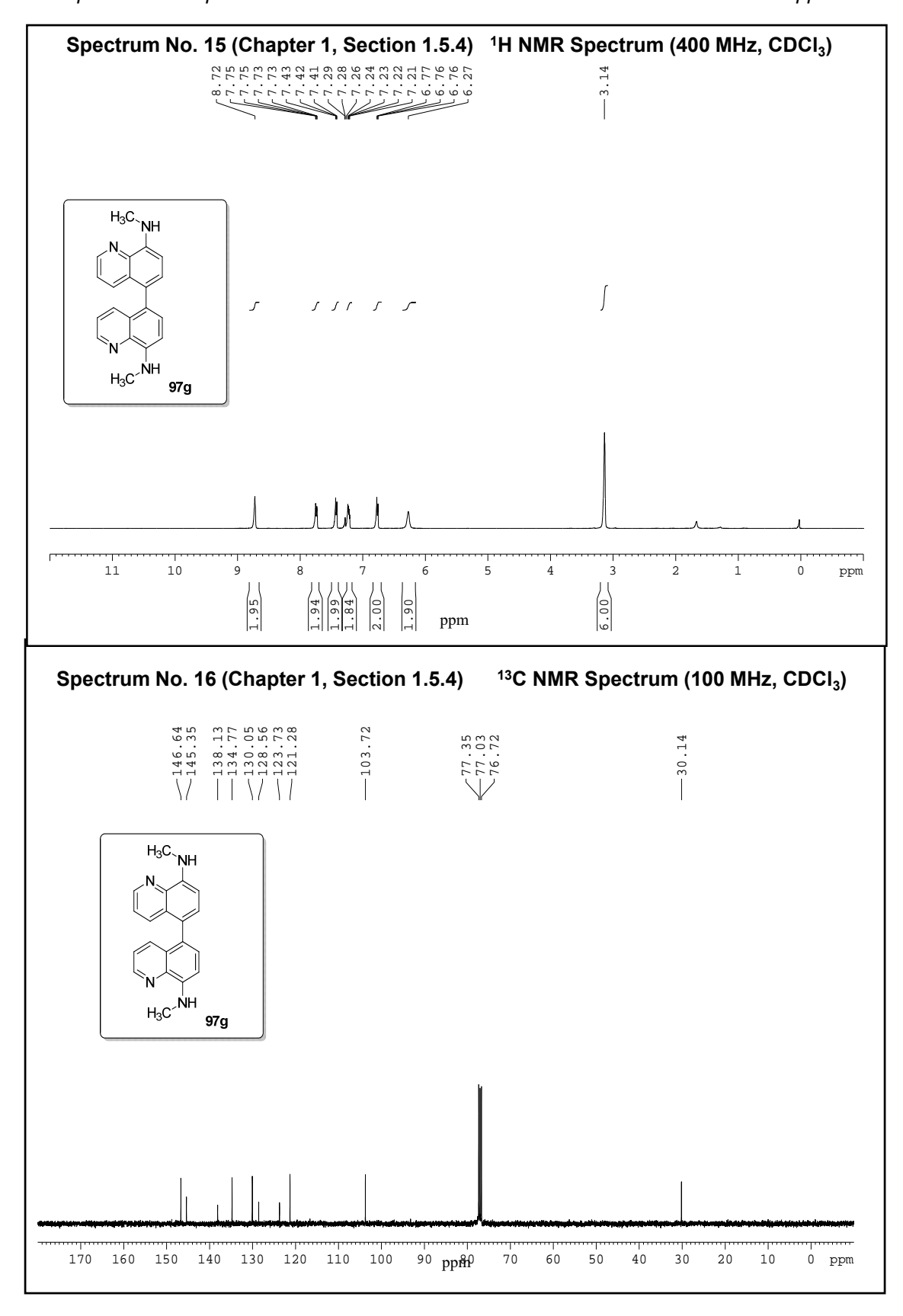


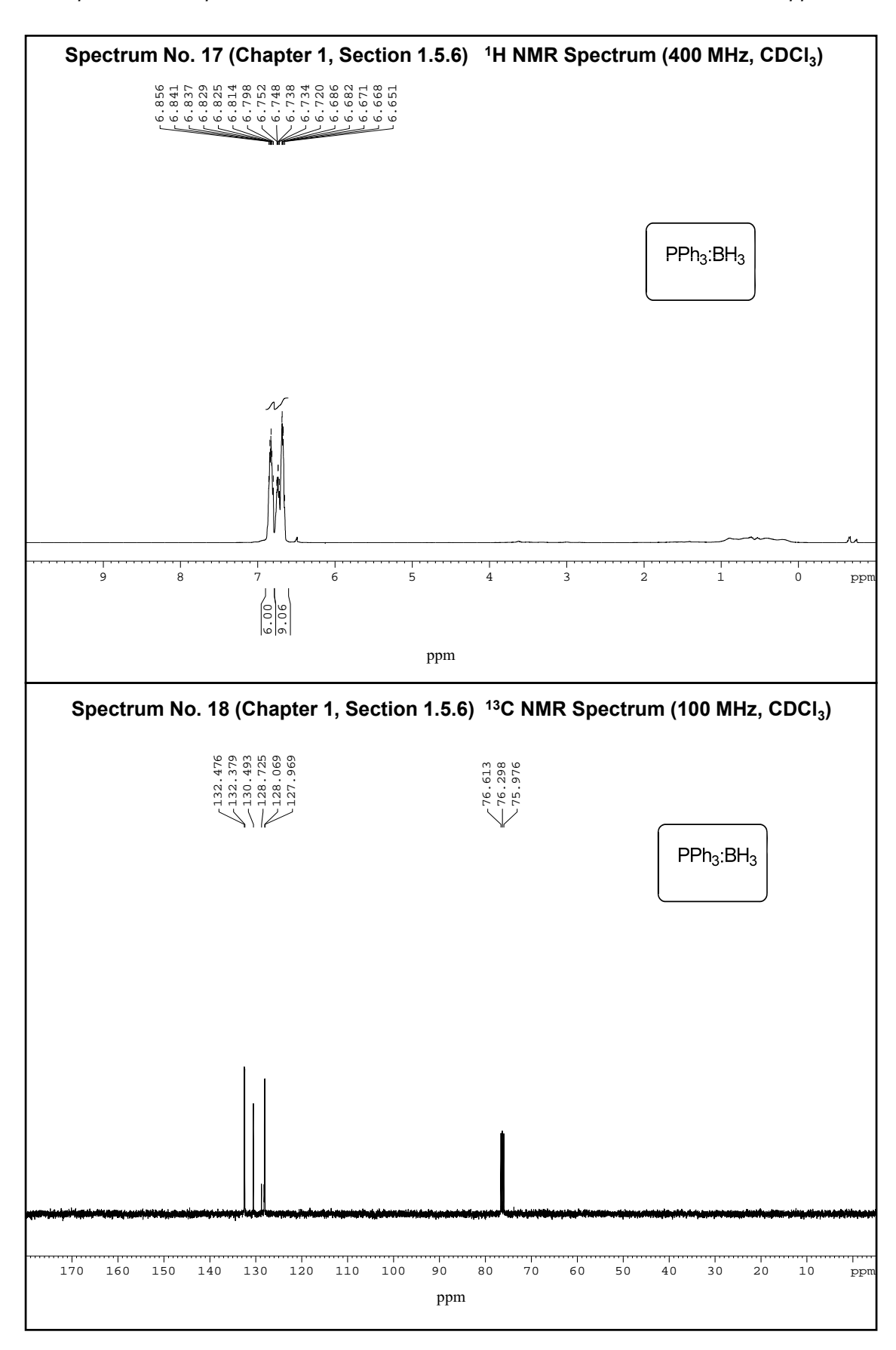


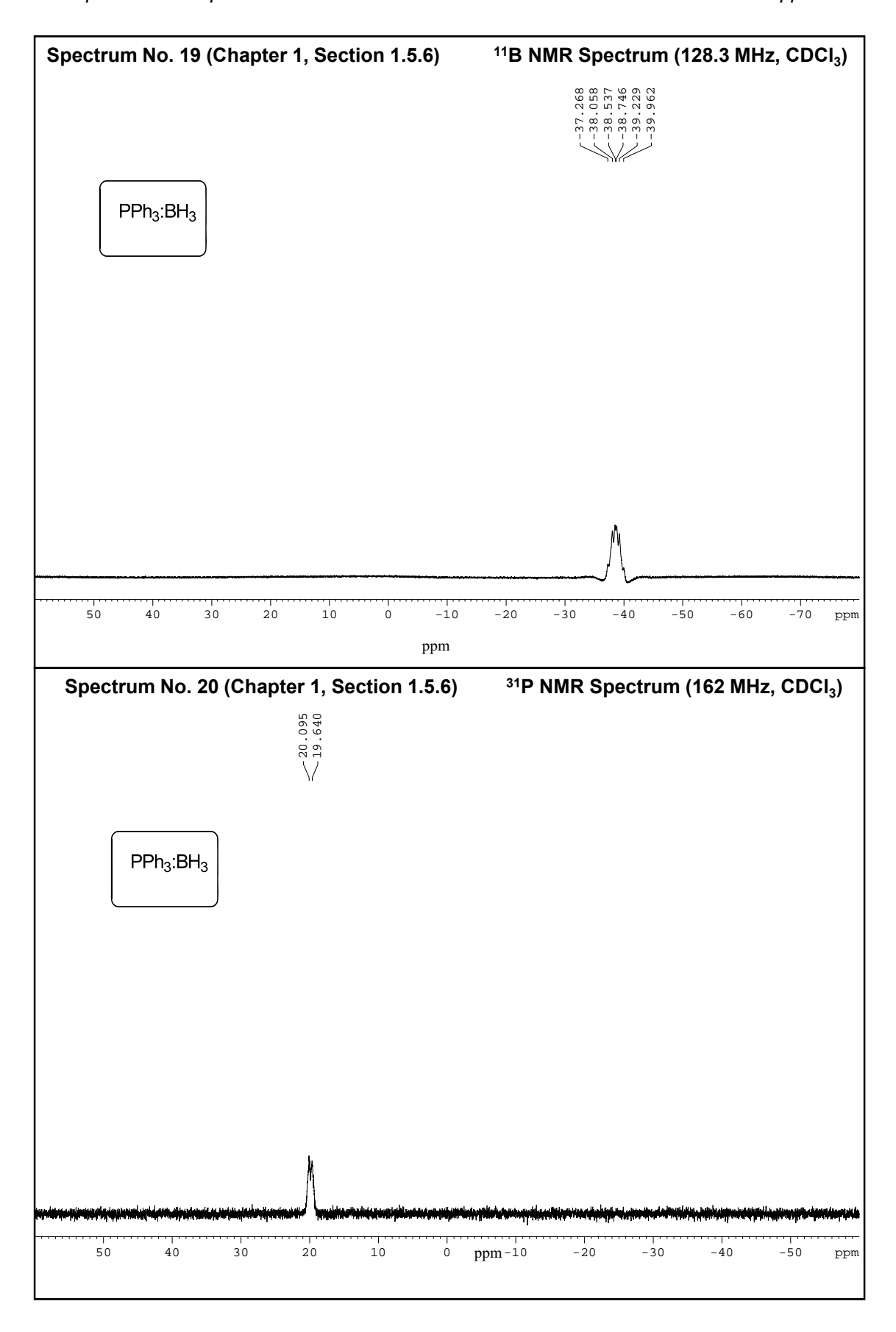


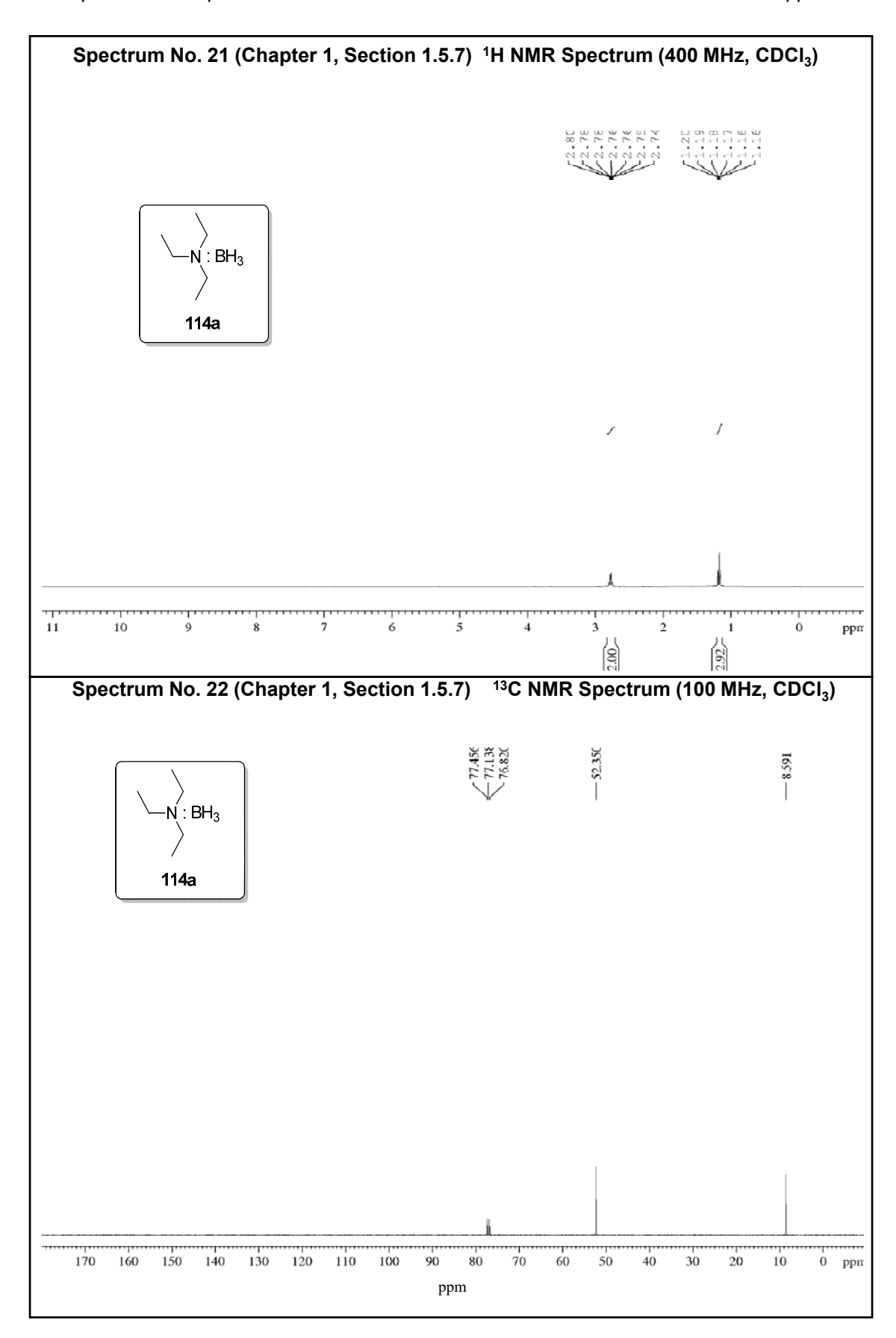


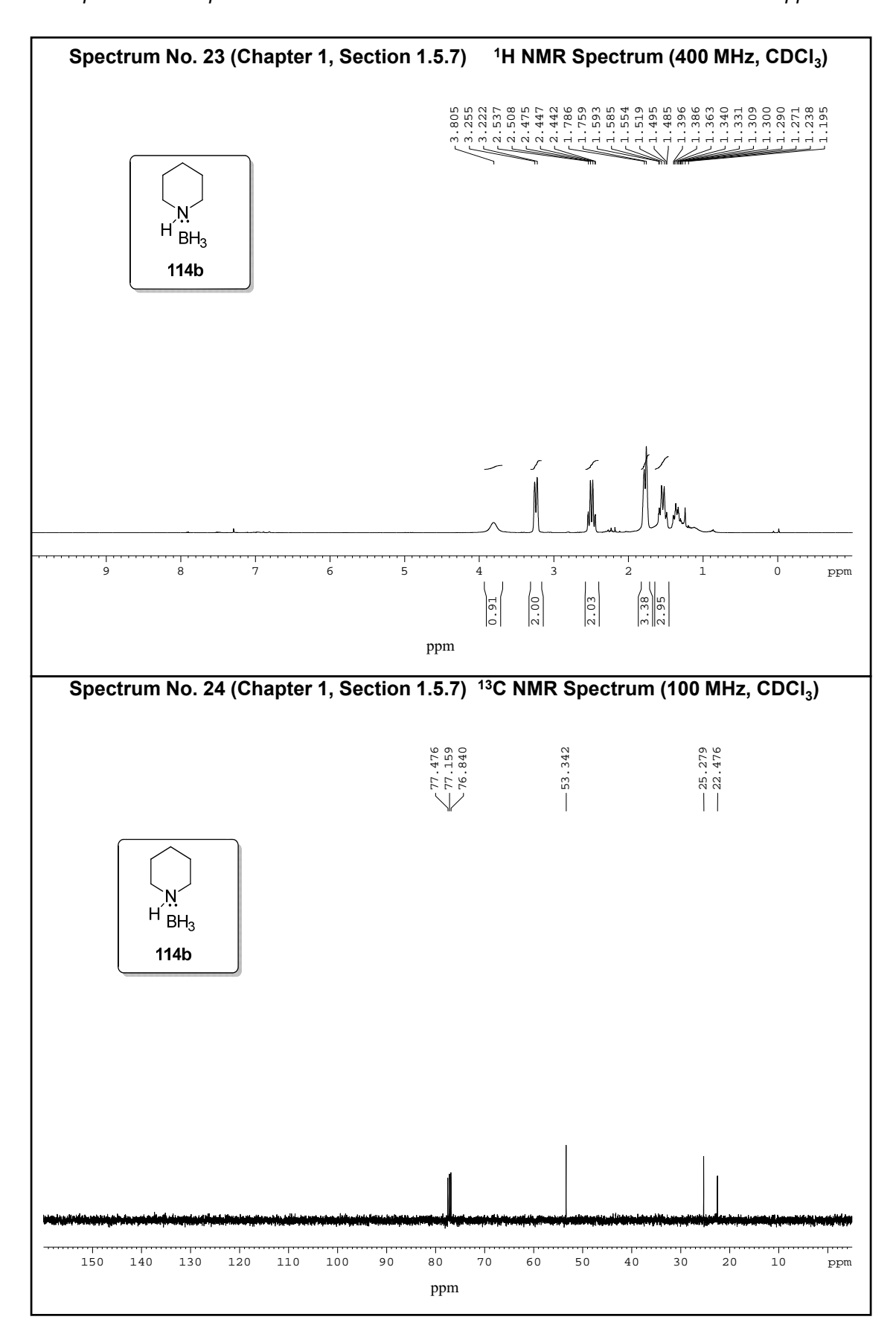


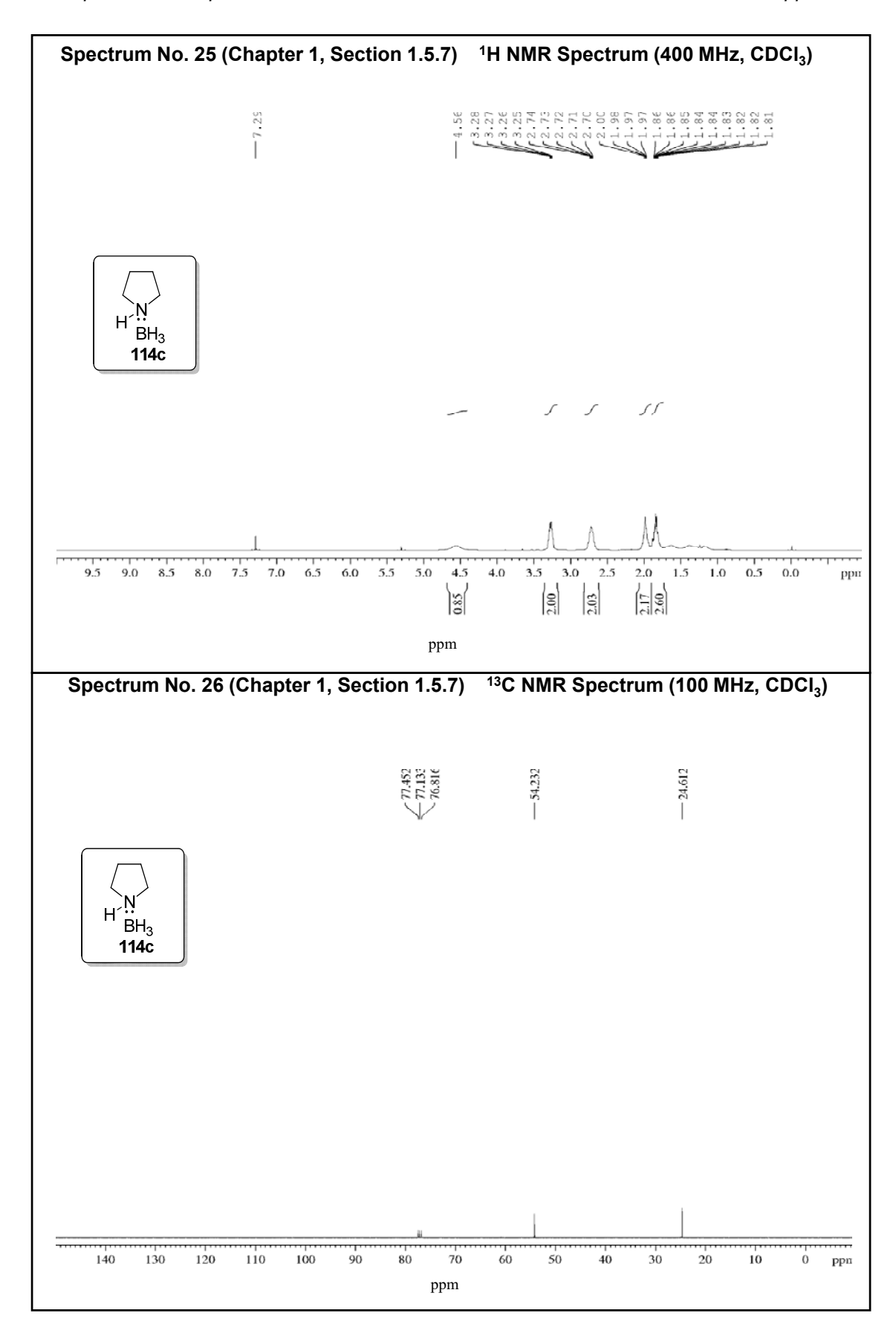


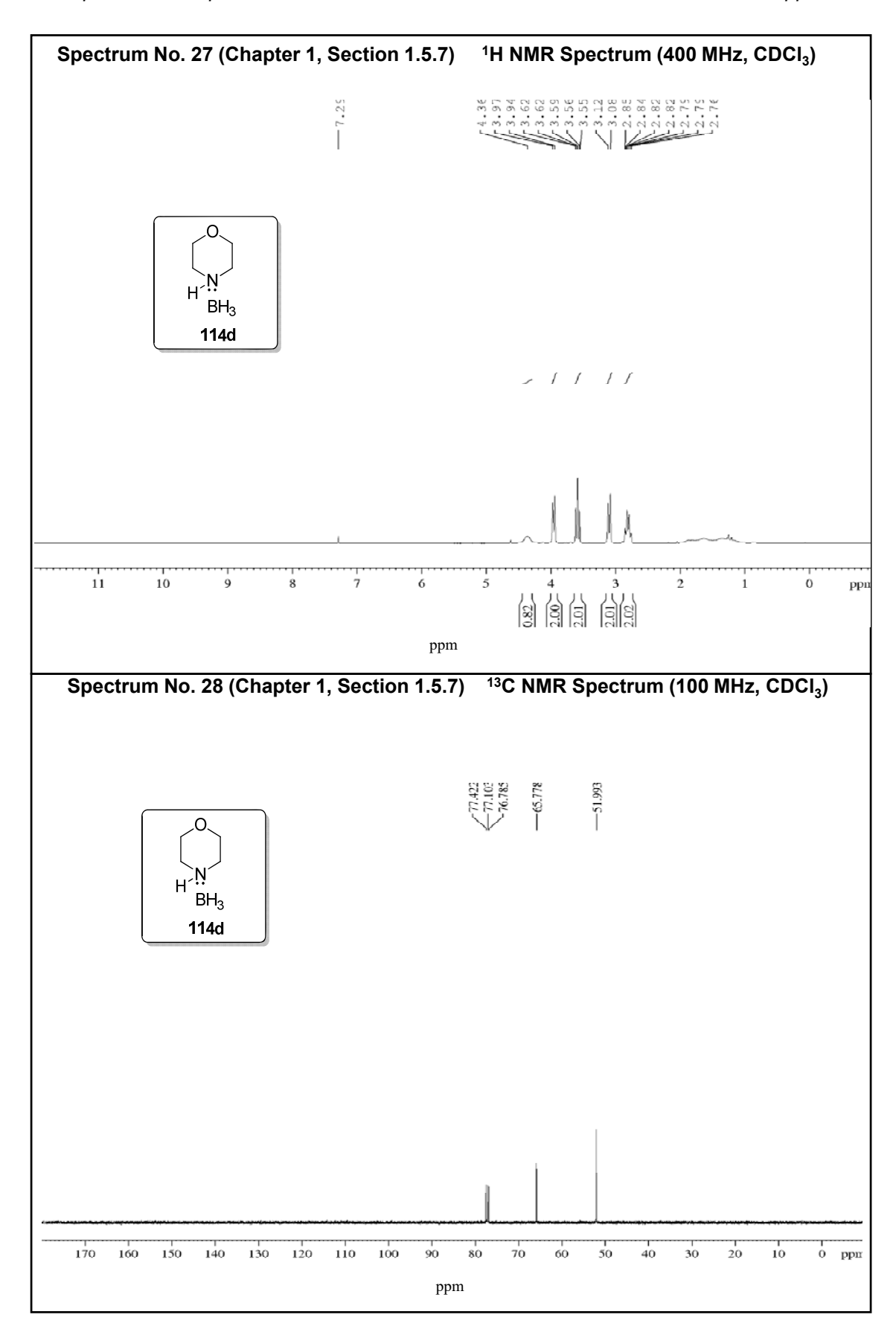


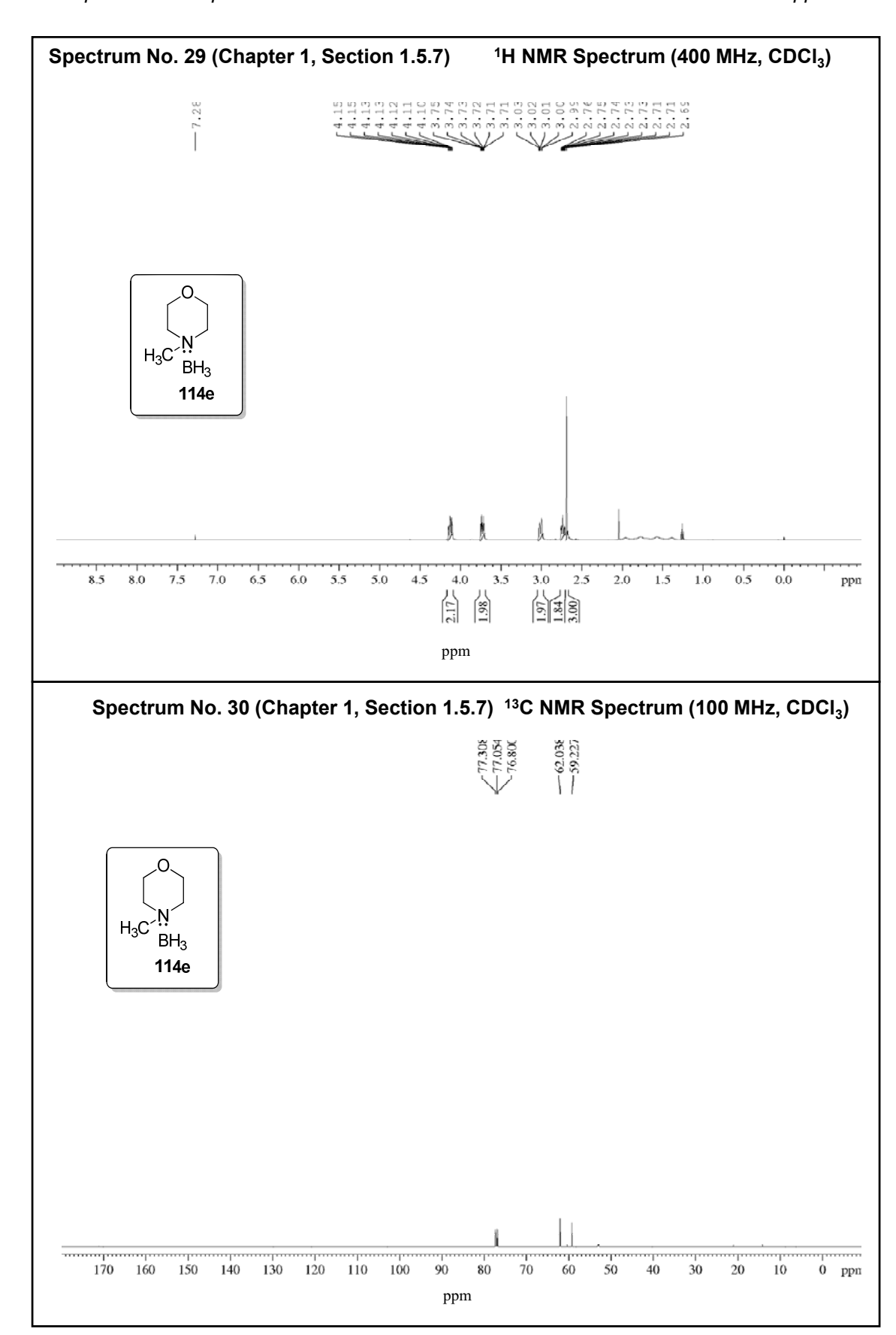


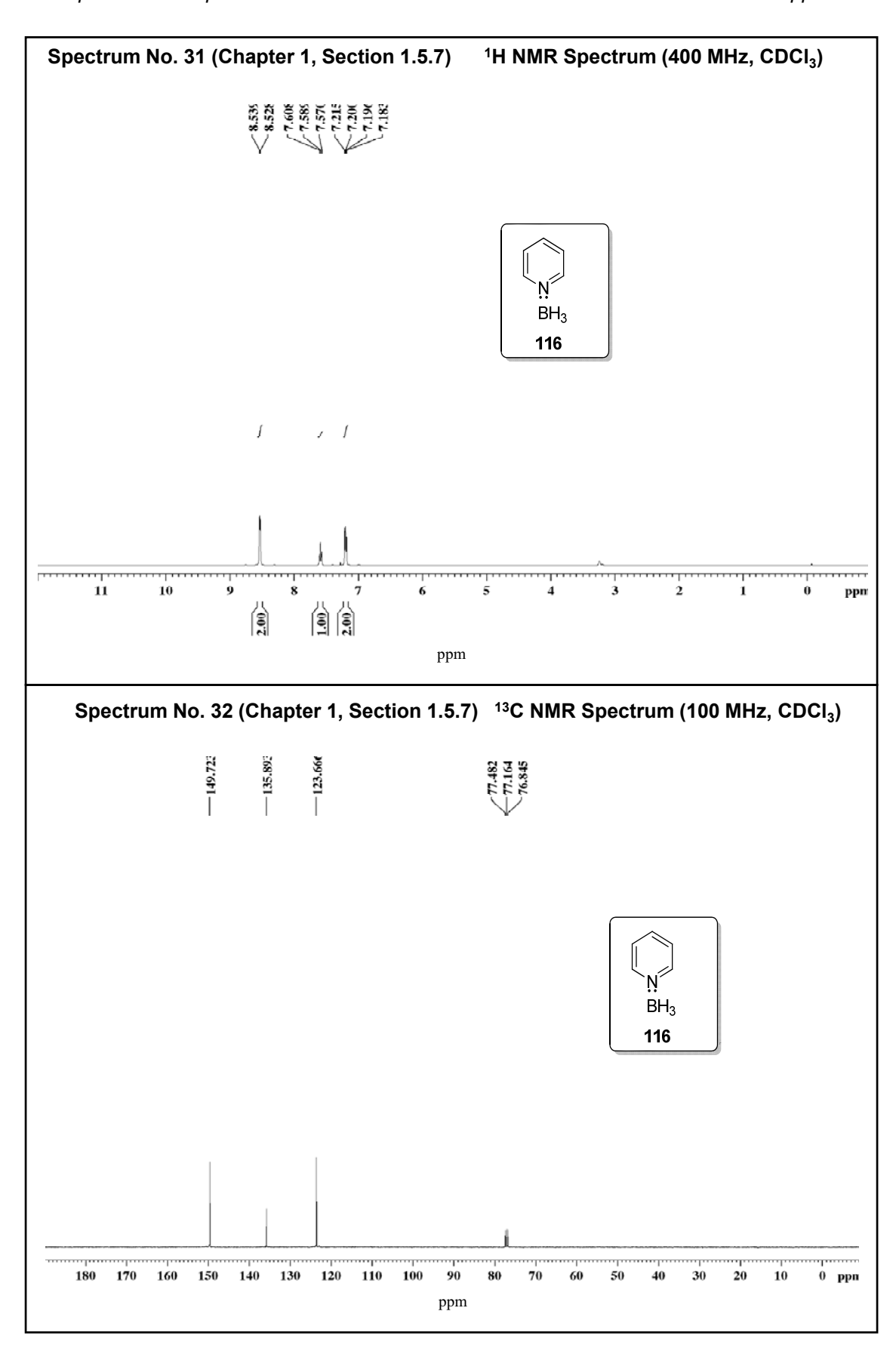


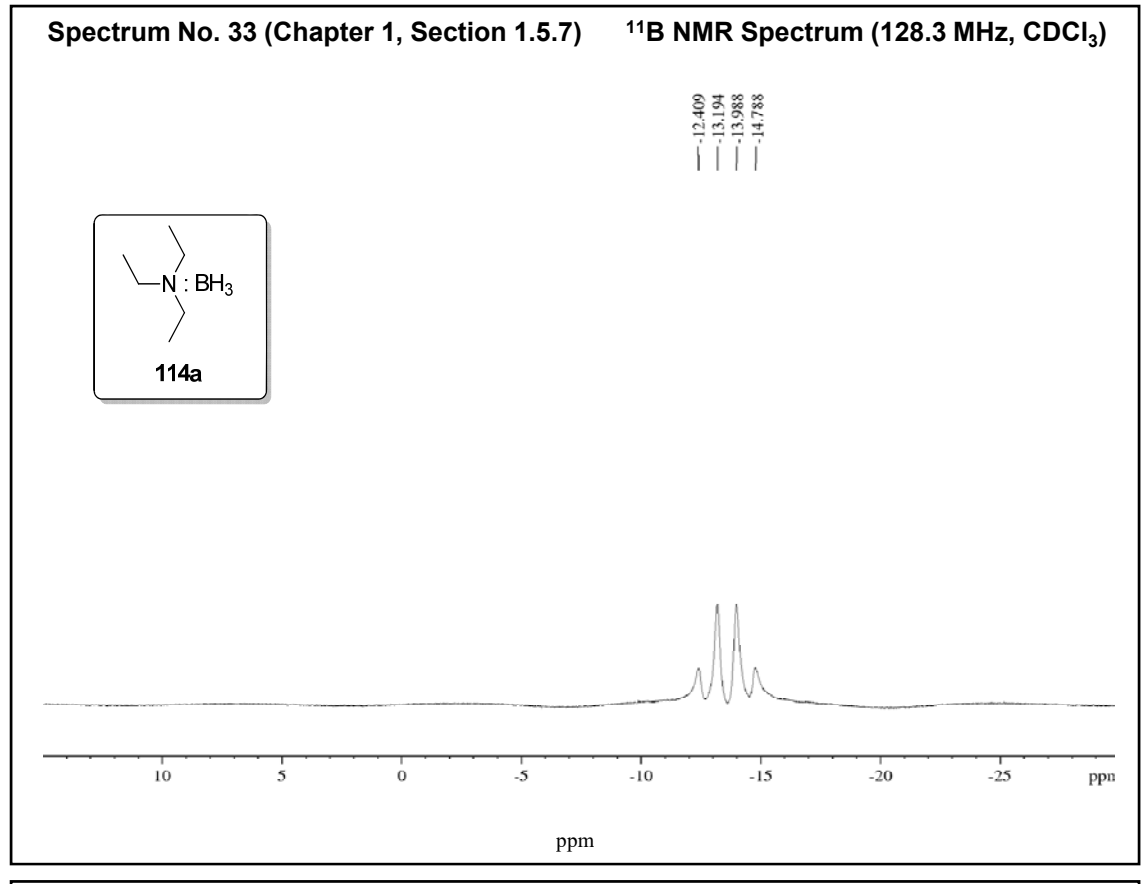


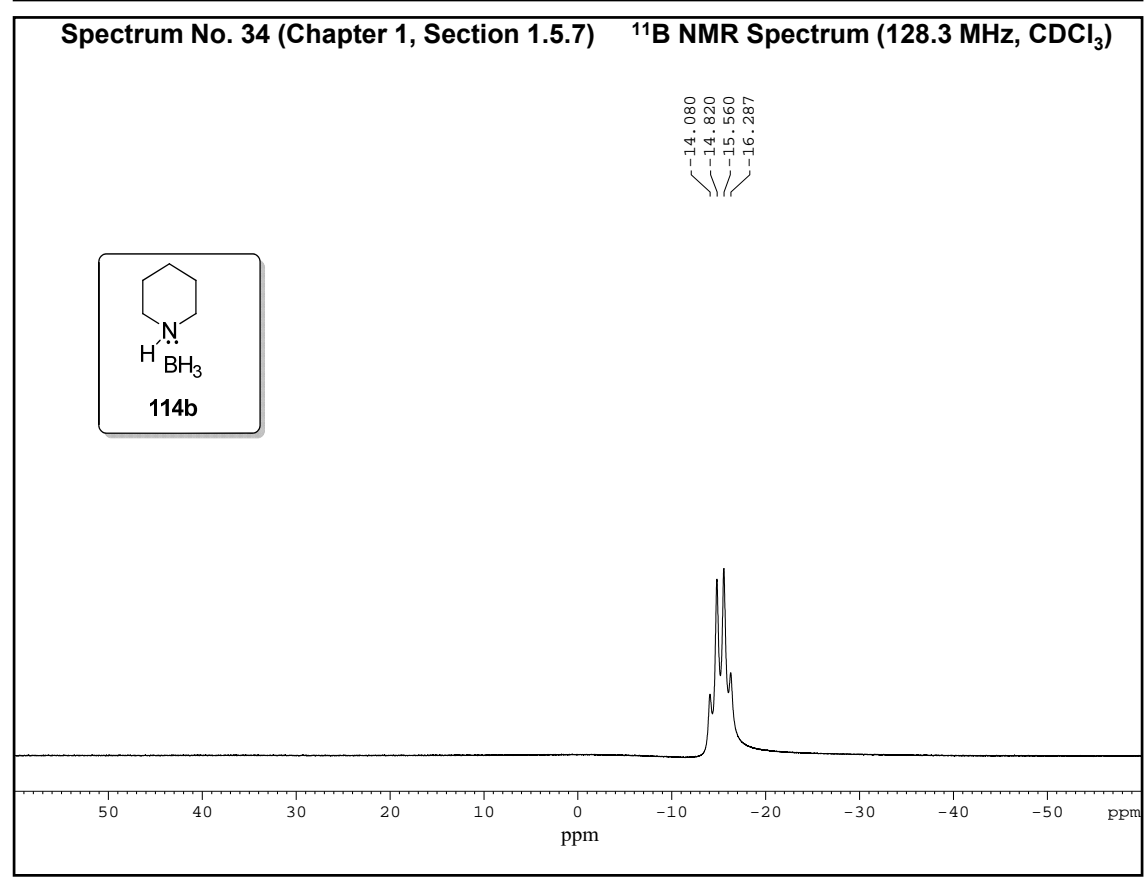


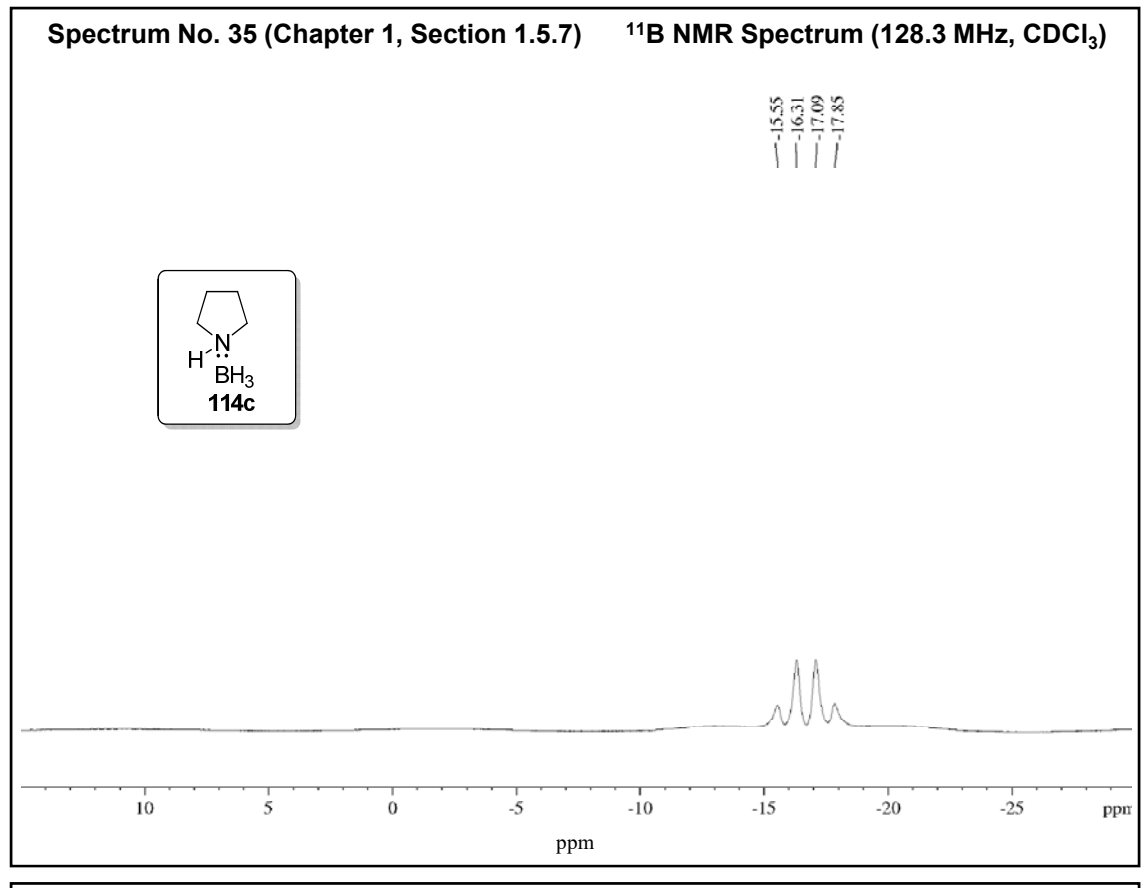


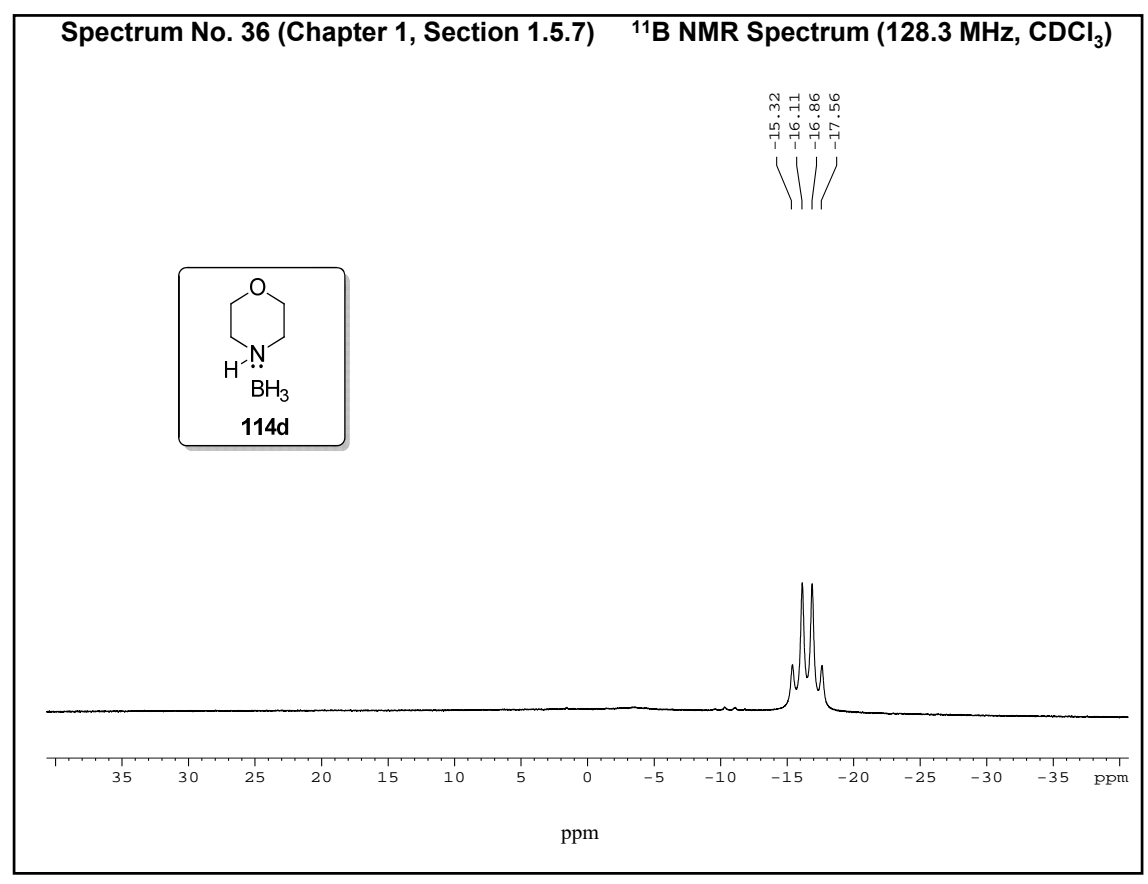


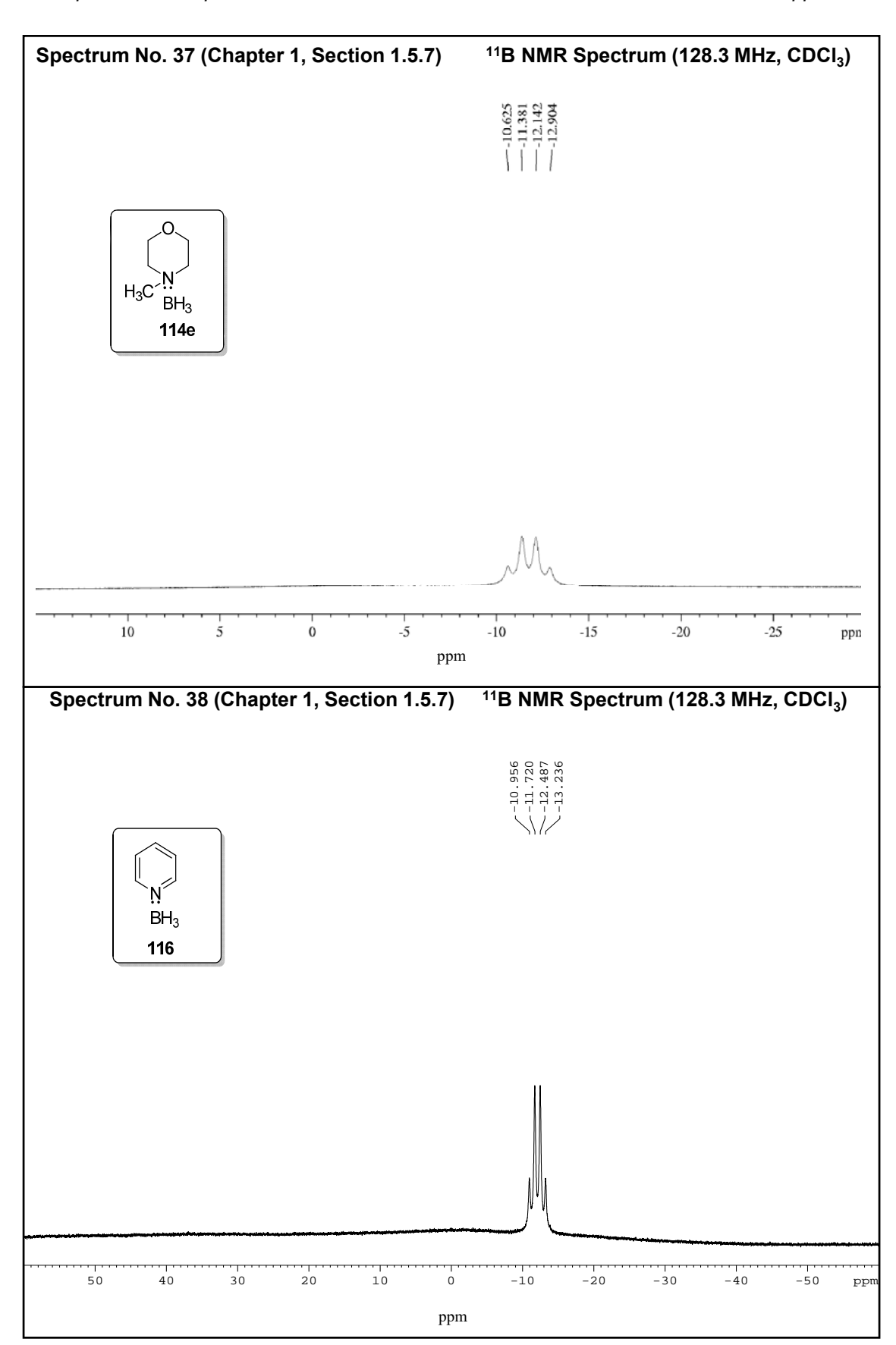


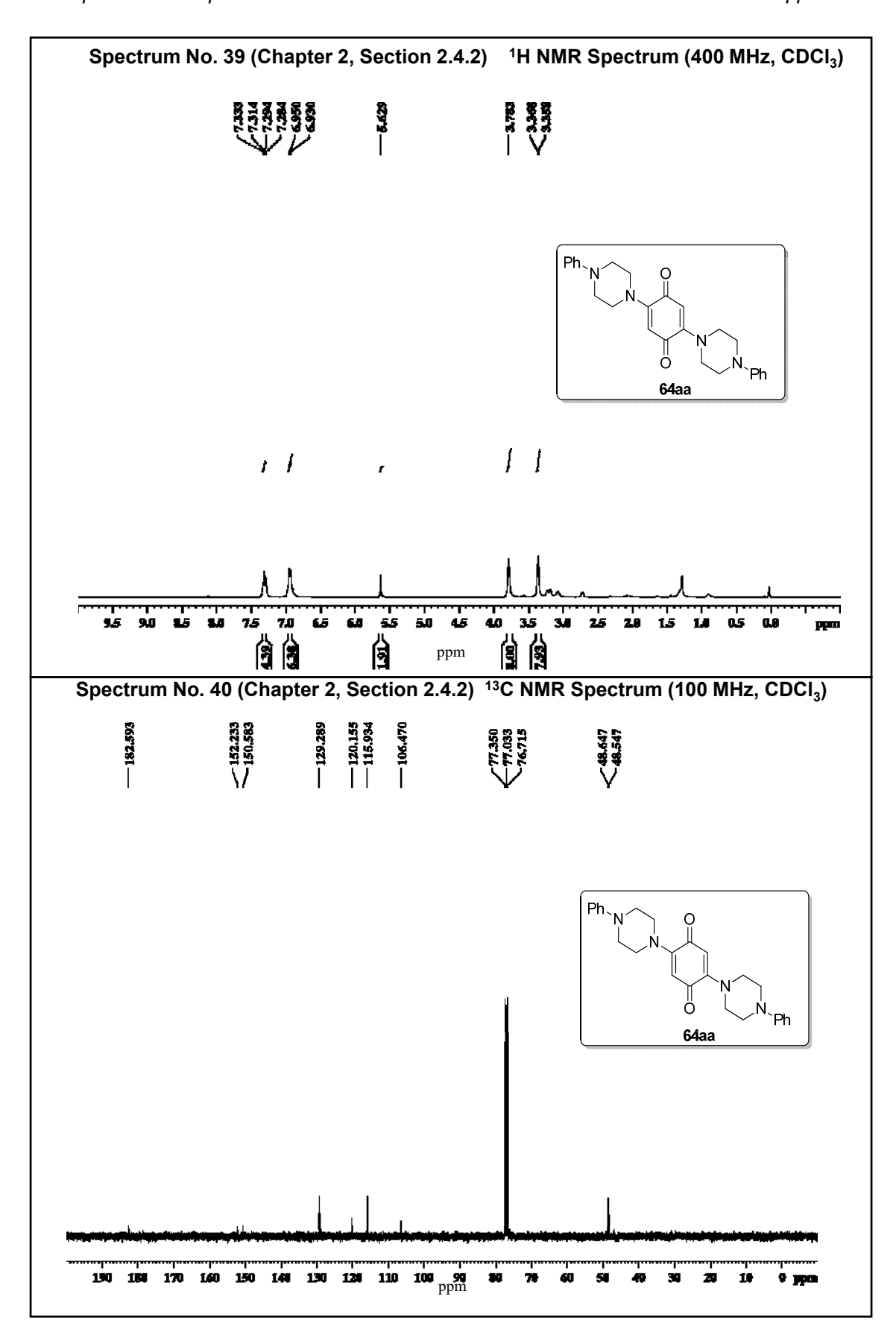


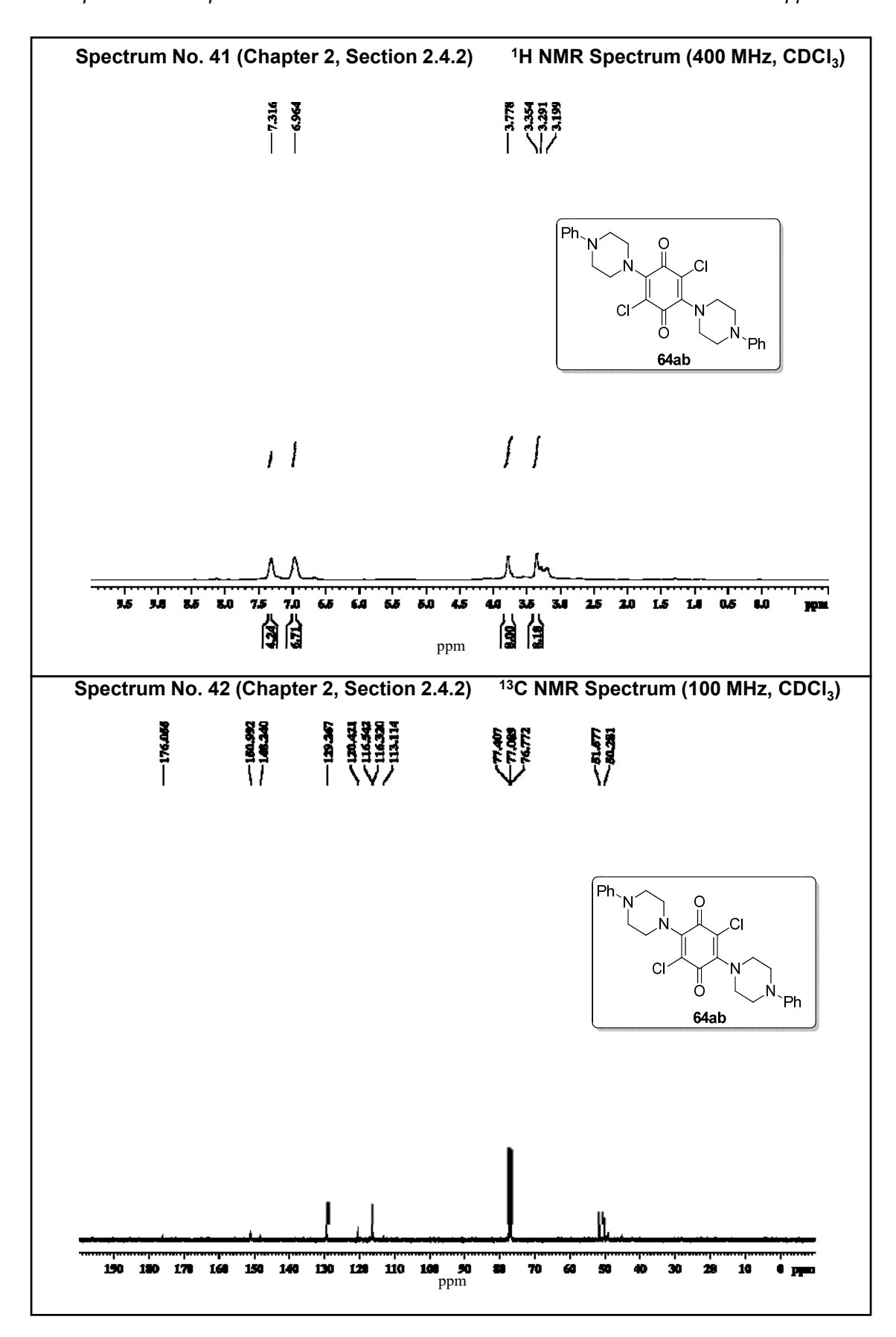


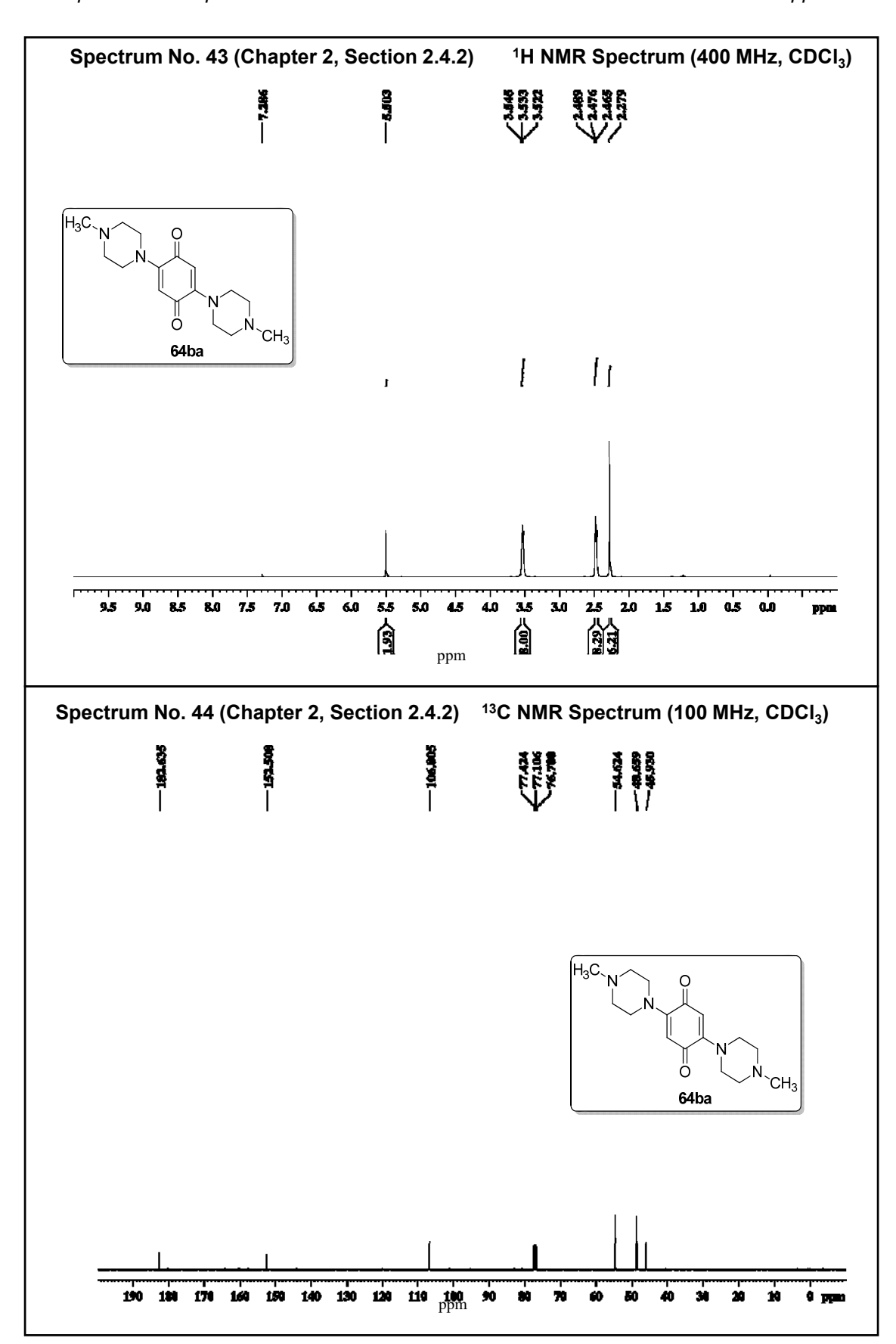


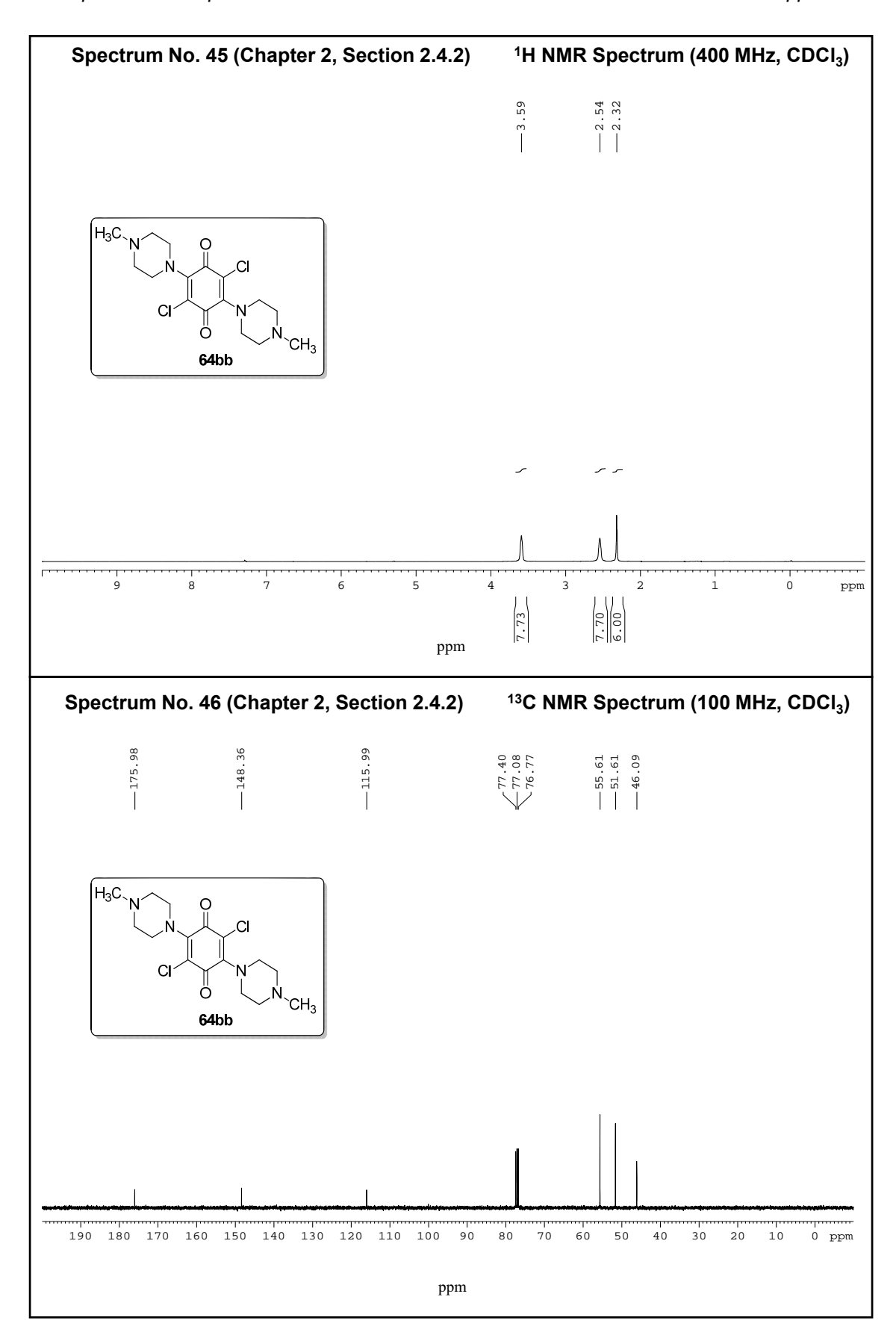


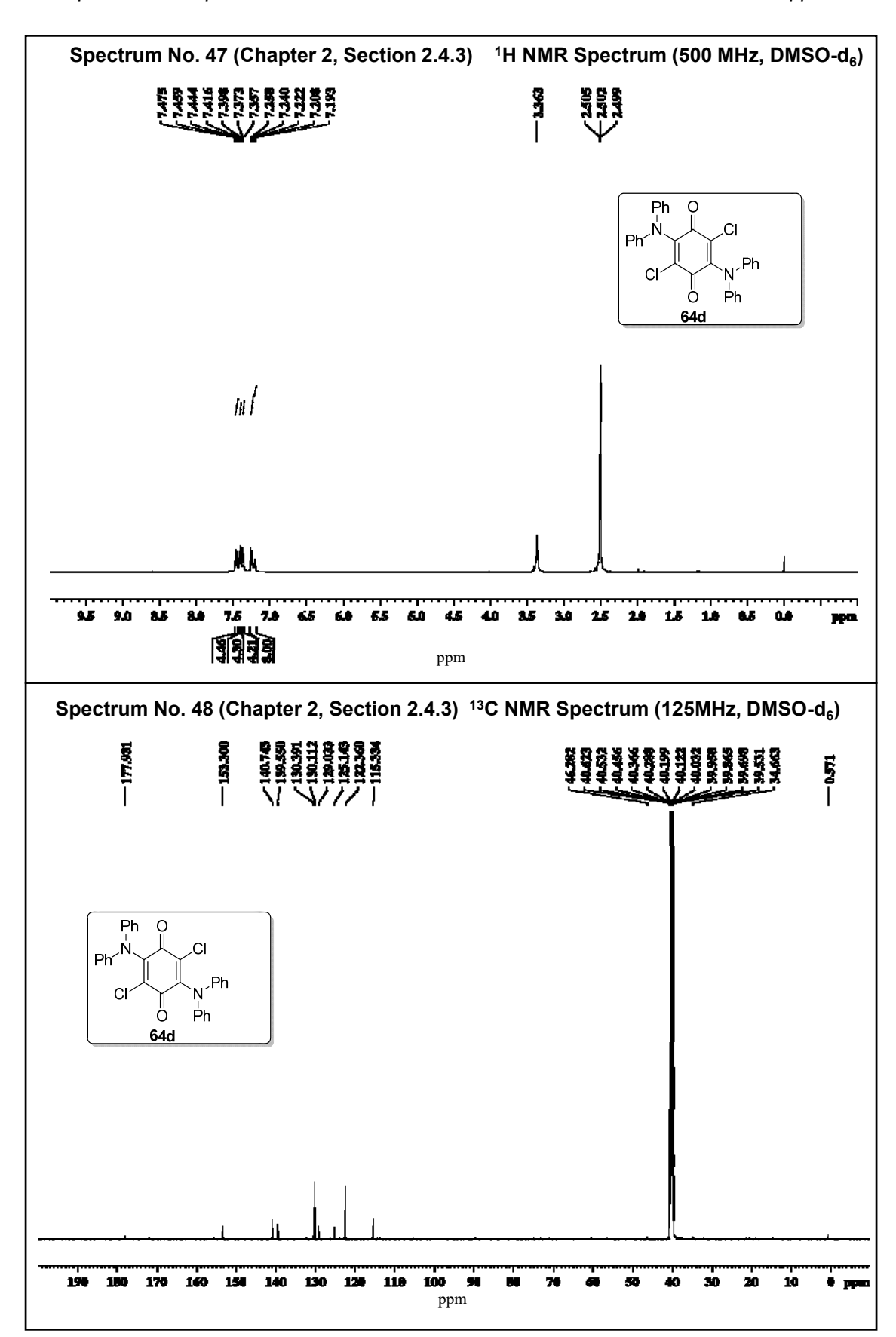


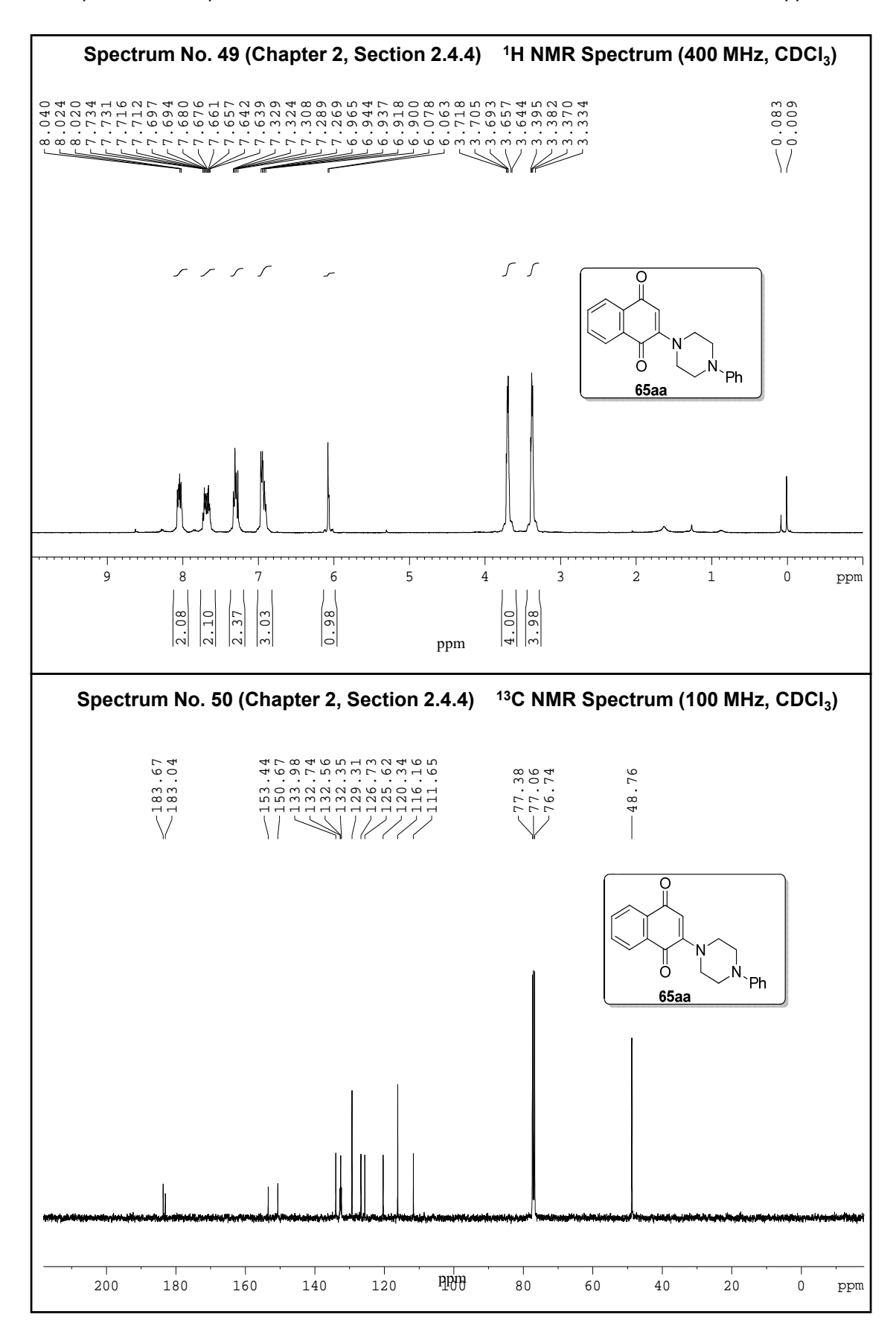


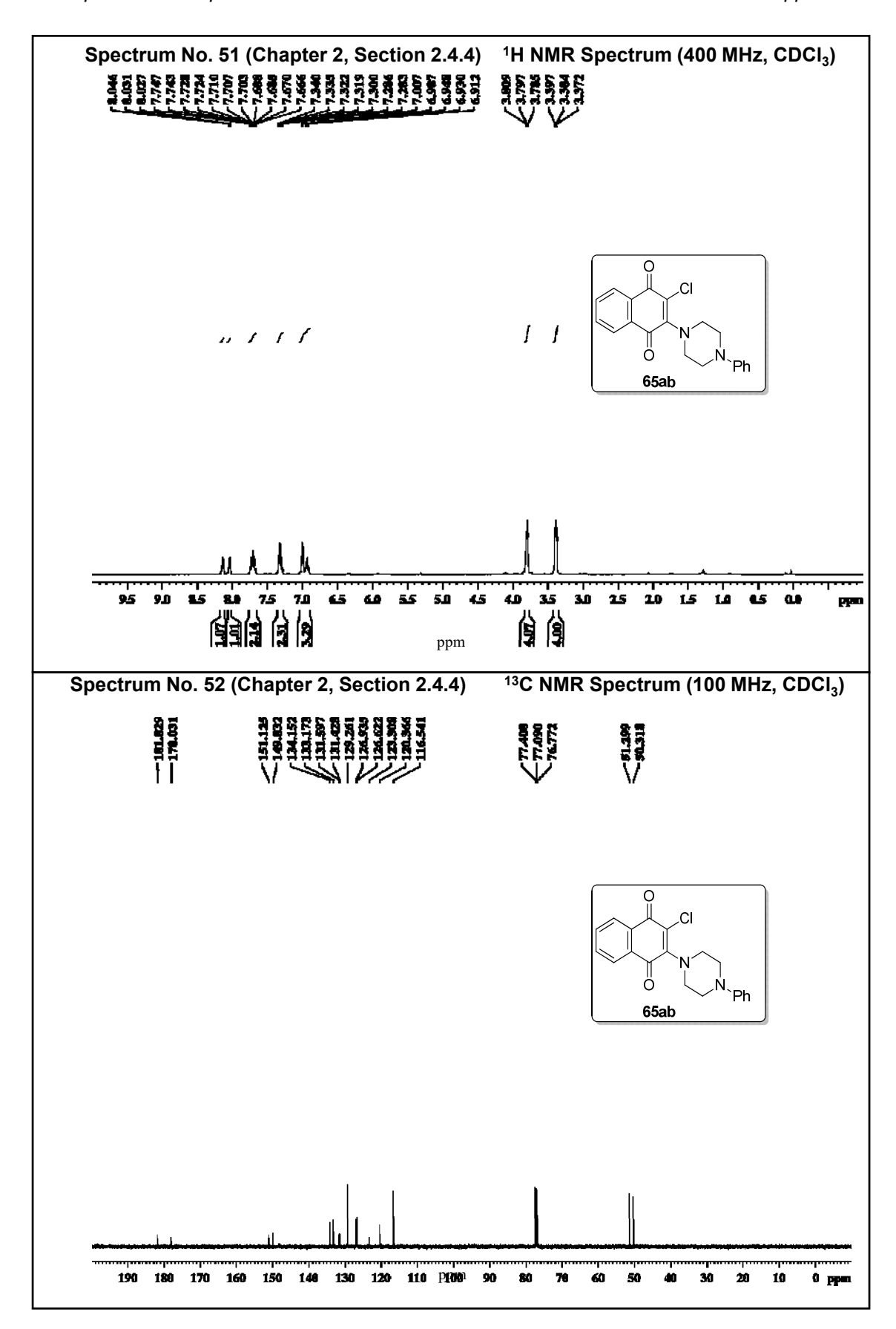


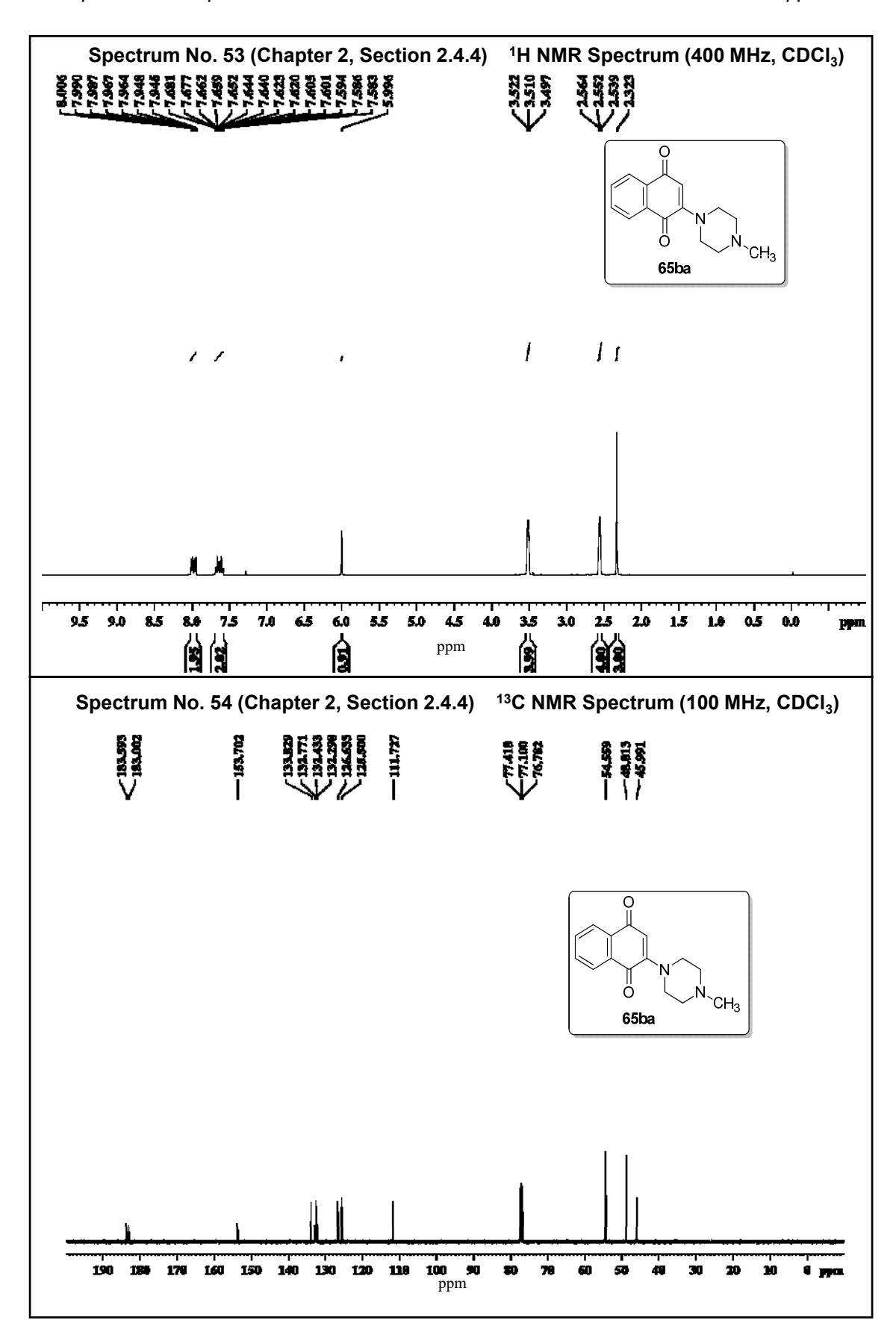


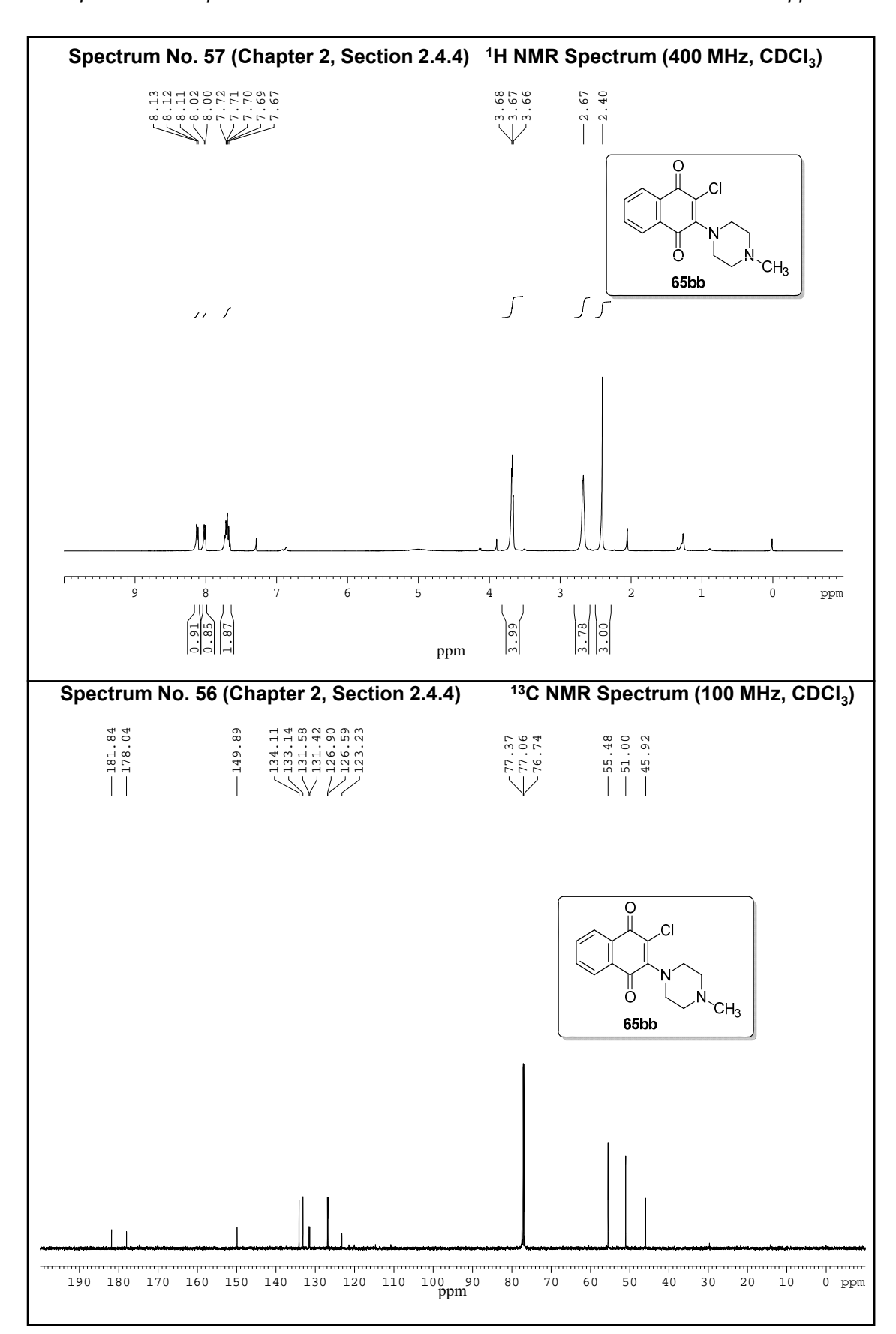


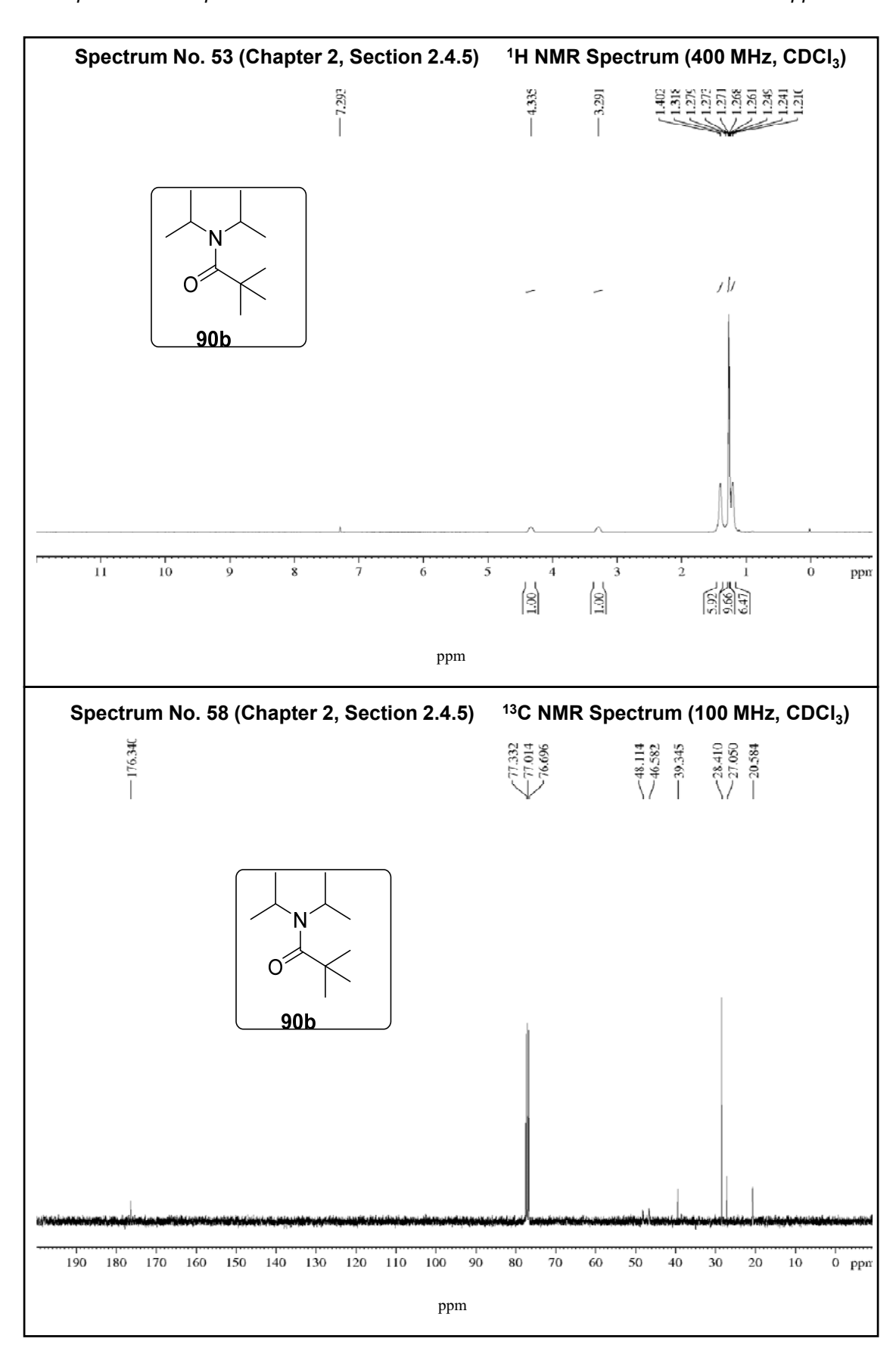


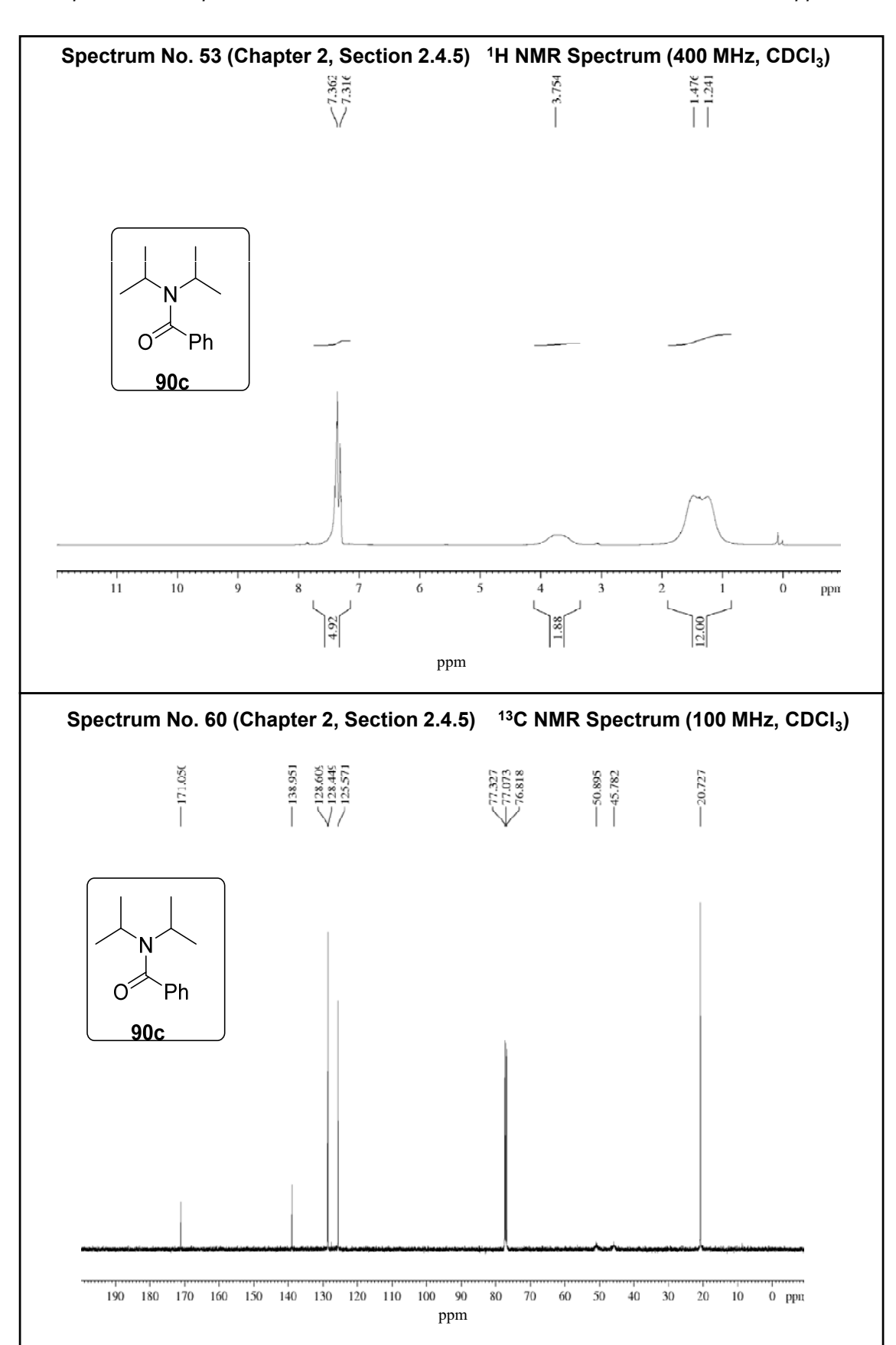


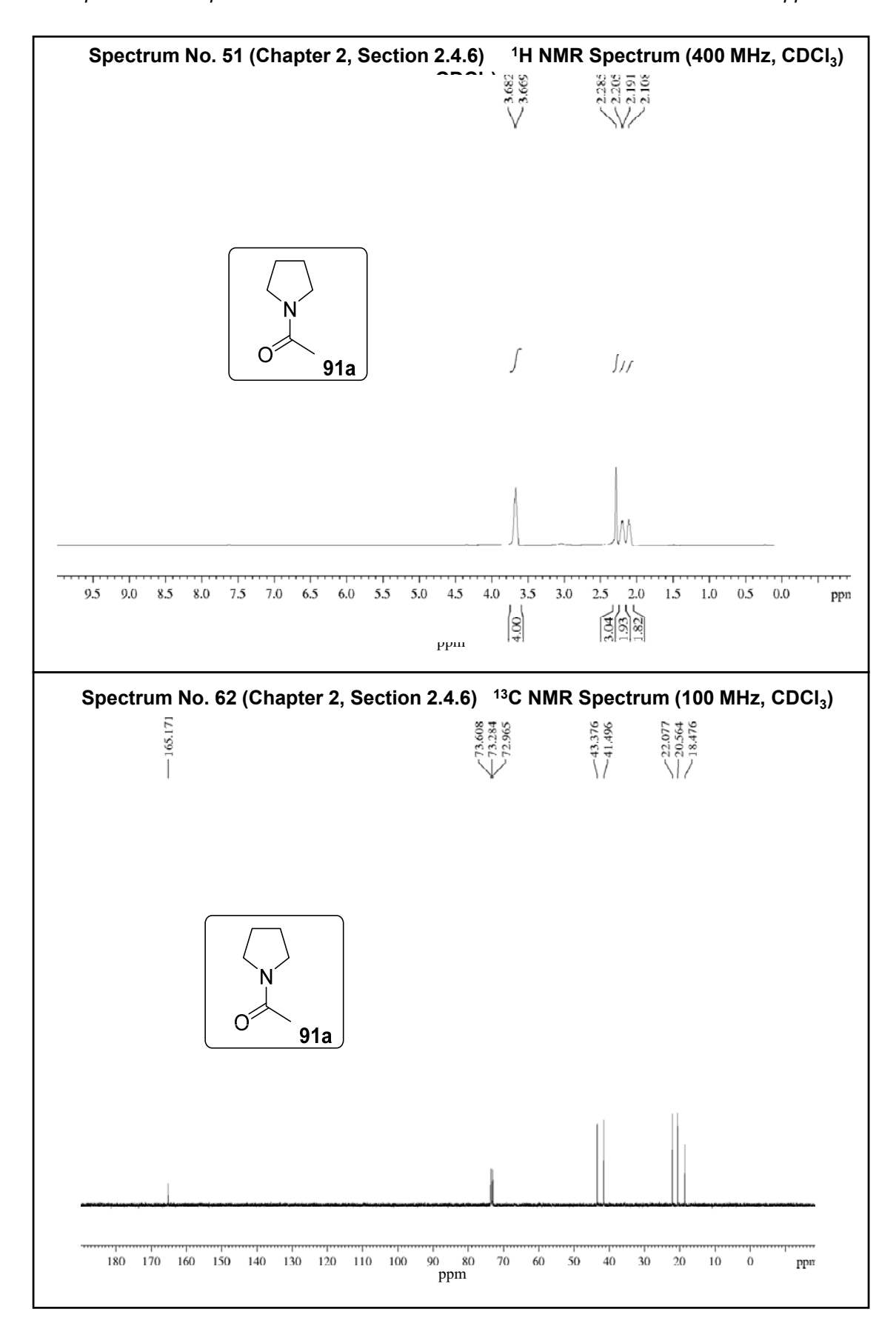


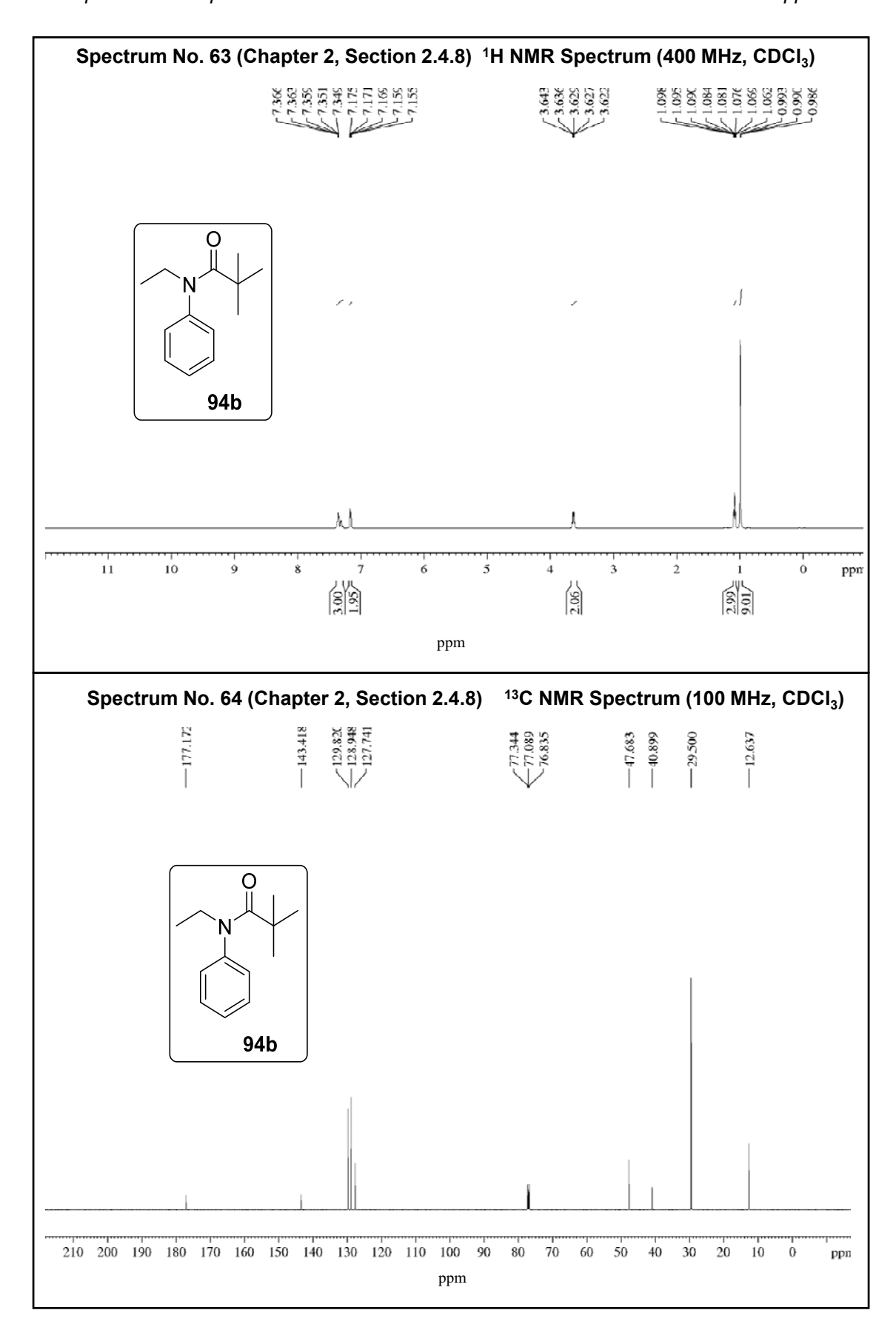


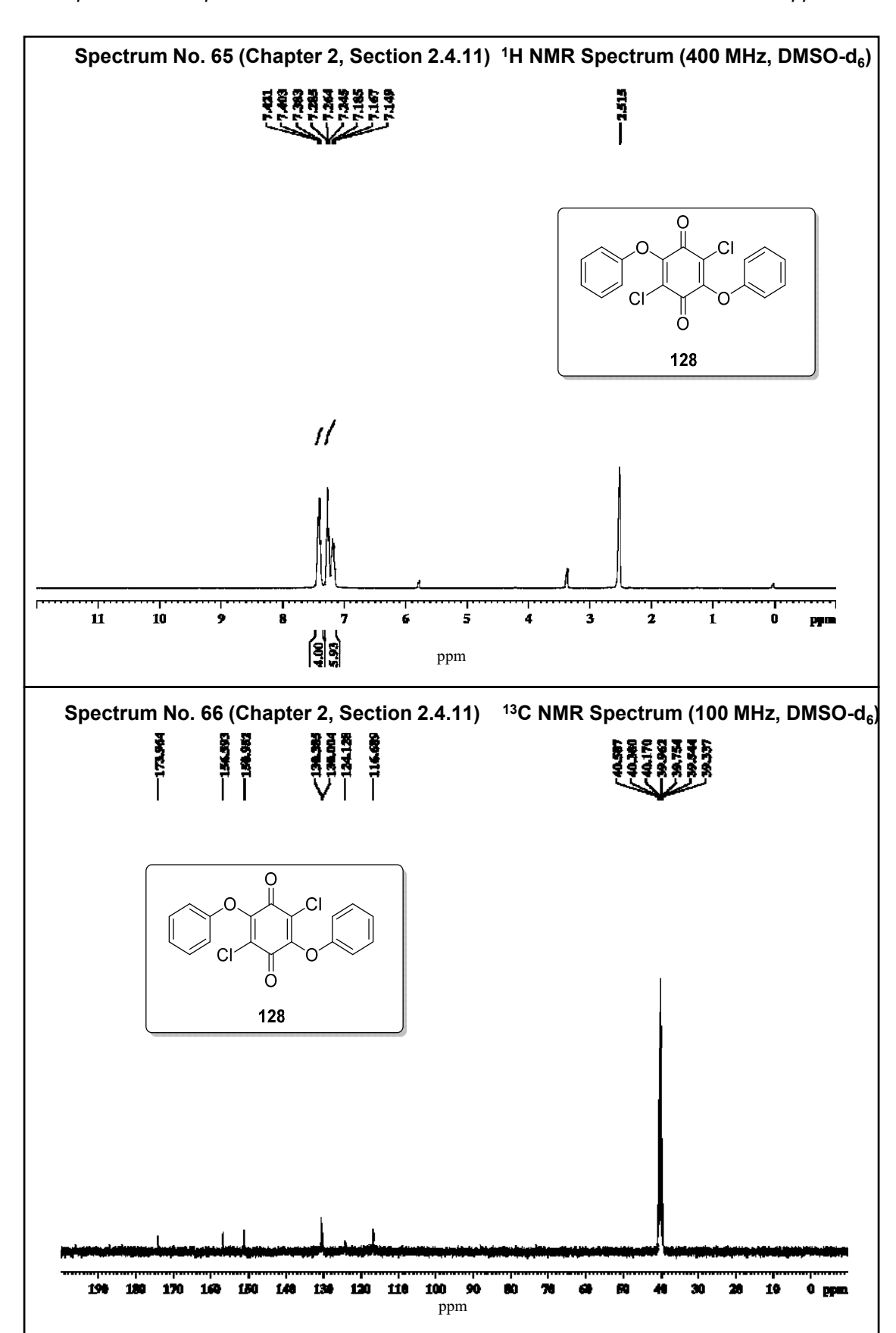


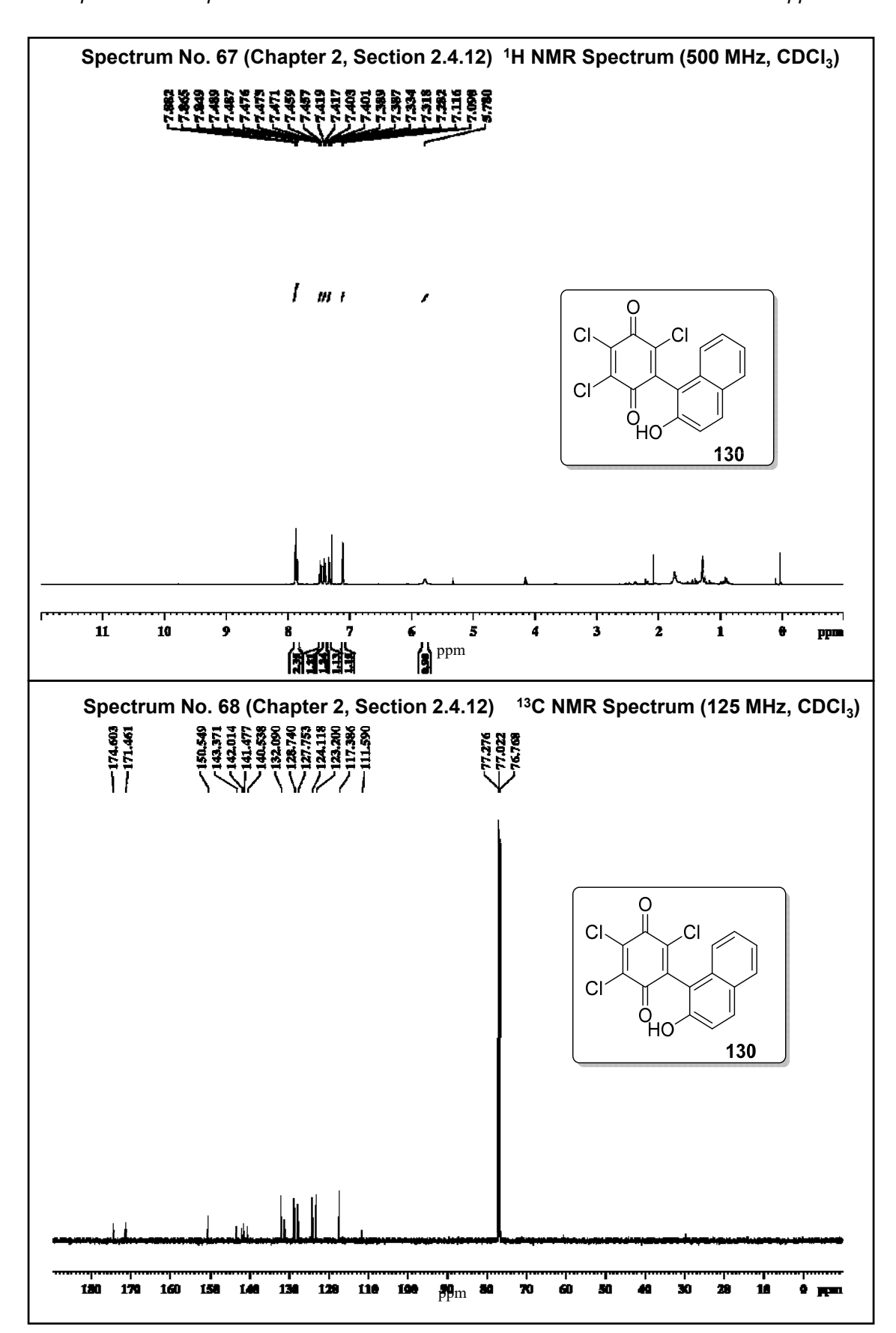












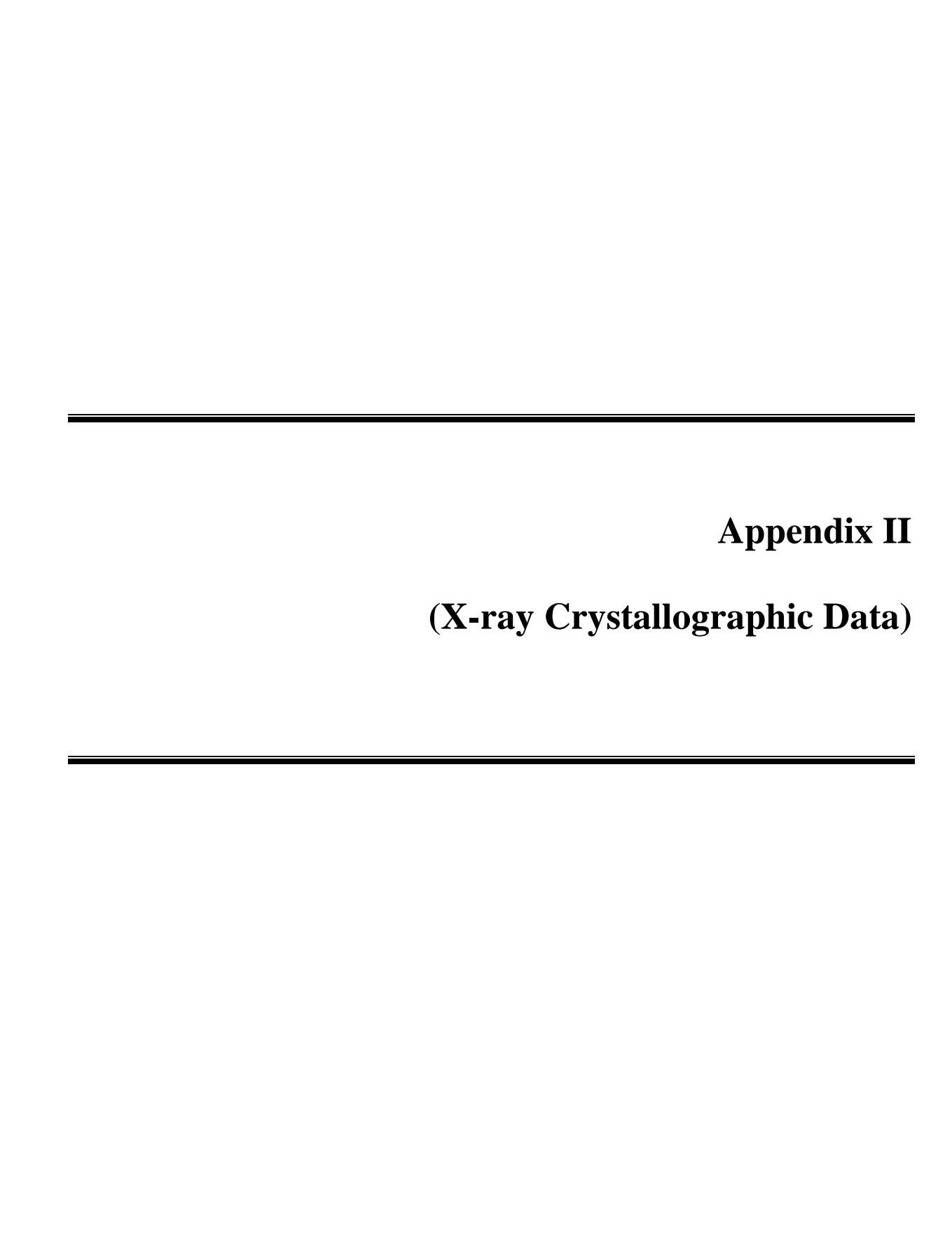


Table 2. Atomic coordinates (x 10⁴) and equivalent isotropic displacement parameters (\mathring{A}^2x 10³) for compound **97g**. U(eq) is defined as one third of the trace of the orthogonalized U^{ij} tensor.

	X	y	Z	U(eq)
		<u>-</u>		
N(1)	1381(3)	7045(3)	3127(2)	39(1)
N(3)	8521(3)	6734(3)	4310(2)	44(1)
N(2)	979(3)	8099(3)	4822(2)	48(1)
N(4)	8904(3)	8193(3)	2743(2)	45(1)
C(4)	3434(3)	7487(3)	3386(2)	31(1)
C(9)	2303(3)	7532(3)	3679(2)	29(1)
C(8)	2084(3)	8089(4)	4581(2)	33(1)
C(15)	7598(3)	7409(3)	3856(2)	33(1)
C(19)	6479(3)	7339(3)	4176(2)	33(1)
C(14)	7815(3)	8195(4)	3036(2)	34(1)
C(11)	5554(3)	8069(4)	3672(2)	34(1)
C(3)	3558(3)	6845(4)	2512(3)	38(1)
C(7)	3002(3)	8576(4)	5146(3)	38(1)
C(5)	4364(3)	8030(4)	3988(2)	35(1)
C(18)	6356(3)	6486(4)	4972(3)	38(1)
C(13)	6904(3)	8894(4)	2572(3)	40(1)
C(12)	5805(3)	8816(4)	2894(3)	39(1)
C(1)	1570(3)	6485(4)	2310(3)	42(1)
C(6)	4110(3)	8536(4)	4844(3)	40(1)
C(17)	7275(4)	5828(4)	5409(3)	49(1)
C(2)	2642(3)	6348(4)	1978(3)	43(1)
C(20)	9199(3)	9071(4)	1977(3)	52(1)
C(16)	8337(4)	5992(4)	5059(3)	51(1)
C(10)	693(4)	8680(5)	5712(3)	59(1)

List of publications

- Synthetic Transformations Using Molecular Oxygen Doped Readily Accessible Carbon Materials; Periasamy, M.; Shanmugaraja, M.; Obula Reddy, P.; Ramusagar, M.; Ananda Rao, G.; *J. Org. Chem.*, **2017**, 82, 4944-4948.
- 2. Ambient Heat Harvesting Organic Electrochemical cell Constructed using Tertiary amines, Amide donors and *p*-chloranil acceptor. Periasamy, M.; Shanmugaraja, M.; Ramusagar, M.; Ramesh, E. (Communicated).
- 3. Oxidative Coupling of 2-naphthol and 1-naphthylamines using the I₂/O₂ Reagent System.; Periasamy, M.; Ramusagar, M.; Ramesh E. (to be communicated).
- 4. Borane Lewis Base Complexes by the Reaction of Oxidatively Doped Polymers with Sodium Borohydride and Lewis Bases; Periasamy, M.; Shanmugaraja, M.; Ramusagar, M.; Suresh, S. (to be communicated).

Posters/Papers presented in symposia

- 1. Borane Lewis Base Complexes by the Reaction of Oxidatively Doped Polymers with Sodium Borohydride and Lewis Bases; Poster Presentation in the *Chemfest-2018* held at School of Chemistry, University of Hyderabad, INDIA.
- Synthetic Transformations Using Molecular Oxygen Adsorbed Carbon Materials;
 Poster Presentation in the *Chemfest-2018* held at School of Chemistry, University of Hyderabad, INDIA.